The Role of Phosphatidylinositol 3-Kinase in P2X7R Gated Signalling in T Lymphocytes

Foster, John

Award date:
2012

Awarding institution:
University of Bath

THE ROLE OF PHOSPHATIDYLINOSITOL 3-KINASE IN P2X7R GATED SIGNALLING IN T LYMPHOCYTES

John Gordon Foster

Submitted for the degree of Doctor of Philosophy (PhD)

University of Bath,

Department of Pharmacy and Pharmacology

Abstract

Background: The role of P2X7R in the immune response has been investigated and this receptor clearly has important roles in inflammation. However, the mechanisms which integrate P2X7R activation with biochemical changes in T lymphocytes such as: proliferation, migration and regulation of adhesion molecule expression are less well understood. Many of these processes are controlled by the PI3K pathway, which is an important signalling cascade involved in development and immunity that it is frequently altered in disease. This study sought to investigate if PI3K was responsible for integrating P2X7R dependent signalling in primary human T lymphocytes, with an emphasis on regulation of the adhesion molecule CD62L.

Results: Whole cell patch clamp electrophysiology is an important technique for characterising ion channel expression. This technique was optimised for the first time in *primary* human naïve $CD4^+$ T lymphocytes and used to show P2X7R expression in this study. The pharmacology of ATP in the process of CD62L down-regulation in these cells was explored using new P2X7R antagonists with improved selectivity over previous compounds. Remarkably, PI3K/mTOR, MAPK and PKC signalling was shown to be dispensable for this down-regulation of cell surface CD62L expression. However, while investigating novel mechanisms for ATP induced CD62L down-regulation, it was revealed that pharmacological modulation of mitochondrial complex I or III, but not inhibition of NADPH oxidase, enhanced P2X7R dependent CD62L down-regulation by increasing ATP potency. The mechanism for this was further explored and this effect may arise from enhanced superoxide generation in the mitochondria of rotenone and antimycin A treated cells. Crucially, although ATP alone did not cause apoptosis of cell, perturbation of the mitochondria of cell with these compounds followed by ATP treatment, revealed P2X7R exposure of phosphatidyl serine.

Discussion: This major new finding may have implications for the clearance of naïve $CD4^+$ T lymphocytes which have undergone mitochondrial damage. A novel protective mechanism for the potential removal of cells with damaged mitochondria is presented, whereby, P2X7R dependent PS exposure occurs only when cells have enhanced mitochondrial ROS generation. Given the potential role of P2X7R in a number of diseases with a mitochondrial element, the findings of this thesis are of great importance for the targeting of P2X7R in inflammation.

Table of Contents

Table of Figures

Table of Tables

Acknowledgements

I would like to thank my supervisors Professor Stephen Ward and Dr Amanda Mackenzie for their help and support throughout my PhD. I would also like to thank Dr. Iain Kilty and Dr. Mark O'Neill at Pfizer, Inc. for their input into this project.

Dr. Richard Parry and other post-doctoral researchers in the department have provided invaluable technical assistance. Dr. Adrian Rogers of the Microscopy and Analysis Suite, Bath was very helpful in assisting with flow cytometry.

To postgraduate colleges past and present, especially Matt and Ed, thank you for your continued friendship.

Mostly I would like to thank my parents and Josie for their love and support through the best and the worst of these past years.

Finally this thesis is dedicated to Rita Herbert (RIP), the reason I have dedicated myself to a career in the sciences.

Abbreviations

ABD	Adaptor binding domain
ADAM	A disintegrin and metalloproteinase
ADAP	Adhesion and degranulation promoting adaptor protein
ADP	Adenosine diphosphate
ALS	Amyotrophic lateral sclerosis
AML	Acute myeloid leukaemia
AMP	Adenosine monophosphate
APC	Antigen presenting cell
ART2	Mono-ADP-ribosyltransferase 2
ATP	Adenosine triphosphate
BBG	Coomassie Brilliant Blue G
BCG	Bacille Calmette-Guerin
B-CLL	B cell chronic lymphoid leukaemia
BCR	B cell receptor
BzATP	2',3'-O-(4-benzoyl-benzoyl) ATP
cAMP	Cyclic adenosine monophosphate
CD45RB	RB isoform of protein tyrosine phosphatase receptor type C
CFSE	Carboxyfluorescein diacetate, succinimidyl ester
CHR	Cysteine rich hand
CLP	Common lymphoid precursor
CRAC	Calcium release activated channel
CTL	Cytotoxic T lymphocyte
DAG	Diacylglycerol
DAMP	Damage associated molecular pattern
DLD	Disintegrin-like domain

DN	Double negative
DP	Double positive
EGF	Epidermal growth factor
ENTPD1 (CD39)	Ectonucleoside triphosphate diphosphohydrolase-1
ER	Endoplasmic reticulum
FasL	Fas ligand
fMLP	N-formyl-methionyl-leucyl-phenylalanine
FOXO	Forkhead box subfamily O
GC	Germinal centre
GEF	Guanine-nucleotide-exchange factor
Glycam-1	Glycosylation dependent cell adhesion molecule 1
GPCR	G-Protein Coupled Receptors
H2DCFDA	2',7'-dichlorodihydrofluorescein diacetate
HA	Influenza hemagglutinin
HEV	High endothelial venule
HSC	Hematopoietic stem cell
HTS	High throughput screening
HVR	Hyper variable region
ICAM1	Intracellular adhesion molecule 1
IFN	Interferon
IKBKE	Inhibitor of NFκ-B Kinase subunit ε
IL	Interleukin
IP(1,4,5)P_3	Inositol(1,4,5)trisphosphate
ITAM	Immunoreceptor tyrosine-based activation motif
LFA-1	Leukocyte function-associated antigen 1
LPS	Lipopolysaccharide
MAdCAM-1	Mucosal vascular addressin cell adhesion molecule 1

MAPK	Mitogen activated protein kinase
MDSCs	Myeloid-Derived Suppressor Cells
MHC	Major histocompatability
MMP	Matrix metalloproteinase
mRNA	Messenger RNA
MS	Multiple sclerosis
mtDNA	Mitochondrial DNA
MTOC	Microtubule-organising centre
mTOR	Mammalian Target of Rapamycin
mTORC2	Mammalian Target Of Rapamycin complex 2
NAD	Nicotinamide adenine dinucleotide
NK	Natural Killer
NKT	Natural Killer T
NLR	NOD like receptor
NO	Nitric oxide
O_2^-	Superoxide
oATP	Periodate-oxidized 2′,3′-dialdehyde ATP
OVA	Ovalbumin
P2X7R	P2X7 receptor
hP2X7R	human P2X7 receptor
mP2X7R	mouse P2X7 receptor
rP2X7R	rat P2X7 receptor
PAMP	Pathogen associated molecular pattern
PBMC	Peripheral Blood Mononuclear Cell
PDK1	Phosphoinositide-dependent kinase-1
PH	Pleckstrin homology
PHA	Phytohaemagglutinin

PHLPP	PH domain leucine-rich repeat protein phosphatases
Pi	Organic phosphate
PI	Propridium Iodide
$PI(3,4,5)P_3$	Phosphatidylinositol(3,4,5)trisphosphate
$PI(4,5)P_2$	Phosphatidylinositol(4,5)bisphosphate
PI3K	Phosphoinositide 3-kinase
PKB	Protein Kinase B
PKC	Protein kinase C
PLC	Phospholipase C
PLD	Phospholipase D
PMA	Phorbol 12-myristate 13-acetate
PNAD	Peripheral node addressin
PPR	Pattern recognition receptor
PS	Phosphatidyl serine
PTEN	Phosphatase and tensin homolog
Q	Quinone
RA	Rheumatoid Arthritis
RBD	Ras binding domain
ROS	Reactive oxygen species
RTK	Receptor tyrosine kinase
S1P	Sphingosine-1-phosphate
S6K	S6 kinase
SAR	Structure activity relationship
sCD62L	Soluble CD62L
SCR	Short consensus repeat
SEB	Staphylococcal enterotoxin B
SERCA	Sarco/endoplasmic reticulum Ca^{2+}-ATPase

SHIP-1	Src homology 2 domain-containing inositol-5-phosphatase-1
SLO	Secondary lymphoid organ
SNP	Single nucleotide polymorphism
SOD	Superoxide dismutase
STIM	Stromal interaction molecule
TACE	Tumour necrosis factor-α converting enzyme
TCP	T-cell precursor
TCR	T cell receptor
TEM	Trans Endothelial Migration
Tfh	Follicular T helper cell
TGF	Tumour growth factor
Th	T helper
TLR	Toll Like Receptor
TMD	Transmembrane domain
TNF	Tumour necrosis factor
TRAPS	TNFR1-associated periodic syndrome
Treg	Regulatory T cell
UCHT-1	University College Hospital T Cell-1
UDP	Uridine diphosphate
USC	Unstained control
UTP	Uridine triphosphate
WCL	Whole cell lysate

1. Introduction

1.1. The Immune System

The immune system exists as an evolved mechanism to protect organisms from infection. It comprises organs, tissues, cells and small soluble factors which interact to maintain a homeostatic healthy organism. Some factors are relatively static, for instance skin and epithelial cells act as barriers to infection, whereas others are induced and act rapidly such as the recruitment of cells to sites of infection. The response of immune cells to pathogens is termed inflammation (Figure 1.1). Inflammation is heavily regulated and de-regulation can result in poor immunity and susceptibility to pathogens, or over reactive immunity which can lead to chronic inflammation and auto-immune disorders. Resolution of inflammation is therefore critical and involves the suppression of the immune response and the remodelling and repair of damaged tissue and vasculature (1). At this stage “memory” of previous infections can also be acquired through the maintenance of a pool of specially developed memory cell subsets. This process is exploited by pharmaceutical companies and medical professionals to produce vaccinations against diseases (2). In addition, the immune system plays a critical role in immune surveillance to detect the presence of transformed cancerous cells and tissues in the body (3). Cells of the immune system themselves are, however, susceptible to forming cancers such as leukaemia and lymphomas; as well as infection by viruses including Human Immunodeficiency Virus (HIV) (4, 5).

1.1.1. Innate Immunity

The first line of defence against pathogens is innate immunity which consists of anatomical barriers to disease, such as the skin and the epithelial cells lining the lungs and gut. Additional to barrier function, these cells are also able to actively release a number of factors including cytokines, chemokines and can activate the complement system. These cells, when damaged by pathogens, can also release their contents including reactive oxygen species (ROS) and damage associated molecular patterns (DAMPs). One such DAMP is the molecule Adenosine Triphosphate (ATP). Resident macrophages and mast cells, which reside in the surrounding connective tissue, express receptors called Toll Like Receptors (TLRs) on their surface. TLRs are able to recognise DAMPs along with pathogen associated molecular patterns (PAMPs) (6). Fc receptors, which can recognise PAMPs in complex with antibodies, are also expressed on these cells. Receptor

ligation activates macrophages, which opsonise pathogens by a process termed phagocytosis, and mast cells, which can undergo de-granulation to release their inflammatory contents. This latter process by mast cells is largely responsible for allergic responses in mammals (7, 8). Macrophages and mast cells can also release cytokines and soluble chemokines into the surrounding tissue and vasculature. Chemokines can also be expressed on the surface of epithelial cells or released from these cells following activation of TLRs (9). Chemokines act to recruit cells of the innate immune system including neutrophils, eosinophils, basophils and further monocytes/macrophages; this process of cell migration termed chemotaxis will be described further in following sections (10). Cytokines activate and cause the differentiation and proliferation of these infiltrating cells. Once neutrophils encounter pathogens they employ phagocytosis, produce elastase and generate ROS, as part of the respiratory burst to destroy bacteria and resolve infection (11). Infiltrating macrophages can develop along multiple distinct lineages but can be broadly defined as being classically activated (MI) or alternatively activated (MII). Pro-inflammatory MI macrophages differentiate to produce cytokines including: Interferon γ (IFNγ), Interleukin 6 (IL-6), IL-12 and Tumour Necrosis Factor (TNF); whereas, MII macrophages are anti-inflammatory and promote wound healing through the production of IL-10 and Tumour Growth Factor β (TGF-β) (12). Macrophages, along with dendritic cells, are an important bridge between the innate and adaptive immune system. These cells express major histocompatability (MHC) molecules on their cell surface which allows presentation of antigenic components of bacteria to T lymphocytes (13). Once antigen has been immobilised on their surface, dendritic cells migrate into the lymphatic system through draining lymph nodes where they encounter resting (naïve) cells of the adaptive immune system (14, 15). Antigen is presented and, if the cognate receptor specific for that pathogen is present on the adaptive immune cell, the cell becomes activated, clonally expands and an adaptive immune response is initiated.

1.1.2. Adaptive Immunity

The adaptive immune response by lymphocytes can be broadly divided into cellular and humoral responses. B lymphocytes are involved in humoral immunity, whereas, specific T lymphocyte subsets (which will be discussed in detail in the

following section) can act as mediators of cellular or humoral immunity. B lymphocytes are produced in the bone marrow and mature in situ. Mature, but un-activated, naïve B lymphocytes circulate through the lymphatic system, until they encounter antigen specific for membrane bound antibody also termed the B cell receptor (BCR). Activation of B lymphocytes in response to antigen induces proliferation, maturation and class switching of cell surface antibodies. The type of antibody expressed, or released by B lymphocytes, as well as their interaction with T lymphocytes and macrophages, helps to determine the specific adaptive immune response. Antibodies released by B lymphocytes have multiple roles in the adaptive immune response including activation of the complement system, facilitating phagocytosis of bacterial cells and cytotoxicity of virally infected host cells.

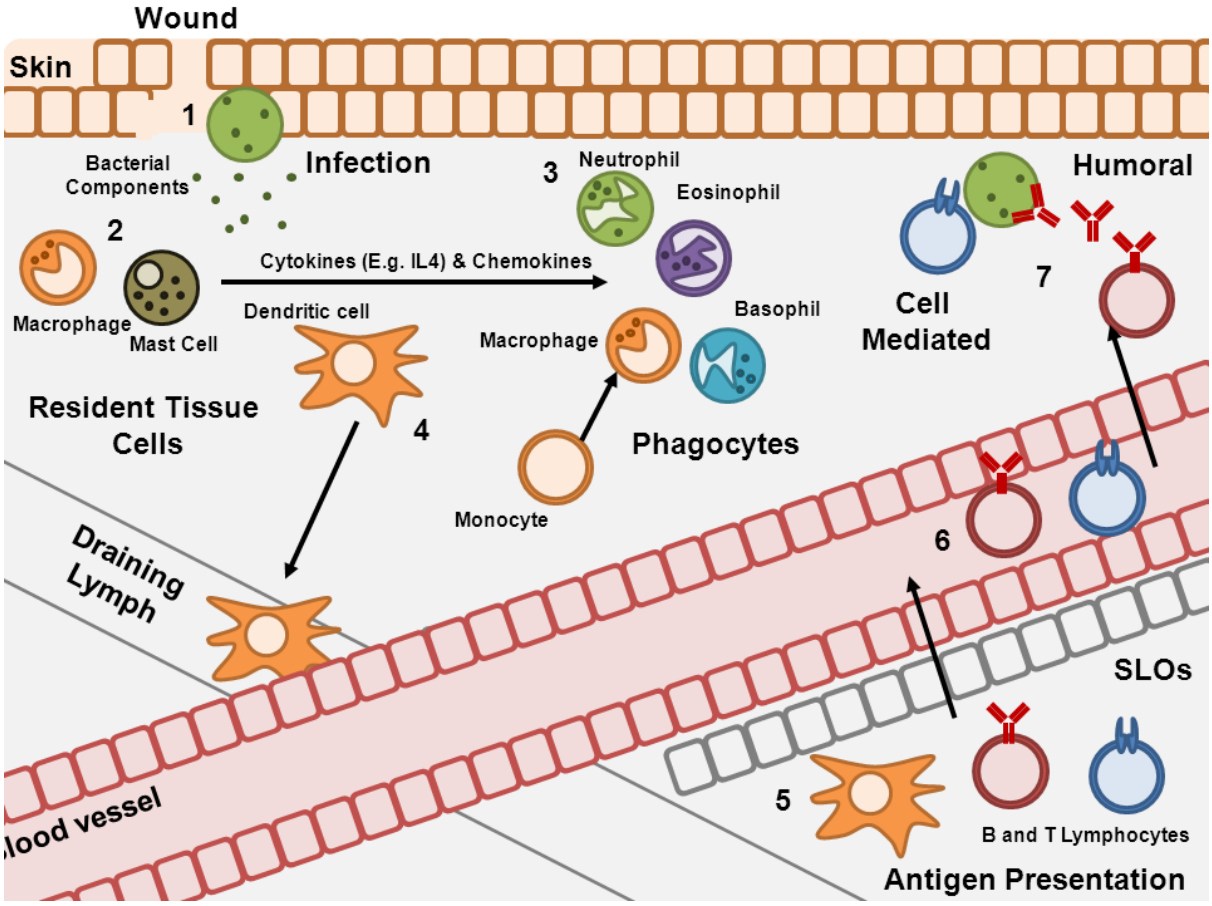

Figure 1.1: Innate and Adaptive Immunity. 1. Skin provides an essential barrier to infection, but when broken pathogens such as bacteria can enter and cause infection. **2.** Resident tissue macrophages and mast cells recognise antigenic components, they then release chemokines and cytokines to recruit and activate circulating phagocytes. **3.** Phagocytes opsonise bacteria and release factors such as elastase, leukotriene and histamine, which is also released by mast cells. **4.** Dendritic cells are professional antigen presenting cells (APCs) which opsonise bacteria and travel through draining lymph to secondary lymphoid organs (SLOs). **5.** Here, dendritic cells present antigenic bacterial components to lymphocytes expressing cognate receptors. **6.** These cells become activated, clonally expand and enter the vasculature where they migrate to peripheral sites of infection. **7.** Lymphocytes are part of the adaptive arm of the immune response and can bring about cell mediated (cytotoxic) or humoral (B cell antibody mediated) killing of bacteria and bacterially infected cells. Finally, the infection is resolved and the wound (**1**) is repaired.

1.2. T Lymphocytes

1.2.1. T lymphocyte maturation

T lymphocyte precursors are produced in the bone marrow and migrate to the thymus, where they mature from double negative ($CD4^-/CD8^-$) to either single positive $CD4^+$ or $CD8^+$ cells expressing the αβ T cell receptor (TCR) (Figure 1.2). The CD4 and CD8 molecules aid binding of T lymphocytes to class II and class I MHC molecules respectively. Double negative cells may also form a subpopulation of γδ T cells, named due to their expression of only the γ and δ chains of the TCR. Somatic gene rearrangement of the V, D and J components of the TCR by the enzymes RAG1 and RAG2 in the thymus is essential for production of a plethora of structurally distinct TCRs. These TCRs are specific only for one antigenic component, and the naïve T lymphocytes produced are only activated once they encounter this specific antigen presented by an APC.

Naïve T lymphocytes have a distinct phenotype characterised by high levels of surface L-selectin (CD62L) expression, expression of the RB isoform of protein tyrosine phosphatase receptor type C (CD45RB) and low levels of the glycoprotein CD44 (16). Naïve cells exist in this $CD62L^{high}$, $CD45RB^{high}$, and $CD44^{low}$ state and survey the lymphatic system for antigen (17, 18). Prior to antigen presentation, naïve $CD4^+$ cells undergo homeostatic proliferation in response to IL-7. Naïve $CD8^+$ cells respond more robustly to IL-7 and, while the cytokines IL-4 and IL-15 also enhance proliferation, IL-7 is indispensable (19, 20). IL-7 can also drive the transition of naïve (independent of antigen) and effector T cells into a memory phenotype (16, 21). IL-7 levels are carefully controlled to maintain proliferation of naïve T cells, however, acting as a co-stimulant IL-7 can drive T cell autoimmune disease (22).

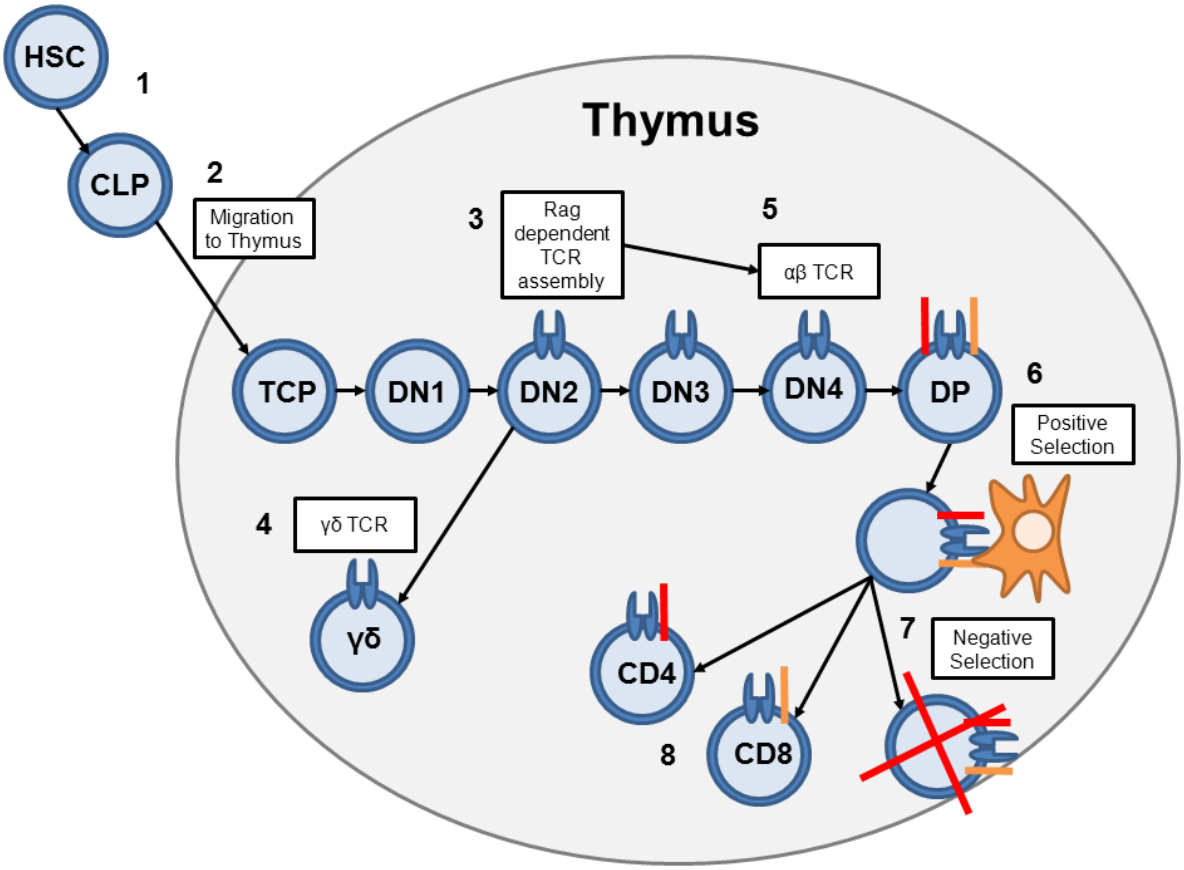

Figure 1.2: T lymphocyte maturation. 1. T lymphocytes originate from hematopoietic stem cells (HSCs) which are produced in the bone marrow and develop into common lymphoid precursor cells (CLPs). **2.** CLPs migrate to the thymus where they develop into committed T-cell precursors (TCPs). These thymocytes are double negative (DN) as they do not express either the CD4 or CD8 co-receptors on their cell surface. C-Kit^{+}, CD44^{high}, CD25^{-} D1 thymocytes develop into DN2 cells which gain CD25 expression and lower the levels of cell surface CD44. **3.** At the DN2 stage, the TCR components begin to rearrange forming either DN3 thymocytes or T lymphocytes which eventually express the γδ TCR (**4**). C-Kit^{-}, CD44^{-}, CD25^{+} DN3 cells, in contrast, express TCRβ and pre-TCRα in complex with CD3. **5.** CD25 expression is lost at the DN4 stage and, as both the CD4 and CD8 co-receptors are expressed, cells become double positive (DP). **6.** Positive selection allows the progression of DP cells which can bind MHC expressed by epithelial cells **7.** DP cells that bind MHC too readily are removed by apoptosis through the process of negative selection. **8.** Finally, single positive CD4^{+} or CD8^{+} cells are produced and leave the thymus.

1.3. T cell activation

1.3.1. TCR

As described above, the TCR is assembled in a RAG1/2 dependent manner from V, D, and J elements by somatic gene rearrangement. Once mature, the TCR forms a membrane complex with constant cell surface CD3γ, δ and two ε co-receptors as well as two intracellular CD3 ζ elements. These form a complete TCR complex as described in the figure below (Figure 1.3). Activation of a T cell is a two signal system, it requires formation of an immunological synapse involving both presentation of cognate peptide to the TCR by the MHC of an APC, and the co-stimulation of CD28 by B7 family ligands expressed on the surface of the APC (Figure 1.4). Super-antigens such as staphylococcal enterotoxin B (SEB) act independent of MHC to activate a large number of αβTCR T lymphocytes, irrespective of the antigen specificity of these cells (23). As well as co-stimulatory signals, co-inhibitory receptors expressed by T lymphocytes can respond to ligands expressed on the surface of APCs (Figure 1.4). If co-stimulation is absent, T lymphocytes become anergic (24). Activated T cells up-regulate CTLA-4 which also acts as a co-receptor for B7 family ligands; ligation of CTLA-4 results in inhibition of T cell function and this is an important step in resolution of adaptive immunity (25). This inhibition of T cell function by CTLA-4 forms a strategy for the treatment of auto-immune disorders and cancer (26–28). Antigen presentation and co-stimulation of T lymphocytes induces activation by initiating a complex signalling cascade involving multiple kinases, increases in free intracellular calcium levels followed by changes in gene transcription and finally global changes in T cell phenotype.

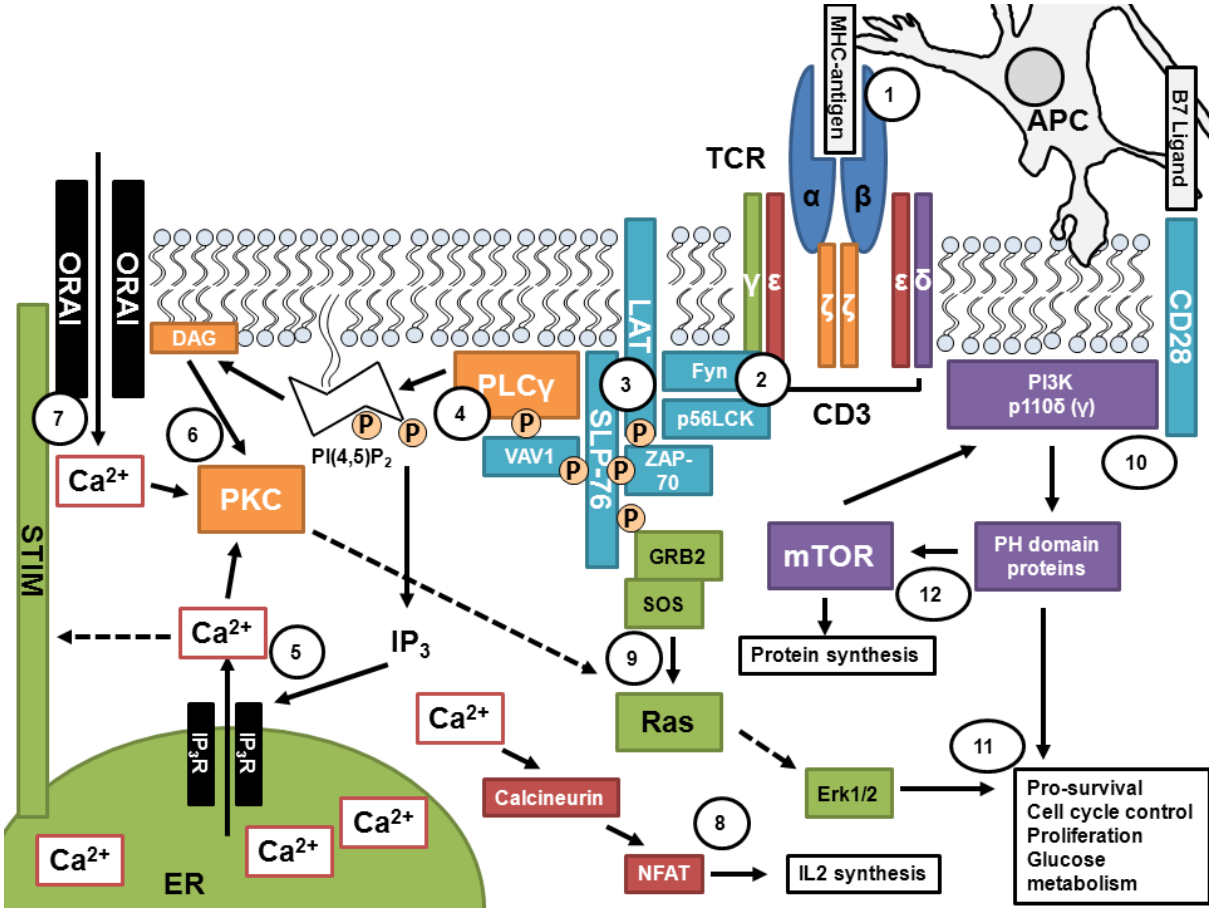

Figure 1.3: Signalling mechanisms down-stream of T lymphocyte activation. 1. Following engagement of the TCR with antigen presented by an APC and presentation of co-stimulatory ligands the sequential activation of a number of signalling pathways occurs. **2.** CD3 subunits contain ITAMs which are phosphorylated by Fyn and p56Lck allowing the recruitment of ZAP70. **3.** ZAP70 becomes tyrosine phosphorylated and phosphorylates SLP76 and LAT. **4.** These act as linkers to recruit PLCγ brings it into close proximity with its substrate PI(4,5)P_2 which is hydrolysed into IP_3 and DAG. **5.** IP_3 acts on IP_3 receptors on the ER which allow release of calcium. **6.** Raised intracellular calcium levels, along with DAG in the plasma membrane, activate PKC. **7.** Calcium release from the ER also causes association of STIM with ORAI channels in the plasma membrane which allow influx of calcium, further raising intracellular levels. **8.** Free calcium (Ca^{2+}) also acts through Calcineurin to activate the transcription factor Nuclear Factor of Activated T cells (NFAT) leading to IL-2 synthesis. **9.** PKC and GRB2/SOS activate the Ras/Erk1/2 pathway. **10.** Activation of the TCR/CD3 complex, as well as engagement of the co-stimulatory receptor CD28 by B7 family ligands on the APC surface, recruits the class I PI3Kδ (as well as PI3Kγ). **11.** The PI3K signalling cascade is important for proliferation and survival of T lymphocytes and can feed into the mTOR pathway which controls protein synthesis (**12**)

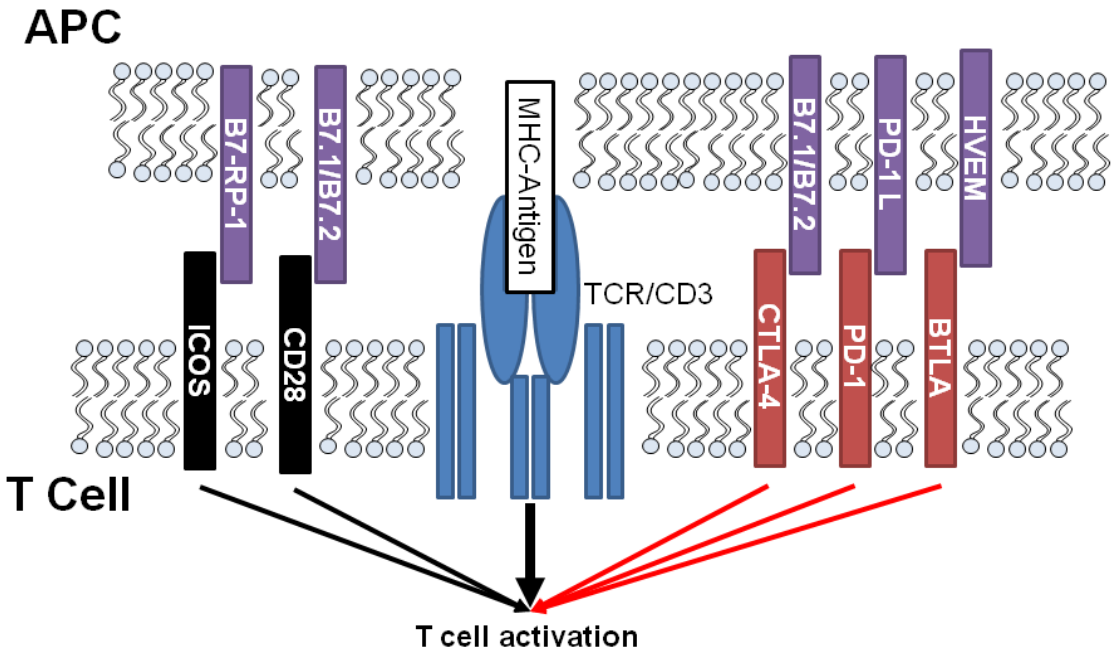

Figure 1.4: Role of co-stimulatory, co-inhibitory receptors and cognate ligands on antigen presenting cells. The TCR is engaged by antigen presented by MHC molecules on an APC and T cell activation is initiated. The ultimate fate of the T cell depends on the mechanism of co-stimulation provided by the APC. Activation of CD28 and ICOS expressed by T lymphocytes promotes the activation of these cells (black arrows) whereas activation of CTLA-4, PD-1 or BTLA causes inhibition of T lymphocyte activation and eventual anergy (red arrows).

1.3.2. Signalling down-stream of the TCR

1.3.2.1. ITAMs

CD3 and CD28 co-receptors contain immunoreceptor tyrosine-based activation motifs (ITAMs) on their intracellular tails, these have the common sequence: $YxxLx_{(7\text{-}12)}YxxL$. This sequence becomes phosphorylated by p56Lck and Fyn following engagement of peptide-MHC with TCR. These ITAMs act to recruit a number of signalling components. The first of these is ZAP70 which is tyrosine phosphorylated and in turn phosphorylates SLP76 and LAT; these act as linkers to recruit a complex of signalling molecules including: VAV1, ITK, GRB2, SOS and PLCγ.

1.3.2.2. PLC and PKC

PLCγ recruitment to the membrane brings it into close contact with its substrate phosphatidylinositol(4,5)bisphosphate ($PI[4,5]P_2$), which is hydrolysed by PLCγ to form the membrane anchored substrate diacylglycerol (DAG) and inositol(1,4,5)trisphosphate ($IP[1,4,5]P_3$). These second messengers activate conventional α, β and γ isoforms of the Protein Kinase C (PKC) family. DAG anchors PKC at the inner leaflet of the plasma membrane and $IP[1,4,5]P_3$ acts to open calcium release channels on the endoplasmic reticulum. Two ions of free Ca^{2+} bind to each PKC protein in a region that is revealed by a conformational change in the protein following DAG binding. Recently the novel PKC isoforms θ, ε and η (but not δ), which are activated by Ca^{2+} alone, were shown to be required for re-localisation of the microtubule-organising centre (MTOC) to the immunological synapse after T lymphocyte activation (29, 30). GRB2 and SOS, along with PKCθ, activate the GTPase Ras which has multiple roles in cell growth (31, 32). Other PKC substrates include PKD1 which associates with a complex containing adhesion and degranulation promoting adaptor protein (ADAP) and SLP76 and RAPL which is responsible for integrin activation (33). Integrin activation allows the adhesion of T cells to APCs during activation and/or the surface of the endothelium.

1.3.2.3. PI3K and mTOR

The phosphoinositide 3-kinase (PI3K) family of lipid kinases has four distinct classes: I, II, III and IV. Little is known about class II and III PI3Ks in T lymphocyte

activation but the class I and mammalian Target of Rapamycin (mTOR), a class IV enzyme, have been extensively studied. Class IA PI3K isoforms are composed of regulatory subunits p85α, p55γ, p50α, p85β, or p55γ in complex with catalytic p110 α, β or δ subunits (Figure 1.5). The single class IB p110γ catalytic subunit is associated with p84/p87 or p101 regulatory subunits. Classically class IA PI3Ks are activated down-stream of a number of cell surface receptor tyrosine kinases (RTKs) including: antigen and co-stimulatory receptors, Fc receptors, adhesion molecules, TLRs and cytokine receptors (34) (Figure 1.6). Whereas, the p110γ catalytic subunit is activated by chemoattractant receptors including those for the ligands C5a, N-formylmethionyl-leucyl-phenylalanine (fMLP), chemokines and sphingosine-1-phosphate (S1P) (14). Promiscuity between Class I PI3Ks and receptor types is a new concept, growing evidence has shown that p110β can be activated through G-Protein Coupled Receptors (GPCRs) and p110γ can be activated via the TCR complex (35, 36).

In the context of TCR signalling, regulatory p85 subunits are recruited to the membrane along with the p110δ catalytic subunit, by the LAT, TRIM and other adaptors (37). PI3K can also be directly activated by the co-stimulatory CD28 and ICOS molecules (38). In T lymphocytes p110δ is largely responsible for integrating signalling downstream of the TCR (39, 40) although there is increasing evidence that p110γ may also play a role (35). Both p110δ and γ have distinct and overlapping roles in T lymphocyte function which will be mentioned briefly in the following sections.

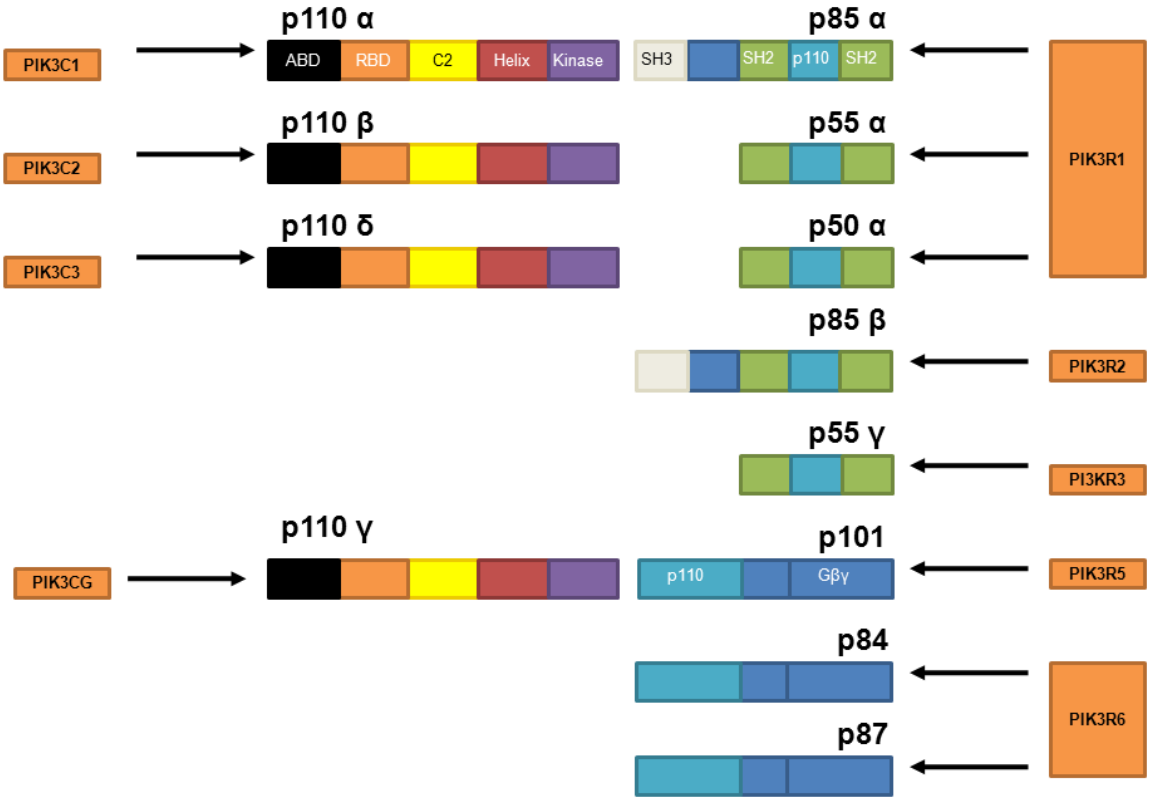

Figure 1.5: Class IA and IB PI3K isoforms. The genes PIK3C1, PIK3C2, PIK3C3 and PIK3CG encode the catalytic p110 α, β, δ and γ isoforms of the class I PI3K family. These catalytic subunits contain a number of important structural domains including: an N-terminal adaptor binding domain (ABD), a Ras binding domain (RBD) and a core structure comprising the C2, helical and kinase domains. Class IA PI3K catalytic subunits can associate with either p85α, p55α or p50α all encoded by PIK3R1 or p85β (PI3KR2) or p55γ (PI3KR3). These regulatory proteins have two proline rich SH3 domains, one Sh2 domain and a p110 binding domain. The single class IB p110γ associates with p101 encoded by PI3KR5 or the PIK3R6 proteins p84 or p87.

Upon activation of class I PI3K, the substrate $PI(4,5)P_2$ is phosphorylated at the D3 position to produce the product phosphatidylinositol(3,4,5)trisphosphate ($PI[3,4,5]P_3$). An increase in $PI(3,4,5)P_3$ levels in the cell membrane is observed following T cell activation and $PI(3,4,5)P_3$ acts to recruit signalling molecules which contain the pleckstrin homology (PH) domain to the plasma membrane (41). These PH domain containing proteins include Phosphoinositide-dependent kinase-1 (PDK1) which, along with mammalian Target Of Rapamycin complex 2 (mTORC2), activates Akt/Protein Kinase B (PKB). Akt is one of the most commonly studied substrates of PI3K and controls cell survival, growth, proliferation and processes such as migration (42). There are three isoforms of Akt: 1, 2 and 3 encoded by distinct genes; Akt 1 and 2 are ubiquitously expressed but Akt 3 has a more restricted expression profile (43). It is becoming increasingly apparent that these Akt isoforms have differing substrate profiles and may regulate cellular processes by different mechanisms. For example, in a model of invasive carcinoma siRNA targeting Akt1 results in increased migration, whereas, targeting Akt2 decreases migration (44, 45). Substrates phosphorylated only by Akt1 include: P21 cip1, SKP2 (46, 47) and paladin; Akt2 phosphorylates MDM2 and AS160 however a large number of substrates, such as BAD and GSK3β, are phosphorylated by both Akt1 and 2.

Full activation of Akt generally requires phosphorylation of both Ser473 by mTORC2 and Thr308 by PDK1. However, this may not be true for all Akt isoforms in all cell types (48). A recent study has also demonstrated that Akt can be phosphorylated and activated independently of PI3K by Inhibitor of NFκ-B Kinase subunit ε (IKBKE) (49). The Ser473 residue can also be de-phosphorylated by a family of PH domain leucine-rich repeat protein phosphatases (PHLPP) (50). PI3K signalling can also be terminated by the actions of phosphatase and tensin homolog(PTEN), which dephosphorylates $PI(3,4,5)P_3$ to $PI(4,5)P_2$. The Src homology 2 domain-containing inositol-5-phosphatase-1 (SHIP-1) dephosphorylates $PI(3,4,5)P_3$ at the 5' position to give the alternative PIP_2, $PI(3,4)P_2$ and this may act to recruit PH domain containing proteins with a different specificity to $PI(3,4,5)P_3$ (51, 52).

mTOR is responsible for regulation of cell metabolism and protein synthesis and mTOR activity is important for T lymphocyte proliferation (53). mTOR can form two signalling complexes mTORC1 and mTORC2 which have different substrate specificities and sensitivities to inhibitors. Akt, through phosphorylation of TSC2 and release of inhibition by Rheb, leads to activation of the protein complex mTORC1. mTORC1 activates S6Kinase which in turn inhibits 4EBP1 to promote cellular growth and proliferation. Much of what is known about mTORC1 has been garnered from the use of a naturally occurring compound called Rapamycin, an immunosuppressant. Rapamycin blocks the interaction between Raptor and mTOR in mTORC1, whereas mTORC2 contains Rictor in place of Raptor and is insensitive to inhibition by Rapamycin.

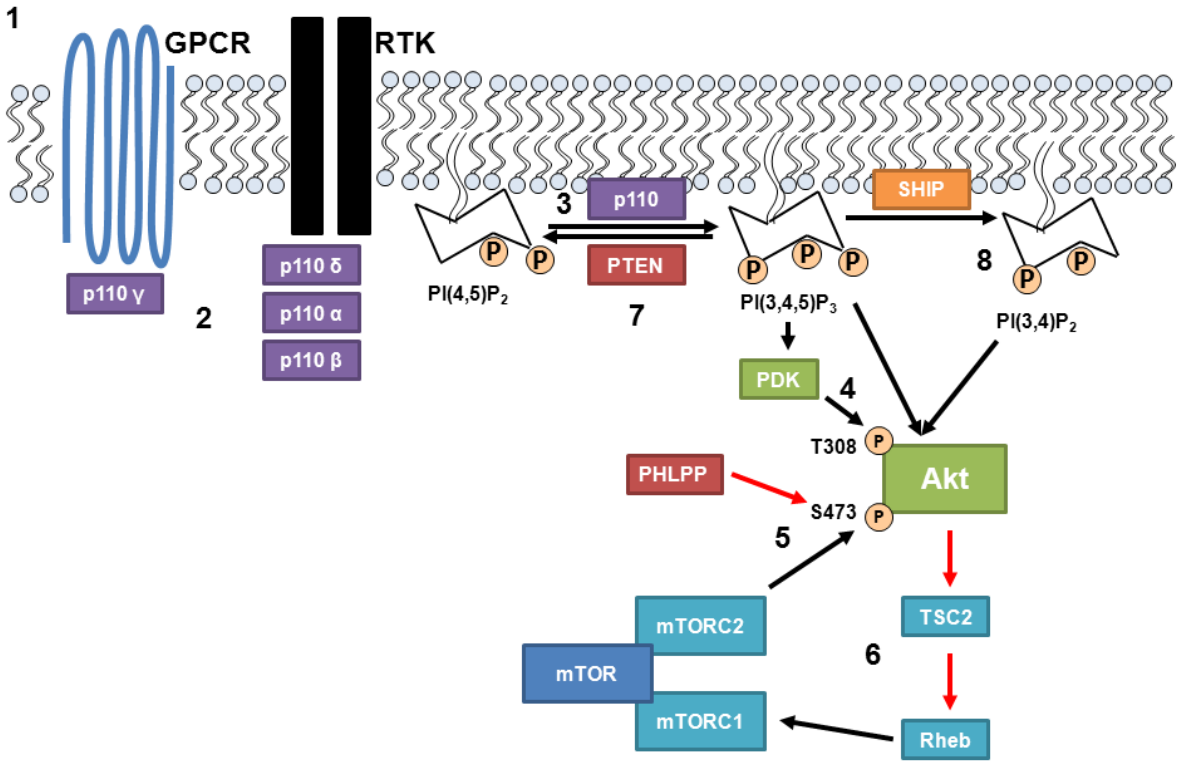

Figure 1.6: PI3K/mTOR signalling. 1. Ligands activate cell surface receptors such as RTKs and GPCRs. 2. Classically class IA PI3K isoforms are activated down-stream of RTKs and the single class IB PI3K isoform is activated down-stream of GPCRs. 3. Class I PI3Ks catalyse the addition of a phosphate group to the 3' region of the inositol ring of $PI(4,5)P_2$ to produce $PI(3,4,5)P_3$. PIP_3 acts as a membrane anchor for proteins with a PH domain. **4.** The increased proximity of two such proteins PDK and Akt/PKB at the membrane leads to phosphorylation of T308 on Akt by PDK. **5.** The kinase mTOR can form one of two signalling complexes: mTORC1 and mTORC2 the latter of which phosphorylates S473 on Akt leading to its activation. This residue can be de-phosphorylated by PHLPP. **6.** Akt through its inhibition of TSC2 (an inhibitor of mTOR signalling) leads to activation of mTORC1. The PIP_3 product of PI3K function can also be de-phosphorylated to $PI(4,5)P_2$ and $PI(3,4)P_2$ by the lipid phosphatases PTEN (**7**) and SHIP1 (**8**) respectively. $PI(3,4)P_2$, in contrast to $PI(4,5)P_2$, can also act as an anchor for PH domain containing proteins including several which PIP_3 cannot bind.

1.3.3. Inhibition of PI3K/mTOR pathway for the treatment of inflammatory and autoimmune disease

As mentioned previously, deregulation of PI3K signalling can lead to the development and progression of diseases such as inflammatory and autoimmune disease and malignancies (54). The p110δ and γ isoforms of PI3K are expressed predominantly in cells of the immune system and control leukocyte activation, differentiation, migration and a whole host of other biochemical processes. Isoform and cell specific roles for PI3K have been investigated intensively using animal mouse models, where p110δ and/or γ have been knocked out or inactivated (55). The important role of these PI3K isoforms in disease has led to the development of PI3K inhibitors as novel therapeutics. Early efforts to target PI3K involved the natural compound Wortmannin and the first synthesised PI3K inhibitor LY294002 (56, 57). These were both useful pharmacological tools; however multiple off target effects and toxicity limited their use as drugs (58, 59). Wortmannin and LY294002 are examples of Pan-isoform PI3K inhibitors, in that they target all four PI3K isoforms. Recently a large number of Pan-isoform PI3K inhibitors have been developed for the treatment of cancer, a number of these can be seen in Table 1.1 below. However, the targeting of PI3K in inflammation and autoimmunity may require a more selective approach. While isoform specific PI3K inhibitors were initially thought impossible to achieve, a number of p110δ and γ selective (as well as dual p110δ/γ) inhibitors have been reported in the literature (Table 1.1). Recently the structure of p110δ in complex with PI3K inhibitors has been solved; this has provided insight into how isoform selectivity of compounds can be obtained (60).

PI3K is not the only point of intervention in the signalling cascade to provide therapeutic potential. The mTORC1 inhibitor Rapamycin was one of the first immunosuppressive drugs developed and has been joined more recently by active site inhibitors of both mTORC1 and mTORC2 (61, 62). The PI3K effector molecule Akt can also be directly inhibited and this may overcome novel PI3K independent Akt activation mechanisms such as IKBKE (63–65).

Compound	Company	Ref	IC_{50} (μM)					Structure
			p110α	p110β	p110δ	p110γ	mTOR	
Wortmannin	N/A	(66)	0.0042					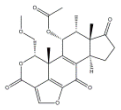
LY294002	Eli Lilly	(56)	1.4					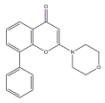
ZSTK474	Zenyaku Kogyo	(67)	0.016	0.044	0.0046	0.049		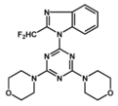
GDC0941	Genentech/ Roche	(68)	0.003	0.033	0.003	0.075		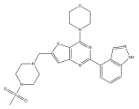
PIK-75		(69)	0.0058	1.3	0.51	0.076		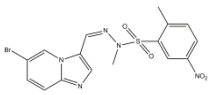
TGX-221		(70)	n/a	0.005	n/a	n/a		
IC-87114	ICOS	(71)	>200	16	0.13	61		
GS-1101 (CAL-101)	Gilead	(72)	0.82	0.565	0.0025	0.089		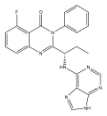
AS-605240	Merck Serono	(73)	0.06	0.27	0.3	0.008		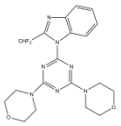
TG-100-115	TargeGen	(74)	1.3	1.2	0.235	0.083		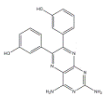
BEZ235	Novartis	(75)	0.004	0.075	0.007	0.005	0.021	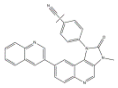
SF1126	Semafore Pharma	(76)	0.356	0.736	3.225	1.774	1.06	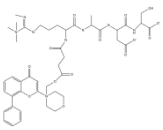
AZD8055	AstraZeneca	(77)	3.59	18.9	3.2	>14.79	0.0008	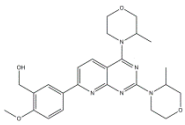
			Akt1		**Akt2**		**Akt3**	
MK2206	Merck	(43)	0.0053		0.012		0.065	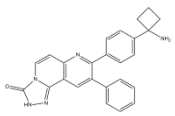

Table 1.1 PI3K Inhibitors

Details for inhibitors of the PI3K/mTOR pathway are given including: the companies responsible for their development, the IC_{50} values against Class I PI3K isoforms, mTOR or Akt as well as their chemical structure. Colour coding indicates the selectivity of compounds: Orange = Pan-PI3K, Blue = Isoform selective, Grey = Dual p110δ/γ selective, Purple = Pan-PI3K/mTOR, Green = mTOR and Red = Akt.

1.4. Role of T lymphocyte subsets in adaptive immunity and inflammation

After exiting the thymus and becoming activated, $CD4^+$ T lymphocytes can differentiate into a number of different T helper (Th) subsets (Figure 1.7). This differentiation depends on the cytokine environment surrounding the cells during activation. Two distinct types of Th cell were initially described in the lab of Robert L Coffman, based upon the how they reacted to specific stimuli and the proteins they produced in response (78, 79). From this point, Th cells were either Th1 cells which facilitated cell based immunity or Th2 cells which were responsible for humoral immunity. This paradigm existed for almost 20 years before the discovery of a lineage of Th cells which responded to IL-23 and produced, among others, the cytokine IL-17. Each $CD4^+$ sub group produces signature cytokines, which have specific roles in supporting the cell mediated or humoral arms of the adaptive immune response. For example, IL-4 produced by Th2 cells supports B lymphocytes whilst inhibiting the generation of Th1 cells. Unrestrained production of cytokines by Th cells can also drive inflammation; indeed, high levels of IL-17 are observed in patients with inflammatory and auto-immune disorders including Rheumatoid Arthritis (RA). More recently several other Th subsets have been discovered including Th9 and Th22 cells (80–83). A suppressive T cell subset, regulatory T cells (Tregs), are characterised by the expression of the transcription factor FOXP3, high surface expression of CD25 and secretion of IL-10. Tregs help control tolerance to self-antigens and therefore play a key role in preventing autoimmune disease. There is on-going debate about the plasticity of these cell

subsets, how they arise and whether they are terminally committed to a specific lineage (84–86).

Naïve $CD8^+$ T lymphocytes differentiate into cytotoxic T lymphocytes (CTLs) when they are activated. CTLs are responsible for detecting pathogen infected cells and survey for signs of cancerous cells. These infected cells, like most cells of the body, are capable of displaying antigen through MHC class I on their surface. Killing of infected cells by CTLs requires tight cell to cell contact followed by release of granules from the CTL. These granules contain perforin (a pore forming protein) and granzymes (serine proteases responsible for lysis of infected cells). CTLs also express Fas ligand (FasL) on their cell surface which, when in contact with Fas Receptor on the surface of infected cells, initiates the programmed cell death of infected cells by the process of apoptosis.

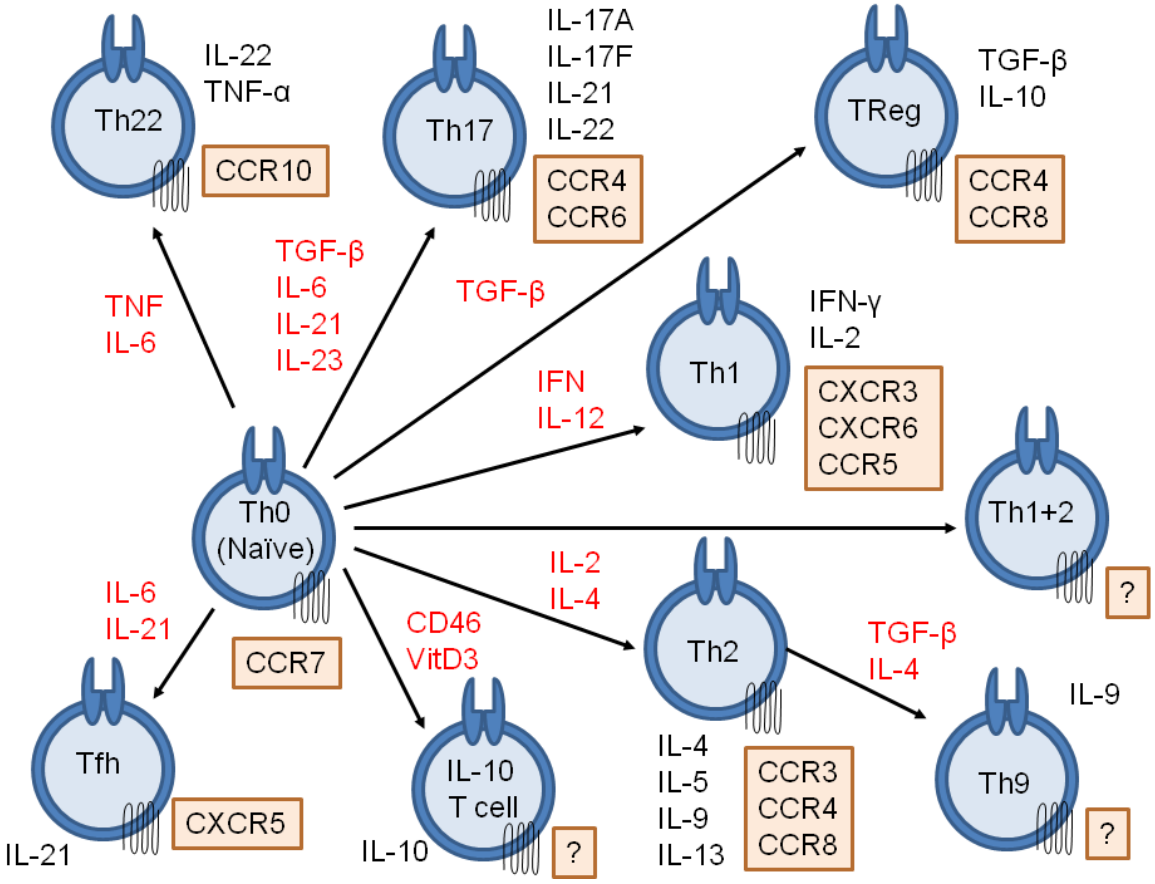

Figure 1.7: T helper subsets generated following activation of naïve $CD4^+$ (Th0) T lymphocytes. Cytokines required to "skew" to a specific subset *in vitro* are given in red. The signature chemokine receptor expression patterns are given in orange boxes and the typical cytokines released by these subsets are written in black. Abbreviations: Follicular T helper cell (Tfh) and regulatory T cell (Treg),

1.5. T cell migration

1.5.1. Circulation of T cells

The trafficking of T lymphocytes is crucial for all stages of their development, activation and subsequent role as effectors of adaptive immunity, described in the previous sections (Figure 1.8). Stem cell precursors of thymocytes migrate from the bone marrow to the thymus for maturation. After maturation, naïve T lymphocytes constantly move through the circulatory and lymphatic systems where they survey resident and non-resident APCs for cognate antigen (87). SLOs have high levels of the chemokines CXCL13, which attracts naïve B lymphocytes and CXCL19 and CXCL21 which attract naïve T lymphocytes. The architecture of SLOs is specifically designed to facilitate the process of antigen surveillance (17) (Figure 1.9). There are two distinct areas of antigen presentation: in B cell follicles follicular dendritic cells present antigen; in the T cell zone it is dendritic cells originating from the bone marrow that are the primary APCs. Dendritic cells can circulate throughout the body, migrating through SLOs, or remain resident in SLOs (88). Naïve T lymphocytes first enter SLOs through high endothelial venules (HEVs) and then move into the T zone to survey antigen. If antigen is presented to cognate TCR on the T cells then they become activated in the manner described in the sections above. These activated T lymphocytes then undergo rapid proliferation by a process termed clonal expansion. A small number of T lymphocytes remain the SLO and aid B lymphocyte activation, proliferation and differentiation in germinal centres (GCs). Activated T lymphocytes down-regulate surface expression of the adhesion molecule CD62L and sphingosine-1-phosphate receptor 1 ($S1P_1$), this allows their egress back into the vasculature (14). Up-regulation of chemokine receptors specific for ligand expressed by peripheral tissues allows the final migration into infected tissues. After resolution of inflammation the memory cells generated migrate either into the blood (effector memory) or to Spleen and SLOs (central memory) (89).

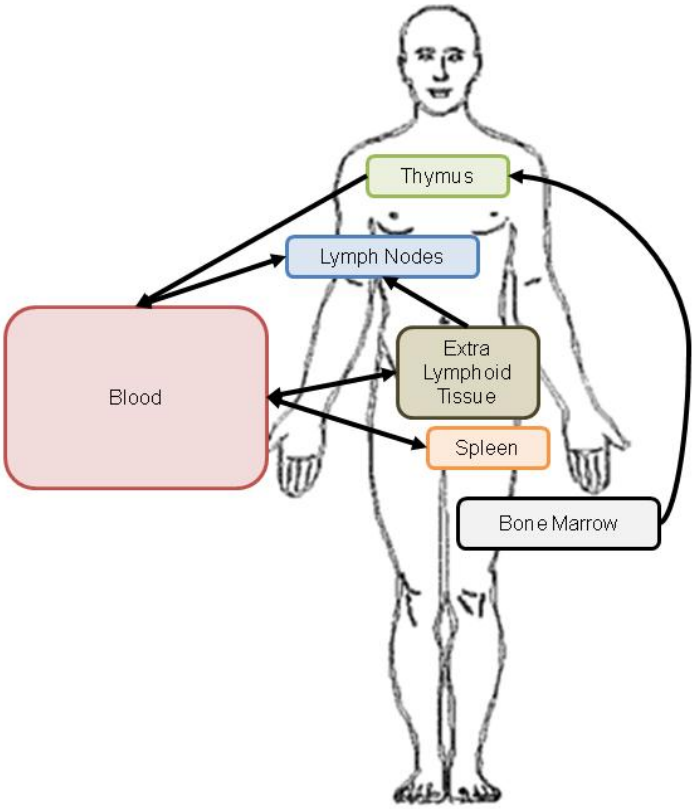

Figure 1.8: Circulation of T cells. T lymphocyte precursors are produced by haematopoiesis in the bone marrow and migrate to the thymus, where they mature from thymocytes into naïve T lymphocytes. Naïve T lymphocytes enter the blood and circulate through secondary lymphoid organs such as the spleen and lymph nodes, as well as extra lymphoid tissue including Peyer's patches. Naïve T lymphocytes survey for APCs with cognate antigen to allow their activation and subsequent migration to the periphery.

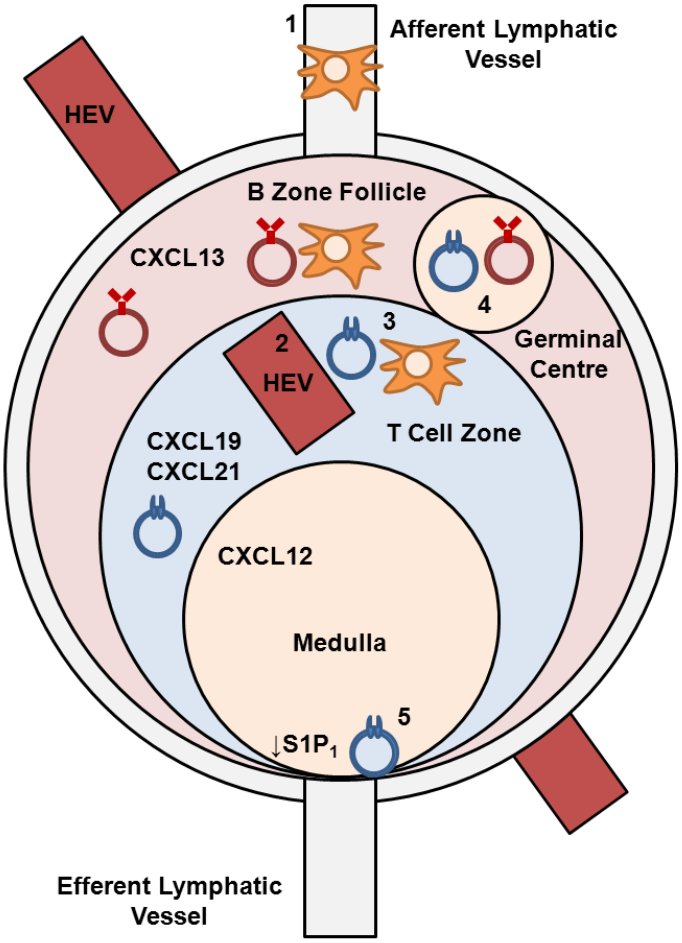

Figure 1.9: Architecture of secondary lymphoid organs. 1. Dendritic cells drain into SLOs through the afferent lymphatic vessel. These cells migrate into the T cell zone where naïve T lymphocytes enter through the HEVs (**2**). **3.** T lymphocytes become activated following antigen presentation and co-stimulation by dendritic cells. **4.** A number of T lymphocytes enter specialised GCs where they aid the activation, proliferation and differentiation of B lymphocytes. **5.** Activated T lymphocytes down-regulate CD62L and S1P1 to allow their egress through the medulla into circulation.

1.5.2. Trans Endothelial Migration (TEM)

Leukocytes are highly motile cells which can infiltrate into tissues; this is crucial to both the innate and adaptive immune response. However, un-restrained cell migration can contribute heavily to inflammatory and autoimmune diseases; therefore, the signalling mechanisms which underpin this process have been explored in great detail with therapeutic intervention in mind.

Entry of naïve lymphocytes into SLOs requires the key migratory processes termed “capture and roll” and TEM. These processes are delicately orchestrated by chemokines, integrins and other adhesion molecules (Figure 1.10). Molecules with chemo-attractant properties can be expressed on the surface of cells, such as on the epithelium and endothelium, or secreted from cells. Leukocytes moving rapidly through blood vessels often come into contact with the endothelial wall under shear flow. Contact allows adhesion molecules to bind to their ligands. For example CD62L binds to its ligands which include peripheral node addressin (PNAD) which is a group of glycoproteins including CD34 (90) and glycosylation dependent cell adhesion molecule 1 (Glycam-1) (91), as well as mucosal vascular addressin cell adhesion molecule 1 (MAdCAM-1) (91). This rolling causes chemokine receptors such as CCR7 (highly expressed on naive $CD4^+$ T lymphocytes) to become activated by their cognate ligands expressed on the HEV (CCL21 for CCR7 (92)). Activation allows binding of leukocyte function-associated antigen 1 (LFA-1) to intracellular adhesion molecule 1 (ICAM1) bringing about firm arrest of cells on the endothelium. Cells spread out and crawl across the endothelium searching for routes to cross the endothelial cell layer.

During crawling, a cell will form a polarised morphology with a leading edge moving towards the source of chemokine and a trailing end termed the uropod. This allows reorganisation of the MTOC, as in formation of the immune synapse, and the mitochondria. In addition there is an organised distribution of signalling molecules within the cell, which occurs through mechanisms including plasma membrane lipid metabolism. This is achieved, in part, by the formation of a network of actin filaments at the leading edge of the cell which is driven by a signalling pathway which includes a number of Rho GTPases. Briefly, the guanine-nucleotide-exchange factors (GEFs) DOCK2 and Tiam1 as well as Cdc42

activate Rac1. PIP_3 accumulation catalysed by PI3K at the leading edge of cells and PTEN accumulation at the uropod is observed early on in cell migration (93, 94). PI3K is indispensable for most leukocyte migration, but, for T lymphocytes it is only require for migration during a naïve and not activated state (95). The recruitment of Akt facilitates F-actin organisation through Rac1. Rac1, along with RhoA and the GEF Vav1, is also responsible for activation of LFA-1 through inside-out signalling (96). Activation of LFA-1 allows its interaction with ICAM-1 and facilitates firm adhesion of cells to the endothelium. Finally cells cross the endothelium by transendothelial migration through a para or transcellular route, the former being the most common (97).

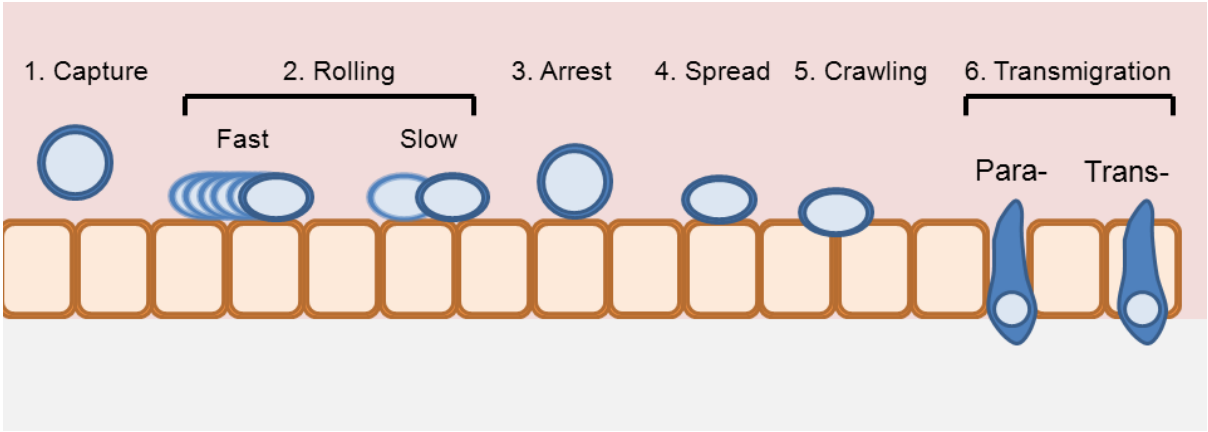

	Capture	Rolling	Arrest	Spread	Crawling	TEM
Adhesion	Selectins e.g CD62L	Selectins e.g CD62L				PCAM1
Signalling		Chemokines		PI3K Src VAV GEFs		
Integrin	VLA-4		LFA-1 VLA-4 $A_4\beta_7$-integrin		MAC1	
Junctional						JAMs

Figure 1.10: Transendothelial migration of leukocytes. Leukocytes circulate through the blood under shear stress. **1.** Selectins such as CD62L bind ligands expressed on endothelial cells and are captured onto the vessel wall. **2.** Leukocytes then begin to slowly roll across the endothelial cells which express further selectin ligands as well as chemokines. This activates the leukocytes and causes up-regulation of integrins on the surface. **3.** These integrins LFA-1 and VLA-4 interact with the endothelial ligands ICAM-1 and VCAM-1 respectively. **4-5** Intracellular signalling mechanisms facilitate the spread and crawling of leukocytes across the endothelium. **6.** Leukocytes finally cross the endothelium through either para- or trans-cellular routes, involving interaction between endothelial junction proteins or cytoskeleton respectively.

1.5.3. CD62L

As described above in section 1.2.1, CD62L, along with CCR7, expressed on naive $CD4^+$ T lymphocytes have essential roles in homing of cells to and entry into SLOs. This is underscored by observations from the CD62L knockout mouse, which shows impaired rolling and homing of leukocytes (98–100). Consequently these mice show altered humoral immune responses (101), reduced skin allograft rejection (102) and impaired responses to inflammatory stimuli (99, 100). The inability of leukocytes to migrate via HEVs results in almost complete loss of leukocytes from the peripheral SLOs, and an increase in the number of these cells in the spleen (100).

Use of an antibody (MEL-4), which blocked leukocyte adherence to HEV (103) led to the identification and cloning of mouse and human CD62L (104, 105); CD62L has since been cloned from a number of other organisms (106). The gene SELL on chromosome 1q23-q25 encodes the 372 amino acid protein CD62L; this is transcribed and translated into a protein of predicted molecular weight 42.19 KDa. Once trafficked to and expressed on the cell surface, CD62L can undergo extensive post-translational modification. As a consequence, when analysed by western blotting, the leukemic T cell line Jurkat showed CD62L banding of ~72 KDa under non-reducing and 80 KDa under reducing conditions (107). Human lymphocytes isolated from serum show CD62L to be 74 kDa in size (108). In contrast, human neutrophils express a 70-120 KDa CD62L protein (107, 108). CD62L contains several structural domains with homology to other protein domains including: a low affinity IgE receptor like (C-lectin) domain, epidermal growth factor (EGF) like domain, two tandem short consensus repeats (SCRs), a trans-membrane domain and an intracellular portion (104) (Figure 1.11).

1.5.4. Mechanisms of CD62L down-regulation

Upon T lymphocyte activation levels of cell surface CD62L are down-regulated (109). T lymphocyte activation by antibodies against CD3 cause loss of surface CD62L expression; the cytokine IL-2 also causes CD62L loss (109, 110). Mitogens such as phytohaemagglutinin (PHA) (109) as well as polysaccharides (111), antibody (IgE) (112), peptide hormone (113), and phorbol 12-myristate 13-acetate (PMA) can also cause CD62L down-regulation. CD62L down-regulation

occurs via direct cleavage of CD62L from the cell surface and the silencing of CD62L gene expression (114, 115). The signalling mechanism regulating these processes involves serine/threonine kinases and these will be discussed in this section (Figure 1.13).

The cleavage of CD62L from leukocytes was shown to be matrix metalloproteinase (MMP) dependent (116, 117) and the “sheddase” responsible for this, tumour necrosis factor-α converting enzyme (TACE/ADAM17), was first cloned in 1997 (118–120). A disintegrin and metalloproteinases (ADAMs) are a group of membrane bound proteins which possess a disintegrin-like domain (Figure 1.11) which can be involved in cell adhesion and a metalloproteinase domain which can cleave a variety of substrates shown in Figure 1.12. ADAM17 is the principle “sheddase” for CD62L; however, there is conflicting evidence that suggests ADAM10 may have an overlapping role in this process (121–124). ADAM protein is produced by the endoplasmic reticulum and inactive ADAM is trafficked to the cell surface where it becomes activated. A number of ADAMS including ADAM17 possess a motif which binds Zinc through cysteine thiol groups, when this is disrupted, for instance by ROS, Zinc binding ADAMs become activated (125). A number of signals can either influence ADAM trafficking or initiate their activation at the cell surface leading to processing of their substrates. Down-regulation of ADAM10/17 substrates by PMA is largely dependent on ADAM17 (122, 126). Increases in intracellular calcium can induce ADAM10 activity and calcium ionophores such as Ionomycin cause substrate processing (122, 126, 127). Observations that PMA causes rapid and significant CD62L down-regulation from leukocytes led to the investigation of PKC as a mediator of CD62L loss. Indeed, PKC regulates CD62L down-regulation (111, 128) through direct phosphorylation of ADAM17 (129). The mitogen activated protein kinase (MAPK) p38 can also phosphorylate threonine residues in ADAM17 in response to the poison cantharidin (130). Activation of p38 results in increased ADAM17 protein at the cell surface, the MAPK Erk1/2 also increases ADAM17 trafficking though threonine phosphorylation (131, 132). Inhibition of MAPK activity with the MEK-1 inhibitor PD98059 causes inhibition of CD62L loss in mouse T lymphocytes following treatment with antibody against CD3 (114).

The same study by Sinclair et al. also highlighted important roles for the PI3K/mTOR pathway in CD62L down-regulation following $CD4^+$ and $CD8^+$ T lymphocyte activation by antibody, TCR peptide and cytokines (114). Using transgenic mouse $CD8^+$ T lymphocytes which all recognise the peptide gp33-41, it was shown that CD62L down-regulation in response to TCR stimulation is Erk1/2 dependent; whereas, IL-2 mediated CD62L loss is mTOR mediated. PI3K, specifically the p110δ catalytic subunit, is required for both TCR and IL-2 induced CD62L down-regulation. The lipid phosphatase PTEN negatively regulates PI3K signalling, loss of PTEN decreases, and gain of PTEN increases, cell surface CD62L expression (114, 133). As mentioned previously, Akt acts down-stream of PI3K, is regulated by mTOR and phosphorylates a broad range of substrates involved in migration and cell survival. Akt substrates include members of the transcription factor forkhead box subfamily O (FOXO). FOXO1 exists in an active state within the nucleus of naïve T lymphocytes and promotes CD62L expression through the transcription factor KLF2 (133–135). FOXO1 can be phosphorylated by activated Akt and this causes its re-localisation to the cytosol (136). Thus activation of the PI3K/mTOR signalling pathway can switch off transcription of CD62L as well as other KFL2 regulated genes, importantly CCR7 and $S1P_1$ (115). It has therefore been suggested, that the immunosuppressant actions of Rapamycin may be, in part, due to maintained KLF2 mediated gene expression and retention of naïve T lymphocytes in SLOs (114, 137).

Patients with acute myeloid leukaemia (AML) and B cell chronic lymphoid leukaemia (B-CLL) show increased soluble CD62L (sCD62L) in their serum (138, 139). sCD62L retains ligand binding function and can prevent the binding of lymphocytes to endothelial cells (108). Myeloid-Derived Suppressor Cells (MDSCs) play a key role in suppressing the immune response to cancer. Immuno-surveillance for tumours requires T lymphocyte homing as described above and MDSCs may interrupt this by causing down-regulation of CD62L on T lymphocytes (140). Primed anti-tumour antigen T cells expressing CD62L and CCR7 are a possible immunotherapy for tumours (141); in contrast the down-regulation of CD62L from the surface of anti-tumour antigen T cells was observed to be required for tumour lytic activity (142).

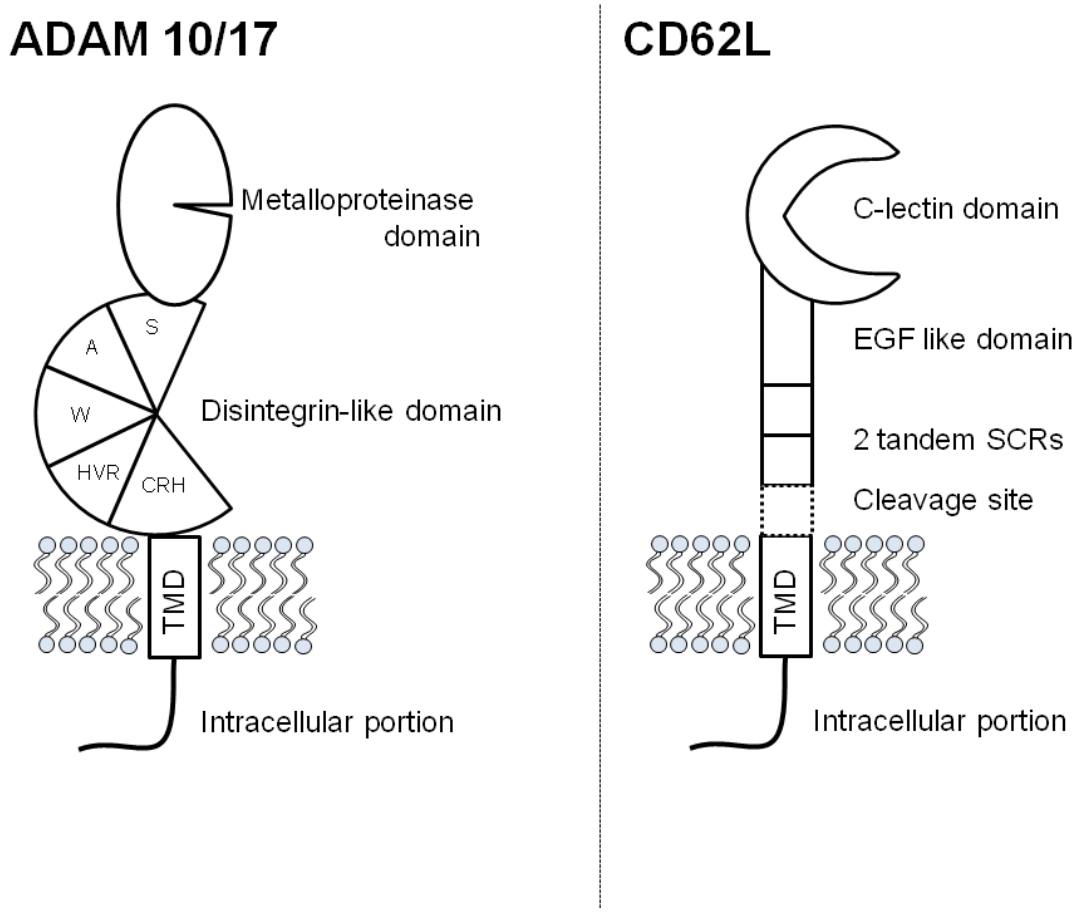

Figure 1.11: Structure of ADAMs 10/17 and their substrate CD62L. Both ADAM10/17 and their substrate CD62L are membrane bound proteins with trans-membrane domains (TMDs) and short intracellular portions. ADAM 10 and 17 both possess the same basic tertiary structure (498). A metalloproteinase domain is responsible for the cleavage of substrates such as CD62L, which has a cleavage site proximal to its TMD. ADAM10 and 17 possess a disintegrin-like domain (DLD) which has shoulder (S) and arm (A) portions, a wrist domain (W), a hyper variable region (HVR) which may be important for substrate binding and a cysteine rich hand (CRH) which is shorter in ADAM10 and 17 compared to other ADAMs. ADAM10 and 17 also do not have calcium binding sites found in the DLD of other ADAMs and have an increased number of disulphide bonds. CD62L has a C-lectin domain which is responsible for substrate binding, an EGF like domain which has calcium binding properties and 2 SCRs, which are also possessed by complement proteins.

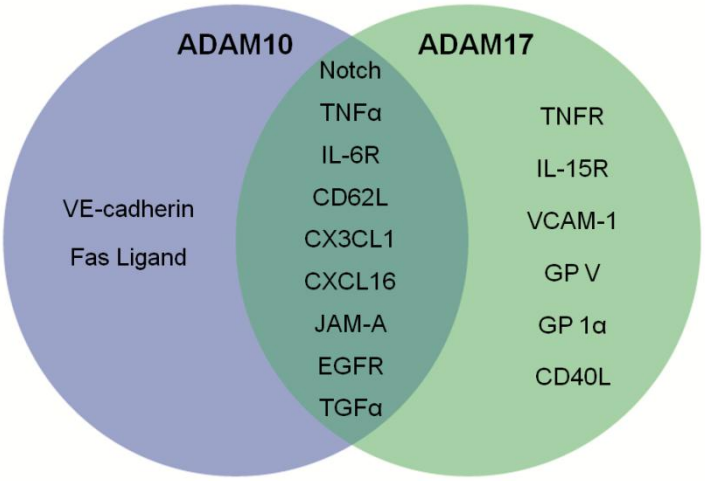

Figure 1.12: Substrate specificity of ADAM10 and ADAM17. Venn diagram displaying the substrates specific for ADAM10 or ADAM17 and the substrates for which both ADAMs can process.

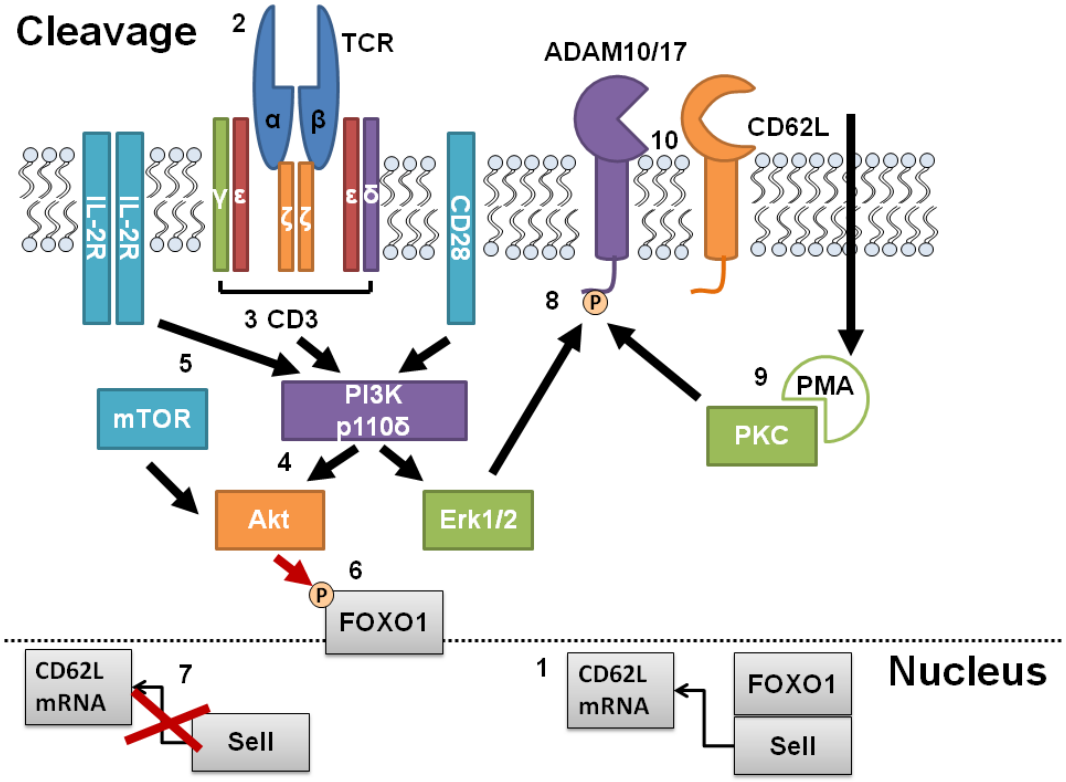

Figure 1.13: Mechanisms of CD62L down-regulation following T lymphocyte activation through TCR or PMA. 1. Under resting conditions, the transcription factor FOXO1 promotes the transcription of the gene Sell to produce CD62L mRNA in naïve T lymphocytes. **2.** Upon activation of the T lymphocytes, or antibody induced activation of CD3, the p110δ isoform of PI3K is activated (**3**). **4.** PI3K along with mTOR, which is activated down-stream of the IL-2 receptor (**5**), activate Akt. **6.** Akt phosphorylates FOXO1 promoting its removal from the nucleus which turns off transcription of CD62L mRNA (**7**). **8.** p110δ can also activate the Erk1/2 signalling pathway, Erk1/2 phosphorylate ADAM17 facilitating its trafficking to the cell surface. **9.** PMA, which activates PKC, also promotes this trafficking. **10.** Activated ADAM10 and 17 cleave cell surface CD62L

1.6. Requirement for cytosolic ATP and calcium in T cell activation

As mentioned previously, activation of some signalling molecules including PKC and the transcription factor NFAT require large increases in the concentration of free intracellular calcium. The phosphorylation of substrates by kinases requires the hydrolysis of ATP and this high energy requirement must be maintained during T cell activation (143). The mechanisms of calcium release by intracellular stores and influx through ion channels and the generation of ATP by respiration will be discussed in this section.

1.6.1. Calcium

As previously mentioned, the activation of the TCR signalling complex causes the hydrolysis of $PI[4,5]P_2$ by PLCγ to DAG and $IP[1,4,5]P_3$. The receptor for $IP[1,4,5]P_3$, IP_3R, is expressed as a tetramer on the surface of the endoplasmic reticulum (ER) (144). Multiple molecules of $IP[1,4,5]P_3$ bind to these receptors which open to release Ca^{2+} from the ER (Figure 1.3). Store operated calcium release is rapid but transient, whereas T cell activation requires a sustained intracellular Ca^{2+} increase for several hours (145–147). Early electrophysiological evidence revealed an inward current in response to T cell activation and this current was dependent on the rise in intracellular Ca^{2+} from ER release (148). Thapsigargin, which blocks sarco/endoplasmic reticulum Ca^{2+}-ATPase (SERCA) resulting in rapid store Ca^{2+} depletion, causes activation of this inward current. The inward current was attributed to the calcium release activated channel (CRAC) which has now been shown to comprise a membrane channel (ORAI) and stromal interaction molecules (STIM) that are calcium sensors expressed on the ER (149–154). Sustained Ca^{2+} influx activates calcineurin which dephosphorylates NFAT, this allows NFAT translocation to the nucleus where it promotes transcription of IL-2, IL-4 and INF-γ (146) (Figure 1.3).

1.6.2. ATP and the mitochondria

Hydrolysis of ATP to ADP and the transfer of a phosphate group to substrates is the basis for the enzymatic action of kinases and an important post-translational modification of substrates. This process of phosphorylation controls protein activation and localisation. ATP is produced by a complex series of biochemical

processes which occur first in the cytosol and then in a specialised organelle called the mitochondria; these processes will now be briefly described. Glucose is the initial input into a process called glycolysis which ends in the oxidation of pyruvate to Acetyl-CoA; this enters the citric acid cycle. Both processes provide NADPH and ADP as substrates to the electron transport chain where oxidative phosphorylation produces ATP (155). These processes are heavily regulated and respond to the energy demands of the cell (143).

Current evolutionary theory describes the mitochondria as a simple prokaryotic organism which may have fused with the cells of simple eukaryotic organisms (156). This produced a symbiotic relationship whereby the mitochondria received nutrients within the eukaryotic cell and the growing need for energy within the eukaryotic cell was met by the production of ATP by the mitochondria. This theory is supported by the observation that mitochondria have genomic DNA distinct to that of the nucleic DNA of the cells in which they reside (157). Mitochondria have a double membrane structure with multiple folds within the inner membrane. Expressed in the membrane are components of the mitochondrial electron transport chain which is responsible for the final process of respiration that produces ATP. This chain consists of five complexes: NADH dehydrogenase (complex I), succinate dehydrogenase (II), cytochrome b-c1 (III), cytochrome c oxidase (IV) and ATP synthase (V). These complexes serve to facilitate the passage of electrons while pumping hydrogen ions into the mitochondrial inter-membrane space. This creates a proton gradient which allows complex V to pump hydrogen ions back into the mitochondrial matrix, a process which drives ATP synthesis (Figure 1.14).

During normal ATP synthesis a small number of electrons may leak out from these complexes and, through their reactivity with H_2O in the matrix, form a number of ROS (158–160). In pathological conditions where the mitochondrial DNA (mtDNA) becomes damaged these complexes may leak a greater number of electrons and mitochondrial ROS can noticeably increase. This results in a phenomenon where further damage to mtDNA and increased ROS generation occur in a cyclical manner; increased mitochondrial ROS can lead to cell death through apoptosis (161–164). A number of diseases exist where mtDNA is damaged or mitochondrial

ROS is increased, for example: TNFR1-associated periodic syndrome (TRAPS) Huntingdon's Disease (165, 166).

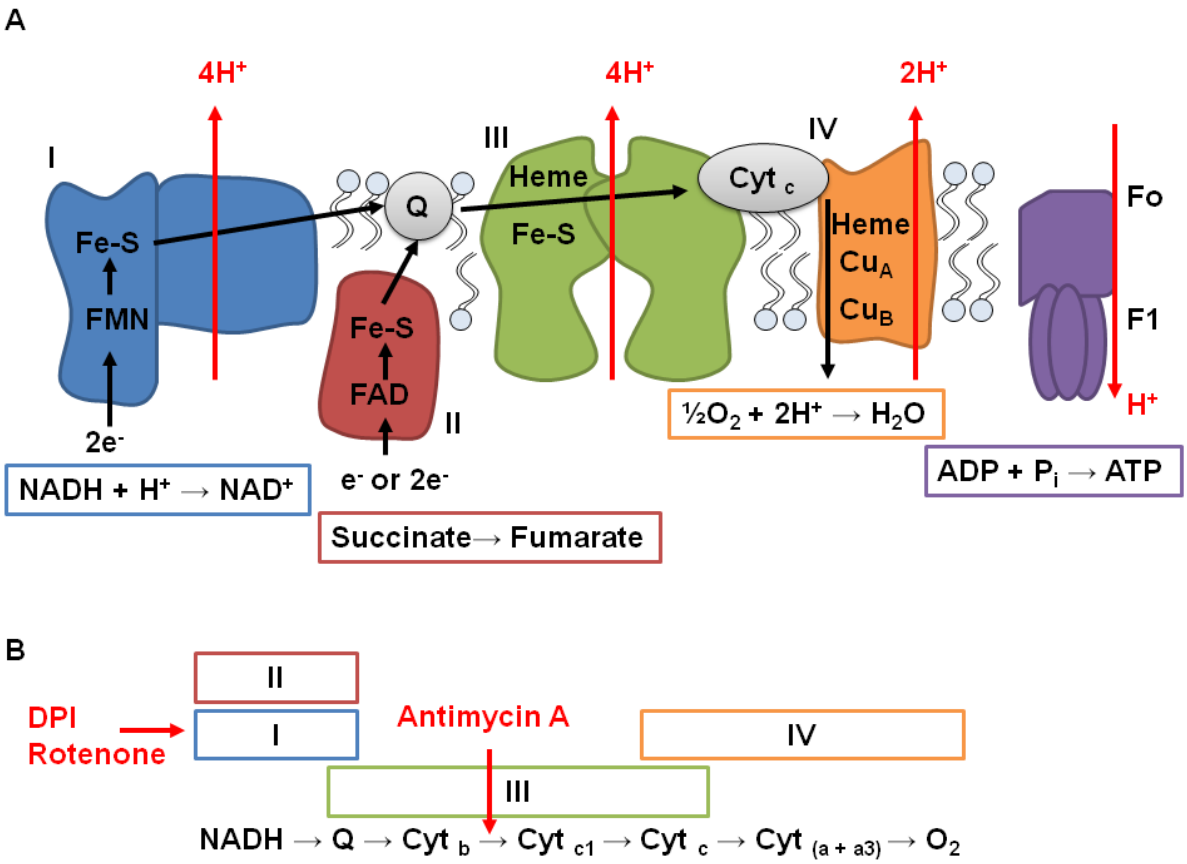

Figure 1.14: The complexes of the mitochondrial electron transport chain. A. The electron donors NADH and Succinate pass electrons through flavin and iron based electron carriers in complex I and II to Quinone (Q) in the mitochondrial membrane. Q shuttles electrons to complex III which is a dimer of subunits containing heme and iron electron carriers. Electrons are passed from complex III to complex IV by soluble cytochrome c in the membrane. Heme and copper carriers in complex VI are the final carrier through which the electrons are passed to oxygen to form water. These reactions allow the passage of protons out of the mitochondrial matrix by complexes I, III and VI. This creates a proton gradient which allows complex V (FoF1) to form ATP from ADP and organic phosphate (Pi). **B.** The basic path of electrons from NADH to O_2 is given with the complexes that facilitate this passage. Agents which uncouple this pathway: DPI, Rotenone and Antimycin A are shown at the complexes which they target.

1.7. Purinergic receptors

1.7.1. P1 and P2 family in inflammation

While investigating novel neurotransmitters, Geoffrey Burnstock discovered that ATP could act as a neurotransmitter, this observation was contrary to opinions held at the time (167). ATP can be released from cells in an autocrine or pancrine manner and is released from dying cells. ATP can be rapidly hydrolysed to adenosine monophosphate (AMP) by cell surface ectonucleoside triphosphate diphosphohydrolase-1 (ENTPD1/CD39) (168, 169) this can be further hydrolysed to adenosine by ecto-5′-nucleotidases such as CD73 (170). CD39 is expressed on cells of the immune system, and in combination with CD73 is important for the function of Treg cells (171, 172). ATP and its metabolites: adenosine diphosphate (ADP), AMP and adenosine, as well as the Uridine based molecules Uridine triphosphate (UTP) and Uridine diphosphate (UDP), stimulate the activation of a class of receptors termed purinergic receptors (Table 1.2).

The P1 adenosine receptor family consists of the A1, A2a, A2b and A3 receptors which are all activated endogenously by adenosine. P1 receptors are GPCRs, the A2a and A2b receptors couple to stimulatory Gs α subunits whereas the A1 and A3 receptors couple to inhibitory Gi/o α subunits (Figure 1.15). The P2 receptor family is subdivided into the P2Y GPCRs and P2X ligand gated ion channels. There are multiple P2Y GPCRs with broad tissue and cellular expression patterns which couple to either: Gs, Gi/o or Gq11 α subunits. The majority of P2Y receptors couple to Gq11 α subunits to activate PLCγ and bring about an increase in intracellular calcium through ER Ca^{2+} release. P2Y receptors respond to a wide variety of purine nucleotides including: ADP, ATP, UDP, UTP and UDP-glucose with differing sensitivities (Table 1.2). P2XRs are a family of 7 ion channels which share sequence homology and all are activated endogenously by ATP. Using electrophysiology a distinct fingerprint for each channel can be elucidated which are shown in Table 1.2. While ATP is the endogenous ligand for P2X receptors, a number of synthetic agonists have been developed as tools to investigate the pharmacology and function of these receptors (Figure 1.16).

	Agonists	Selective Agonists	Selective Antagonists	Tissue Distribution	Signalling
P1 Receptors					
A_1	Adenosine	CPA, CCPA, S-ENBA, GR79236	DPCPX	Nervous system, Cardiac tissue	Gi/o
A_{2A}	Adenosine	CGS21680, HENECA, ATL-146e	ZM241385, SCH58261	Immune cells, Nervous system, Vasculature, Platelets	Gs
A_{2B}	Adenosine	Bay60-6583	MRS1754, MRS1706, PSB1115	Vasculature	Gs
A_3	Adenosine	2-Cl-IB-MECA, IB-MECA	MRS1220, VUF5574, MRS1523, MRS1191	Nervous system, Cardiac tissue, Mast cells	Gi/o
P2Y Receptors					
$P2Y_1$	ADP>ATP	2-MeSADP, ADPβS, MRS2365	MRS2500, MRS2279, MRS2179, PIT	Brain, vascular endothelia, platelets	Gq/11
$P2Y_2$	UTP=ATP	UTPγS, Ap4A		Epithelial cells, endothelial smooth muscle	Gq/11
$P2Y_4$	UTP>ATP	UTPγS	ATP	Placenta	Gq/11
$P2Y_6$	UDP>>UTP >ATP	UDP, 2-phenacylUDP	MRS2578	Spleen, smooth muscle, airway epithelia	Gq/11
$P2Y_{11}$	ATP>UTP	ARC67085, NAD+, NAADP+		Spleen, granulocytes	Gs, Gq/11
$P2Y_{12}$	ADP>>ATP	ADP, 2-MeSADP	ATP, ARL66096	Glial cells, spinal cord, platelets	Gi/o
$P2Y_{13}$	ADP>>ATP		MRS2211	Spleen, brain, lymph nodes, bone marrow	Gi/o
$P2Y_{14}$	UDP-glucose	MRS2690			Gq/11

P2X Receptors					
$P2X_1$	ATP	L-βγ-meATP, αβ-meATP	TNP-ATP, Ip5I, NF023, NF449	Smooth muscle, platelets	
$P2X_2$	ATP			Sensory neurones, brain, pancreas	
$P2X_3$	ATP	αβ-meATP	TNP-ATP, A317491, RO3	Nociceptive sensory neurones	
$P2X_4$	ATP			Brain, testis, colon	
$P2X_5$	ATP			Heart, adrenal medulla	
$P2X_6$	ATP			Brain	
$P2X_7$	ATP		KN62, KN04, A-438079, A-740003, AZ11645373, AZ10606120, CE-224,535, AZD9056	Macrophages, mast cells, microglia, T and B lymphocytes	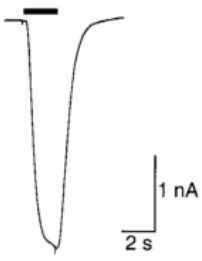

Table 1.2: The purinergic receptor family

The endogenous agonists, selective agonists, antagonists, tissue distribution and function of the purinergic receptor family are given. The signalling pathways which P1 and P2Y receptors couple to are highlighted. For P2X receptors example traces of rat P2X7R expressed in HEK293 cells are reproduced. Cells treated with 0.03 (P2X1-4,6) or 1 mM (P2X7) the black bar above each current represents ATP treatment (173).

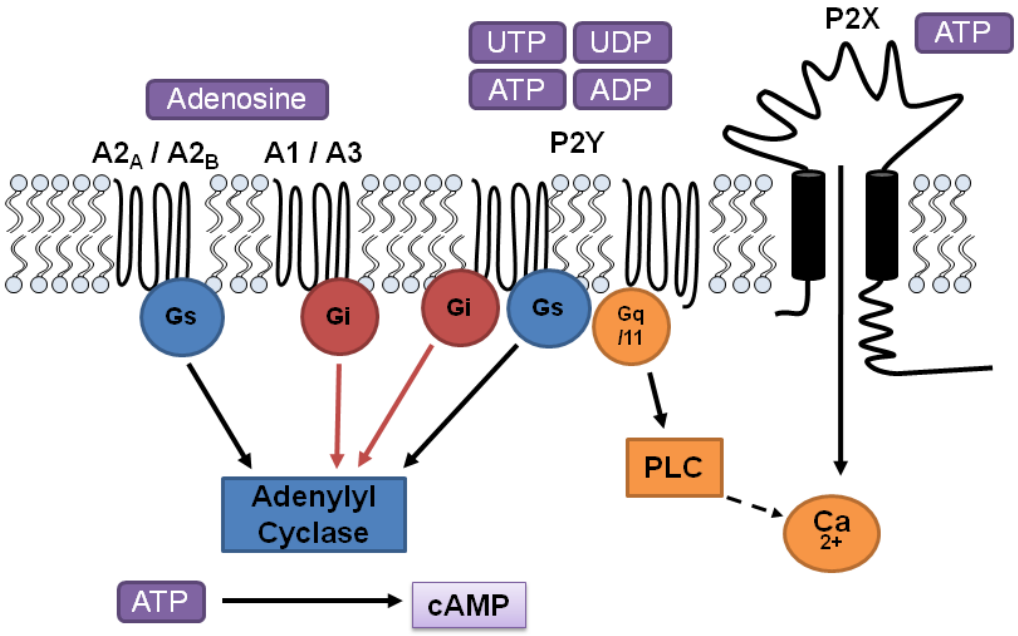

Figure: 1.15: The purinergic receptor family. P1 adenosine receptors are GPCRs activated by adenosine which couple to either Gs (A2A and A2B) or Gi (A1 and A3) subunits. Gs coupled receptors stimulate the activation of adenylyl cyclase which forms cAMP from ATP; whereas, Gi coupled receptors inhibit this process (red arrows). P2Y receptors are also GPCRs which are activated by a number of adenine and uracil based nucleotides to couple to Gs, Gi or Gq11 subunits. The Gq11 subunit promotes calcium release from intracellular stores via PLC activation. P2X receptors are activated by ATP and act as cation channels raising levels of intracellular calcium and sodium, as well as effluxing potassium ions.

1.7.2. Expression of Purinergic receptors by cells of the immune system

A1 receptors are not expressed by T lymphocytes; both A2a and A2b receptors are expressed and may have roles in activation (174, 175). A3 receptors are expressed at low levels on resting T lymphocytes but up-regulated upon activation with PHA (176) and are expressed by the leukemic T cell line Jurkat (177). Tregs express high levels of CD39 and CD73 on their cell surface and, therefore, have the potential to hydrolyse ATP and then AMP to generate large amounts of adenosine (170, 172). This adenosine can act upon Tregs in an autocrine manner or on effector T cells in a paracrine manner. A2a receptor is broadly anti-inflammatory and is the pre-dominant adenosine receptor expressed by activated T lymphocytes. Adenosine acting on effector T lymphocytes reduces the production of pro-inflammatory cytokines and up-regulates production of the immune-suppressant IL-10 (178). $CD8^+$ CTLs express A2a and A2b receptors and adenosine inhibits FasL expression and degranulation, significantly impairing the cytotoxic response (179). Inhibition of Natural Killer cells by adenosine is an important feature to consider in the context of tumour surveillance (180). APCs, especially dendritic cells, are also influenced by adenosine. Immature dendritic cells express mostly A2b receptors but upon activation switch to an $A2a^+$ phenotype, this alters their response to adenosine. The immunosuppressive action of adenosine through A2a receptors is mediated by Gs coupled cyclic adenosine monophosphate (cAMP) generation (179, 181).

Messenger RNA (mRNA) for all P2YR is detected in leukocytes: monocytes express highest levels of P2Y2 and P2Y13 whereas lymphocytes expressed highest levels of P2Y12 (182) as well as P2Y2 (183). Little is known about the role of P2Y receptors in T lymphocyte function. Activation of P2Y12 receptors expressed by dendritic cells has the indirect effect of enhancing T lymphocyte activation (184). T lymphocytes express the fast gated P2X1 receptor which is highly sensitive to ATP, responding to low micromolar concentrations but rapidly desensitising (185). P2X4 receptors which respond to 10 -100 μM ATP with a slower current, which is enhanced by the molecule Ivermectin, are also expressed by T lymphocytes (186–188). Finally, the P2X7 receptor (P2X7R, although

originally named P2Z) is also expressed and responds to millimolar concentrations of ATP with a slow inward current (189). B lymphocytes also express these three P2X receptors as well as P2X2 (190). P2X7R is the focus of this work and its structural features, activation and the current understanding of its role in T lymphocyte function will be described in detail in the following sections.

1.7.3. P2X7R activation by ATP

Before cloning of the P2X7R, the subsequent use of molecular techniques and development of antibodies against the receptor, expression of the P2Z/P2X7R channel was explored by the ability of high millimolar concentrations ATP to induce biochemical changes in cells. Activation of P2X receptors causes a rapid increase in intracellular Ca^{2+} levels, unlike P2Y receptors this does not occur through release from intracellular stores, Ca^{2+} and Na^{+} influx and K^{+} efflux occurs through the trimeric complex (191). This has been measured through electrophysiology or using ion specific fluorescent dyes (192). ATP is the endogenous agonist of all P2X receptors as well as some P2Y receptors, a number of synthetic ligands for P2X receptors have also been developed and they are detailed in Figure 1.16.

The regions and residues of P2X receptors which contribute to ATP binding have been investigated in a number of elegant molecular experiments and most of these findings can be applied to the binding of ATP to P2X7R.The ectodomain of P2X7R is thought to be solely responsible for agonist binding, as highlighted by a study of HEK293 cells expressing rat P2X7R (rP2X7R) (193). Study of P2X2R expressed in HEK293 cells with specific residues sequentially changed to alanine revealed a number of residues in a region proximal to TMD1, which were hypothesised to be important for activation of the receptor by ATP (194). Of these, four lysine residues Lys69, Lys71, Lys188 and Lys308, could have a role in co-ordinating the binding of α and γ phosphates of ATP due to their positive charge (194). Lys193 and Lys311 are essential for binding of ATP to human P2X7R (hP2X7R) expressed in Xenopus oocytes (195); Ile67 was also identified as being required for ATP binding by rat P2X2R. A polymorphism in hP2X7R, which results in the substitution of the charged Arg307 residue of P2X7R for an uncharged glutamine, revealed that Arg307 present in the ATP binding region of P2X7R is

important for activation of the receptor (196). It was determined through studies of human P2X2/3 heterotrimers expressed in HEK293 cells, that lysine residues from adjacent receptor subunits were required for ATP binding (197). The crystal structure of a zebrafish P2X4R homotrimer confirms the close proximity of residues from two P2X4 subunits forming the putative ATP binding pocket (198). This binding pocket contains a unique ATP binding motif, comprised of highly conserved basic and polar residues, homologous to those described above (199). Comparison of the closed state and ATP-bound open state revealed important features of P2XR activation. Upon ATP binding, the subunits undergo conformational changes to open the receptor in an “iris-like” manner; this may allow entry of cations laterally into the pore (199).

An analogue of ATP 2’,3’-O-(4-benzoyl-benzoyl) ATP (BzATP) is often used to activate and study P2X7R. This is in part due to the observations that it is marginally more selective than ATP; of rat P2XRs it has only been reported to activate rP2X1R, rP2X2R and rP2X7R (185). BzATP is more potent than ATP at rP2X7R but less potent than ATP at rP2X1 and rP2X2 (185). Mouse P2X7R (mP2X7R) is also more sensitive to BzATP than ATP but this agonist difference is less significant than at rP2X7R due to differences in amino acid residues between the two species (193). BzATP is also more potent than ATP at the recombinant hP2X7R (200).

ATP is required in its deprotonated ATP^{4-} state for activation of P2X7R (201) and a number of divalent cations have been suggested to inhibit P2X7R activation through both quenching ATP^{4-} and allosteric modulation of the receptor. In dye uptake experiments, extracellular Ca^{2+} or Mg^{2+} reduce the potency of BzATP at the hP2X7R (cDNA expressed in HEK293 cells) (202). Experiments involving HEK293 cells expressing rP2X7R assessed a larger range of divalent cations and demonstrated that they inhibited P2X7R with varying potencies (203). Zinc (Zn^{2+}), which inhibits rP2X7R expressed in HEK293 cells potentiates ATP responses and inhibits BzATP responses in HEK293 cells expressing mP2X7R (203, 204). Extracellular Mg^{2+} blocks a number of P2X7R dependent processes including: ATP induced activation of PKD (205), cell shrinkage (206) (also blocked by Cu^{2+} and partially by Zn^{2+}) and CD62L (207) and CD23 shedding (208) (also blocked by Mn^{2+}, Ca^{2+} and Ba^{2+}).

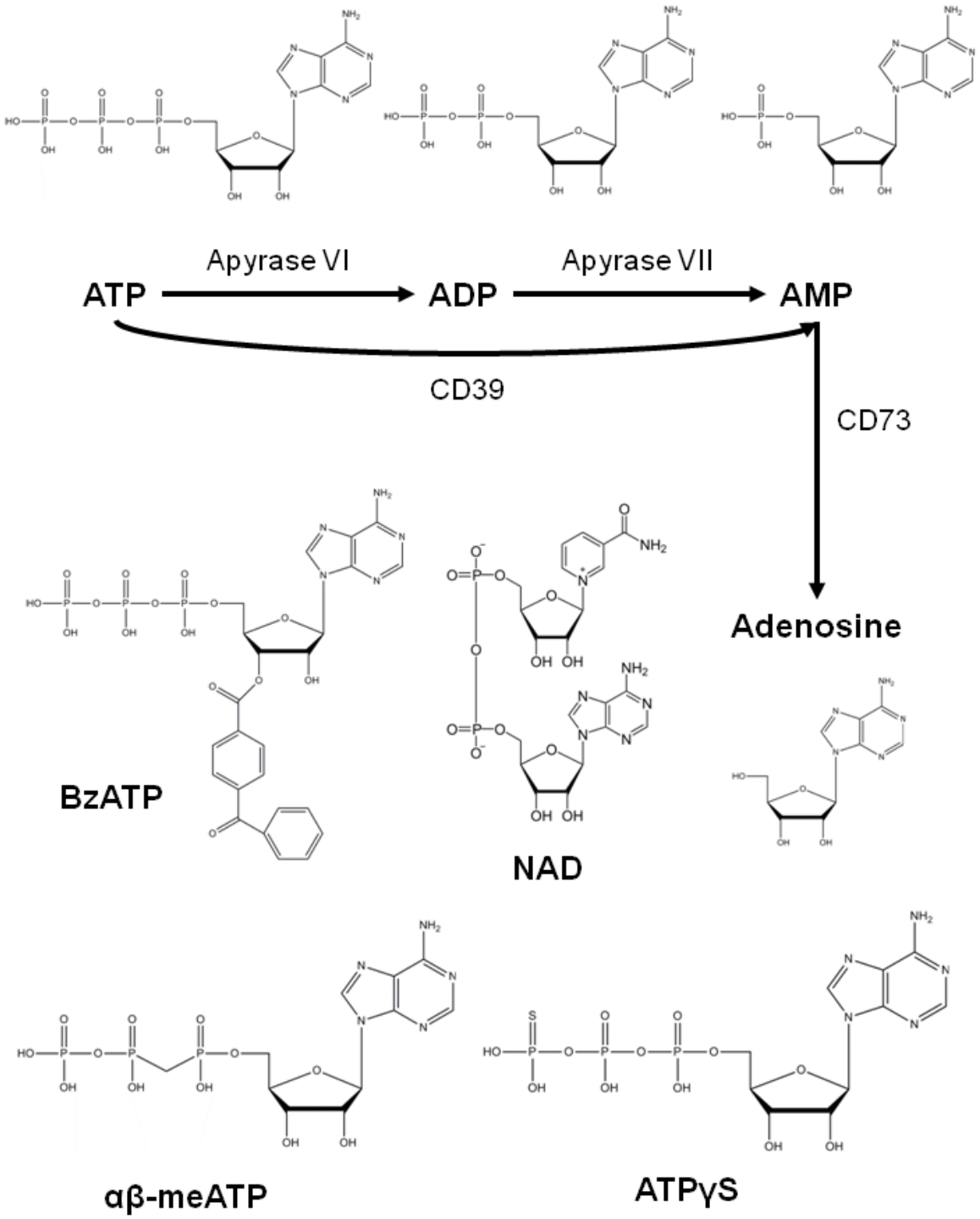

Figure 1.16: P2X agonists. ATP is the endogenous ligand of P2X receptors. Apyrases catalyse the hydrolysis of ATP: grade VI apyrase preferentially converts ATP to ADP whereas grade VII apyrase preferentially converts ADP to AMP. These are compounds extracted from potato; however, cell membrane bound ATPases are found in the body. CD39 hydrolyses ATP to AMP and CD73 further hydrolyses this to adenosine. A methyl group can be introduced into ATP between the α and β phosphates to create the synthetic ligand αβ-meATP. A sulphur atom can also be introduced to the γ phosphate to give ATPγS. 2',3'-O-(4-benzoyl-benzoyl) ATP (BzATP) is a potent agonist for P2X7 receptors but can also activate other P2X receptors. NAD is a substrate for ART2, which in mice can be used to ADP ribosylate P2X7R.

1.7.4. P2X7R antagonists

The progress of P2X7R antagonist development has been relatively slow. Periodate-oxidized 2′,3′-dialdehyde ATP (oATP) was the first P2X7R antagonist described in 1993 from its ability to prevent pore formation in response to ATP in the J774 murine macrophage cell line (209) (Figure 1.17). The actions of oATP are very slow (1-2 hour incubation required), the inhibition is irreversible and off target effects were observed soon after its synthesis (209, 210). Nevertheless, oATP was a key tool in early pre cloning experiments with P2Z/P2X7R (207, 211). Other compounds such as Suramin and PPADS are broad spectrum P2X antagonists which inhibit P2X7R activation, but at much higher concentrations than other P2XRs (185, 200). KN-62 is an isoquinoline derivative first reported for its ability to inhibit calmodulin-dependent kinase II; however, it was subsequently discovered to inhibit P2X7R (200, 212, 213). Coomassie Brilliant Blue G (BBG) was also identified as an inhibitor of the rat P2X7R (214).

Until the mid-2000s these compounds represented the core pharmacological tools for the study of P2X7R and their lack of selectivity, coupled with non-selective agonists, hampered research efforts. Pharmaceutical companies were keen to investigate P2X7R antagonism as a novel therapeutic intervention for a number of inflammatory disorders; indeed two mouse P2X7R knockout models were created by GlaxoSmithKline and Pfizer. A number of second generation, more specific and selective P2X7R inhibitors were developed by structure activity relationship (SAR) based synthesis approaches; compounds from AstraZeneca and Abbott Laboratories are excellent examples of this approach (215). The antagonists A438079 and A740003 are highly selective inhibitors developed by Abbott from series of tetrazole and cyanoguanidine derivative compounds respectively. Both are competitive P2X7R inhibitors that show superior *in vitro* potency compared to the first generation P2X7R antagonists described above and have very little effect on other P2X and P2Y receptors at concentrations up to 100 μM (216–218). These compounds also show promise for the treatment of chronic pain as they are effective in *in vivo* rat models of nociception (217, 218). AstraZeneca also identified a series of cyclic imides and a series of adamantane amides as P2X7R antagonists, using a high throughput screening (HTS) and SAR approach (219, 220); these studies led to the development of two lead compounds AZ116453743

and AZ10606120. AZ116453743 is a potent *in vitro* inhibitor of human P2X7R expressed by HEK293 cells or endogenously expressed by THP-1 monocytic cells (221). Interestingly, this compound showed species specificity, being more potent at human than rat P2X7R. Pharmacological observations suggest that this compound is most likely a non-competitive inhibitor of P2X7R (221).

A number of P2X7R antagonists have entered clinical trials, but have so far been unsuccessful in the treatment of inflammatory disorders. For example AZD9056, another AstraZeneca P2X7R antagonist, failed to show efficacy in a phase II trial for treatment of RA (222). Another trial showed that, in patients with Methotrexate insensitive RA, Pfizer's P2X7R antagonist CE-224,535 was not efficacious (223).

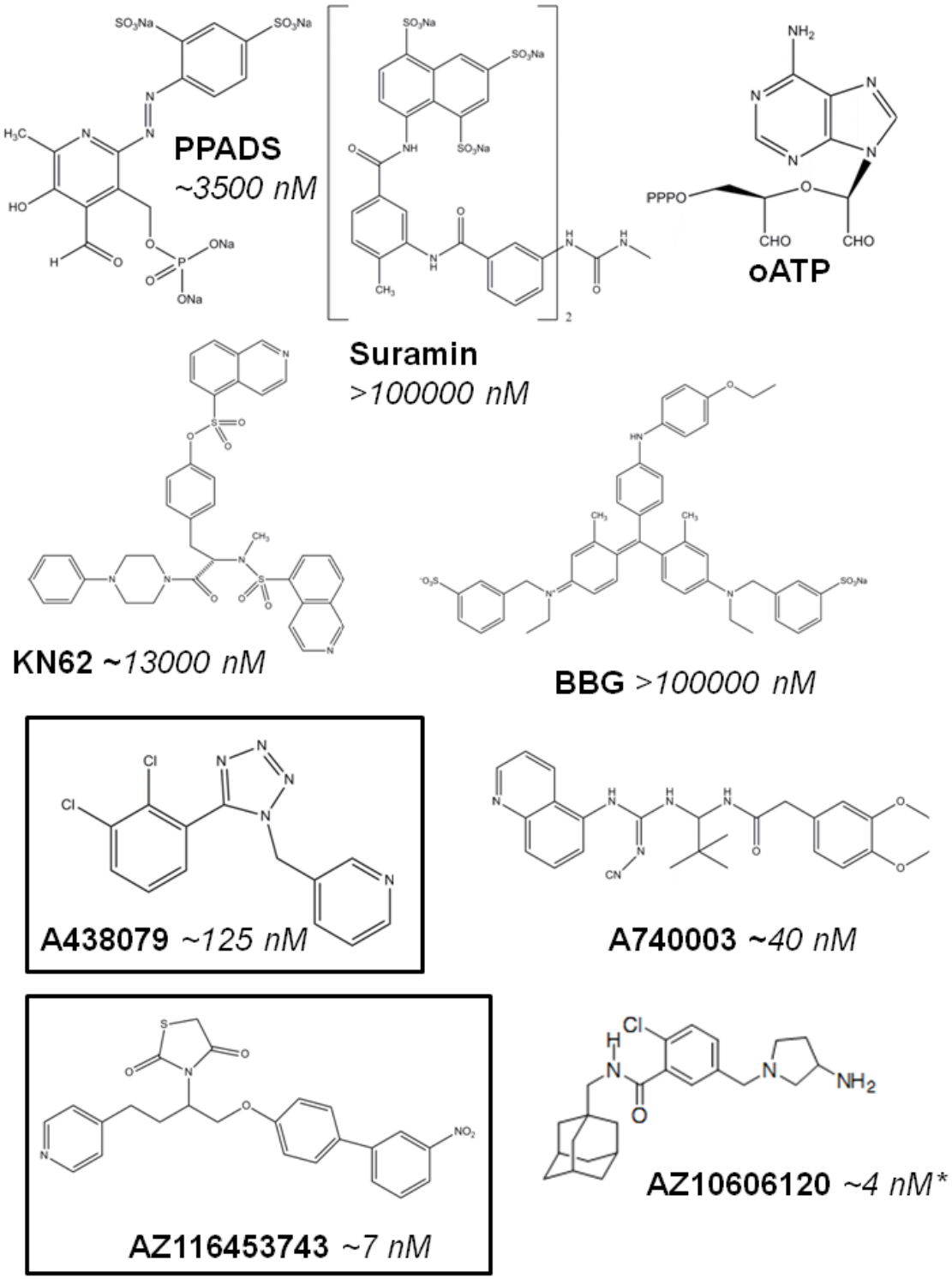

Figure 1.17: P2X antagonists. Structures for inhibitors of P2XR and P2X7R are given in this figure. The broad spectrum P2XR inhibitors PPADS and Suramin are presented alongside first generation P2X7R inhibitors oATP, KN62 and BBG. Specific P2X7R antagonists developed by Abbot Laboratories (A438079 and A740003) and AstraZeneca (AZ116453743 and AZ10606120) are also displayed. The antagonists used in this study are highlighted with a black box. IC_{50} values are presented in italics after compound names. These were calculated from pIC50 values for the inhibition of calcium influx in HEK293 cells expressing human P2X7R previously published (353).

1.7.5. P2X7R structure

cDNA for hP2X7R was first cloned in 1997 (the mouse receptor was cloned a year later (224)); it is present at 12q24.31 at the chromosomal level and the full length receptor subunit is encoded by 13 exons giving a receptor of 595 amino acids in length (189, 225). P2X7R was identified as the molecular identity for a receptor (P2Z) which responds to high, millimolar, concentrations of ATP by first opening a cationic selective channel, followed by delayed opening of a membrane associated pore (192). P2X receptor subunits form into hetero- or homo-trimeric complexes and biochemical and pharmacological approaches have been employed to determine association of P2X receptor subunits in these complexes. A number of hetero-trimeric receptor complexes have been identified including P2X1/P2X2, P2X1/P2X4, P2X1/P2X5, P2X2/P2X3, P2X2/P2X6, and P2X4/P2X6 (226–233). P2X7R was previously thought to only form homo-trimeric associations; however, recent evidence suggest that it may partner with P2X4 (234).

Until recently the tertiary structure of P2X receptors was based on low resolution crystal structures, as well as a raft of studies investigating contributions of individual and groups of amino acids to P2XR trafficking, ATP biding and their subsequent activation (235). The publication of a high resolution crystal structure of Zebrafish P2X4R (198) in a closed or open state confirmed many key features identified by molecular studies (199, 236).

P2X receptor subunits share common structure with intracellular N- and C-terminus regions, two transmembrane domains (TMD1 and TMD2) joined by a large extracellular loop region (Figure 1.18). The number of amino acids that make up each P2X receptor varies largely with P2X7R being the largest due to a long C-terminus. This C-terminus is key for a number of P2X7R functions including trafficking to the plasma membrane (237–240).

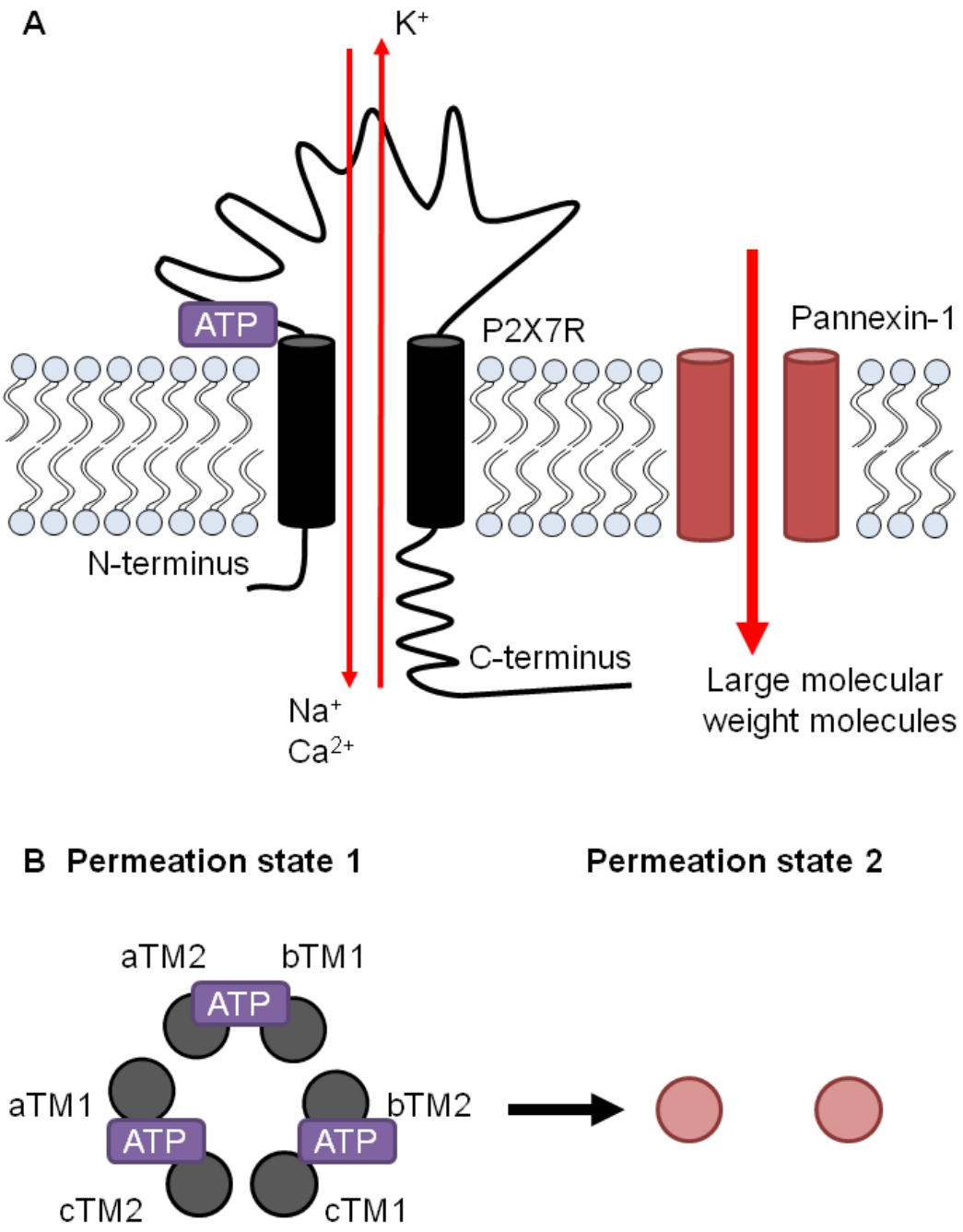

Figure 1.18: P2X7R structure and function. A. Side on view of the plasma membrane. As described briefly in Figure 1.15 P2X receptors (such as P2X7R) are activated by ATP and couple to the influx of Ca^{2+} and Na^{+} into cells and the efflux of K^{+}. **B. Top-down view of the plasma membrane.** This first permeation state can be followed by a second permeation state whereby prolonged P2X7R activation leads to the opening of a membrane associated pore. Biochemical evidence suggests this pore is the hemichannel Pannexin-1. Molecular and crystallography experiments suggest that ATP binds to a region between TM1 of one P2X subunit and TM2 of an adjacent P2X subunit. P2X7Rs have been shown to form both homotrimers and herterotrimers with P2X4Rs.

1.7.6. P2X7R expression

The use of molecular and biochemical techniques have revealed that P2X7R is expressed in almost every tissue of the rat body (241). A number of individual studies have confirmed expression in primary human cells i.e. those that have been isolated from tissues and cells of the human body without subsequent immortalisation as cell lines. The levels of P2X7R expression can differ greatly between cell types, but it is clear that cells of the immune system express high levels of P2X7R (242). However, it is unclear if neutrophils express functional cell surface P2X7R. P2X7R mRNA has been detected in human peripheral blood neutrophils and BzATP evokes a rapid transient increase in intracellular Ca^{2+} (243). However, expression of P2X7R in neutrophils could only be detected by flow cytometry after cells were permeabilised (242). One study demonstrated that in response to BzATP human neutrophils do not produce currents in patch clamp configuration, uptake ethidium bromide or generate ROS (244); neutrophils were also resistant to CD62L down-regulation induced by BzATP (245). Monocyte cell lines and primary human monocytes express high levels of P2X7R which has an important role in IL-1β processing in these cells and its subsequent release in microvesicles (246–249). Dendritic cells, Langerhans cells and Mast cells all express functional P2X7Rs (250–252). B lymphocytes also express P2X7R (242), although little is known about the physiological role of the receptor in these cells. Expression of P2X7R is increased in B lymphocytes from patients with B-CLL (253) and may provide a marker of evolutive (advanced) B-CLL (254).

Even before the cloning of human P2X7R, a receptor for high millimolar concentrations of ATP was detected in murine T lymphocytes (191). Since then, the expression of P2X7R has been detected in mixed populations of T lymphocytes as well as T lymphocyte subsets (242). Thymocytes express P2X7R where it has an important role in cellular death (206, 255–258). Splenocytes also express P2X7R, with splenic T lymphocytes expressing higher levels than splenic B lymphocytes (206). Naïve $CD4^+$ and $CD8^+$ T lymphocytes from mice express P2X7R (259, 260). Human peripheral $CD4^+$ and $CD8^+$ T lymphocytes express P2X7R mRNA (245, 261) and protein expression in $CD4^+$ cells has been confirmed by fluorescence microscopy (261). Although $CD8^+$ T lymphocytes express P2X7R, in mice the expression of P2X7R by $CD8^+$ cells was restricted to

intraepithelial cells (262). $CD8^+$ T lymphocytes from the spleen expressed very low levels of P2X7R, but its expression could be up-regulated by retinoic acid (262). In mouse studies it was apparent that $CD4^+/CD25^+$ Tregs expressed high levels of P2X7R (263). This subpopulation of cells were more sensitive to the effects of ATP than $CD4^+/CD25^-$ cells and a role for P2X7R in apoptosis of Tregs was revealed (259, 263–266).

1.8. P2X7R function in cells of the immune system

The actions of P2X7R and its endogenous ligand ATP have been investigated in the context of T and B lymphocyte mediated immunity. It has roles in different cell subsets, from thymocytes where it appears to have a role in cell death, naïve T lymphocytes where it may aid activation, through to differentiated subsets such as Tregs.

1.8.1. Proliferation

The observations that B lymphocytes from patients with B-CLL express high levels of P2X7R and that transfection of P2X7R deficient B cell lines with human P2X7R allowed serum independent growth, suggested a role for P2X7R in proliferation (254, 267). The broadly non-selective P2X7R antagonist oATP inhibits the proliferation of murine naïve $CD4^+$ T lymphocytes stimulated with anti-CD3 and anti-CD28 antibodies (268). oATP and another broad spectrum P2X antagonist PPADS inhibited Erk phosphorylation 16 hours post activation of T lymphocytes. A proportion of calcium influx following T lymphocyte activation was inhibited by oATP, this suggests P2X7R may be involved in the global calcium response of T lymphocytes. Release of ATP following activation of $CD4^+$ T lymphocytes was shown to act in an autocrine manner through P2X7R to mediate: calcium influx, IL-2 production and NFAT activation (261). The same group also reported that P2X1 and P2X4 receptors play a role in these processes following T lymphocyte activation and, unlike P2X7R, locate to the immunological synapse (188). This most recent study also suggests that ATP release following T lymphocyte activation is through the Pannexin-1 hemichannel.

1.8.2. Pore formation and cell death

Before cloning of the receptor, P2X7R (then P2Z) was distinguished from other P2X receptors by the ability of its activation to couple to the uptake of large molecular weight molecules (such as the dye ethidium bromide) into cells (269). Pore formation in response to ATP was exploited in the form of biochemical assays as a method of determining functional expression of P2X7R before it's cloning in 1996; this method is still frequently used. Indeed, P2X7R was first identified in murine T lymphocytes through increased intracellular calcium levels coupled with ethidium bromide uptake following ATP treatment (191). Extraceullar calcium influx by P2X7R is rapid and dye uptake was shown to be slower, this suggested two permeation states for P2X7R (270) (Figure 1.18).

The molecular identity of the pore that mediates this second permeation state has been the topic of much investigation. An initial theory that multiple P2X7Rs associate in the membrane to form a pore permeable to molecules larger than cations was discounted (173). Co-expression of the hemichannel Pannexin-1 with P2X7R was required to induce cell death through pore formation in zebrafish oocytes and this was inhibited by carbenoxolone (a channel blocker) (271). Transfection of siRNA against Pannexin-1 also reduced dye uptake induced by BzATP in cell lines (271, 272). Pannexin-1 may represent a route for the release of ATP from cells, which acts in an autocrine manner to activate P2X receptors on the cell surface (188, 268).

Pore formation by activation of P2X7R and subsequent opening of Pannexin-1 leads to biochemical changes in cells and has been linked to IL-1β release from macrophages (273, 274). Initially, work with mouse thymocytes revealed that prolonged ATP treatment resulted in the death of these cells through both apoptosis and necrosis (201, 255, 275). Apoptosis of cells in response to ATP was later shown to involve activation of caspases (276) and DNA fragmentation (275). Other global apoptotic events occur including exposure of phosphatidyl serine (PS), membrane blebbing, microvesicle shedding and cell shrinkage (277, 278). A number of mechanisms have been proposed for how P2X7R activation couples to cell death including: mitochondria, Erk1/2 MAPK activation and ROCK1 (255, 277, 279) (Figure 1.19). The Pannexin-1 pore is involved in apoptosis, where it is

allows the release of ATP from thymocytes, this acts as a chemoattractant for macrophages (280).

A novel mechanism of P2X7R dependent cell death was discovered in mouse T lymphocytes which, unlike human T lymphocytes, express cell surface enzyme called mono-ADP-ribosyltransferase 2 (ART2) (281, 282). It is expressed by the majority of post thymic $CD4^+$ and $CD8^+$ T lymphocytes; however, it is down-regulated upon treatment of T lymphocytes with PMA in an MMP dependent manner (281, 283). Nicotinamide adenine dinucleotide (NAD^+) is a co-enzyme present in the cytosol of cells which may be released through lysis of cells such as erythrocytes (284). ART2 enzymes use NAD^+ as a substrate to ADP-ribosylate P2X7R at Arg125 which leads to the irreversible activation of the receptor (285, 286). This activation of P2X7R by NAD^+ through ART2 leads to cell death, measured by annexin V binding to externalised PS and uptake of propridium Iodide (PI) (286). Genetic deletion of ART2 in these mice prevented NAD^+ induced cell death (266, 286, 287), $P2X7^{-/-}$ mice were also protected (262, 265, 266, 288) and pharmacological inhibition of P2X7R was effective at blocking cell death (265, 286). Higher concentrations of NAD^+ than those required for cell death induced via ART2-P2X7R activation also cause activation of a delayed P2X7R independent cell death pathway (289). Cell death induced by NAD^+ has been observed in murine $CD4^+/CD25^+$ Tregs (265, 266), Natural Killer T (NKT) cells (288), intestinal $CD8^+$ T lymphocytes (262). Murine naïve $CD4^+$ and $CD8^+$ T lymphocytes isolated from lymph nodes may be more sensitive to NAD^+ induced cell death than activated or memory T lymphocytes (260). In addition to inducing cell death, activation of P2X7R through this NAD-ART2 mechanism also causes shedding of CD62L from the surface of mouse T lymphocytes (284, 286). Antibodies against ART2 are able to prevent both cellular death and CD62L down-regulation *in vitro* (284) and their use *in vivo* inhibits the development of autoimmune type 1 diabetes in mice (290).

1.8.3. P2X7R, NADPH oxidase and activation of the inflammasome

As mentioned previously in section 1.1.1, PAMPs from bacteria are recognised by pattern recognition receptors (PPRs) such as cell surface and intracellular TLRs as well as intracellular NOD like receptors (NLRs) (291, 292). The role of ATP as a

DAMP extends far beyond causing cell death in lymphocytes. Through its receptor, P2X7R, ATP can act as a co-stimulatory signal for PAMP primed macrophages, causing the maturation and release of cytokines such as IL-1β and IL-18. This point of convergence between PAMPS, such as LPS and the DAMP ATP, is the activation of inflammasomes. Other inflammasome activating DAMPs include uric acid crystals, asbestos and UV light (291). There are three types of inflammasome, the NALP1, NALP3 and IPAF inflammasomes, which are involved in recruiting and activating caspases, through CARD domains in associated proteins. Caspases can have roles in the apoptosis of cells as well as the cleavage and maturation of cytokines. For example caspase 1 is activated by the NALP3 inflammasome and can both promote apoptosis and cleavage of pro- to mature-IL-1β (Figure 1.19). Production of pro-IL1β is increased by LPS, the subsequent maturation and release of this cytokine, as well as the associated IL-18, requires activation of P2X7R by ATP (247, 293). The cellular mechanism involved in the activation of NALP3 by ATP requires the efflux of potassium ions (which can be recapitulated by the K^+/H^+ antiporter nigericin) and superoxide generation by NADPH oxidase (246, 248).

NADPH oxidase has previously been mentioned in the context of the respiratory burst employed by neutrophils to kill opsonised cells (section 1.1.1), however, this enzyme complex has other important biological functions within cells such as inflammasome activation. NADPH oxidase comprises a family of enzyme complexes NOX1, 2, 3, 4, 5 and DUOX 1 and 2. NOX2 is comprised of membrane associated gp91phox and p22phox subunits and the intracellular p40phox, p47phox and p67phox. GTPases such as Rac1 or 2 also associate with the NADPH oxidase complex. The NOX2 enzyme complex is responsible for increased superoxide generation in response to ATP in macrophages; ATP has been shown to cause the translocation of the p67phox subunit to the plasma membrane of the monocytic leukemic THP-1 cell line (246). Loss of NOX2 in a $NOX2^{-/-}$ mouse causes increased number of pro-inflammatory $CD11^+$ cells and profoundly affects the differentiation of Treg and Th17 cells and leads to the development of arthritis in these mice (294). However, whether P2X7R activation couples to NADPH oxidase in T lymphocytes is unclear.

1.8.4. P2X7R, *Mycobacterium tuberculosis* and Autophagy

Mycobacterium tuberculosis (M. tuberculosis) is a pathogen which causes infection predominantly of the lungs. The disease has previously been managed by vaccination and antibiotics; however, in some areas of the world heavy resistance to these antibiotics has developed. The immune response to *M. tuberculosis* has been extensively studied an may lead to novel treatments for infection by this pathogen (295). Macrophages are important for the defence against *M. tuberculosis* infection; one mechanism employed by these cells is the process of autophagy (296). In this process macrophages actively opsonise *M. tuberculosis* and portions of its cytoplasm and contain them within double membrane vesicles, termed autophagosomes (297). Autophagosomes vesicles are then trafficked to and destroyed by lysosomes. The mechanisms involved in autophagy have been investigated and involve a complex of the class III PI3K Vps34 with other proteins including Beclin-1 (297). A novel role for macrophage P2X7R in the killing of *M. tuberculosis* was suggested following the observation that ATP and BzATP enhanced apoptosis of bacille Calmette-Guerin (BCG) infected cells (298). Indeed, ATPases secreted by *M. tuberculosis* may form a mechanism to prevent ATP induced killing of pathogen infected cells (299). Other purinergic receptors may also integrate stimulation by ATP with pathogen clearance (300, 301). The mechanism of clearance was shown to involve autophagy which required phospholipase D (PLD) activity (300, 302) (303). Killing of *M. tuberculosis* by purines also involves nitric oxide (NO); however, this is independent of P2X7R (301, 302). This process of autophagy also enhances the processing and secretion of the inflammatory cytokine IL-1β (304). Microglial cells also undergo autophagosome formation in response to a model of *Escherichia coli (E. coli)* infection (305). The importance of P2X7R in clearance of *M. tuberculosis* is underscored by single nucleotide polymorphisms (SNPs) of P2X7R which determine the response to pathogen infection (306–308).

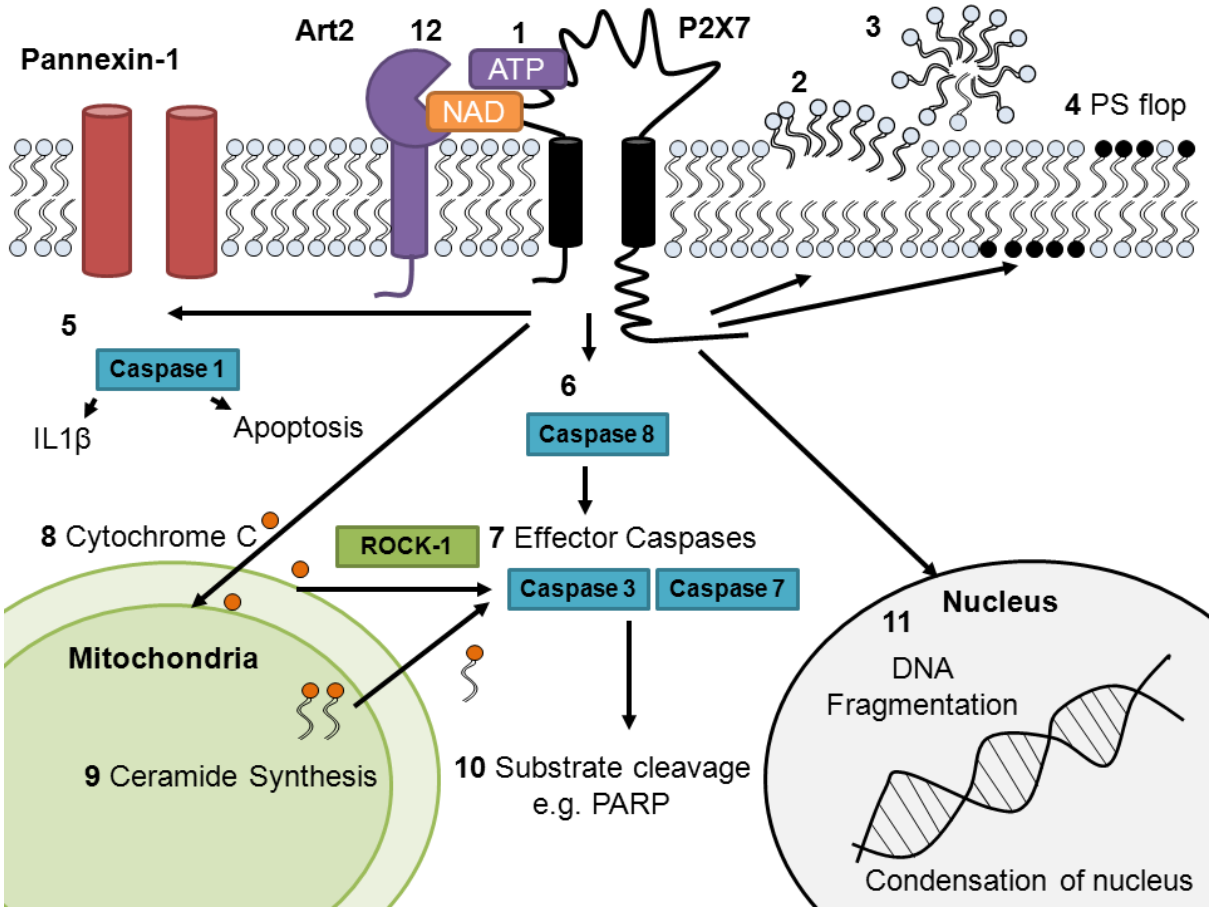

Figure 1.19: Apoptosis induced by P2X7R activation. 1. P2X7R is activated by ATP or BzATP which causes the induction of apoptosis. Reversible changes in the plasma membrane occur rapidly following activation of P2X7. **2.** Firstly rapid blebbing of the membrane occurs which can eventually lead to the shedding of microvesicles (**3**); cells subsequently shrink in size.**4.** Phosphatidyl Serine (PS) is restricted to the inner leaflet of healthy cells however it can be translocated to the cell surface following activation of P2X7R. Externalised PS acts as an important "find me" signal for phagocytes to remove apoptotic cellular material. P2X7R activation also causes activation of a number of key apoptotic proteases termed caspases. **5.** Caspase 1 forms part of the "inflammasome" which is responsible for IL-1β processing; but, independent of this it can promote apoptosis **6 and 7** Caspase 8 is also activated down-stream of P2X7R which can in turn activate the effector caspases 3 and 7.Two mitochondrial mechanisms for effector caspase activation have been observed in macrophages and thymocytes **8.** Prolonged activation of P2X7R can lead to the release of cytochrome C from the mitochondria, which activates caspase 3 and 7 through ROCK-1 activation. **9.** *De novo* synthesis of ceramide in the mitochondria in response to ATP can also activate these effector caspases. **10.** Caspase 3 and 7 are responsible for the cleavage of intracellular proteins during apoptosis. **11.** ATP can also induce Fragmentation of DNA and condensation of the nucleus. **12.** In mouse T lymphocytes apoptosis can be induced by irreversible activation of P2X7R through ADP-ribosylation by the enzyme ART2 using NAD^+ as a substrate.

1.8.5. Cell surface molecule regulation

As mentioned previously, CD62L is an important molecule for naïve $CD4^+$ T lymphocyte homing through its interaction with HEVs allowing transendothelial migration into SLOs. The mechanisms for its regulation have also been discussed in the context of lymphocyte activation, however activation of P2X7R by ATP/BzATP or NAD^+ via ART2 has also been shown to cause CD62L down-regulation. It was initially observed that mouse B lymphocytes isolated from spleen did not flux calcium in response to ATP (191). To investigate P2X7R on human B lymphocytes cells were isolated from patients with BCLL because B lymphocytes are the predominant peripheral immune cell type (190). BCLL B lymphocytes are more responsive to ATP than B lymphocytes isolated from healthy human donors (309). In patients with BCLL levels of cleaved soluble CD62L (sCD62L) correlate with cell number (310) and treatment of CLL B lymphocytes with ATP causes rapid loss of cell surface CD62L (207, 208). CD62L loss in response to ATP/BzATP was rapid, dependent on agonist concentration and blocked by KN-62, oATP and the ADAM17 inhibitor R 31-9790 (207, 208, 212). BzATP is more potent than ATP at inducing CD62L down-regulation; loss of CD62L was independent of extracellular calcium but the process was inhibited by Mg^{2+} (207). T lymphocytes are also sensitive to ATP induced CD62L down-regulation, in mice both $CD4^+$ and $CD8^+$ T lymphocytes are able to undergo ATP induced CD62L down-regulation however $CD4^+/CD25^+$ T lymphocytes appeared even more sensitive to this process (263). Indeed, lymphocytes isolated from mice deficient in P2X7R do not down-regulate CD62L in response to ATP or NAD^+ (284, 311). A study of human PBMC revealed that both naïve $CD4^+$ and naive $CD8^+$ T lymphocytes down-regulate CD62L in response to BzATP and this was inhibited by oATP and KN-62 (245). Other cell surface molecules are also regulated by ATP through P2X7R activation including CD21 (245), CD23 (208, 312) and CD27 (313). The mechanism integrating P2X7R activation by ATP to CD27 processing involved activation of MMPs however this was not mediated by Erk1/2, p38 MAPK or PI3K signalling (313). Activation of P2X7R by ATP and BzATP has also been linked to the release of MMP9 in a calcium dependent manner from monocytes (314). Ultimately, the mechanisms that couple the activation of P2X7R by ATP or BzATP to a decrease in cell surface expression of CD62L are at present unclear.

1.8.6. Migration

As mentioned previously, the role of migration in the co-ordination of lymphocytes within the body is critical to their function. Although little research has focussed on the role of P2X7R in lymphocyte migration, a number of other studies have explored the role of purines in the migration of immune cells.

Purinergic regulation of migration has been most extensively investigated in the context of neuronal inflammation. The expression of both P2X7 and P2Y1 receptors where identified in progenitors of oligodendrocytes. Here P2Y1 is involved in the migration of progenitors prior to their development into mature oligodendrites (315, 316). Microglia from $P2Y12^{-/-}$ mice show reduced ruffling of their membrane and impaired migration towards ADP and ATP (317). P2Y1 and P2Y12 also facilitate migration of microglial cells in response to ADP, a process which is enhanced by TGFβ and reduced by LPS (318). ATP also acts as a chemo-attractant for microglial cells through increased activation of MMP9 (319). This process was inhibited by P2Y antagonists and the pan-isoform PI3K inhibitor Wortmannin, suggesting the involvement of PI3K downstream of either P2Y1 or P2Y12. Indeed, another study demonstrated that Akt, phosphorylated in response to ADP, is involved in microglial migration through the P2Y12 receptor (320). Silencing of P2X4 expression in microglia, using Lentiviral mediated introduction of anti-P2X4 shRNA, significantly reduced migration towards ATP (321). This suggests that both ionotropic and metabotropic P2 receptors are involved in migration of microglia towards nucleotides.

Following injury to epithelial cells there is an increase in calcium levels in these cells, apyrase inhibited this process indicating a role for purinergic receptor signalling (322). These changes were mimicked by purinergic agonists including ATP and ATPγS and facilitated paxcillin phosphorylation and migration of these cells. In human umbilical vein endothelial cells (HUVECs) P2X4 and P2X6 receptors where shown to co-localise with VE-cadherin, an important junctional protein (323). Therefore, purines may play a role migration during in wound healing, following infection and inflammation (Figure 1.1). P2Y2, 11, 13 and P2X1, 4 and 7 receptors are expressed by macrophages; evidence suggests that P2Y11 receptors facilitate migration of these cells. However, migration was not directional and did not require the PI3K signalling effector Akt (324). The migration of other

innate cells, such as neutrophils, is influenced by purines; indeed, chemotaxis towards IL-8 requires the function of P2Y2 receptors (325). Another study, which previously showed a role for P2Y2 in neutrophil migration, also suggests a mechanism whereby the hydrolysis of ATP to adenosine acts to promote neutrophil migration through A3Rs (326). This co-requirement for P1 and P2 receptors for migration was also observed in microglial cells. As mentioned above, microglia migrate towards the nucleotides ATP, ADP and AMP and interestingly this migration requires expression of the ecto-ATPase CD39 (327). Neutrophil migration also requires the activity of CD39 (328, 329).

Analysis of proteins which associated with rat P2X7R *in vitro* revealed interactions of this receptor with integrins and cytoskeletal components (330). Indeed, human eosinophils phosphorylate actin and up-regulate the integrin CD11 in response to ATP (331). PX7R can also be activated by αvβ3 integrin signalling in astrocytes, where it is required for calcium influx in response to the glycoprotein Thy-1 (332). P2X7R has also been shown to influence expression of the adhesion molecule CD62L described in the sections above.

1.8.7. Signalling

The P2X7R dependent functions described above require integration of P2X7R activation into biochemical changes within the cell, either through increased intracellular calcium levels and/or through activation of protein signalling cascades. While several studies have looked at P2X7R dependent signalling in T lymphocytes, a wider raft of studies in other cell types may also be relevant to lymphocytes and are also discussed here (Figure 1.20). Murine thymocytes isolated from mice show increased phosphorylation of the MAPKs Erk1/2 and p38, as well as JNK1/2 and the Src family kinases p56Lck and p59Fyn after ATP treatment (255). In these cells Erk1/2 phosphorylation was inhibited by oATP and ablated in thymocytes from $P2X7R^{-/-}$ mice. Mouse splenocytes also phosphorylated Erk1/2 in response to ATP through activation of MEK (206). Mouse Tregs from P2X7R deficient mice showed significantly reduced Erk1/2 phosphorylation in response to anti-CD3 antibody +/- IL-6 (259). The enhanced anti-CD3 antibody + TGFβ dependent generation of mouse Treg cells from naïve

$CD4^+$ T lymphocytes *in vitro* using the mTOR inhibitor Everolimus requires P2X7R expression (333).

Mouse thymocytes do not phosphorylate Akt after ATP treatment indicating that the PI3K signalling pathway may not be activated down-stream of P2X7R in these cells (255). In human 1321N1 astrocytoma cells transfected with rat P2X7R, stimulation with BzATP, ATP and UTP caused phosphorylation of Akt on Ser473 indicating that both P2Y and P2X receptors can cause activation of the PI3K pathway (334). Phosphorylation of both Ser473 and Thr308 was dependent on BzATP concentration, was rapid and sustained for up to two hours. Extracellular and intracellular calcium were both required for Akt phosphorylation as was the activity of PI3K and Src kinase.

In the microglial cell line MG6, the mTOR pathway was activated by millimolar concentrations of ATP. Moderate mTOR phosphorylation and robust S6K phosphorylation were observed (305); this study also revealed a slight increase in AMPKα phosphorylation following ATP treatment. In astrocyte and microglial cell lines Erk1/2, phosphorylation was observed in response to BzATP (305, 335, 336) and in primary rat astrocytes this effect was enhanced by co-application of arachidonic acid (335, 337). The mechanism for BzATP induced Erk1/2 phosphorylation required upstream activation of MEK and PKC as well as both extracellular and intracellular calcium. Pyk2, a protein tyrosine kinase which is activated by both increases in intracellular calcium concentration and PKC was also required (336, 338).

The novel PKC isoform PKCδ can be phosphorylated following ATP/BzATP treatment of cells (205, 336). Osteoblasts and osteoclasts express P2X7R and its role in bone function may be of importance in osteoporosis (339). Mouse osteoclasts translocate PKCα from the cytosol to the cell membrane in response to BzATP in a P2X7R dependent manner, this was shown in the RAW 264.7 macrophage cell line to require extracellular calcium (340). PKCβ1 was also recruited to the membrane following BzATP treatment; however, this translocation was significantly more transient than for PKCα. In contrast, PKCδ did not show BzATP induced translocation. Primary rabbit osteoclasts demonstrate BzATP induced NF-κB nuclear translocation through activation of P2X7R (341). Mouse

embryonic stem (mES) cells express functional P2X7Rs (342) where it is involved in survival, but may also cause cell death following prolonged activation. ATP induced proliferation of mES cells required PKC activity and ATP induced the relocation of PKCα, δ and ζ from the cytosol to the membrane (343). It is unclear however if P2X7R was responsible for these effects, as its involvement was not assessed in this study. In these cells Erk1/2 was phosphorylated down-stream of Akt.

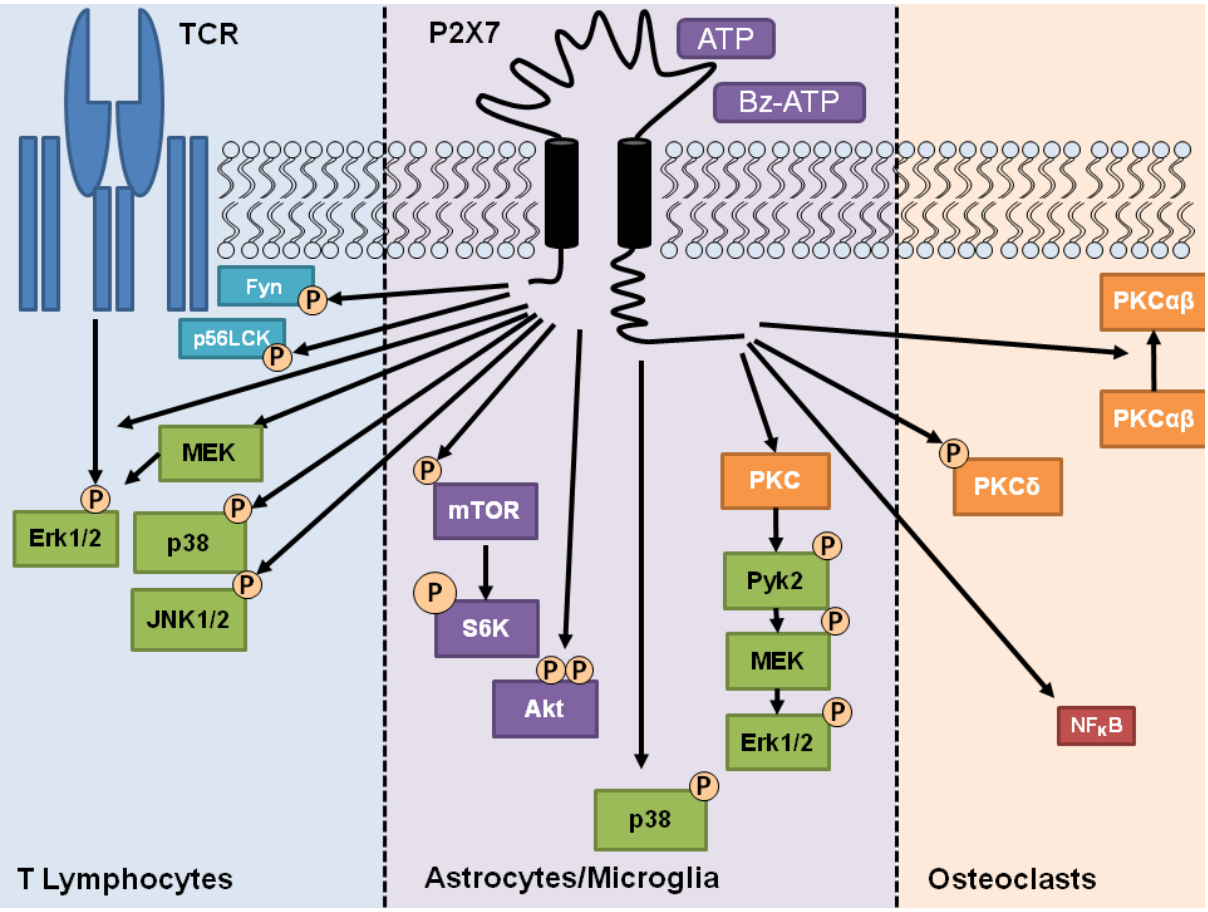

Figure 1.20: Signalling via P2X7R. Studies have revealed that ATP or BzATP can induce activation of signalling cascades and phosphorylation of a number of different proteins. **Left**: In mouse thymocytes members of the MAPK family (green) are activated by BzATP. PX7R activation also phosphorylates the TCR signalling components p56Lck and Fyn. In Treg cells Erk1/2 phosphorylation in response to anti-CD3 and IL-6 partially requires P2X7R. **Centre:** Microglial cells activate the mTOR signalling cascade in response to ATP. BzATP caused activation of the Erk1/2 pathway in both astrocyte and microglia cell lines through the cascade described. p38 MAPK is also activated via P2X7R. **Right:** In osteoclasts BzATP causes translocation of PKCα/β and phosphorylation but not translocation of PKCδ. NFAT was translocated to the nucleus following P2X7R activation.

1.9. P2X7R knockout mice and P2X7R in human disease

In an effort to confirm the role of P2X7R in immune processes before the development of suitably selective antagonists, the pharmaceutical companies Pfizer and GlaxoSmithKline developed mice lacking P2X7R (344, 345). Both mouse strains were generated on a B57BL/6 background with the P2X7R gene targeted at either exon 1 (GlaxoSmithKline) or exon 13 (Pfizer), resulting in viable and fertile mice lacking P2X7R expression (Figure 1.21). These P2X7R deficient mouse strains were initially used to confirm processes previously attributed to P2Z/P2X7R such as: IL-1β processing, pore formation and cell death (345, 346). A more detailed analysis of these $P2X7R^{-/-}$ mice using established models of specific diseases, as well as pharmacological inhibition of P2X7R in wild type mice, revealed a role for P2X7R in the pathology of a number of inflammatory and autoimmune diseases. P2X7R is involved in multiple sclerosis [MS] (347–350), amyotrophic lateral sclerosis [ALS] (351), pain (217, 218, 352–357), hepatitis (262, 288), osteoporosis (339, 358) and RA (311).

However, there have been significant discrepancies between results obtained from each of the two $P2X7R^{-/-}$ mouse strains. For example in one study P2X7R deficiency was associated with decreased disease incidence and clinical score in mice lacking P2X7R in a MOG35-55 peptide model of MS (349). In another study $P2X7R^{-/-}$ mice actually showed increased clinical scoring for EAE disease, through increased proliferative ability and decreased apoptosis of lymphocytes from these mice (348). Sharp et al. used mice provided by GlaxoSmithKline (349) whereas Chen et al. used $P2X7R^{-/-}$ mice provided by Pfizer (348). A possible explanation for this has only recently been elucidated and involved the discovery of alternative splicing of the P2X7R.

P2X7R exhibits a large number of SNPs, which can cause loss or gain of receptor function and as such have been implicated in a number of diseases including depression (359) and *M. Tuberculosis* infection (307, 360).

1.10. Splice variants: A potential caveat to studying P2X7R

A recent study revealed that the human P2X7R, like other P2X receptors (173, 361, 362), can undergo alternative splicing to produce splice variants of the full length receptor (363). So far, little has been studied in the context of human

P2X7R (364) however mouse P2X7R is also alternatively spliced and has led to a re-evaluation of data gleaned from the two P2X7R knockout mice models. An initial study by Taylor et al. revealed that T lymphocytes from GlaxoSmithKline $P2X7R^{-/-}$ mice exhibited enhanced PS exposure, cell death and CD62L down-regulation in response to ATP treatment (365). Cells from these mice did not express exon 1 of P2X7R (this is the site where the gene is targeted for deletion), however exon 3 was detectable in these cells. The group postulated that a splice variant of P2X7R escaped deletion in these mice, this was confirmed by the discovery of the K splice variant of P2X7R in mice (365, 366). The tissue expression of the K splice variant has been investigated as well as cell specific expression (342, 366). This splice variant has an alternative exon 1 compared to the wild type P2X7R and therefore is not removed by the GlaxoSmithKline targeting strategy, but it is removed in the Pfizer mouse. The electrophysiology of P2X7K differs from the full length P2X7A when expressed in HEK293 cells. P2X7K has a much longer channel inactivation time following withdrawal of agonist; it also has an increased sensitivity to ATP which may explain the enhanced responses observed in the GlaxoSmithKline $P2X7R^{-/-}$ mice. Rat P2X7K showed enhanced pore formation and membrane blebbing compared to P2X7A. Recently, a further two splice variants have been identified in the mouse which have shortened exon 13s ($P2X7_{13b}$ and $P2X7_{13c}$) resulting in expression of truncated P2X7Rs (367). These isoforms are present in the wild type mouse, deleted from the GlaxoSmithKline $P2X7R^{-/-}$ mouse but $P2X7_{13b}$ (and to a lesser extent $P2X7_{13c}$) was observed in Pfizer $P2X7R^{-/-}$ mice; an additional “hybrid” P2X7R isoform was identified in the Pfizer $P2X7R^{-/-}$ mouse. The electrophysiology of the cloned receptors showed that $P2X7_{13b}$ and the hybrid have significantly reduced currents compared to P2X7A and co-expression of P2X7A and $P2X7_{13b}$ attenuated currents.

In the study which first identified the human P2X7R splice variants two of these isoforms where cloned and studied: P2X7B which has a truncated C-terminal domain and P2X7H which lacks TMD1. P2X7H is non-functional and, although P2X7B couples to calcium influx, its activation does not cause pore formation or apoptosis when it is expressed alone. However, when P2X7B was co-expressed with P2XA it in fact caused an enhancement of pore formation and apoptosis.

These isoforms were both expressed in a wide variety of tissues; however, P2X7B was expressed at a higher level than P2X7H. The relative levels of P2X7A and B vary between the studies and require further investigation. A more recent study also identified another truncated P2X7R splice variant (P2X7J) which lacks not only the C-terminus but also TMD2 and part of the extracellular loop (368). P2X7J was cloned from the CaSki cervical cancer cell line and was sub-cloned into HEK293 and MDCK cell lines for evaluation. When expressed alone P2X7J did not couple to pore formation or apoptosis of cells and only partially increased intracellular calcium levels; however, when co-expressed with wild type P2X7A it acted as dominant-negative isoform partially inhibiting these processes. Epithelial cells from the cornea from both healthy and diabetic humans express both isoforms but at varying levels (364).

If these isoforms of P2X7R can form heterotrimers in primary cells, then the pharmacology of the P2X7R and its down-stream functions will depend on the association of these full length (P2X7A), function enhancing (P2X7B) and non-functional (P2X7H and J) isoforms. Cloning and characterisation of the remaining P2X7R splice variants and the detailed analysis of these isoforms in primary tissues and cells will be important for understanding of P2X7R function in the future. The discovery of splice variants of the human P2X7R, coupled with the large number of SNPs for this receptor may explain, in part, why studies involving P2X7R antagonists in human subjects have not been successful.

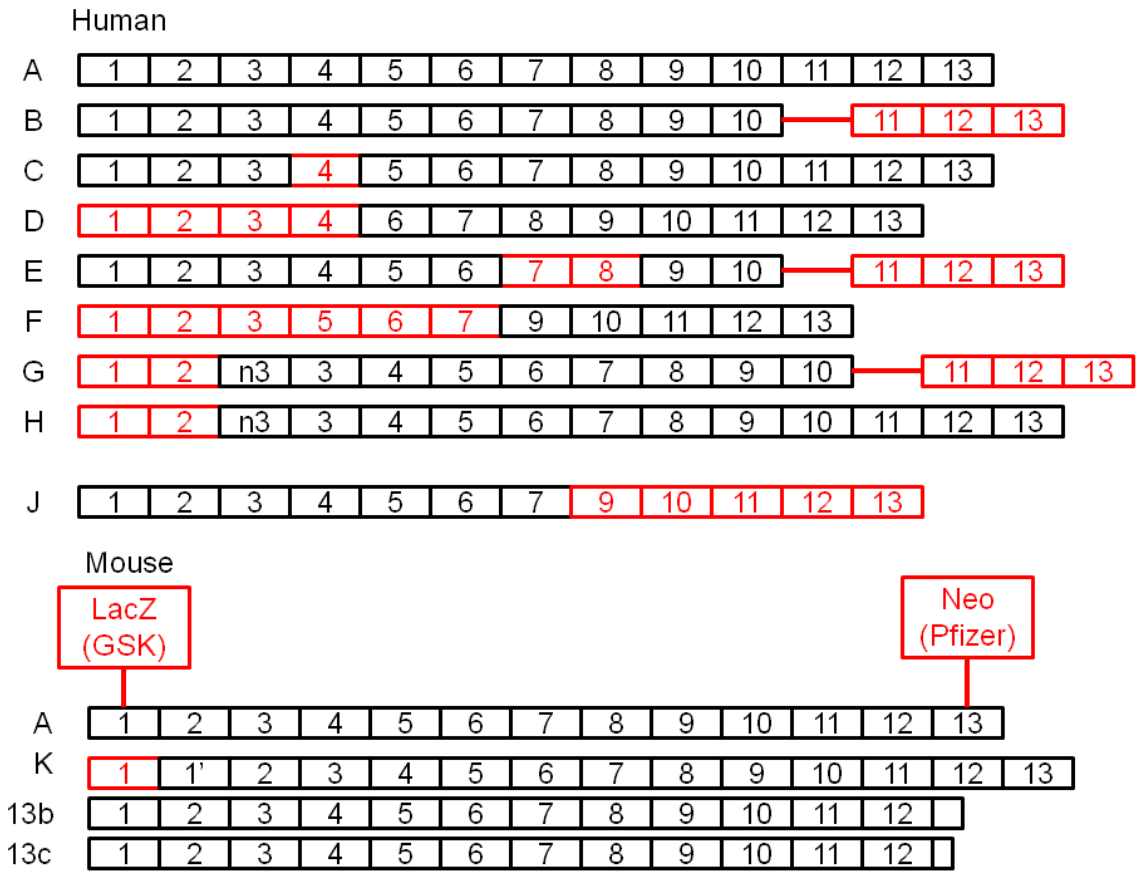

Figure 1.21: P2X7R Splice variants in humans and mice. P2X7R has been reported to undergo alternative splicing in human and murine cells (240, 363, 366–368). The exons present in the full length (A) and other isoforms B-K and 13b and 13c are given in boxes. Where exons are present in the isoform they are given in black and where they are absent, due to alternative start and stop codons, they are given in red. The alternative n3 and 1' exons as well as the shorter 13b and 13c exons are also given. The intro between exon 10 and 11 which inserts a new stop codon is shown as a red line. The strategies for developing P2X7 knockout mice adopted by GlaxoSmithKline and Pfizer use a LacZ and Neomycin Cassette inserted into exons 1 and 13 respectively. P2X7K escapes the GlaxoSmithKline strategy and P2X13b and c escape the Pfizer strategy.

1.11. Summary

In summary, the function of T lymphocytes, particularly their circulation and homing to SLOs and peripheral sites of inflammation are tightly regulated processes. P2X7R expressed by T lymphocytes has a number of functions which include regulation of proliferation and adhesion molecules. Evidence from a wide variety of cell lines has shown P2X7R to activate multiple signalling pathways; however, the role of these signalling mechanisms coupling P2X7R activation to biochemical function in T lymphocytes is poorly understood. P2X7R is associated with a number of inflammatory and autoimmune disorders and while the receptor represents a novel therapeutic route of intervention, little progress has been made in translation to medicine. While chemical synthesis has provided P2X7R antagonists with vastly improved selectivity and potency, a better understanding of how P2X7R transduces its signals in T lymphocytes may improve its potential targeting in these diseases. In addition much pre-clinical work involving P2X7R has taken place in mice; however, the recent discovery of alternative splicing of the P2X7R in both mouse and human genomes has added further complexity. In addition, species differences are observed also observed for P2X7R activity (e.g. activation of P2X7R by ART2/NAD in mice). It was therefore the intention of this study to investigate the potential signalling mechanisms coupling P2X7R activation to changes in T lymphocyte function, with an initial emphasis on PI3K signalling.

1.12. Aims and Objectives

The aims of this project were three fold and designed to investigate the role of PI3K in ATP-gated P2X7 receptor signalling in lymphocytes.

1) Confirm expression of P2X7R in Leukemic T cell lines and primary human T lymphocytes
2) To confirm functional expression of P2X7R by use of biochemical assays and determine which processes to investigate the role of PI3K signalling in
3) To investigate if PI3K signalling couples to P2X7R dependent processes using a pharmacological approach with small molecule inhibitors

2. Materials and Methods

2.1. Materials and compounds list

Unless otherwise stated all materials were purchased from Sigma Aldrich, Poole, Dorset, UK.

2.2. Cell culture

2.2.1. Cell lines

THP-1 human acute monocytic leukaemia cell line (European collection of cell cultures, ECACC, Salisbury, UK) and leukemic T cell line J6 Jurkats (Cancer Research UK) were cultured in RMPI-1640 media supplemented with 10% FCS, 10 µg/ml penicillin and 10 µg/ml streptomycin (All: Gibco, Invitrogen, Paisley, UK). The acute monocytic leukaemia cell line THP-1 was differentiated into macrophage-like cells by overnight incubation with 10 ng/ml IFN-γ and 25 ng/ml Lipopolysaccharide (LPS). Cells were cultured in cell culture flasks with a surface area of 75 cm^2 at 37^oC with a constant supply of air mixed with 5% CO_2. Cultures were maintained by changing media every 2-3 days and kept at a confluency of approximately $0.5x10^6$ cells per ml. Cultured cells were discarded after 12 weeks and replaced with frozen cell stocks stored in cryo-tubes in liquid nitrogen tanks.

2.2.2. Isolation of Peripheral Blood Mononuclear Cells (PBMCs) from whole blood

Syringes were prepared with heparin as an anti-coagulant (2 Units/ml whole blood) and blood was removed from an arm vein of a healthy human volunteer. Blood was mixed with RMPI-1640 without supplements at a ratio of 1:1 and 25-35 ml was layered onto 15 ml lymphoprep (Axis Shield, Oslo, Norway). Preparations were then centrifuged at 1,500 rpm (250 g) for 30 minutes, ending with an unassisted stop. A sterile Pasteur pipette was used to remove the PBMC layer and transfer these cells to a fresh centrifuge tube. Cells were then washed 3 times by the addition of RMPI-1640 without supplements and centrifugation at 250g for 10 minutes.

2.2.3. Clonal expansion of αβTCR T cells

After washing, freshly isolated PBMC was re-suspended in fully supplemented RMPI-1640 at a volume equal to that of the initial volume of whole blood drawn from the donor. SEB was added at a final concentration of 1 µg/ml for 72 hours.

Cells were then washed 3 times to remove SEB before addition of twice the original volume of fully supplemented RMPI-1640 and 36 U/ml IL-2. To maintain cells, the volume of culture medium was doubled every 2 days and fresh IL-2 added. Cells were used between 9-11 days post isolation and rested in fully supplemented RMPI-1640 without IL-2 overnight before use.

2.2.4. Isolation of Naive CD4+ T lymphocytes from PBMC

High purity naive $CD4^+$ T lymphocytes were isolated from PBMC using a negative selection cell isolation kit [#130-094-131] from Miltenyi Biotec, Bisley Ltd., Surrey. After washing, freshly isolated PBMC were counted. PBMCs were re-suspended in 40 µl MACS buffer (PBS + 2 mM EDTA + 0.5% BSA, pH 7.4 – sterile filtered) per 10^7 cells. A cocktail of biotin conjugated antibodies labelling non-naïve $CD4^+$ cells was then added, 10 µl per 10^7 cells, and cells placed at 4^oC for 10 minutes. Labelling was stopped by the addition of 10 ml of ice cold MACS buffer and centrifugation at 250 g for 10 minutes. Supernatant was discarded; cells re-suspended in fresh MACS buffer 80 µl per 10^7 cells and anti-biotin micro-beads added: 20 µl per 10^7. Cells were incubated for 15 minutes at 4^oC followed by addition of 10 ml of ice cold MACS buffer and centrifugation at 250 g for 10 minutes. Supernatant was discarded and cells re-suspended in 500 µl fresh MACS buffer. Cells were passed through a pre-washed LS column [#130-042-401] and collected in a fresh centrifuge tube. The column was washed 3 times with 3 ml MACS buffer. Cells were centrifuged and washed into fully supplemented RMPI-1640 for immediate use in assays or activation and subsequent long-term culture.

2.2.5. Isolation of splenocytes from mice

Spleens from Cd1 mice were removed and disaggregated through a 40 µm filter. Red blood cells were removed by centrifugation through a layer of Lymphoprep and the remaining splenocytes were washed three times in serum free RPMI 1640 by centrifugation at 250 g for 5 minutes. Cells were finally re-suspended at a concentration of $5x10^6$/ml in complete RPMI 1640 and used immediately in experiments.

2.3. Coupling of anti-CD3/CD28 antibodies to micro-beads

Antibodies raised against human CD3 (clone: UCHT-1) and human CD28 (clone: 9.3) were added, 75 µg each, to a 0.1 M borate buffer (pH 9.5). This antibody solution was added to 4 x 10^8 magnetic Dynabeads® (Invitrogen, Paisly, UK) and rotated overnight at 37^{o}C. The next day the beads were held with a magnet and borate buffer was removed. Using the bead wash solution (Table 2.1), beads were washed three times for 10 minutes, once for 30 minutes and then overnight by rotation at 4^{o}C. The following day beads were re-suspended in 10 ml bead wash solution for storage at 4^{o}C; 40 x 10^6 anti-CD3/CD28 antibody coated beads/ml. Before use, beads were washed 3 times in phosphate buffered saline, re-suspended in supplement free RPMI-1640 and added to cells at the indicated ratios.

2.4. Stimulation and protein isolation

For stimulations, cells were re-suspended in supplement free RMPI-1640 at a concentration of 2x10^6 and rested for 30 minutes in a 37^{o}C water bath. Inhibitors or appropriate vehicle was applied to cells for indicated times before the addition of stimulants. After stimulation, cells were centrifuged for 30 seconds, supernatant removed and cells re-suspended in 50 µl NP40 lysis buffer per 1x10^6 cells (containing protease and phosphatase inhibitors as described in Table 2.2).

For analysis of protein expression cells were removed from culture, washed and cells re-suspended in 50 µl NP-40 lysis buffer per 1x10^6 cells. After re-suspension in lysis buffer cells were rotated at 4^{o}C for 15-30 minutes to assist lysis, after which debris was removed by centrifugation at 13,000 rpm 4^{o}C for 10 minutes and the supernatant containing protein was stored at briefly at -20^{o}C before immunoblotting.

For measurement of CD62L released into the supernatant, cells were stimulated as described above except cells were at a concentration of 5x10^6 cells/ml. After stimulation, centrifugation for 30 seconds was used to pellet cells. The supernatant was removed and placed into a new micro-centrifuge tube and 350 µl ice cold 100% acetone was added per 500 µl supernatant. Cells were placed on ice for 10 minutes followed by centrifugation at 13,000 rpm 4^{o}C for 10 minutes. The supernatant was discarded and precipitated protein was re-suspended in 50 µl NP40 lysis buffer.

2.5. Immunoblotting

Acrylamide gels were cast to the desired percentage for optimum resolution of different protein sizes. A resolving phase containing Tris-HCl pH 6.8 was first cast followed by a stacking phase containing Tris-HCl pH 8.8, with a comb to leave impressions for loading protein. 5 µl 5 x sample buffer (SDS and 2-Mercapto-Ethanol) was added to 20 µl protein in NP-40 lysis buffer and samples were boiled at 100^{o}C for 5 minutes. Samples were briefly centrifuged and then 20 µl of each sample was loaded onto the acrylamide gel. The gel tank was filled with running buffer and electrodes connected to the tank. Proteins were separated by electrophoresis first by passing through the stacking phase at 75 V for 15 minutes, followed by 150 V through the resolving phase until the desired molecular weight markers were adequately separated.

Markers and proteins were transferred from the gel onto nitrocellulose membrane at 40 mA per membrane for 1 hour using semi-dry buffer and apparatus. The membrane was blocked with 5% milk in TBST (Tris buffered saline + 0.05% Tween 20) for 1 hour at room temperature. The membrane was then washed once briefly in TBST to remove excess milk, before being sealed in a plastic bag with the primary antibody. Primary antibodies were diluted as described (Table 2.3) in TBST + 1% BSA + 0.01% sodium azide and membranes were incubated overnight in 5 ml diluted primary antibody per membrane.

The next day the membrane was removed from the bag and placed in a tray. The membrane was washed 3 x 5 minutes in TBST before incubation in HRP-conjugated secondary antibody (raised against the same species as the primary antibody) diluted 1:10000 in TBST for 1-2 hours at room temperature. The membrane was then washed 3 x 5 minutes in TBST and once in TBS. Amersham™ ECL detection reagents (GE Healthcare, Little Chalfont, Buckinghamshire, UK) were mixed 1:1, placed over the membrane and allowed to cover the membrane for 1 minute. The membrane was then sealed in cling film and covered by X-ray film [Fuji Medical X-Ray Film 100 NIF 18 x 24] (Fisher Scientific) inside a film cassette. After the desired time, the film was removed and developed using a developer (Photon Imaging Systems, Swindon, Wilts, UK).

To assess the relative phosphorylation levels of the signalling proteins Akt, Erk1/2 and S6 ribosomal subunit, the intensity of phosphorylated protein detected by immunoblotting with specific antibodies was normalised to total levels of Akt or Erk1/2 protein. This was achieved using Image J software: developed film was scanned and intensity of background image was subtracted from protein bands, these bands were then normalised as described above.

2.6. Gelatin Zymography

Naïve $CD4^+$ T lymphocytes were freshly isolated or leukemic T cell line Jurkat removed from culture, cells were washed before treatment with PMA or ATP. Cells were briefly centrifuged at 300 g for 30 seconds, the supernatant was collected and the cell pellet lysed as for immunoblotting except EDTA, protease and phosphatase inhibitors were removed from the lysis buffer (Table 2.2). Gelatin gels containing 0.1% w/v Gelatin were prepared, samples were added to the gel without boiling and proteins were separated using SDS-PAGE. Gels were developed the same protocol as Ghosh et al: gels were washed in developing solution (Table 2.4) with 2.5 % Triton X 100 for 1 hour (369). After a second 5 minute wash, gels were developed overnight in developing solution with 1 % Triton X 100. This allows proteases separated by SDS-PAGE to break down the gelatin within the gel. Finally gels were stained with Coomassie blue for 30 minutes and washed with destain solution containing methanol and acetic acid.

2.7. Electrophysiology

Naïve $CD4^+$ T lymphocytes were freshly isolated from peripheral human blood and pipette in to a custom made cell bath filled with external buffer solution (Table 2.5). The bath was carefully fixed onto an Olympus IX71 inverted microscope (Olympus, Southend-on-Sea, Essex, UK). Cells were allowed to settle on to the bottom of the bath for 15-20 minutes.

Borosilicate glass capillaries with filaments [GC150TF-10 Part #30-0066] (Harvard Apparatus, Kent, UK) were pulled into points using a Narishige PC-10 micropipette puller (Digitimer, Welwyn Garden City, Hertfordshire, UK). Pipettes were polished using a Narishige MF-830 microforge to give a filled resistance of 3-6 MΩ, when placed into the cell bath. Pipettes were back-filled with internal solution (Table 2.6)

using a 1 ml syringe attached to a MF28-G5 syringe filter (World Precision Instruments, Sarasota, FL, USA). Filled pipettes were tapped to remove bubbles and fixed over the silver chloride electrode, this was fitted to a HEKA head-stage. The head-stage was attached to a Marzhauser Micromanipulator MM-33 (Intracel, Roysten, Hertfordshire, UK) which was used for coarse manipulation to position the pipette in the cell bath.

The pipette was positioned carefully over a cell and fine manipulation was used to bring the pipette into contact with the cell (Figure 2.1). Using a syringe attached to the electrode and pipette, a small amount of negative pressure was applied to attach the pipette to the cell before further pressure was applied to form a seal of at least 1 GΩ resistance. Using a HEKA patch clamp EPC10 amplifier (Digitimer) and HEKA patch master 2.11 software the cell was voltage clamped at -60 mV and changes in the current required to maintain this voltage were recorded. Experiments were performed at ambient room temperature.

Once a seal was formed and the cell voltage clamped, external buffer solution was passed over the cell through polyethylene tubing (Portex LTD, Smiths Medical, Hythe, Kent, UK). Excess external solution was removed from the bath using a pump [Dymax 5] (Charles Austen Pumps LTD, Byfleet, Surrey, UK) allowing the constant washing of cells with external buffer solution.

Agonist and antagonist solutions were applied to the cells using a rapid solution changer (RSC) [RSC-200] (Biologic Science Instruments, Claix, France). Solutions were suspended above the RSC in syringes and allowed to pass by gravity through tubing; a remotely controlled valve determined when solutions were passed through tubing into borosilicate glass capillaries with filaments [GC100TF-10 Part #30-0035] attached to the RSC. RSC positioning over the cell and valve opening and closing were controlled by RSC software. Solutions were applied using the RSC as described above and changes in current were recorded using HEKA patch master 2.11 software. Information from the HEKA amplifier was also passed through a Power lab 2/20 data acquisition system (ADInstruments, Oxford, UK) and recorded on chart recorder Chart V4.0.1 software.

All equipment was mounted on an anti-vibration table [Isolate System 2000] (Intracel, Roysten, Hertfordshire, UK). All equipment was earthed to reduce

electrical interference and during recordings a small earthed sheet of foil was placed over the microscope to limit external interference.

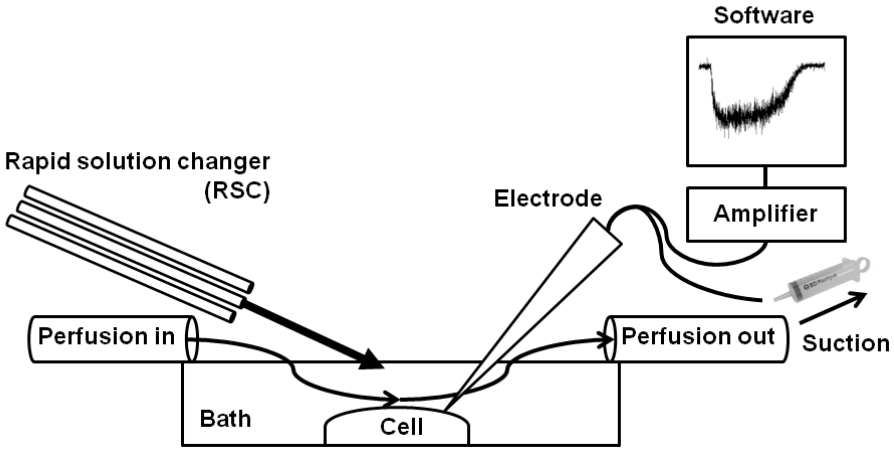

Figure 2.1 Electrophysiology apparatus. A cell is rested at the bottom of the bath surrounded by external buffer with divalent cations (Table 2.4). This solution is slowly perfused over the cell through a drip feed pipe and removed using an aspirating pump. An electrode is introduced into the bath, suction is applied through the electrode to form a seal with the cell of >1 GΩ resistance. The cell voltage is "clamped" at -60 mV and changes in the current across the membrane are recorded. Solutions containing agonists/antagonists are applied by the RSC using the protocols described in Figure 3.3. Changes in membrane current are recorded and represented in graphical form on a personal computer using HEKA software.

2.8. Ethidium bromide Uptake

Freshly isolated naïve $CD4^+$ T lymphocytes were re-suspended external buffer solution (Table 2.5) containing 25 μM ethidium bromide at a concentration of $1x10^6$ cells per ml. 90 μl of cell suspension was placed into each well of a 96 well black bottom plate. The plate was then placed into a FluoStar Optima plate reader (BMG Labtech) at 37^{o}C and allowed to rest for 5 minutes. Cells were excited at 544 nm and emission collected at 590 nm every 30-90 seconds. Baseline fluorescence was recorded before the application of vehicle or ATP. At the end of the experiment cells were lysed by addition of 0.2% Triton X-100 to give a value for maximum ethidium bromide fluorescence, all data points were then normalised to the maximum fluorescence. Finally, linear regression was used to determine the

rate of fluorescence increase (change in percent maximum fluorescence per minute) in the first 15 minutes prior to ATP addition using the below equations.

$$Percent\ maximum\ fluorescence = \frac{Fluorescence}{Fluorescence\ after\ Triton\ X100} \times 100$$

$$\frac{Percent\ Max\ Fluorescence\ before\ agonist}{Percent\ Max\ Fluorescence\ 900s\ after\ agonist} \div Time\ between\ recordings\ (s) \times 60$$

2.9. Cellular Death Assays

2.9.1. Apoptosis

Freshly isolated naïve $CD4^+$ T lymphocytes were treated with ATP at the indicated concentrations. 250,000 cells per point were washed twice in ice cold PBS and then re-suspended to a concentration of $1x10^6$ cells/ml in annexin V binding buffer (10 mM HEPES pH 7.4, 140 mM NaCl, 2.5 mM $CaCl_2$, 0.1% BSA). APC conjugated annexin V (Southern Biotec, Birmingham, Alabama, USA) was then added to each tube 10 µl/$1x10^6$ cells and cells incubated on ice protected from light for 15 minutes. Further binding buffer was added followed by propridium Iodide (PI) 2 µg/$1x10^6$ cells. Cells were immediately analysed by flow cytometry.

2.9.2. LDH measurement

Freshly isolated naïve $CD4^+$ T lymphocytes were re-suspended in phenol red free RMPI-1640 without supplements at a concentration of $1x10^6$ cells/ml. 90 µl of cell suspension was added to each well of a sterile 96 well plate and each condition was performed in triplicate. Vehicle or antagonists were added before agonists were added for the indicated times and the plate was incubated at 37°C with a constant supply of air mixed with 5% CO_2. 0.2% Triton X-100 was added to three wells for 5 minutes to rupture cell membranes and cause the maximum release of LDH from cells. The plate was centrifuged at 250 g for 10 minutes with a brake assisted stop and 50 µl of supernatant for each well was transferred to a new clear bottomed 96 well plate using a multi-channel pipette. Three wells were left blank to measure absorbance of the plate alone, three wells were filled with 50 µl phenol red free RMPI-1640 without supplements to measure absorbance of the medium and LDH positive control (Bovine heart LDH 1:5000 dilution in PBS) was also

added to three wells. LDH assay reagent [G1780] was mixed according to the manufacturer's instructions (Promega, Southampton, UK) and 50 µl added to each well. The plate was covered in foil to protect from light and incubated at room temperature for 30 minutes. The LDH reaction and colorimetric reaction to produce a red product are described below.

$$NAD^+ + Lactate \xrightarrow{LDH} Pyruvate + NADH$$

$$NADH + INT \xrightarrow{Diaphorase} NAD^+ + Formazan\ (Red)$$

To stop the LDH reaction 50 µl 1 M acetic acid was added to each well, bubbles were carefully removed and absorbance recorded at 490 nm.

2.10. Proliferation

The Cell Trace CFSE Cell Proliferation Kit (C34554) (Invitrogen, Paisly, UK) was used to measure proliferation of cells according to the manufacturer's instructions. Carboxyfluorescein diacetate succinimidyl ester (CFSE) is cell permeable, binds DNA and emits fluorescence at 517 nM when excited at 492 nm. After each mitotic cell division the two daughter cells receive half the CFSE labelled DNA from the parent cell each; therefore, the fluorescence intensity effectively halves. This can be used to determine the proliferative capabilities of cells under specific treatment conditions. Briefly, freshly isolated naive CD4+ T lymphocytes were re-suspended at a concentration of $1x10^6$/ml in PBS + 0.1% BSA. CFSE was added for a final concentration of 5 µM and cells incubated in the dark at 37^oC for 15 minutes. Cells were washed once into fresh complete RMPI-1640 and incubated in the dark at 37^oC for a further 30 minutes. Cells were then washed again into fresh complete RMPI-1640 and a small number of freshly labelled cells were analysed by flow cytometry for incorporation of CFSE at day 0 alongside unlabelled naive CD4+ T lymphocytes (unlabelled control). Remaining cells were pre-treated with vehicle or inhibitors as indicated. Cells were then activated by the addition of anti-CD3/CD28 antibody coated beads to cells at a ratio of 3:1 plus the addition of 36 Units/ml recombinant IL-2. After 7 days cells were analysed for CFSE fluorescence using flow cytometry; population gates were set around peaks and the percentage of cells in each division counted.

2.11. *In vitro* migration assays

2.11.1. Neuroprobe chamber assay

A chamber based *in vitro* migration assay was used as described (95). Freshly isolated naive CD4+ t lymphocytes were re-suspended at a concentration of $3.2x10^6$ cells/ml in phenol red free RMPI-1640 with 0.01% BSA (chemotaxis media) added. Cells were pre-treated with vehicle or inhibitors at the indicated concentrations. To equilibrate a fresh Neuroprobe chemotaxis plate (Chemo® Tx101-5 Receptor Technologies) PBS was added to each well and the plate placed in a 37^{o}C 5% CO_2 incubator for 1 hour. PBS was then aspirated from the plate and replaced with 29 µl of either plain chemotaxis media or chemokine diluted in chemotaxis media at the given concentrations. The supplied 5 µM pore membrane was placed over the plate and 25 µl of cell suspension carefully applied to each well as a bubble using a pipette (Figure 2.2 A-C). The plate was then incubated in a 37^{o}C 5% CO_2 incubator for 3 hours. A single piece of Wattmann paper was quickly passed evenly across the membrane to remove cells which have not moved from the top bubble. Centrifugation at 300 g for 10 minutes without a brake assisted stop allowed collection of cells which had passed through the membrane into the bottom well. The membrane was removed and cells from each well were placed in 300 µl PBS for analysis by flow cytometry. A gate was set for "live" cell size, based upon $CD4^+$ labelling of freshly isolated naive $CD4^+$ T lymphocytes, and the number of cells counted within this gate in 30 seconds was recorded for each sample (well).

2.11.2. IBIDI live cell microscopy

For multi-parameter analysis of cell migration across a fibronectin coated surface an µ-Slide assay #80301 (IBIDI, Martinsried, Germany) system was employed as described here (370). Each µ-Slide chamber was coated with pre-warmed (37^{o}C) 45 µg/ml fibronectin for 1 hour at room temperature before washing twice with ultra-pure MilliQ water. One µ-Slide chamber was then filled with chemotaxis media followed by addition of 18 µl of chemokine into the top part of the chamber (Figure 2.2 D). Chemokine was used at 100 nM to give an approximate concentration of 33 nM at the bridge area by diffusion, according to the manufacture's product information (Figure 2.2 E). Freshly isolated naive $CD4^+$ T lymphocytes were re-suspended in chemotaxis media to a concentration of $1x10^7$

cells/ml and 6 µl cell suspension pipetted into the bridge area using the hole provided (Figure 2.2 D). The µ-Slide was placed into an environmental chamber heated to 37^{o}C attached to a Zeiss LSM 510 Meta and a chemokine gradient allowed to form over 15 minutes. An area of cells at the top of the bridge was selected by the criterion that it must contain at least 25 cells. A time series of 60 images were recorded every 15 seconds for 15 minutes. Cells were tracked using Image J software, the Manual Tracking plug-in (Fabrice Cordelières) and using the Chemotaxis and Migration Tool (Gerhard Trapp and Elias Horn). A total of 20 cells were tracked per condition.

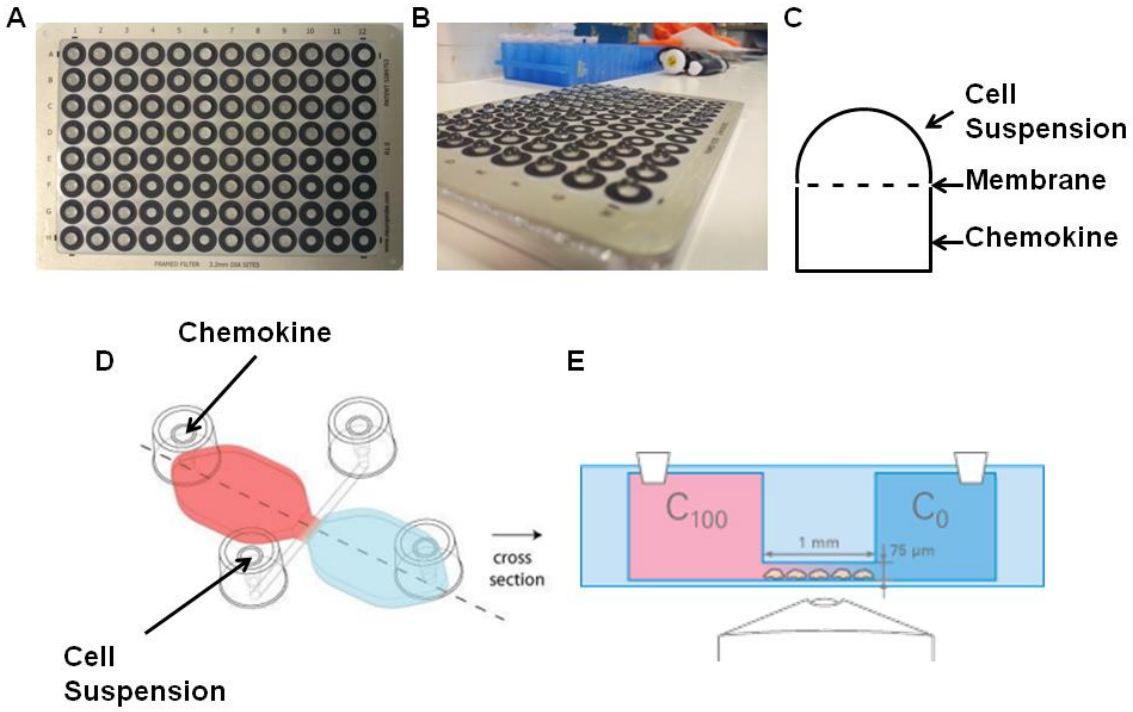

Figure 2.2 Apparatus for measuring *In vitro* cell migration. A. Top down view of a 96 well Neuroprobe plate. **B.** Side on view of a 96 well Neuroprobe plate showing cell suspension bubbles on the surface. **C.** Cartoon showing a bubble of cell suspension on the surface of the membrane, with chemokine in the bottom chamber. Cells migrate towards chemokine through the membrane and are retained in the bottom chamber. Cells are then counted as described. **D.** Top down view of IBIDI µslide. Chemokine and cells are added where indicated. **E.** Side on view of IBIDI µslide showing chemokine gradient ($C_{0\text{-}100}$) and the bridge where cell migration is recorded using confocal microscopy.

2.12. CD62L and CCR7 expression by Flow Cytometry

Freshly isolated naive $CD4^+$ T lymphocytes, SEB activated T lymphocytes or the leukemic T cell line Jurkat were re-suspended in fully supplemented RMPI-1640 at a concentration of $1x10^6$ cells per ml in a 24 well plate. Vehicle or antagonist was added to cells before addition of agonist for the indicated time period. Cells were transferred to micro-centrifuge tubes and centrifuged for 30 seconds, ice cold FACS buffer (PBS + 2% FCS) was added to wash cells and the process repeated a second time. After washing, cells were re-suspended in 100 µl FACS buffer + 1 µl FITC-conjugated anti-CD62L antibody clone DREG-56 (eBioscience, Hatfield, UK) or isotype control IgGκ1 (R and D Systems, Abingdon, UK). Alternatively cells were also labelled with APC-conjugated anti-CCR7 antibody clone 3D12 or isotype control IgG2aκ (Both: eBioscience, Hatfield, UK). Cells were labelled with antibody on ice for 1 hour and washed twice more in FACS buffer. Finally cells were re-suspended in PBS and placed into 5 ml round bottomed tubes (VWR, Lutterworth, Leicestershire, UK) for analysis by flow cytometry. Fluorescent labelling of cells was recorded using a BD FACS Canto II flow cytometer (BD Biosciences, Oxford, UK) and analysed using BD FACS Diva software.

Mean fluorescence index (MFI) was used to describe the level of CD62L expression. For measuring the effect of inhibitors on anti-CD3, anti-CD3/CD28 antibody coated beads or ATP treatment, the change in MFI following treatment was first analysed by a t-test to check for significance. Following this, the vehicle control MFI was set as 100% CD62L expression and all other treatment groups were normalised as percent of control MFI (%). Initial (control) CD62L MFI was variable between donors; therefore normalising to control allows easy comparison of responses between experiments. One Way ANOVA followed by Tukey's post-test was used to compare the loss of cell surface CD62L observed for DMSO versus inhibitor treated groups.

2.13. Reactive Oxygen Species Generation

Cells were re-suspended in supplement free RMPI-1640 and labelled with 10 mM 2',7'-dichlorodihydrofluorescein diacetate (H2DCFDA, Invitrogen, Paisley, UK) at room temperature protected from light for 45 minutes. Cells were then washed into external buffer solution (Table 2.5) and re-suspended at a concentration of $1x10^6$

cells per ml. 90 µl of cell suspension was placed into each well of a 96 well black bottom plate. The plate was then placed into a FluoStar Optima plate reader (BMG Labtech) at 37°C and allowed to rest for 5 minutes. Cells were excited at 485 nm and emission collected at 520 nm every 30-90 seconds. Baseline fluorescence was recorded before the application of vehicle or ATP. Samples were stimulated in three triplicate wells per treatment group. Linear regression was performed on to determine the rate of ROS generation per minute using the below equation:

$$\frac{DCF\ fluorescence\ before\ agonist}{DCF\ fluorescence\ 3600s\ after\ agonist} \div Time\ between\ recordings\ (s) \times 60$$

To measure mitochondrial O_2^- levels cells were loaded with 2.5 µM MitoSOX Red (Invitrogen, Paisley, UK) for 30 minutes at 37°C protected from light. Cells were then washed, treated with agonist for the indicated time, washed into PBS and analysed using flow cytometry. Cells were excited at 488 nm and emission recorded at 585/42 nm.

2.14. Statistical analysis

Data were normalised as described above and in figure legends, statistical analysis was performed using GraphPad Prism software. Graphical representations of data include mean values ± standard error of the mean (SEM) or ± standard deviation (STDEV) for n≥3 and n=2 respectively. For normalised data a One Way ANOVA followed by Tukey's post-test was performed to analyse significance between treatment groups. For all experiments the following marks are used to indicate the levels of significance:

*/#/^ p<0.05

**/##/^^ p<0.01

***/###/^^^ p<0.001

For CD62L experiments mean fluorescent index (MFI) for vehicle and agonist treatment was first compared using a paired one-way Student's t-test, then data was normalised and analysed as described above to compare inhibitor treated groups.

2.15. Appendix of Tables

Component	Concentration
Phosphate buffered saline (without Ca^{2+} and Mg^{2+})	-
Human AB serum	3% v/v
Sodium Azide	1% v/v
EDTA pH 8.0	2 mM

Table 2.1: *Antibody bead wash solution*

Component	Concentration	Protease/phosphatase inhibitor target
H_2O	-	
Tris-HCl pH 7.5	50 mM	
NaCl	150 mM	
Nonident P-40 (NP-40)	1% v/v	
EDTA	5 mM	
Sodium Vanadate	1 mM	Tyrosine Phosphatases, ATPases, Phosphate Transferring Enzymes
Sodium Molybdate	1 mM	Acid and Phosphoprotein Phosphatases
Sodium Fluoride	10 mM	Serine/Threonine Phosphatases
PMSF	40 µg/ml	Serine Proteases
Pepstatin A	0.7 µg/ml	Acidic Proteases
Aprotinin	10 µg/ml	Lipoprotein Lipases
Leupeptin	10 µg/ml	Serine and Thiol Proteases
Soybean Trypsin Inhibitor	10 µg/ml	Trypsin

Table 2.2: *Composition of NP40 lysis buffer and targets of protease and phosphatase inhibitors*

Primary Antibody	Host Species	Final Concentration (µg/ml)	Source
P2X7R	Rabbit	0.2	Santa Cruz
CD62L	Mouse	0.5	E-bioscience
P-Erk1/2	Rabbit	(1:1000 dilution)	Cell Signalling Technologies
P-Akt	Rabbit	0.4	Santa Cruz
P-S6 Ribosomal Subunit	Rabbit	(1:1000 dilution)	Cell Signalling Technologies
Erk1	Rabbit	0.2	Santa Cruz
Akt1	Goat	0.2	Santa Cruz

Table 2.3: *Antibodies used for Immunoblotting*

Where dilutions are given in brackets information about the initial antibody concentration was unavailable.

Component	Concentration
H_2O	-
Tris-HCl pH 7.0	50 mM
Calcium Chloride	6.5 mM
Zinc Chloride	5 µM
Sodium Azide	0.5 g/L
Triton X 100	0-2.5 % as required

Table 2.4: *Composition of Gelatin Zymography Developing Buffer.*

Component	Concentration
H_2O	-
Sodium Chloride	147 mM
Potassium Chloride	2 mM
Calcium Chloride	2 mM
Magnesium Chloride	1 mM
Hepes	10 mM
D-Glucose	12 mM
	pH 7.4 with Sodium Hydroxide

Table 2.5: *Composition of external buffer solution used for methods 2.5, 2.6 and 2.7.*

Component	**Concentration**
H_2O	-
Potassium Chloride	147 mM
Hepes	10 mM
EGTA	1 mM
	pH 7.4 with Potassium Hydroxide

Table 2.6*:* Composition of internal solution for electrophysiology experiments.

3. Chapter 3: Expression and Electrophysiology of P2X7R in Human Naïve $CD4^+$ T Lymphocytes

3.1. Expression of P2X7R in T lymphocytes

3.1.1. Rationale

P2X7R was first cloned in 1997 (189) and its expression was identified in the majority of tissues (241). High levels of P2X7R expression is observed in cells of the immune system including: monocytes, Natural Killer (NK) cells, B and T lymphocytes (242). Before investigating the role of P2X7R in human T lymphocyte function, it was necessary to confirm functional expression of P2X7R in these cells. PCR and immuno-blotting are commonly used to confirm expression of P2X7R at the mRNA and protein levels respectively. Functional expression can also be confirmed by a number of well-established assays. Activation of P2X7R induces influx of Ca^{2+} and Na^{+} and efflux of K^{+} ions which can all be measured using fluorescent dyes. This movement of ions causes a change in the current across the cell membrane which can be measured using electrophysiological techniques. The ability to measure current across cell membranes by fixing (clamping) the cell voltage was initially developed by Cole et al. in the late 1940s and involved a circuit combining an external and internal electrode. This technique was further developed in the 1950s by Hodgkin and Huxley (371). A breakthrough came in the 1970s and 80s, when Neher and Sakmann developed the patch clamp technique, this allowed the measurement of currents through single channels on cells (372). The voltage patch clamp technique (described in materials and methods and here (342)) has been used here to investigate the changes in membrane current in response to agonists and antagonists. Prolonged P2X7R activation can also result in the influx of large molecules through the opening of a membrane associated pore, Pannexin-1 (191, 270, 271, 274). A biochemical assay employing large molecular weight fluorescent dyes such as ethidium bromide can be used to indirectly measure activation of P2X7R (246, 342).

3.1.2. Aim

The aim of these initial experiments is to confirm expression of P2X7R at the protein level and demonstrate using electrophysiology and an ethidium bromide uptake assay that this protein functions as an ion channel and induces

biochemical changes in T lymphocytes. The role of P2X7R in cell proliferation and death will also be investigated briefly.

3.1.3. P2X7R protein is expressed in Leukemic cell lines and human naïve CD4$^+$ T lymphocytes

The leukemic T cell line Jurkat was established from a 14 year old boy with acute T cell leukaemia. This cell line was identified for its ability to produce high levels of the cytokine IL-2; T cell signalling mechanisms were also explored using the leukemic T cell line Jurkat (373–376). It was subsequently discovered that this cell line has aberrant signalling pathways; lack of SHIP and PTEN expression leads to high basal levels of PI(3,4,5)P_3 and constitutive PI3K signalling pathway activation (377). Other leukemic T cell lines include CEM, a cell line derived from an acute lymphoblastic leukaemia in a 4 year old girl. Cell lines have also been developed for studying other cell types such as monocytes; for example, the THP-1 acute monocytic leukaemia cell line (378). THP-1 monocytic leukaemia cells can be differentiated into a macrophage-like cell type by stimulation with PMA or IFN-γ and LPS (379). P2X7R is expressed by the THP-1 monocytic leukaemia cell line and its expression levels are up-regulated following differentiation into macrophage-like cells (380, 381). Treatment of induced macrophage-like cells with ATP causes them to process and release the pro-inflammatory cytokine IL-1β, a process which requires P2X7R activity (246–248). Therefore, the THP-1 acute monocytic leukaemia cell line was used as a positive control for P2X7R expression and function in biochemical assays in this study.

While P2X7R expression has previously been shown in leukemic cell lines, and primary murine and human T lymphocytes it is necessary to confirm this in the cells used for this study. Protein lysates were isolated as described in materials and methods, separated using SDS-PAGE and immunoblotted for P2X7R. Full length P2X7R is 595 amino acids in length (189) and its molecular weight based on this sequence is 68.57 KDa (calculated using P2X7R sequence Accession number: ACS72266 and protein molecular weight tool from www.sciencegateway.org/tools/proteinmw.htm). P2X receptors are subject to a number of post translational modifications including glycosylation (382) and palmitoylation (383). P2X7R is also known to undergo alternative splicing to

produce a number of splice variants of varying size described in more detail in the introduction to this study (240, 363, 366, 384) (Figure 1.21). A rabbit polyclonal antibody raised against human P2X7R that recognises amino acid residues 331-595 of the C-terminus (Santa Cruz P2X7R (H-265)) was used for immunoblotting. This antibody reveals 6 bands indicated by arrows in the top panel of Figure 3.1. In the cell lines and samples from primary cells a band, sometimes appearing as a doublet, between 55 and 72 KDa and is the strongest band in these samples. The largest band is between 95 and 130 KDa which only appears in leukemic cell lines; a band at approximately 72 KDa is faintly visible in all samples except THP-1 acute monocytic leukaemia cell line and naïve $CD4^+$ donor 2. THP1 and Jurkat cell lines also display 1 and 2 band(s) respectively between 43 and 55 KDa, but these are not observed elsewhere. The membrane was stripped and re-probed, using antibody against Erk1 (that also recognises Erk2), to determine the level of protein loaded and transferred to the immunoblot. Protein levels varied across the samples and this may account for the difference in the intensity of bands observed with anti-P2X7R antibody.

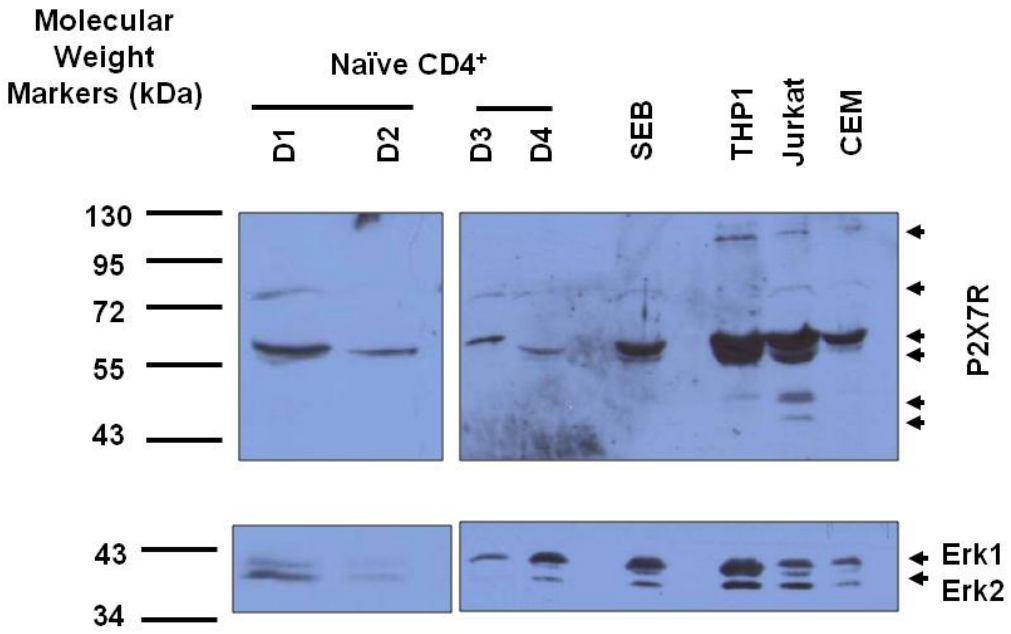

Figure 3.1: Expression of P2X7R protein in leukemic cell lines and human naïve CD4$^+$ and SEB activated T lymphocytes. Naive CD4$^+$ T lymphocytes were freshly isolated from four healthy donors (D1-4); SEB cells were expanded from PBMC as described in materials and methods and removed from ex vivo culture after 9 days. THP1, Jurkat and CEM leukemic cell lines were cultured as described and cells removed from culture. All cells were lysed as described, loaded onto poly-acrylamide gels and proteins separated under reducing conditions using SDS-PAGE. Proteins were transferred to nitro-cellulose membrane, blocked and immunoblotted for P2X7R using anti-P2X7R antibody (Santa Cruz clone: H-265). Membranes were stripped of antibody, blocked and re-probed for Erk1/2 using anti-Erk1 (Santa Cruz). For naïve CD4$^+$ T lymphocytes the blot is representative of 6 donors investigated. For leukemic cell lines and SEB activated T lymphocytes the blot is representative of multiple experiments.

3.1.4. Electrophysiology of P2X7R channel in T lymphocytes

Whole cell patch clamp technique was used to investigate the electrophysiological properties of P2X7R in the leukemic T cell line Jurkat and primary human naïve $CD4^+$ T lymphocytes. Human T lymphocytes expanded *ex vivo* by SEB or PHA were also very briefly investigated. The whole cell patch clamp technique allows the measurement of membrane capacitance, which is defined as "the quantity of charge that must be moved across unit area of the membrane to produce a unit change in membrane potential" (385). Membrane capacitance is measured in Farads (F) and gives an indication of the size of a cell. The membrane capacitance for the leukemic T cell line Jurkat and naïve $CD4^+$ T lymphocytes, as well as *ex vivo* SEB or PHA activated T lymphocytes, is given in Figure 3.2. The membrane capacitance of the leukemic T cell line Jurkat ranged from 1.19 pF to 16.39 pF and the mean membrane capacitance was 7.92 pF ± 0.99 (n=81 cells ± SEM). For naïve $CD4^+$ T lymphocytes it ranged from 1.19 pF to 11.54 with a mean capacitance of 2.53 ± 0.45 pF (n=24 cells ± SEM). Naïve $CD4^+$ T lymphocytes had significantly lower membrane capacitance than the leukemic T cell line Jurkat and T cells expanded *ex vivo* using SEB. For post-analysis of recorded currents, the change in current was normalised to the membrane capacitance recorded for that cell at the beginning of the experiment to give the current density (pA/pF).

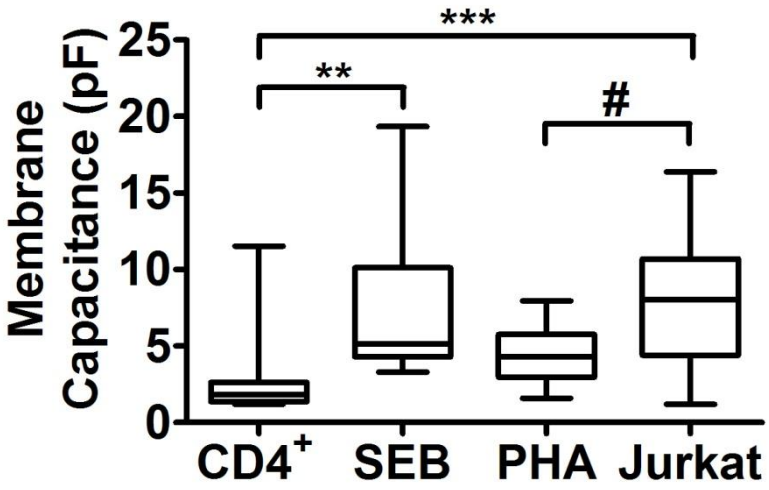

Figure 3.2: Membrane capacitance of different T lymphocytes. Cells were isolated or removed from culture (9 days post activation for SEB and PHA expanded cells). Whole cell seal with resistance >1GΩ was achieved as described and the membrane capacitance was recorded from HEKA patch master 2.11 software. Data is displayed as box and whisker diagrams and analysed by One Way ANOVA followed by Tukey's post hoc test #p<0.05, **p<0.01 and ***p<0.001. Lower (l) and upper (u) 95% confidence intervals and number of cells (n) for each cell type: $CD4^+$ l=1.58, u=3.49 and n=23; SEB l=3.22, u=12.23 and n=8; PHA l=3.23, u=5.84 and n=12; and Jurkat l=7.08, u=8.75 and n=81.

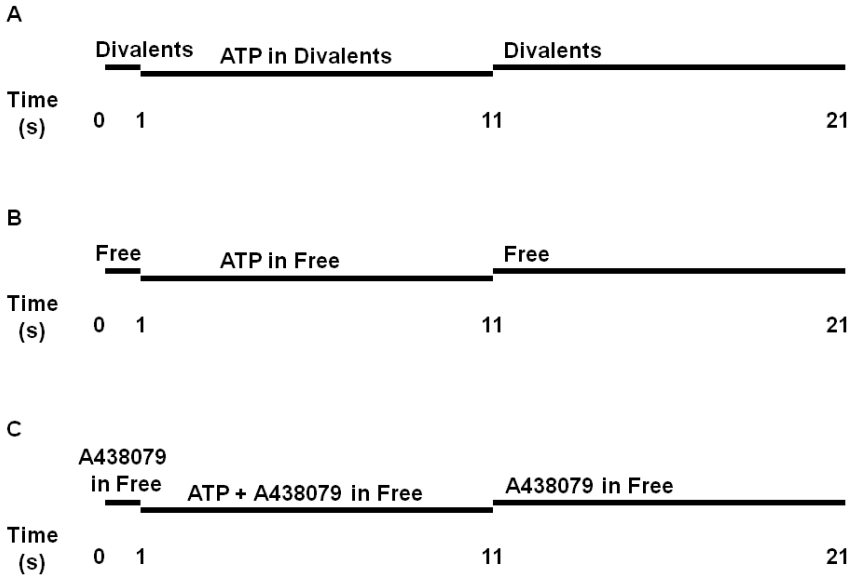

Figure 3.3: Protocols for ATP application. Agonists and/or antagonists were applied in the solution described in Table 2.5, with or without (Free) divalent cations at the indicated points, for the required time periods. After 21 seconds all tubes from the rapid solution changer were switched off and the slow perfusion of divalent cation containing buffer was the only feed into the cell bath. A rest period of 60 seconds was taken between applications of the protocols, to allow full cleansing of the cell bath by the slow perfusion system.

Agonists and antagonists were applied using the protocols in Figure 3.3 using the rapid solution changer (RSC). Protocol A was used to apply ATP in buffer containing divalent cations ($MgCl_2$ and $CaCl_2$); Protocol B to apply ATP in buffer free from divalent cations and Protocol C was used to apply ATP in divalent cation free buffer in the presence of the P2X7R antagonist A438079.

3.1.4.1. Leukemic T cell Line Jurkat

The leukemic T cell line Jurkat was initially used to set up the whole cell patch clamp technique for human T lymphocytes, as Western Blotting indicated that these cells expressed high levels of protein recognised by the anti-P2X7R antibody (Figure 3.1). P2X7R is activated by high millimolar concentrations of ATP and small inward currents were observed in response to 5 mM ATP applied for 10 seconds in buffer containing 2 mM $CaCl_2$ and 1 mM $MgCl_2$ (Figure 3.4 A). When $CaCl_2$ and $MgCl_2$ were removed from the application buffer the current density of response induced by 10 second 5 mM ATP application was increased (Figure 3.4 B). The inhibitory effect of these divalent cations was significant (Figure 3.4 C). The ability of ATP to induce currents in the leukemic T cell line Jurkat was dependent on the concentration of ATP applied for 10 seconds (Figure 3.4 D). Interestingly, application of 0.1 mM ATP caused a small outward current (Figure 3.4 D). Small inward currents were observed with 1 and 3 mM ATP treatment however 5 mM ATP produced a noticeably larger current. The P2X7R competitive antagonist A438079 was applied prior to, and during, 10 second 5 mM ATP (in divalent free buffer). Use of 3 µM A438079 almost completely blocked the response to 5 mM ATP, suggesting that a major component of the inward current in response to ATP is due to activation of the P2X7R channel (Figure 3.4 E and F).

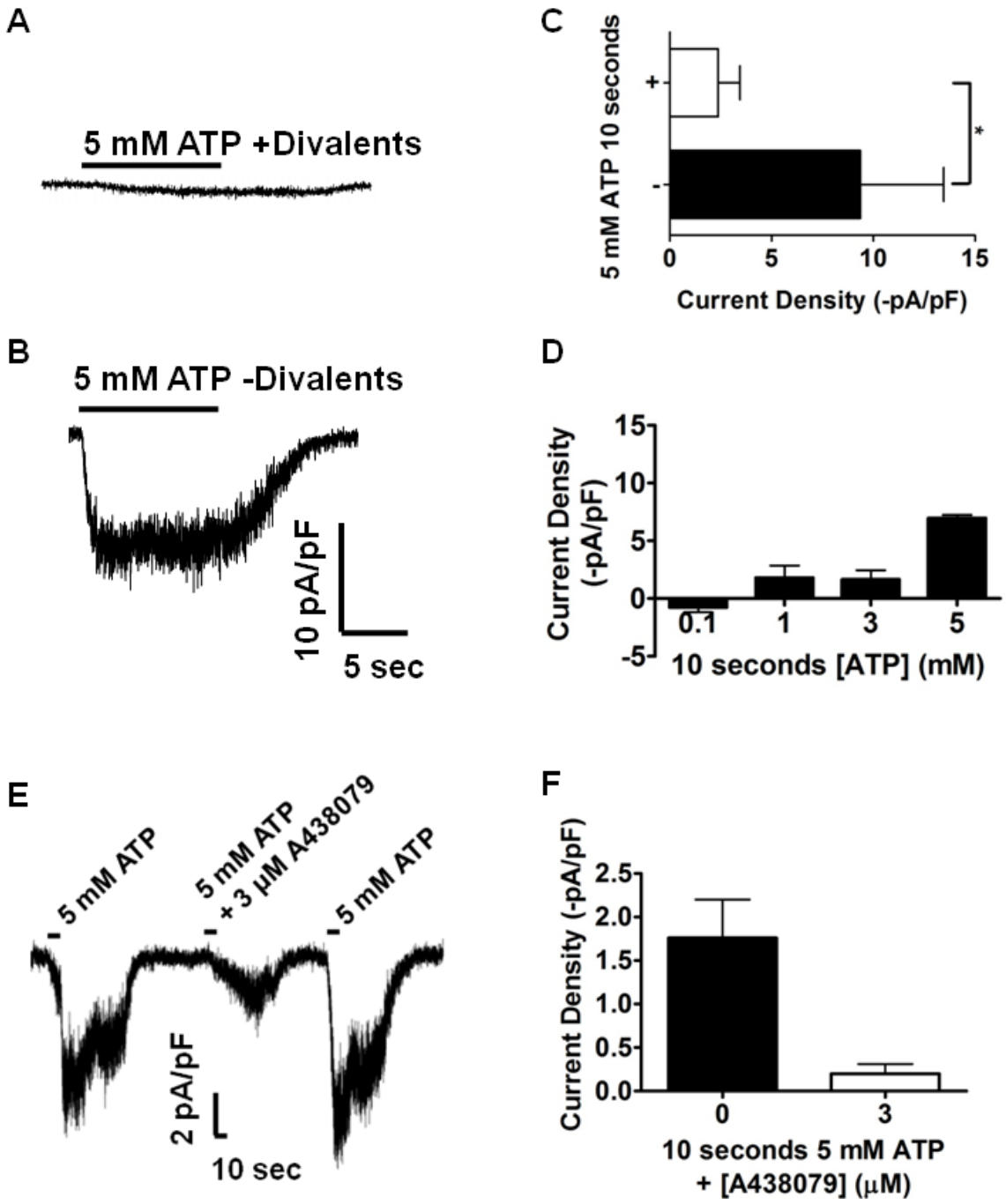

Figure 3.4: Electrophysiology of P2X7R in the leukemic T cell line Jurkat. Whole cell patch clamp electrophysiology was used to voltage clamp cells at -60mV; change in current was measured in response to ATP. **A.** 5 mM ATP was applied for 10 seconds in buffer containing $CaCl_2$ and $MgCl_2$. **B.** 5 mM ATP was applied for 10 seconds in buffer free from $CaCl_2$ and $MgCl_2$. **C.** Current density in presence and absence of divalent cations is compared. **D.** Increasing concentrations of ATP were applied for 10 seconds followed by 60 second pause. **E.** 5 mM ATP was applied for 10 seconds in the presence or absence of 3 µM A438079. **F**. Current density when ATP was applied in the presence or absence of 3 µM A438079 is compared. Currents are from single representative cells and data are the mean of at least 3 independent experiments ± SEM, except **E and F** n=2 ± range. Student paired t-test was performed to compare treatments *p<0.05

3.1.4.2. Activated primary T lymphocytes

Having established the voltage clamp technique using the leukemic T cell line Jurkat, it was desirable to apply this to the investigation of P2X7R expression in primary human T lymphocytes. Naïve $CD4^+$ T lymphocytes were to be the focus of subsequent functional experiments, however the electrophysiology of primary human T lymphocytes activated *ex vivo* by SEB or PHA was briefly investigated. Whole cell patch clamp recordings revealed a small inward current upon 10 second application of 5 mM ATP in both SEB and PHA expanded T lymphocytes (n=1).

3.1.4.3. Naïve $CD4^+$ T lymphocytes

Similar to the leukemic T cell line Jurkat, naïve $CD4^+$ T lymphocyte freshly isolated from peripheral human blood demonstrated inward currents in response to 10 second application of 5 mM ATP. These currents were sensitive to inclusion of divalent cations in the application buffer. Application of 5 mM ATP in $CaCl_2$ and $MgCl_2$ buffer caused an inward current, this was increased when ATP was applied in $CaCl_2$ and $MgCl_2$ free buffer (Figure 3.5 A and B). Although this difference was marked, it was not significant (Figure 3.5 C). Consecutive application of ATP at increasing concentrations, with 60 seconds between applications, reveals concentration dependence for ATP in evoking inward currents. Low concentrations (0.01 and 0.1 mM) of ATP caused very small outward currents but higher concentrations (1, 3 and 5 mM) of ATP caused inward currents (Figure 3.5 D). The requirement for high millimolar concentrations of ATP is characteristic of the pharmacology of the P2X7R, and use of A438079 confirmed P2X7R involvement. Pre-treatment of cells with 10 μM A438079 caused a significant inhibition of current evoked by 10 second 5 mM ATP application (Figure 3.5 E and F).

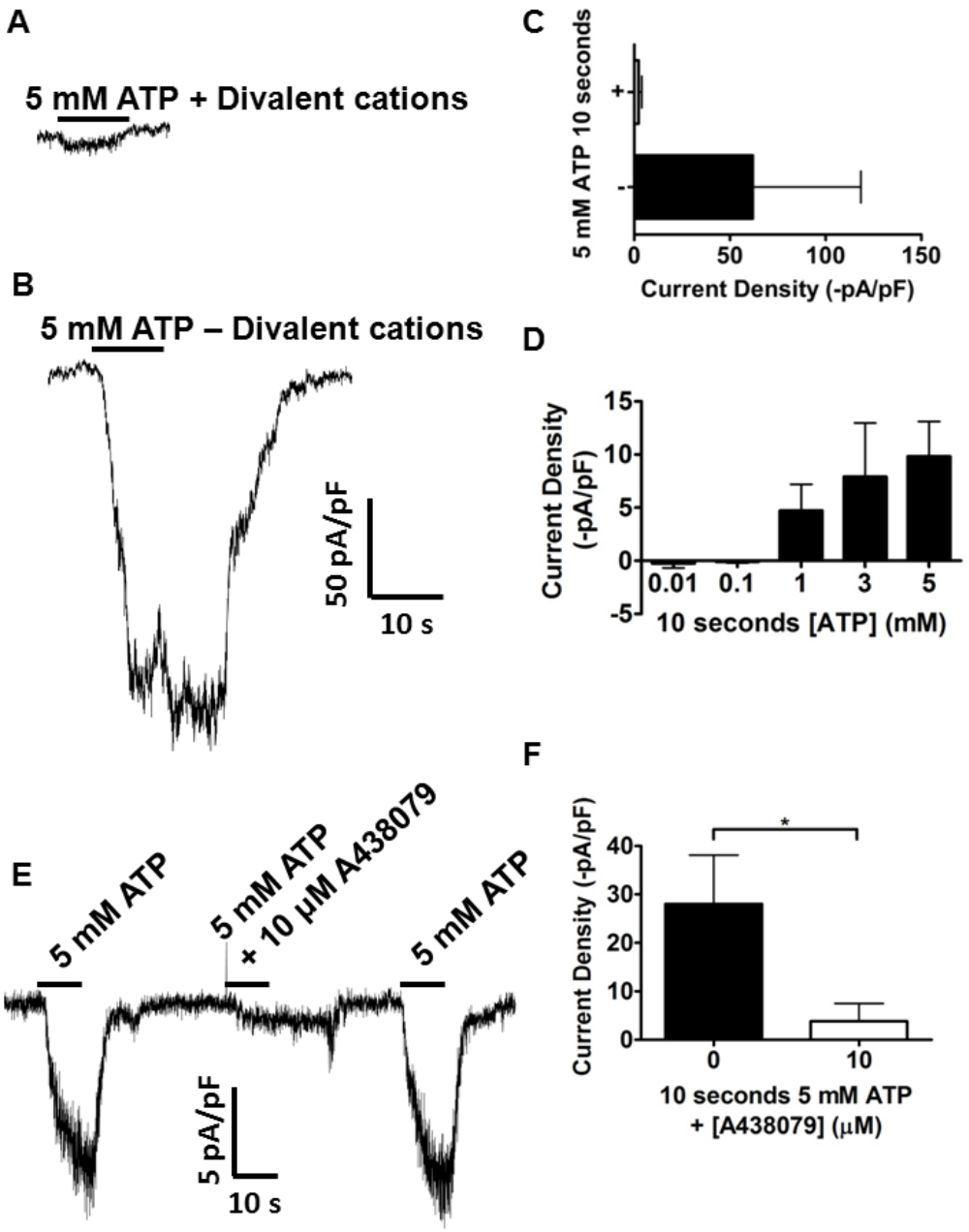

Figure 3.5: Electrophysiology of P2X7R in Naive CD4$^+$ T lymphocytes. Whole cell patch clamp electrophysiology was used to voltage clamp cells at -60mV; change in current was measured in response to ATP. **A.** 5 mM ATP was applied for 10 seconds in buffer containing $CaCl_2$ and $MgCl_2$. **B.** 5 mM ATP was applied for 10 seconds in buffer free from $CaCl_2$ and $MgCl_2$. **C.** Current density in presence and absence of divalent cations is compared. **D.** Increasing concentrations of ATP were applied for 10 seconds followed by 60 second pause. **E.** 5 mM ATP was applied for 10 seconds in the presence or absence of 10 µM A438079. **F**. Current density when ATP was applied in the presence or absence of 10 µM A438079 is compared. Currents are from single cells and representative of experiments conducted in cells from at least 3 independent donors. Data are the mean of at least 3 independent experiments using cells from different donors ± SEM. Student paired t test was performed to compare treatments *$p<0.05$

3.1.5. ATP causes the uptake of large molecular weight molecules into primary human T lymphocytes and leukemic cell lines

As described in the previous section, short (10 second) application of ATP causes the movement of ions across the cell membrane by the activation of P2X7R. Prolonged application of ATP has been shown to lead to a second permeation state through the opening of associated Pannexin-1 hemichannels (271, 274), this leads to the uptake of large molecular weight molecules. Before cloning of the P2X7R, the proposed receptor P2Z was identified by the ability of ATP to cause activation of this second permeation state and subsequent cell death. Therefore, this thesis sought to use an assay for measurement of pore formation, by uptake of the large molecular weight dye ethidium bromide, to provide further evidence for P2X7R expression on human naïve $CD4^+$ T lymphocytes. Previous work in our group has demonstrated that ATP couples to ethidium bromide uptake in HEK293 cells transfected with mouse or rat P2X7R, RAW 264.7 and J774.2 murine macrophage cell lines, primary mouse BMDMs and LPS/IFNγ differentiated human acute monocytic leukaemia cell line THP-1 (204, 246). THP-1 cells differentiated with LPS and IFNγ were used as a positive control to optimise an ethidium bromide assay for measuring pore formation.

[ATP] (mM)	**0**	**1**	**3**	**5**	EC_{50}
THP-1	0.09 ± 0.02	0.302 ± 0.04	0.51 ± 0.1	0.89** ± 0.01	1.65 mM
Naïve $CD4^+$	0.04 ± 0.03	0.22 ± 0.09	0.37 ± 0.09	0.51** ± 0.14	1.47 mM
SEB Activated	0.15 ± 0.02	0.25* ± 0.01	0.54** ±0.01	0.67*** ± 0.01	
Jurkat	0.04 ± 0.02	0.08 ± 0.02	0.22** ± 0.01	0.31** ± 0.03	

Table 3.1: Effect of ATP on ethidium bromide uptake in primary cells and cell lines

Values are given for the rate of ethidium bromide uptake over 15 minutes (normalised to Triton X-100 control) after vehicle or 1, 3, 5 mM ATP treatment (%ΔMax.min-1 ± SEM). The final column also gives the EC_{50} values where they have been calculated for that cell type. One Way ANOVA followed by Tukey's post-test used to determine significance *p<0.05, **p<0.01 and ***p<0.001.

3.1.5.1. Ethidium bromide uptake in THPs

THP1 cells differentiated overnight with LPS and IFNγ and treated with ATP showed an increased rate of ethidium bromide uptake, compared to vehicle treatment (Figure 3.6 A and Table 3.1). This was concentration dependent and the EC_{50} for ATP induced ethidium bromide uptake is 1.65 mM (Figure 3.6 B and Table 3.1). This value is similar to that previously published by our group under the same experimental conditions (246).

3.1.5.2. Ethidium bromide uptake in naïve $CD4^+$ T lymphocytes

Naive $CD4^+$ T lymphocytes freshly isolated from peripheral human blood also show an increase in the rate of ethidium bromide uptake following ATP treatment (Figure 3.7 A and Table 3.1). Rate of ethidium bromide uptake in response to 15 minute vehicle treatment increased significantly following treatment with 5 mM ATP. This effect of ATP was concentration dependent with an EC_{50} of 1.47 mM (Figure 3.7 B and Table 3.1). Un-expectedly, the P2X7R inhibitor A438079 at 10 μM failed to inhibit 5 mM ATP induced ethidium bromide uptake (Figure 3.7 C).

3.1.5.3. Ethidium bromide uptake in SEB activated T lymphocytes

Similarly to human naïve $CD4^+$ T lymphocytes, human T lymphocytes clonally expanded from PBMC using SEB showed increased ethidium bromide uptake in response to ATP (Figure 3.8 A). This response was greater and significant at lower concentrations than for naive cells, with significant increases for 1, 3 and 5 mM ATP treatment (Table 3.1). In SEB activated T lymphocytes 3 mM ATP induced ethidium bromide uptake was significantly inhibited by the exclusion of $CaCl_2$ and $MgCl_2$ in the external buffer solution (Figure 3.8 B).However, there were no significant differences with 1 or 5 mM treatment.

3.1.5.4. Ethidium bromide uptake in the leukemic T cell line Jurkat

The final cell type assessed for their ability to incorporate ethidium bromide following ATP treatment were cells from the leukemic T cell line Jurkat. As with SEB activated T lymphocytes, Jurkat cells also showed increased ethidium bromide uptake in response to ATP with significant increases at 3 and 5 mM (Figure 3.8 C and Table 3.1). ATP induced ethidium bromide uptake was also sensitive to divalent cations (Figure 3.8 D).

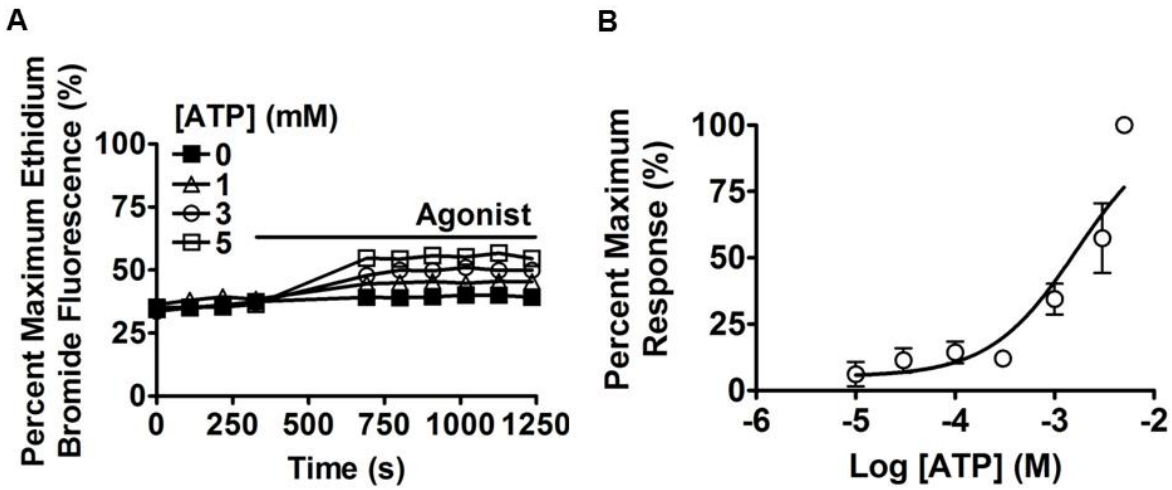

Figure 3.6: ATP induced uptake of ethidium bromide in differentiated THP1 acute monocytic leukaemia cells. THP1 acute monocytic leukaemia cells were differentiated overnight with IFNγ and LPS in a 96 well plate as described (246). Cells were washed and media replaced with physiological buffer containing ethidium bromide. Changes in fluorescence were recorded using a FluoStar Optima plate reader as described and normalised to a percentage of maximum uptake using Triton X-100. **A.** Example kinetic showing the addition of agonist followed by readings for 15 minutes. Rate of ethidium bromide uptake was calculated over the 15 minute period post agonist application and the effect of vehicle compared to increasing concentrations of ATP. **B.** The mean response to 5 mM ATP was set at 100% and other concentrations normalised to this for a concentration response curve (n=3). Prism Graph Pad was used to fit a sigmoidal concentration response curve.

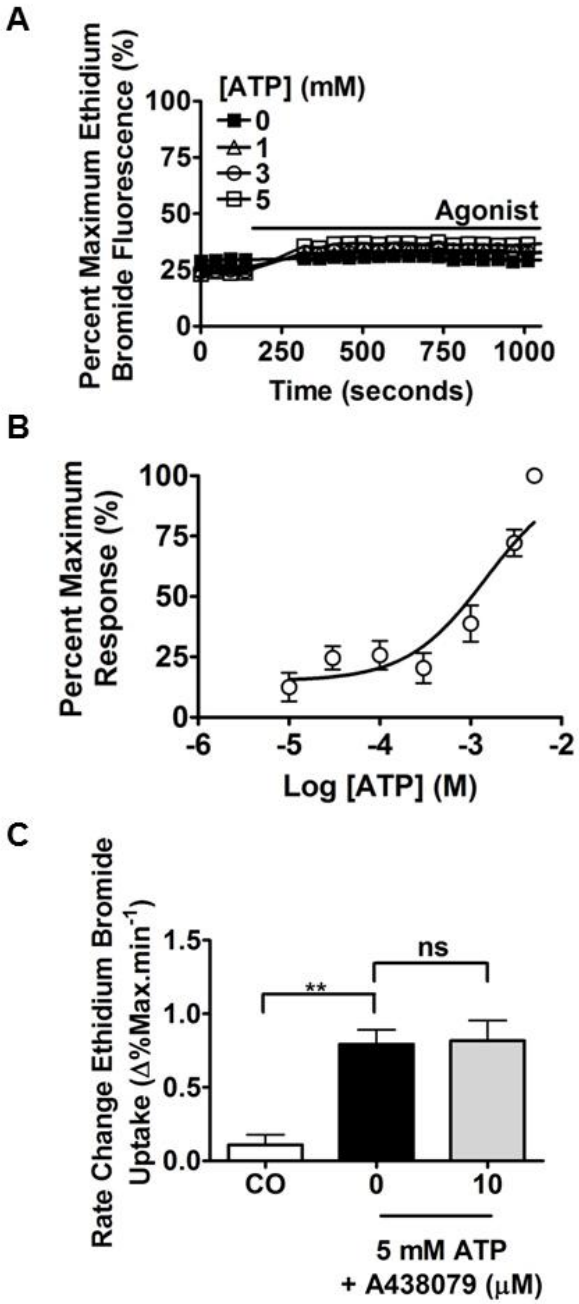

Figure 3.7: ATP induced uptake of ethidium bromide in human naïve CD4$^+$ T lymphocytes. Freshly isolated naïve CD4$^+$ T lymphocytes were washed and media replaced with physiological buffer containing ethidium bromide. Changes in fluorescence were recorded using a FluoStar Optima plate reader as described and normalised to a percentage of maximum uptake using Triton X-100. **A.** Example kinetic showing the addition of agonist followed by readings for 15 minutes. Rate of ethidium bromide uptake was calculated over the 15 minute period post agonist application and the effect of vehicle compared to increasing concentrations of ATP. **B.** The mean response to 5 mM ATP was set at 100% and other concentrations normalised to this for a concentration response curve (n=4). Prism Graph Pad was used to fit a sigmoidal concentration response curve. **C.** Cells were pre-treated with 10 μM A438079 for 30 minutes before ATP application and measurement of ethidium bromide uptake (n=4). One Way ANOVA followed by Tukey's post-test used to determine significance **p<0.01

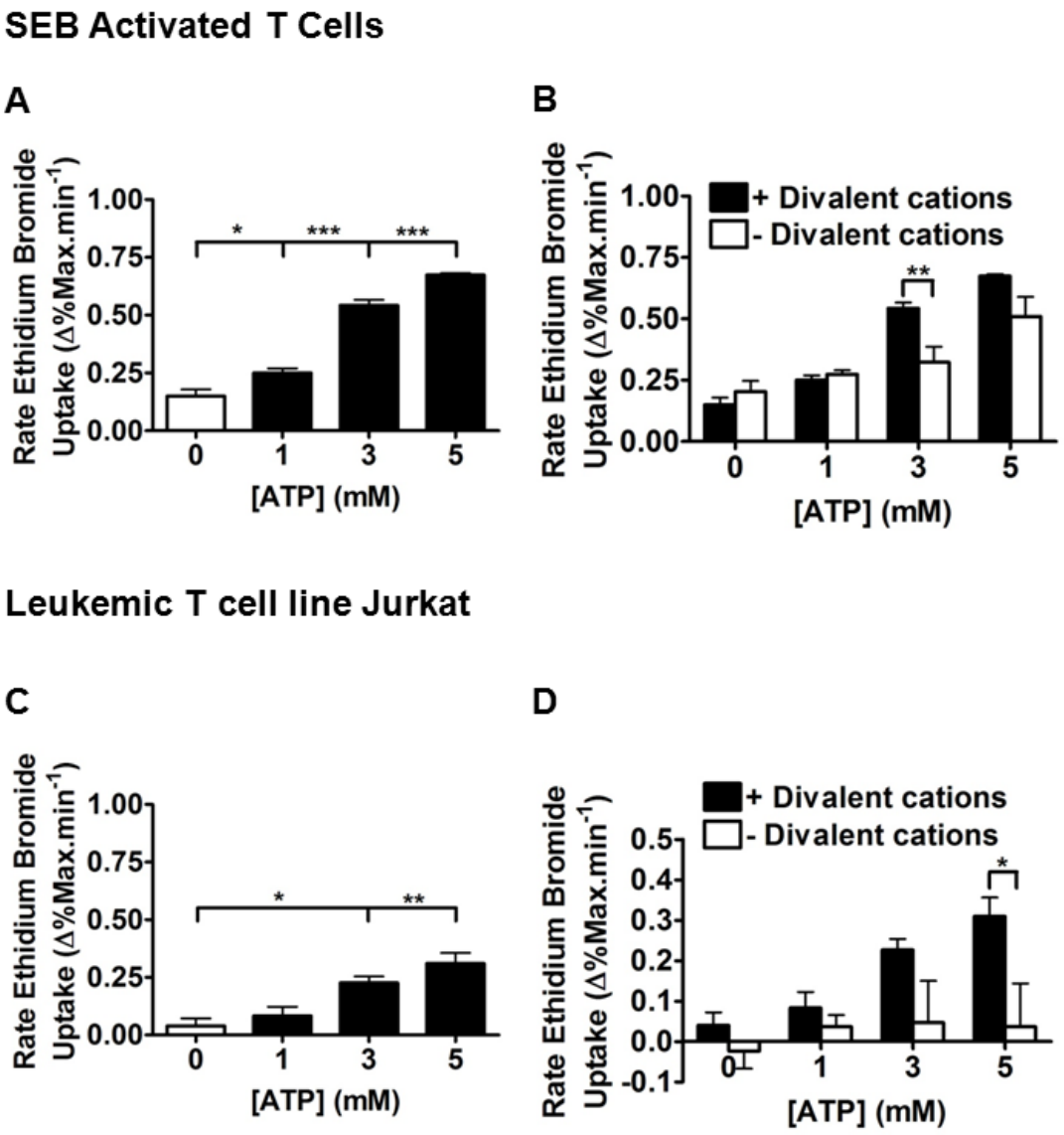

Figure 3.8: ATP induced uptake of ethidium bromide in SEB activated T lymphocytes and the leukemic T cell line Jurkat. Jurkat T cells were removed from culture and washed on day of use. T lymphocytes were activated and clonally expanded from PBMC as described. 8 Days post activation cells were washed and rested overnight in complete RMPI-1640 without IL-2. The following day, cells were removed from culture, washed and media replaced with physiological buffer containing ethidium bromide. Changes in fluorescence were recorded using a FluoStar Optima plate reader, as described and normalised to a percentage of maximum uptake using Triton X-100. For **A.** SEBs and **C.** Jurkats the rate of ethidium bromide uptake was calculated over a 15 minute period post agonist application and the effect of vehicle compared to increasing concentrations of ATP (n=3). For **B.** SEBs and **D.** Jurkats before ATP application cells were re-suspended in ethidium bromide containing physiological buffer or physiological buffer without $MgCl_2$ and $CaCl_2$ (n=3). **A.** and **C.** One Way ANOVA followed by Tukey's post-test used to determine significance *p<0.05, **p<0.01 and ***p<0.001 **B.** and **D.** Two Way ANOVA followed by post-test used to determine significance between groups *p<0.05 and **p<0.01

3.2. Effect of ATP on naïve $CD4^+$ cell death

Pore formation by activation of P2X7R has been proposed as a component of an ATP induced cell death (201, 255, 275). Cell death is an important process and is required for negative selection of T lymphocytes (386–388). The thymic selection and clearance of thymic T lymphocytes are tightly controlled processes, and apoptosis of cells occurs in response to specific stimuli (389). The death of T lymphocytes in the periphery is also required for resolution of inflammation (390). Mature T lymphocytes undergo apoptosis, and the less regulated process of necrotic cell death, during inflammation in response to DAMPS such as ATP. The P2X7R has been extensively investigated for its ability to cause cellular death in a wide variety of cell lines and mouse and human primary cells (391). In the context of murine T cells a raft of studies have focussed on the ability of the enzyme ART2 to irreversibly activate P2X7R by ADP ribosylation leading to a number of P2X7R dependent processes including cell death (206, 260, 262, 263, 265, 266, 284–286, 288, 289, 392). However, human T lymphocytes do not express ART2 or a homologous enzyme, therefore P2X7R induced cell death in human T lymphocytes must be investigated in the context of activation by ATP or BzATP. This current work sought to briefly establish whether human naïve $CD4^+$ T lymphocytes stimulated by ATP would undergo apoptosis and/or necrosis.

3.2.1. Apoptosis

As described previously, apoptosis is a tightly controlled process of cell death by which cells are destroyed without the leaking of their cellular contents into the extracellular space (393). This is coordinated by a complex signalling cascade of caspase activation, cleavage of intracellular proteins, exocytosis of cellular contents in “blebs” and eventual shrinkage of cells and phagocytosis of apoptotic material. A key early step in apoptosis is the loss of lipid membrane structure with PS being “flopped” to the outer leaflet of the cell membrane; this aids phagocytosis (394). PS externalisation can be measured using the protein annexin V; a fluorescent form of annexin V can bind cell surface PS and allow measurement by flow cytometry. ATP has previously been shown to cause cell shrinkage and externalisation of PS in murine thymocytes and $CD4^+$ T lymphocytes (395, 396). Human primary naive $CD4^+$ T lymphocytes were treated with 3 mM ATP for increasing periods of time; although ATP caused a noticeable

increase in annexin V fluorescence this was not significant (Figure 3.9 A). Cells were treated for 1 hour with increasing concentrations of ATP from 1-5 mM and again visible but insignificant increases in annexin V binding were observed (Figure 3.9 B).

Another marker of apoptosis is uptake of the large molecular weight dye PI, which enters the cell and binds to DNA; this causes its fluorescence to increase. Cells were treated with ATP for 5 or 60 minutes before labelling with annexin V and staining with PI; example dual staining plots can be seen in Figure 3.9 C. The percentage of cells which were positive for binding of annexin V and uptake of PI increased after 5 to 60 minutes treatment with 3 mM ATP (Figure 3.9 D).

ATP induced apoptosis is accompanied by a reduction in cell size (shrinkage), for mouse $CD4^+$ T lymphocytes this was required for PS exposure (206, 278). However, human naïve $CD4^+$ T lymphocytes did not significantly shrink in response to 1 hour ATP 1-5 mM treatment (Figure 3.9 E).

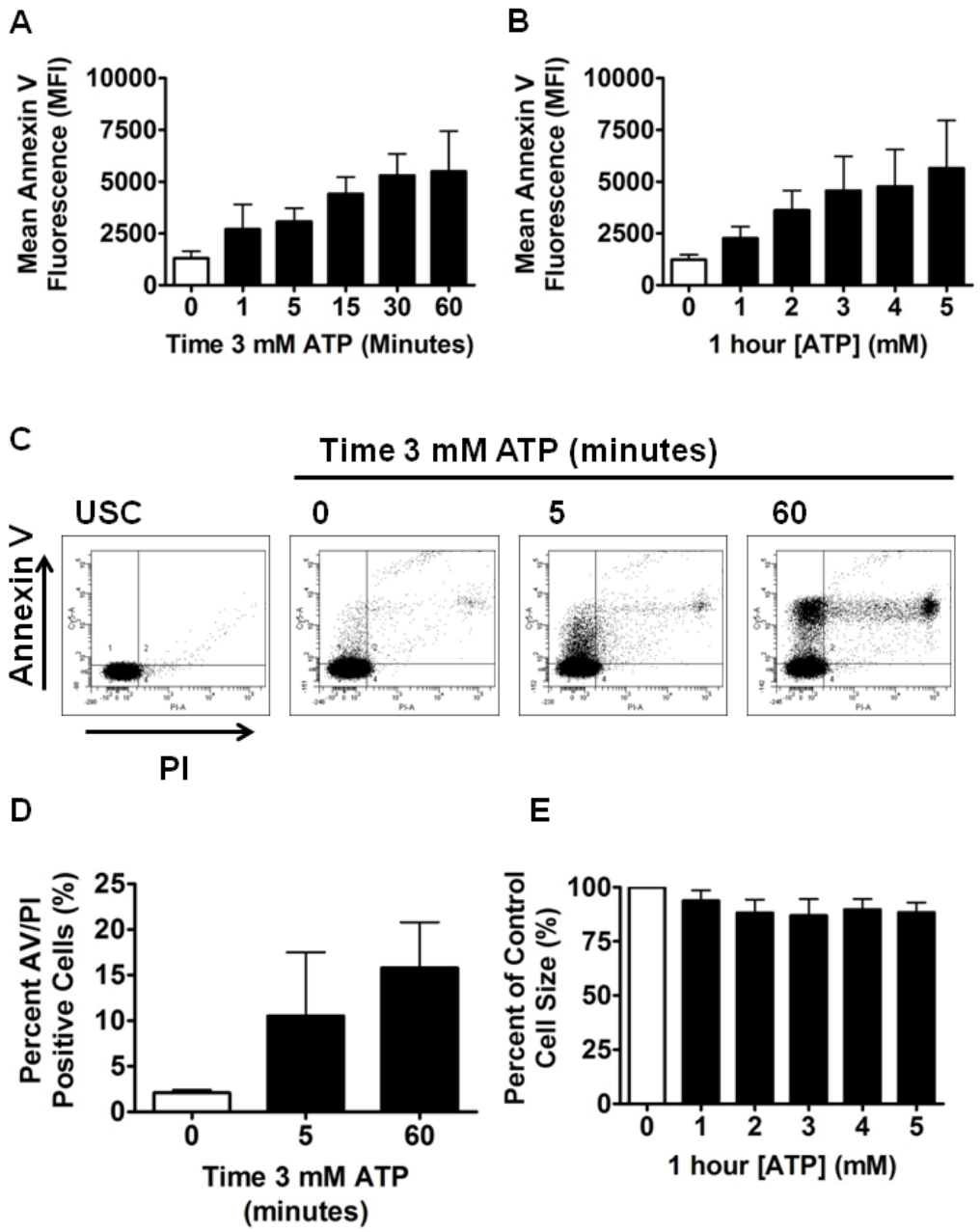

Figure 3.9: Measurement of PI uptake and PS exposure in naïve CD4$^+$ T lymphocytes treated with ATP. Naïve CD4$^+$ T lymphocytes were freshly isolated from peripheral human blood and re-suspended in complete RMPI-1640. **A.** Cells were treated with 3 mM ATP for increasing periods of time or **B.** with increasing concentrations of ATP for 1 hour. Cell surface PS was quantified by measurement of Annexin V binding, as described in materials and methods (n=4). **C.** Cells were treated with vehicle or 3 mM ATP for 5 or 60 minutes before staining with Annexin V and PI. Representative dual staining plots are given including an unstained control (USC), which was used to set the quadratic gate with 1% of cells in Annexin V and PI single positive gates. **D.** The percentage of cells which were dual Annexin V$^+$/PI$^+$ following vehicle or ATP treatment are given (n=2 ± range). **E.** Cells were treated with increasing concentrations of ATP for 1 hour and cell size measured as forward scattered light using flow cytometry. The size of vehicle treated cells was set as 100% and treatments normalised as a percentage of this. One Way ANOVA followed by Tukey's post-test was used to determine significance.

3.2.2. Necrosis

Necrosis is a form of cellular death that occurs in pathological conditions and can be caused by a wide variety of stimulants. It is often un-restrained and can lead to the “bursting” of cells and the release of intracellular contents into the extracellular space. T lymphocytes have been shown to undergo necrotic cell death in response to ATP (206, 255). An early marker of necrosis is the incorporation of dyes such as PI into cells; however, results presented here have already shown ATP not to couple to significant PI uptake. Additionally, as necrotic cells leak cellular contents the level of this release can be used to quantify necrotic cell death. Specifically, the release of the enzyme lactate dehydrogenase (LDH) is a common method for identifying cells undergoing necrosis (342, 397). Supernatant of cells treated with vehicle or ATP were collected and assayed for LDH content, as described in materials and methods. After subtraction of LDH detection in medium alone, naïve $CD4^+$ T lymphocytes show a basal release of 8.94 ± 1.38 % (n=3 ± SEM) of maximum cellular LDH. No significant increase in LDH release was observed after treatment with 0.01-5 mM ATP (Figure 3.10 A). Cells pre-treated for 30 minutes with increasing concentrations of A438079 (0.01-10 μM) followed by 1 hour 3 mM ATP treatment showed markedly lower levels of LDH release compared to both 3 mM ATP plus vehicle pre-treatment (Figure 3.10 B). As 3 mM ATP alone does not increase LDH release, it is possible that the effect of A438079 is an effect on basal LDH release, although this was not investigated further. Finally inhibition of caspases with the broad spectrum inhibitor Z-VAD-FMK had no effect on LDH release in response to 1 hour treatment with 3 mM ATP (Figure 3.10 C).

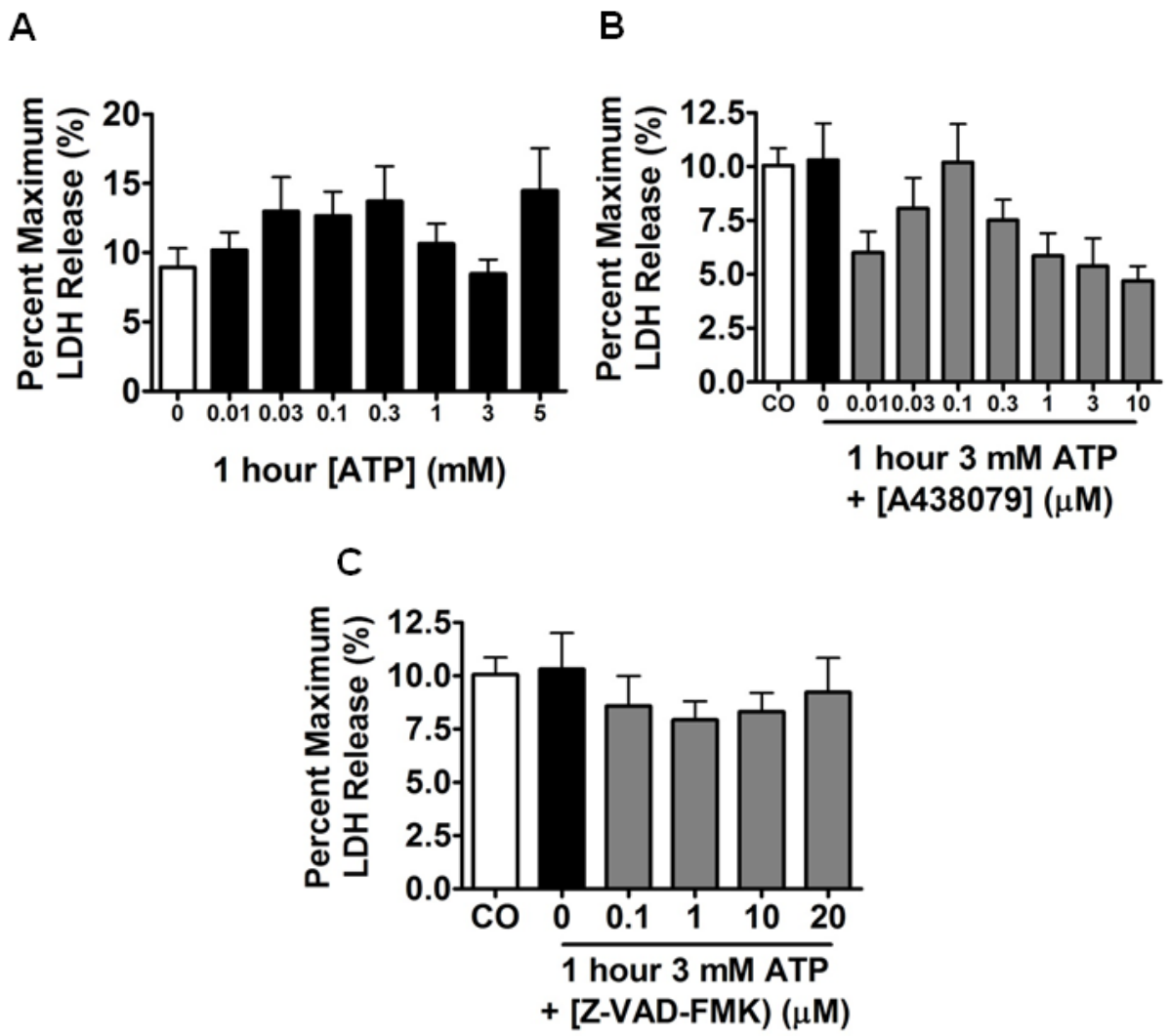

Figure 3.10: Measurement of LDH release in naïve CD4$^+$ T lymphocytes treated with ATP. Naïve CD4$^+$ T lymphocytes were freshly isolated from peripheral human blood and re-suspended in complete RMPI-1640 without phenol red. **A.** Cells were treated with increasing concentrations of ATP for 1 hour, or cells were pre-treated with increasing concentrations of A438079 (**B**) or Z-VAD-FMK (**C**) for 30 minutes before treatment with 3 mM ATP for 1 hour. Supernatant was collected from cells and LDH levels measured as described (n=3). One Way ANOVA was performed followed by Tukey's post test to determine significance.

3.3. Effect of P2X7R inhibition on T lymphocyte proliferation

P2X1, P2X4 and P2X7 receptors have been implicated in human T lymphocyte activation and proliferation. Silencing of P2X7R expression by siRNA or use of the Suramin and oATP demonstrate a role for this receptor in anti-CD3 antibody induced calcium mobilisation, NFAT activation and IL-2 mRNA production (188, 261, 268). In this present study, the role of P2X7R in activation of human naïve $CD4^+$ T lymphocytes was investigated using the selective P2X7R antagonist A438079. The ability of this compound to inhibit T cell proliferation following anti-CD3/CD28 antibody coated bead and IL-2 treatment was investigated. Cells labelled with CFSE were pre-treated with 10 μM A438079 for 30 minutes followed by anti-CD3/CD28 + IL-2 activation, as described in materials and methods. No significant differences in the number of cells in each division of CFSE intensity were observed between vehicle and A438079 treated cells (Figure 3.11 A and B). No significant differences between DMSO and 10 μM A438079 treated cells were observed in any division, including the final 6th division (Figure 3.11 C) (n=3 $p>0.05$).

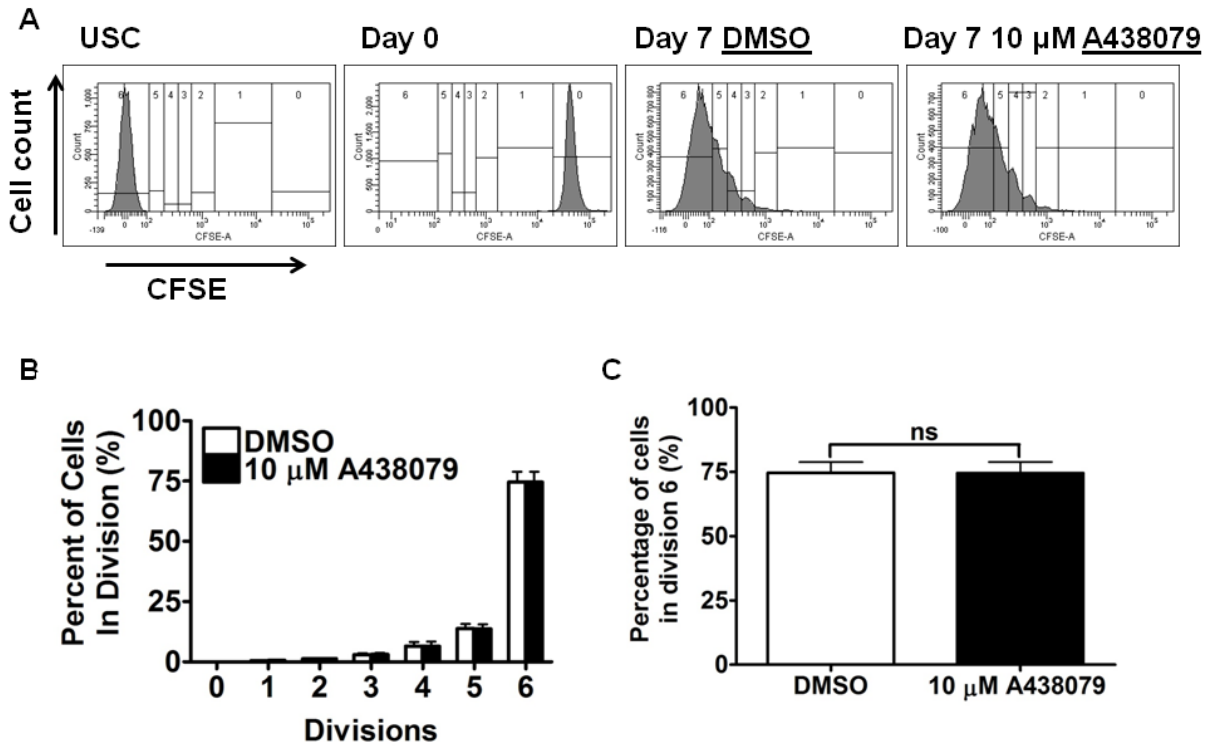

Figure 3.11: Effect of P2X7R inhibition on proliferation of human T lymphocytes. Freshly isolated naïve $CD4^+$ T lymphocytes were labelled with CFSE as described. Cells were analysed on the same day (Day 0) or pre-treated with vehicle (DMSO) or 10 µM A438079 for 30 minutes followed by addition of anti-CD3/CD28 antibody coated beads to cells at a ratio of 3:1. IL2 was added at a final concentration of 36 Units/ml and cells cultured for 7 days before analysis for CFSE fluorescence. **A.** Representative flow cytometry histograms displaying population divisions 0-6. **B.** The effect of A438079 on percentage of cells in each division (n=3). **C.** Statistical analysis of percentage of cells in final division 6 (minimum CFSE fluorescence) (n=3). Two Way ANOVA followed by post-test used to determine significance

3.4. Results Section 3 Summary

- P2X7R protein is expressed by leukemic THP-1 monocyte, Jurkat and CEM T cell lines, as well as primary SEB activated human T cells and naive $CD4^+$ T lymphocytes
- Using voltage clamp electrophysiology, cation sensitive inward currents in response to ATP are observed
- These currents are dependent on ATP concentration and inhibited by the P2X7R antagonist A438079
- Following ATP treatment, significant increases in the rate of ethidium bromide uptake were observed in the acute monocytic leukaemia cell line THP-1, leukemic T cell line Jurkat, human SEB activated and naive $CD4^+$ T lymphocytes
- ATP does not cause significant PS externalisation or PI uptake
- LDH release is not affected by ATP
- Inhibition of P2X7R does not affect T lymphocyte proliferation

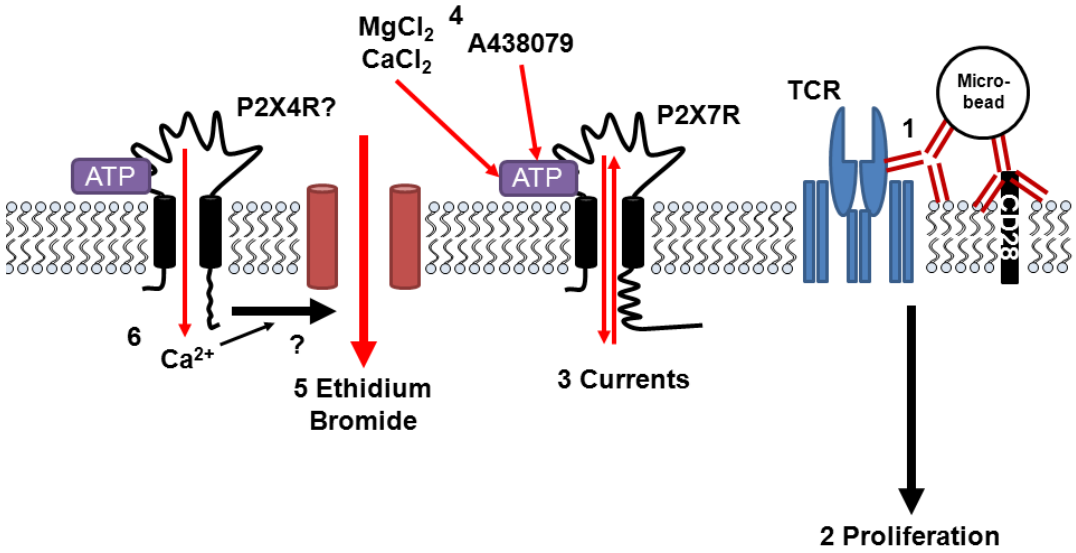

Figure 3.12: Expression of P2X7R by T lymphocytes summary. 1. Anti-CD3/CD28 antibody coated beads activate human naïve $CD4^+$ T lymphocytes; this induces proliferation of these cells, independent of P2X7R (**2**). **3.** ATP causes inward currents in the leukemic T cell line Jurkat and human naïve $CD4^+$ T lymphocytes. **4.** These currents are sensitive to inclusion of divalent cations in the ATP application buffer; currents were also inhibited by the competitive P2X7R antagonist A438079. **5.** The rate of ethidium bromide uptake is increased by ATP, however this process is insensitive to A438079 suggesting involvement of other P2XRs such as P2X4R. **6.** In the leukemic T cell line Jurkat and SEB activated T lymphocytes ethidium bromide uptake was partially dependent on external $CaCl_2$ and $MgCL_2$.

3.5. Results Chapter 3 Discussion

3.5.1. P2X7R Expression

Immunoblotting confirmed that P2X7R is expressed in a number leukemic cell lines and importantly in primary human naïve $CD4^+$ T lymphocytes. The antibody used in this study recognised several bands of varying sizes and there may be biochemical explanations for this. As mentioned previously, P2X7R can be alternatively spliced to produce nine different mRNA transcripts (363). The antibody used in this study recognises a region of the C-terminus of P2X7R and therefore would not be expected to detect the four splice variants which have a truncated c-terminus. This leaves five isoforms including the full length P2X7A receptor, one of which lacks the exon 4 (P2X7C) and three which have alternative start codons (P2X7D, F and H). As P2X7C only lacks a small portion of the receptor it could represent the lower part of the doublet observed in Figure 3.1. The D, F and H transcripts could potentially lead to the expression of shorter P2X7R protein which could correspond to the two bands observed between 54 and 43 kDa in the Jurkat and THP-1 samples. P2X7R is highly glycosylated and the band above the 72 kDa marker may be a highly glycosylated P2X7A receptor, whereas the band below 72 kDa may represent P2X7A in a less glycosylated state as observed by A. Nicke (398). P2X7R can form homotrimeric subunit arrangements or heterotrimeric complexes with P2X4R, either of these conformations could explain the band just below 130 kDa. The fact that these experiments were performed under reducing conditions makes this unlikely, but not an impossibility. While the antibody used here would not be expected to detect P2X7B, E, G or J splice variants; these could still be expressed in T lymphocytes.

The full length P2X7A and truncated P2X7B isoforms are expressed widely throughout cells of the immune system, including naïve and activated $CD4^+$ T lymphocytes, and the P2X7H isoform is expressed at lower levels (363). Although these are the only splice variants studied so far, it is apparent that loss of TM1 or truncation of the C-terminus causes partial or complete loss of P2X7R induced pore formation and cell death (363). Co-expression of the cloned P2XB isoform with P2XA in fact enhances pore formation (240). The relative expression of these P2X7R isoforms and the pattern of their association in primary cells will therefore likely influence the function of these P2X7R complexes. This may help explain

differences between P2X7R responses in healthy human donors and isoform expression may even correlate with disease promotion or progression. Although this is yet to be determined, single nucleotide polymorphism of the P2X7R do correlate with a number of diseases and conditions including: depression (359), *M. Tuberculosis* infection (307, 360) and pain (399).

3.5.2. Analysis of electrophysiological properties of P2X7

Much of what is known about P2X7R electrophysiology has been determined using P2X7R receptors cloned from mouse, rat or human cells. There are notable differences between receptors cloned from these species, therefore the results presented here will be compared with the electrophysiology of human P2X7R (400). Activation of human P2X7R cloned from B lymphocytes and expressed in Xenopus oocytes caused an inward current which increased first exponentially then in a second slower more linear phase (401). In this thesis a similar activation kinetic was observed for both the leukemic T cell line Jurkat and human naïve $CD4^+$ T lymphocytes (Figure 3.3 and 3.4). Little research has been conducted on the electrophysiology of P2X7R in primary cells; however, ATP activates a rapid inward current in murine thymocytes (402). This thesis is therefore novel in its use of voltage clamping to investigate P2X7R expression in primary human T lymphocytes. The P2X7R antagonist A438079 has previously been shown to block 100 μM BzATP evoked currents in 1321N1 cells expressing human P2X7R with a pIC_{50} value of 6.6 (216). The experimental conditions are not directly comparable to those used in this study; however for the leukemic T cell line Jurkat 3 μM A438079 did not completely abolish currents whereas 1 μM A438079 was sufficient in the study by Nelson et al (216).

Divalent cations have previously been shown to inhibit P2X7R activation and the activity of P2X7R in a number of assays, including: ethidium bromide uptake, cell shrinkage and adhesion molecule shedding (CD62L and CD23) (202–208). ATP can be applied in a solution with low concentrations of divalents (252) or nominally free of divalent cations (cations are not added but EDTA or EGTA are also not added to remove contaminating ions) (342) to enhance detection of P2X7R activity.

By using voltage clamp electrophysiology and a dye uptake assay, a large range of divalent cations were compared for their action on the rat P2X7R expressed in HEK293 cells (203). When cells were treated with 30 µM BzATP, Ca^{2+} inhibited 50% of currents and dye uptake at 3.2 and 2.2 mM respectively, whereas Mg^{2+} IC_{50} values were lower at 2.2 and 0.82 mM for these two assays. In this thesis, currents recorded from the leukemic T cell line Jurkat and human naïve $CD4^+$ T lymphocytes in response to 5 mM ATP were diminished when 2 mM $CaCl_2$ and 1 mM $MgCl_2$ were present. Studies have reported species differences for cloned P2X7R; indeed, BzATP is more potent at rat P2X7R than the mouse or human receptor for both currents and dye uptake (400). These species differences can also apply to the effect of divalent cations at the receptor. For example, Zn^{2+} is inhibitory at rat P2X7R but may inhibit or potentiate mouse P2X7R, depending on whether BzATP or ATP is used as the agonist (204). This was measured using ethidium bromide uptake as a read out of P2X7R activation. For human P2X7R transfected into HEK293 cells, 1 mM $CaCl_2$ blocked 38% and 1 mM $MgCl_2$ blocked 50% of YO-PRO-1 uptake into cells stimulated with BzATP (202). This study is in contrast to data presented in this thesis for ATP induced ethidium bromide uptake in the leukemic T cell line Jurkat and SEB activated T lymphocytes. Here, for these two cell types removal of extracellular $CaCl_2$ and $MgCl_2$ in fact inhibited ethidium bromide uptake in response to ATP, this was clearest in the leukemic T cell line Jurkat. It is unclear whether this is due to differences in the agonist, dye or native cell versus recombinant system used in these studies. Additionally, the study by Michel et al. used an external buffer solution containing 280 mM sucrose, whereas this thesis used 147 mM NaCl. Whether it is $CaCl_2$ or $MgCl_2$ that is required for pore formation is also unclear, however one study has shown that external Ca^{2+} is partially required for 1 mM ATP induced PS translocation in mouse thymocytes (256).

Under physiological conditions the extracellular environment would be expected to contain Mg^{2+} and Ca^{2+} ions. With this in mind, although electrophysiology was conducted under divalent free conditions, all other experiments were performed using buffer or culture media containing these ions unless otherwise stated.

3.5.3. Pore formation by leukemic cell lines and human T lymphocytes

Voltage patch clamp experiments focussed on brief 10 second applications of ATP; however prolonged ATP treatment has been associated with opening of a membrane associated pore, Pannexin-1. The THP-1 acute monocytic leukaemia cell line was used to establish an ethidium bromide assay. This assay revealed significant ethidium bromide uptake by the leukemic T cell line Jurkat, SEB activated T lymphocytes and human naïve $CD4^+$ T lymphocytes. Although the P2X7 antagonist A438079 has been shown to potently inhibit Yo-Pro uptake in THP-1 cells with a pIC50 value of 6.7 (216). This is in contrast to the observation here, that 10 μM A438079 was insufficient to inhibit ATP induced ethidium bromide uptake in naïve $CD4^+$ T lymphocytes (Figure 3.7). P2X2R and P2X4R can both couple to pore formation and could therefore be responsible for the A438079 insensitive ethidium bromide uptake observed in this study (403, 404). As expression of only P2X1R, P2X4R and P2X7R has been reported in T lymphocytes, it is most likely that P2X4 is responsible for this pore formation. P2X4R expression was not explored in this study and no selective P2X4R antagonists have been reported in the literature. A molecule, Ivermectin, can potentiate activation of P2X4R and has been used to investigate the role of this receptor in a number of processes (186). However, recently it has been observed that Ivermectin can actually interact with human P2X7R (405). Recent studies have reported a close association between the function of P2X4R and P2X7R; for example shRNA mediated silencing of P2X4 reduces ATP induced LDH release in macrophages (406, 407). ATP induced IL-1β release from macrophages isolated from $P2X7^{-/-}$ mice is promoted by Ivermectin (408). Interestingly, this study by Seil et al. also showed Ivermectin to potentiate 30μM ATP induced Yo-Pro-1 uptake in macrophages from $P2X7^{-/-}$ mice.

3.5.4. Involvement of P2X7R in T lymphocyte death and activation

The opening of Pannexin-1 hemichannels following P2X7R activation is important in the process of ATP induced apoptosis (Figure 1.19). The observation that ATP did not cause significant translocation of PS, nor did it cause a significant increase in PI uptake is in contrast to previous studies (277, 284). The observation that significant ethidium bromide, but not PI, uptake was not seen in naïve $CD4^+$ T

lymphocytes treated with ATP is in agreement with a study of murine T lymphocytes (191). Ethidium bromide is 314 Da and PI is 415 Da suggesting that the pore activated in T lymphocytes following ATP treatment has a cut off somewhere between the size of these two molecules. Indeed, for B lymphocytes this has been suggested to be approximately 320 Da, much smaller than the proposed cut off of 900 Da for other cell types (409). In this thesis, PI and ethidium bromide uptake were not directly compared under the same conditions so it is unclear why one dye was omitted whilst the other was allowed entry. One caveat to measuring ATP induced apoptosis using PS translocation as a marker, is that PS exposure has been suggested as a non-apoptotic signalling mechanism involving activation of P2X7R in murine $CD4^+$ T lymphocytes (395). P2X7R activation may also lead to necrotic cell death; however this was ruled out using an LDH release assay. The observation that antagonism of P2X7R partially reduces basal release of LDH suggests the receptor may play a role in naïve $CD4^+$ T lymphocyte survival.

Several studies have explored the role of P2X7R in T lymphocyte activation (188, 261, 268), however in this thesis pre-treatment of naive $CD4^+$ T lymphocytes with A438079 before anti-CD3/CD28 antibody and IL-2 treatment did not affect their ability to proliferate. The fact that long term culture of these cells was performed in the presence of IL-2 may have masked a possible role for P2X7R in NFAT activation and IL-2 transcription by these cells as seen by Woehrle et al. However, oATP was still able to inhibit T lymphocyte proliferation when cells were cultured with anti-CD3 and anti-CD28 antibodies in combination with IL-2 (at a higher concentration than used in this thesis) (188). oATP has P2X7R independent immuno-suppressant activity (210), therefore it may have non-specific effects that the specific P2X7R antagonist A438079, used here, does not. In published studies, small interfering RNA (siRNA) was also used to investigate inhibit P2X7R and demonstrate a role for it in T cell activation (188, 261). Gene silencing may provide a more robust system to investigate the role of P2X7R in T cell activation and proliferation than pharmacological inhibition.

4. Chapter 4: CD62L Processing

4.1. Mechanisms of loss of surface CD62L expression from human T lymphocytes

4.1.1. Rationale

CD62L is highly expressed on the surface of neutrophils, B cells and naïve and central memory T lymphocytes (18, 107, 410) (Figure 11.1). Recognition and binding to its substrates aids the homing of lymphocytes to secondary lymphoid organs (SLOs), as well as the initial tethering and rolling phases of extravasation into peripheral tissues (Figure 1.10). Activation of lymphocytes by a number of stimuli can lead to the down-regulation of CD62L surface expression (112, 113). In murine naïve $CD4^+$ and $CD8^+$ T lymphocytes the mechanisms for down-regulation in response to soluble anti-CD3 antibody have been elucidated (Section 1.5.4 and Figure 1.13) (114). There is evidence that these pathways may also be involved in the same process in human lymphocytes (133). The molecule PMA activates PKC to cause CD62L processing through ADAM17 and subsequent loss of cell surface expression. These well characterised PKC and CD3 dependent mechanisms were initially used to establish a protocol for measuring cell surface expression of CD62L, as well as the mechanisms involved in its processing from the cell surface.

CD62L is not only down-regulated in response to T lymphocyte activation or PMA stimulation; a number of other extracellular signalling molecules can lead to CD62L loss. One of these is ATP which activates purinergic receptors, such as P2X7R which was characterised in naïve $CD4^+$ T lymphocytes in Chapter 3. ATP induced CD62L down-regulation has been previously reported from B and T lymphocytes (245). The down-regulation of CD62L from the surface of cells from human patients with B cell chronic lymphocytic leukaemia has been shown to involve ATP and P2X7R (208). However, studies involving ATP induced CD62L loss from the surface of T lymphocytes has mainly focused on mouse cells. As stated previously in the context of cellular death mouse T lymphocytes express ART2 which facilitates irreversible activation of P2X7R by NAD (Section 1.8.2 and Figure 1.19). This activation also causes CD62L loss and the role of NAD and P2X7R in this process has been investigated (262, 266, 284–286, 288, 289, 392). The effect of the P2X7R ligands ATP and BzATP on CD62L expression in mouse

T lymphocytes has also been studied. Few studies have used primary human T lymphocytes and only one uses naïve $CD4^+$ T lymphocytes; however, these are stimulated within a population of PMBCs and not isolated themselves (208, 245, 411). This can provide confounding factors from bystander cells. There are also species differences between a number of processes in human and mouse T lymphocytes, these differences will become apparent in the context of anti-CD3/CD28 antibody induced CD62L down-regulation in this section.

4.1.2. Aim

To isolate high purity naïve $CD4^+$ T lymphocytes from healthy donors and explore the pharmacology of the P2X7R agonist ATP and P2X7R antagonists, before trying to elucidate a mechanism of CD62L down-regulation. It was first desirable to establish a positive control for assessing signalling mechanisms involved in CD62L processing. An established method of T cell activation was employed, this involved *ex vivo* culture of isolated human naïve $CD4^+$ T lymphocytes with micro beads (Dynabeads®, Invitrogen, Paisley, UK) coated with anti-CD3/CD28 antibodies. Signalling mechanisms responsible for CD62L down-regulation will then be explored and compared to previously published studies (24, 412). This will allow P2X7R dependent down-regulation of cell surface CD62L to be explored in detail and the mechanisms coupling ATP to CD62L loss to be elucidated.

4.1.3. Anti-CD3/CD28 antibody coated bead mediated CD62L down-regulation

Studies using murine T lymphocytes demonstrated that treatment with soluble anti-CD3 antibodies could lead to significant CD62L down-regulation within 4 hours (114). In this study, these treatment conditions were sufficient to show that inhibition of PI3K by LY294002 and MEK by PD98059 prevented CD3 mediated CD62L down-regulation. Here it is shown that treatment of freshly isolated naïve $CD4^+$ T lymphocytes with 5 µg/ml soluble anti-CD3 antibodies (UCHT-1 clone) was also sufficient to cause significant loss of cell surface CD62L expression (Figure 4.1 A and B).

A stronger activation signal for naïve T lymphocytes is the co-stimulation of CD3 and CD28 co-receptors (24). Cross-linking of anti-CD3 (UCHT1 clone is used in this thesis) antibody by coating of micro beads was able to cause a greater down-regulation of cell surface CD62L expression (Figure 4.1 A and C). Additional coating of beads with anti-CD28 antibody further enhanced CD62L down-regulation (Figure 4.1 A and C). Using anti-CD3/CD28 antibody coated microbeads a time-course of T cell activation was initially performed, this was to determine the earliest time point where CD62L down-regulation became significant. Significant down-regulation was shown to occur after an 18 hour treatment of cells with anti-CD3/CD28 microbeads (Figure 4.1 C and D).

4.1.4. Involvement of MMPs

ADAM 17 is the proposed MMP responsible for down-regulation of cell surface CD62L expression in response to a number of stimuli. This has been determined using inhibitors of MMPs such as Ro31-9790 (117) or silencing of MMP mRNA using siRNA (121). Here, a broad spectrum inhibitor of MMPs GM6001 was used to see if anti-CD3/CD28 antibody treatment down-regulated CD62L through the activity of MMPs. GM6001 is a dipeptide based inhibitor of MMP activity, which binds at the zinc active site of the enzyme. It has activity against a broad range of MMPs with Ki values in the nM to low µM range, it also inhibits the function of ADAM17 ectodomain (413). However, pre-treatment with GM6001 had no effect on anti-CD3/CD28 antibody induced down-regulation of cell surface CD62L (Figure 4.1 E).

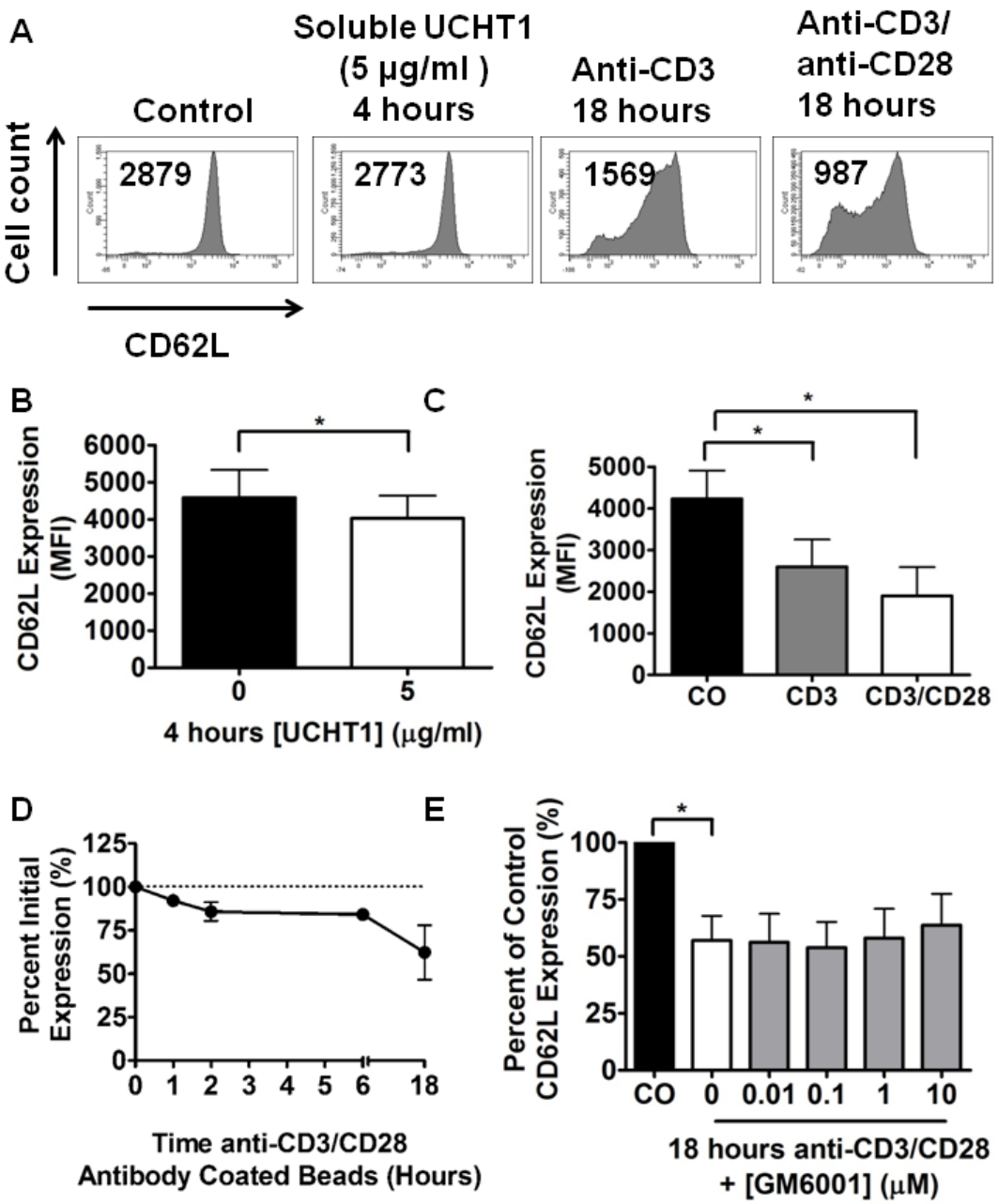

Figure 4.1: Activation of naive CD4$^+$ T lymphocytes induces CD62L down-regulation. A. Representative histograms of CD62L expression measured as described by flow cytometry. Freshly isolated naïve CD4$^+$ T lymphocytes were treated with vehicle, **B.** 5 µg/ml UCHT1 for 4 hours or **C.** anti-CD3 or anti-CD3/CD28 antibody coated beads for 18 hours (n=3). Surface CD62L expression was measured by flow cytometry, as described. Student's t-test was used to compare treatments *p<0.05. For future experiments the effect of bead treatment on MFI was analysed by Student's t-test, CD62L MFI was then normalised as a percent of control (100%) expression. Treatment groups were then analysed by One Way ANOVA followed by Tukey's post-test. **D.** Cells were treated with anti-CD3/CD28 antibody coated beads for indicated time points and CD62L expression measured (n=3). **E.** Cells were pre-treated for 30 minutes with vehicle (DMSO) or indicated concentrations of GM6001 before anti-CD3/CD28 antibody coated bead treatment (n=4).

4.1.5. PI3K/mTOR and Erk1/2 MAPK signalling is not required for anti-CD3/CD28 induced loss of cell surface CD62L expression

A panel of commercially available small molecule inhibitors of intracellular signalling proteins (Table 4.1) were used to determine the signalling mechanism of anti-CD3/CD28 mediated down-regulation of cell surface CD62L expression.

Compound	**Target**	**Source**	**IC_{50} Values**	**Ref**
LY294002	Pan-isoform PI3K	Sigma Aldrich	(See table 1.1) 1-3 µM	(56)
ZSTK474	Pan-isoform PI3K	Gift	(See table 1.1) 0.0046 – 0.049 µM	(414)
IC871114	p110δ PI3K	Gift	(See table 1.1) p110δ = 0.13 µM	(71)
PD98059	MEK1/2	Calbiochem	MEK1 = 2-7 µM MEK2 = 50 µM	(415)
Gö6976	PKC	Calbiochem	PKCα = 2.3 nM PKCβ1 = 6.2 nM	(416)
Rottlerin	PKC	Calbiochem	PKCδ = 3-6 µM PKCα,β,γ = 30-42 µM Mitochondrial uncoupling = 10 µM	(417, 418)
PP2	Src kinases	Sigma Aldrich	Lck = 4 nM Fyn = 5 nM	(419)
Rapamycin	mTOR	Sigma Aldrich	~1 nM	(420)

Table 4.1: Small molecule, cell permeable inhibitors of signalling proteins.

Inhibitors acquired from the sources mentioned here, are displayed with their primary target. The IC_{50} values for inhibition of these signalling proteins, as described in the references, are also displayed.

LY294002, a pan-isoform PI3K inhibitor, was unable to inhibit CD62L down-regulation in response to 18 hour anti-CD3 antibody coated bead treatment (Figure 4.2 A). Reduced CD62L surface expression following 18 hour anti-CD3/CD28 antibody coated bead treatment was not inhibited by LY24002 or ZSTK474, another pan-isoform PI3K inhibitor (Figure 4.2 B and C). This suggests that the PI3K pathway is not involved in CD62L down-regulation in response to anti-CD3/CD28 treatment, however the role of PI3K δ was still explored, as this is the isoform involved in murine CD62L processing (114). Use of the selective PI3K δ inhibitor IC87114 had no effect on anti-CD3/CD28 induced CD62L cell surface loss (Figure 4.2 D).

It is of note that, whilst LY294002 had no inhibitory effect on anti-CD3/CD28 induced CD62L down-regulation, a marked but statistically insignificant *enhancement* of CD62L down-regulation was observed. Anti-CD3/CD28 antibody coated beads plus DMSO control caused a mean down-regulation of 59.17 % ± 21.5 (n=3 ± SEM) when cells were pre-treated with 10 μM LY294002 down-regulation was increased to 74.63 ± 9.88 (n=3 ± SEM). Further down-regulation was seen when using 20 μM LY294002 (n=2 data not shown) and when using anti-CD3 coated antibody beads as a stimulus.

Erk1/2 kinase can phosphorylate ADAM17 on Thr735 which mediates its trafficking to the cell surface and subsequent maturation of the pro form of ADAM17 (132). Indeed, in mice inhibition of MEK upstream of Erk1/2 with PD98059 prevented anti-CD3 induced CD62L down-regulation (114). However, with 18 hour anti-CD3/ CD28 induced CD62L loss in human T lymphocytes PD98059 had no significant effect (Figure 4.2 E).

Nutrient uptake during T lymphocyte activation is very important and expression of the amino acid transport CD69 is increased upon activation (145). mTOR is an important component of the nutrient sensing pathway, it is required for T lymphocyte activation and proliferation (53). mTOR has also been shown to be involved in CD62L down-regulation in mouse naïve $CD8^+$ cells following stimulation of cells with IL-2 (114). In this thesis, Rapamycin was used to inhibit mTOR prior to activation with anti-CD3/ CD28; however no significant inhibition of CD62L loss was observed (Figure 4.2 F).

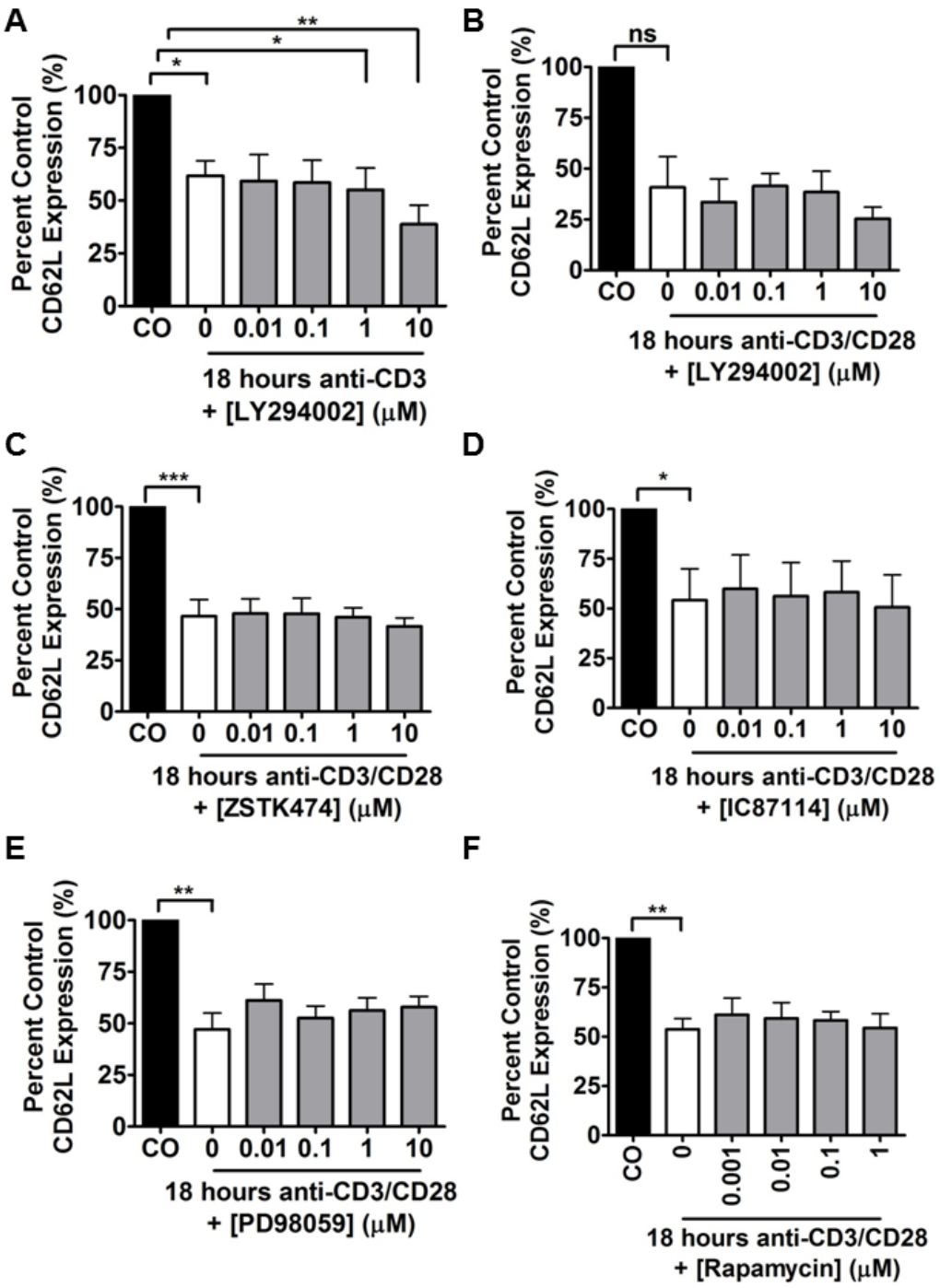

Figure 4.2: PI3K/mTOR and Erk1/2 MAPK signalling is not required for anti-CD3/CD28 induced loss of cell surface CD62L expression. Freshly isolated naive CD4 T lymphocytes were pre-treated with vehicle (DMSO) or small molecule inhibitors at the given concentrations: **A.** and **B.** LY294002 for 1 hour (n=3) **C.** ZSTK474 (n=6) **D.** IC87114 (n=5) **E.** PD98059 (n=6) **F.** Rapamycin (n=3) for 30 minutes. Cells were then treated with **A.** anti-CD3 or **B-F**. anti-CD3/CD28 antibody coated beads for 18 hours. CD62L expression was analysed by flow cytometry as described, the effect of bead treatment on MFI was analysed by Student's t-test *p<0.05 **p<0.01 ***p<0.001. CD62L MFI was then normalised as a percent of control (100%) expression, DMSO treated groups were compared to inhibitors by One Way ANOVA followed by Tukey's post-test *p<0.05 **p<0.01 ***p<0.001.

4.1.6. Activation of mouse splenocytes by anti-CD3 antibody and signalling mechanisms involved in loss of cell surface CD62L expression

As mentioned, the initial experiments to explore the mechanisms of TCR induced CD62L down-regulation involved mouse $CD4^+$ and $CD8^+$ T lymphocytes (114). Therefore, these experiments were briefly repeated using mouse splenocytes to confirm the involvement of PI3K and MEK/Erk1/2 in this process. Treatment of mouse splenocytes with soluble anti-CD3 antibody (Clone 2C11) had noticeably more effect on CD62L expression than anti-CD3 antibody on human $CD4^+$ T lymphocytes. Species differences may therefore explain why little cell surface CD62L was lost with soluble anti-CD3 antibody alone and that immobilisation and/or combination with anti-CD28 antibody was required for more robust CD62L loss from human naïve $CD4^+$ T lymphocytes. Pre-treatment with LY294002 or PD98059 appears to partially inhibit CD62L loss induced by anti-CD3 antibody treatment, but not to the same extent observed by Sinclair et al (Figure 4.3).

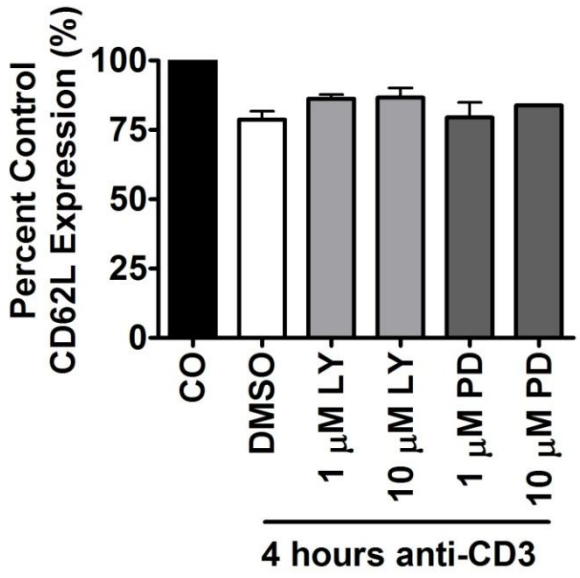

Figure 4.3: Effect of PI3K and MEK inhibition on anti-CD3 antibody induced CD62L loss in mouse splenocytes. Mouse splenocytes were isolated from mouse spleens as described and re-suspended at a concentration of 5 x 10^6 cells/ml. Cells were pre-treated with vehicle (DMSO) or indicated concentrations of LY294002 or PD98059 for 1 hour and 30 minutes respectively. Cells were then treated for 4 hours with 5 µg/ml anti-CD3 antibody (clone: 2C11).CD62L expression was measured by flow cytometry as described (n=2 ± STDEV).

4.1.7. Validation of small molecule inhibitor of signalling proteins

As a further positive control, SEB activated T lymphocytes were pre-treated with LY294002, PD98059, IC87114 or Rapamycin for indicated time periods before treatment with 10 µg/ml soluble anti-CD3 antibody for 5 minutes. SEB activated T lymphocytes were used for these experiments because they are easier to obtain in large numbers and contain higher protein levels than naïve CD4+ T lymphocytes. These compounds inhibited the phosphorylation of MAPK and PI3K signalling pathway components as expected following T lymphocyte activation (Figure 4.4).

Cells pre-treated with vehicle (DMSO) followed by 5 minute 10 µg/ml anti-CD3 antibody treatment showed markedly enhanced phosphorylation of Akt on Ser473, Erk1 on Thr202 and Erk2 on Tyr204, and S6 ribosomal subunit protein (S6) on Ser235 and Ser236 (Figure 4.4). Activation of the PI3K signalling cascade can lead to the phosphorylation of all three of these proteins. Pre-treatment with 10 µM LY294002, 10 µM ZSTK474 or 1 µM IC87114 completely abolished Akt phosphorylation (Figure 4.4 A). Both LY294002 (Figure 4.4 A and B) and IC87114 had a small inhibitory effect on Erk1/2 and S6 phosphorylation, however ZSTK474 ablated anti-CD3 antibody induced phosphorylation of all three proteins (Figure 4.4 A). Activation of MEK leads to phosphorylation of Erk1/2 and MEK can be inhibited by PD98059. As expected, pre-treatment with 10 µM PD98059 completely inhibited Erk1/2 phosphorylation and also partially inhibited Akt phosphorylation (Figure 4.4 A and C). The protein mTOR is part of the PI3K signalling cascade and controls protein synthesis through activation of S6 ribosomal subunit, via S6 kinase (S6K). Pre-treatment with 1 µM Rapamycin partially inhibited S6 phosphorylation in response to anti-CD3 antibody stimulation (Figure 4.4 D).

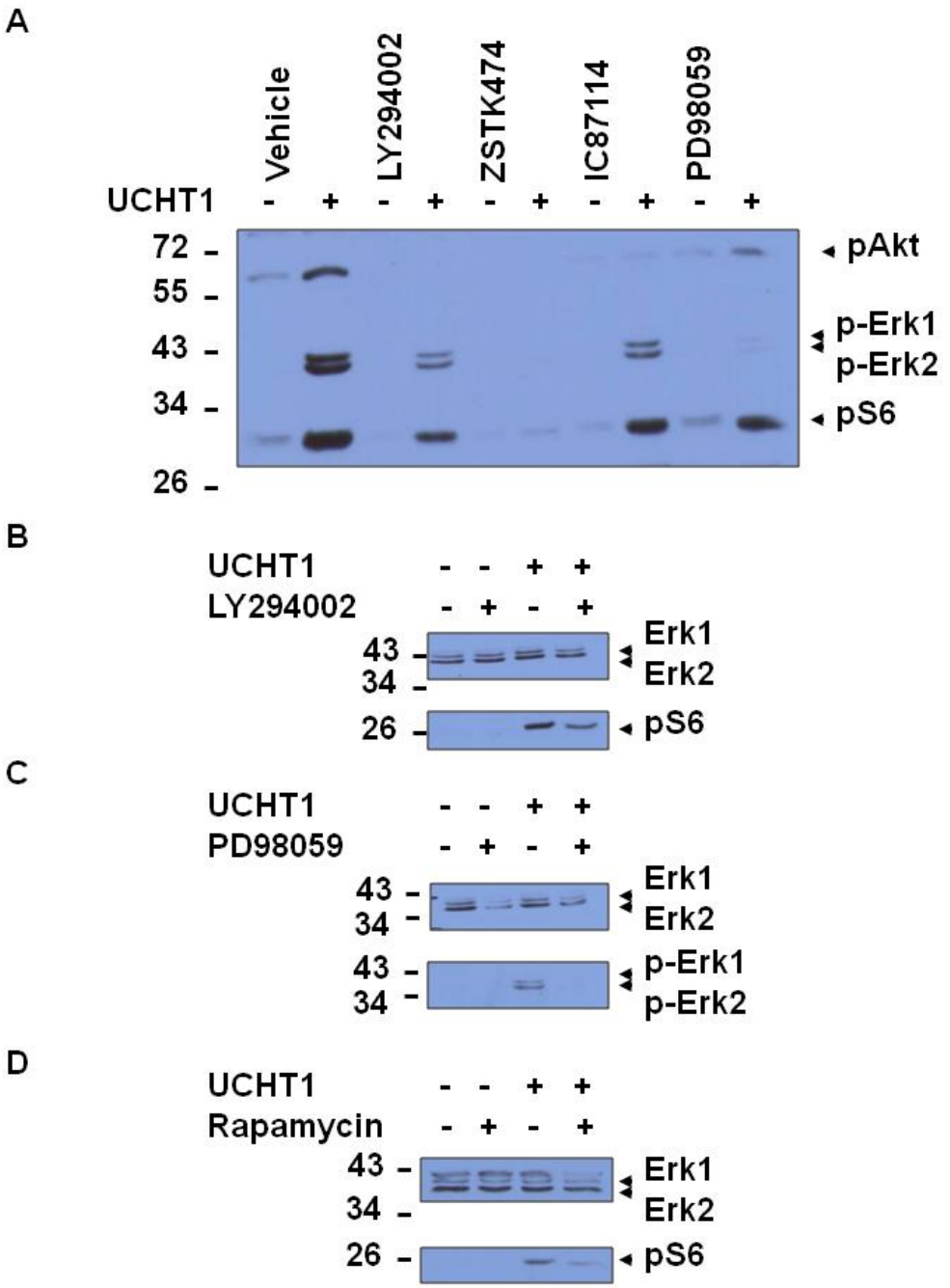

Figure 4.4: Validation of small molecule kinase inhibitors in activated T lymphocytes. SEB activated T lymphocytes were expanded from PBMC as described in materials and methods, IL-2 removed on day 8 and cells removed from ex vivo culture after 9 days. Cells were pre-treated for 30 minutes with vehicle (DMSO), 10 µM ZSTK474, 1 µM IC87114, 10 µM PD98059, 1 µM Rapamycin or for 1 hour with 10 µM LY294002. Cells were then treated with vehicle (media) or 10 µg/ml anti-CD3 antibody (UCHT1) for 10 minutes. All cells were lysed as described, loaded onto poly-acrylamide gels and proteins separated under reducing conditions using SDS-PAGE. Proteins were transferred to nitro-cellulose membrane, blocked and immuno-blotted for: pAkt (Ser473), pErk1/2 (Thr202 and Tyr204/Thr185 and Tyr187) and pS6 (Ser235 and Ser236). Membranes were stripped of antibody, blocked and re-probed for Erk1/2 using anti-Erk1 antibody (Santa Cruz). **A** n=2 and **B-D** n=1

4.1.8. Cell surface loss of CD62L following long term *ex vivo* culture.

Initial experiments focussed on 18 hour treatment of naïve $CD4^+$ T lymphocytes with anti-CD3/CD28, as this was the earliest time point where significant down-regulation of CD62L from the surface of these cells was observed. However, it was possible that the effects of PI3K and/or Erk1/2 inhibition would not be apparent until $CD4^+$ T lymphocytes were fully activated over a longer time period. PI3K and mTOR can control CD62L expression at the transcriptional level, through Akt mediated suppression of FOXO1 and repression of the SELL gene for CD62L (114, 115). Therefore, the effect of the pan-isoform PI3K inhibitor LY294002 and the MEK inhibitor PD98059 on surface levels of CD62L expression on human $CD4^+$ T lymphocytes over a 7 day period of *ex vivo* culture was explored. It is important to note that for long term culture the protocol required to maintain T lymphocytes is different, it requires an anti-CD3/CD28 antibody bead to cell ratio of 3:1 and the addition of 36 Units/ml IL-2. IL-2 has a role in CD62L down-regulation; therefore this system is not directly comparable to 18 hour anti-CD3/CD28 treatment alone (109, 110). After one day, cells treated with DMSO alone expressed 17.11 % ± 4.84 (n=3 ± SEM) of their initial cell surface CD62L levels (Figure 4.5). Over time CD62L levels increased: 29.67 % ± 8.71 after 2 days and 226.4 % ± 110.01 at 7 days. Pre-treatment with 10 μM LY294002 or 10 μM PD98059 has no effect on anti-CD3/CD28 antibody induced CD62L loss over 7 days.

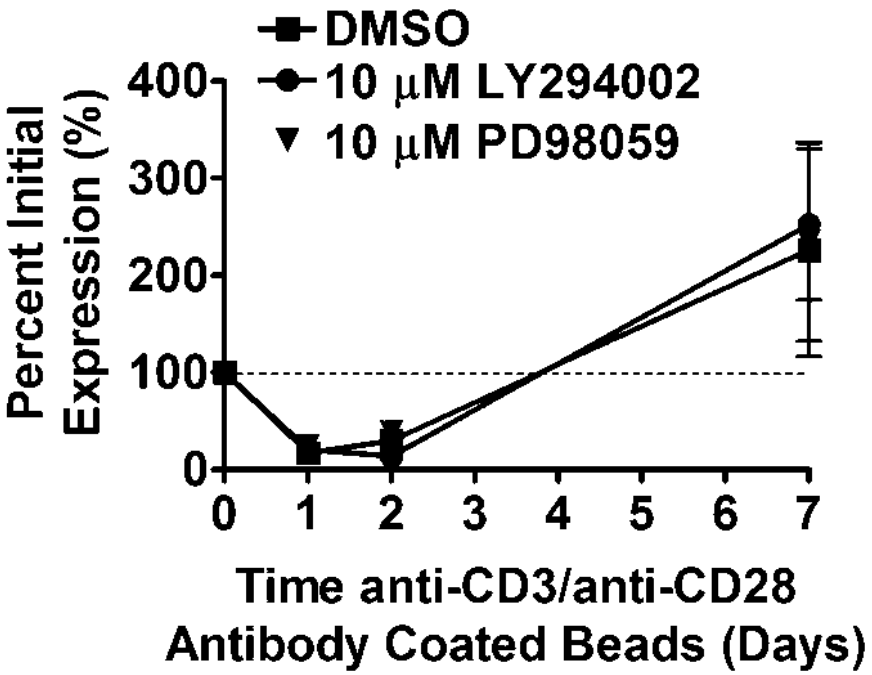

Figure 4.5: PI3K and Erk1/2 are not required for modulating CD62L expression levels over 7 days. Freshly isolated naive CD4 T lymphocytes were pre-treated with vehicle (DMSO) or 10 μM PD98059 for 30 minutes, or 10 μM LY294002 for 1 hour. Cells were then treated with anti-CD3/CD28 antibody coated beads at a ratio of 3:1 (beads:cells). 36 Units/ml IL-2 was added on day 0 and added again every 48 hours, along with a doubling of media volume. Cells were removed from culture at 0, 1, 2 and 7 days post activation and CD62L expression measured by flow cytometry as described (n=3 ± SEM). To compare treatment groups a Two Way ANOVA was performed followed by post hoc test.

4.1.9. CCR7 also undergoes down-regulation following T lymphocyte activation

In addition to CD62L, naïve $CD4^+$ T lymphocytes express high levels of the chemokine receptor CCR7; this was confirmed by dual staining of freshly isolated cells for both CD62L and CCR7. Initially 83.05 ± 7.37 % (n=4 ± SEM) of cells were $CD62L^+/CCR7^+$ (Figure 4.6 A). As for CD62L, the change in CCR7 expression was measured using the mean fluorescent index (MFI). After 18 hour treatment with anti-CD3/CD28 antibody coated beads a significant loss of cell surface CCR7 was observed (Figure 4.6 B and C). The same signalling pathways investigated for CD62L down-regulation were assessed for their involvement in CCR7 processing (Figure 4.6 D). Inhibition of PI3K by the pan-isoform inhibitor LY294002 and ZSTK474, as well as the PI3Kδ inhibitor IC87114, caused partial restoration of CCR7 surface expression lost after anti-CD3/CD28 treatment. This was also seen when cells were pre-treated with the Src kinase inhibitor PP2. Like CD62L, CCR7 is down-regulated initially at 1-2 days post activation, but after 7 days levels return to normal (Figure 4.6 E).

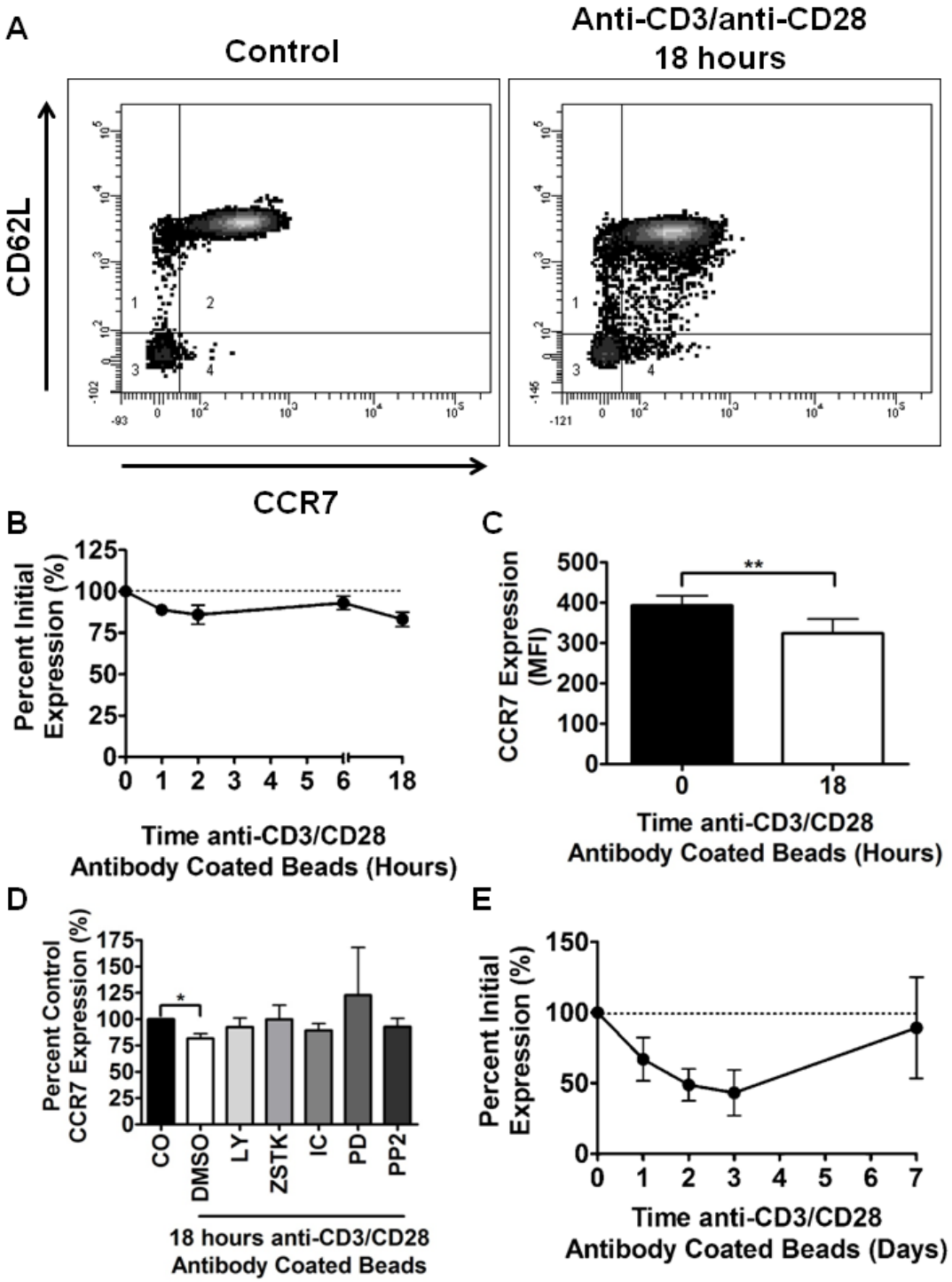

Figure 4.6: Cell surface expression of CCR7 is down-regulated following T lymphocyte activation and may require PI3K and Erk1/2 signalling. A. Freshly isolated naïve $CD4^+$ T lymphocytes were treated with anti-CD3/CD28 antibody coated beads, stained for CD62L and CCR7 and dual staining measured using flow cytometry. **B.** Cells were treated for up to 18 hours and CCR7 surface expression measured (n=4). **C.** Analysis of significant CCR7 MFI decrease at 18 hours by Student's t-test **p<0.01 (n=3). **D.** Cells were pre-treated with vehicle, 1 μM IC87114, 10 μM LY294002, 10 μM ZSTK474, 10 μM PP2 or 10 μM PD98059. Cells were then treated with anti-CD3/CD28 antibody coated beads for 18 hours. CCR7 surface expression was then measured (n=4). **E.** The effect of 7 day anti-CD3/CD28 antibody coated beads on cell surface CCR7 expression (n=3).

4.1.10. Effect of PMA and ATP on cell surface CD62L expression on human naïve $CD4^+$ T lymphocytes and the leukemic T cell line Jurkat

Having established an assay for measuring changes in cell surface expression of CD62L and confirmed P2X7R expression on the leukemic T cell line Jurkat and human naïve $CD4^+$ T lymphocytes (Results Chapter 3), the ability of PMA and ATP to induce cell surface CD62L loss was investigated. Vehicle treated naïve $CD4^+$ T lymphocytes show uniformly high levels of CD62L expression (Figure 4.7 A), however the leukemic T cell line Jurkat expresses very low levels of CD62L (Figure 4.7 B). In naïve $CD4^+$ T lymphocytes both PMA and ATP significantly induced loss of cell surface CD62L (Figure 4.7 A), whereas the leukemic T cell line Jurkat responded only to PMA (Figure 4.7 B).

PMA has been used to investigate CD62L processing in a number of cell types (121, 421). Here the loss of cell surface CD62L expression from the leukemic T cell line Jurkat and naïve $CD4^+$ T lymphocytes with PMA was dependent on PMA concentration (Figure 4.8 A and B). Using concentration response curves, EC_{50} values for PMA on CD62L down-regulation were determined for both cells types: Jurkat EC_{50} = 12.24 nM and naïve $CD4^+$ EC_{50} = 12.68 nM.

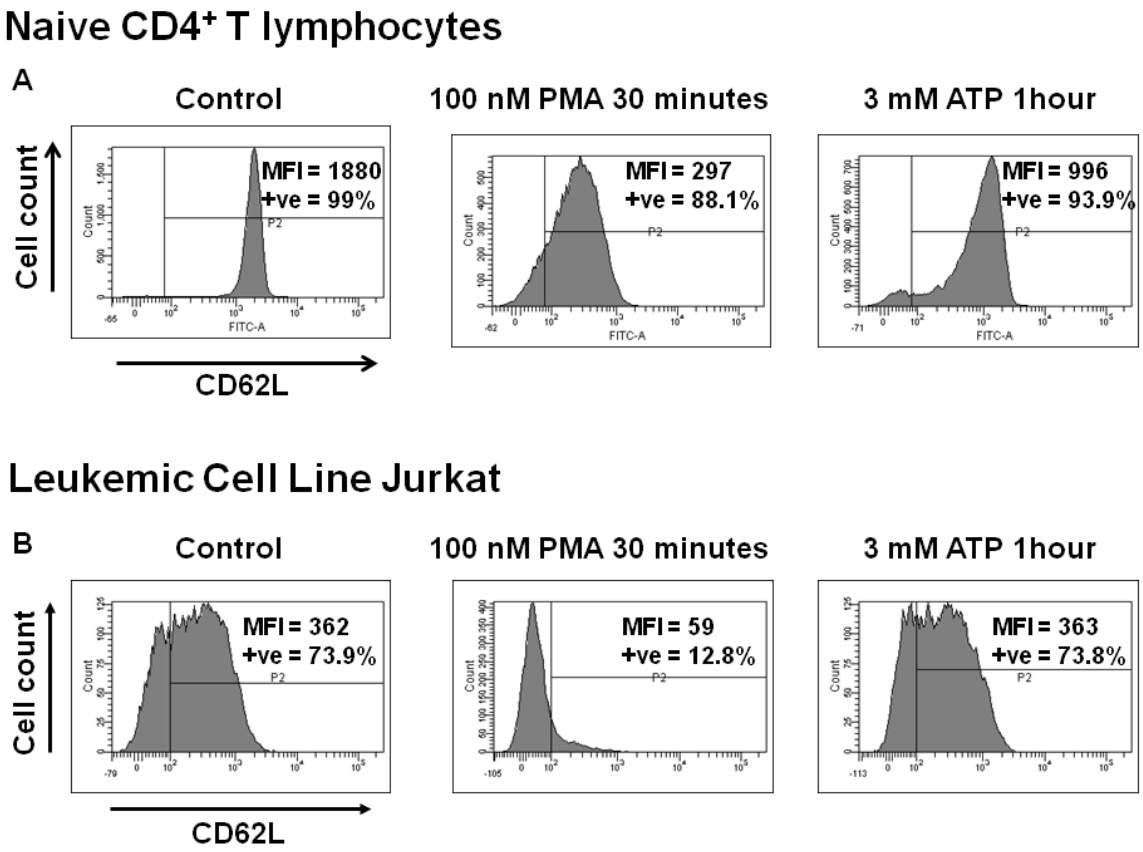

Figure 4.7: The effect of PMA and ATP on CD62L surface expression on the leukemic T cell line Jurkat and human naïve CD4$^+$ T lymphocytes A. Freshly isolated human naive CD4$^+$ T lymphocytes were treated with vehicle, 100 nM PMA for 30 minutes or 3 mM ATP for 1 hour. Surface CD62L expression was measured by flow cytometry as described. Representative histograms of CD62L expression are given, with the mean fluorescence index (MFI) displayed. A gate (P2) has been set to include 1% of cells from the isotype control; CD62L positive (+ve) cells from control and treatment groups are those which fall within this gate. **B**. The leukemic T cell line Jurkat was also treated under the same conditions and analysed for surface CD62L expression.

4.1.11. Loss of cell surface CD62L from human naïve $CD4^+$ T lymphocytes is dependent on ATP concentration

To explore the concentrations of ATP required to elicit a significant down-regulation of CD62L in the leukemic T cell line Jurkat and human naïve $CD4^+$ T lymphocytes, non-cumulative dose response experiments were performed (Figure 4.8 C and D). After 5 minute or 1 hour treatment with ATP, naïve $CD4^+$ T lymphocytes showed significantly decreased cell surface CD62L expression (Figure 4.8 C). This effect was dependent on ATP concentration with EC_{50} values of 877 µM and 888.6 µM for 5 minutes and 1 hour treatments respectively. The EC_{50} values for both time points are close to 1 mM which is typical for the pharmacology of P2X7R and less indicative of P2X1R or P2X4R. However, no down-regulation was observed in the leukemic T cell line Jurkat after 1 hour treatment with ATP at concentrations from 0.01 – 5 mM. As described above, PMA can induce significant CD62L loss in this cell line, therefore PMA acted as a positive control for CD62L down-regulation in these experiments.

4.1.12. Loss of cell surface CD62L from human naïve $CD4^+$ T lymphocytes is rapid and sustained

Next, the kinetics of ATP induced CD62L down-regulation were investigated; 3 mM ATP was chosen because it is a suboptimal concentration above the EC_{50} for both 5 minute and 1 hour ATP treatment described above. Here, significant CD62L down-regulation was observed from naïve $CD4^+$ T lymphocytes after 5 minutes and after 15 minutes of treatment only 59.67 ± 6.45 % (n=3 ± SEM) of cell surface CD62L remained (Figure 4.8 E). Significant loss of CD62L expression was maintained for up to 6 hours, although cell surface expression began to increase; at 6 hours cells expressed 70.53 ± 6.45 % (n=3 ± SEM). The leukemic T cell line Jurkat did not display CD62L down-regulation in response to 3 mM ATP treatment at any time point from 1 – 60 minutes (Figure 4.8 F). As expected, cell surface loss of CD62L expression by the leukemic T cell line Jurkat was observed in response to PMA treatment.

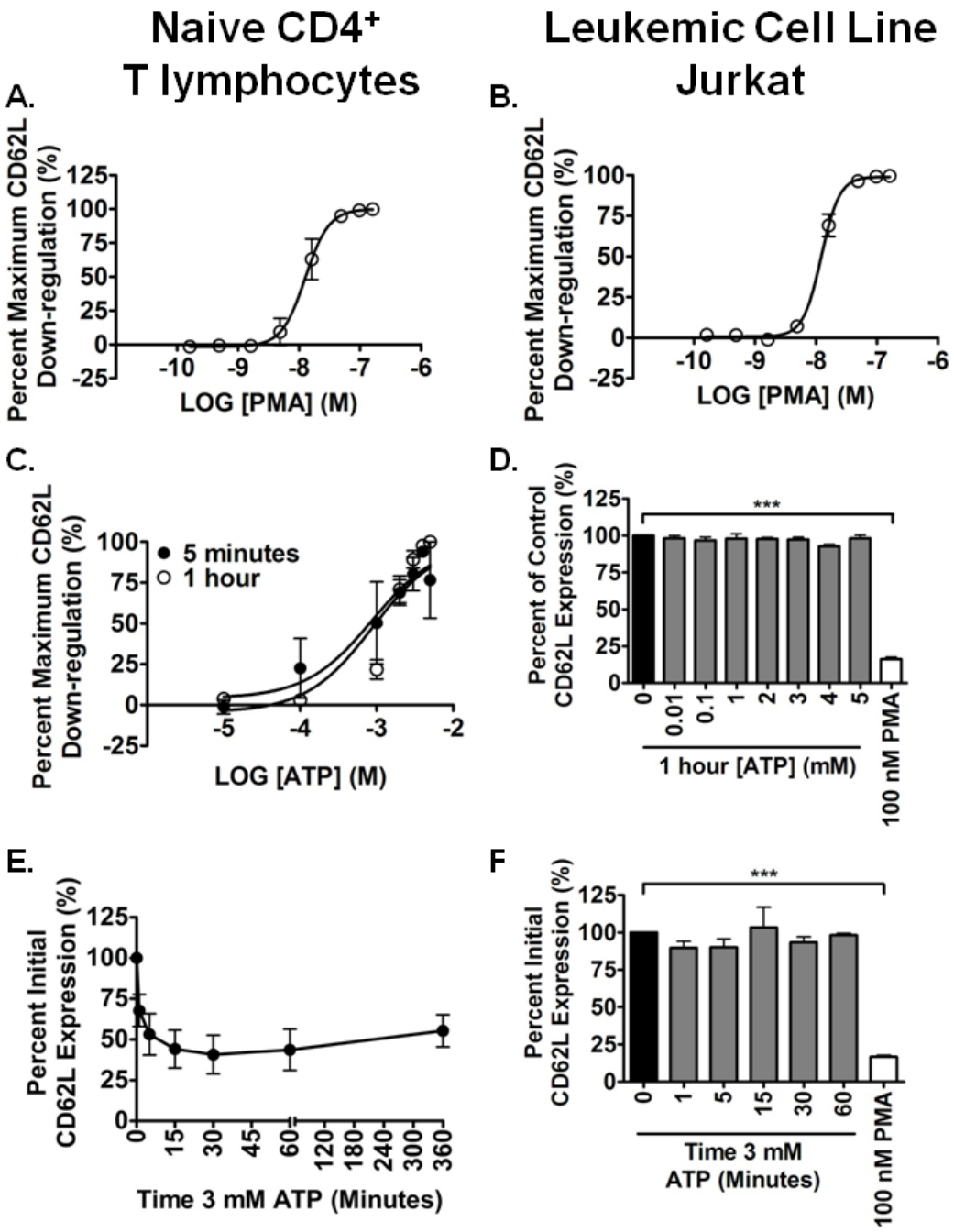

Figure 4.8: PMA and ATP induce CD62L down-regulation from naïve CD4$^+$ T lymphocytes and the leukemic T cell line Jurkat. Freshly isolated naïve CD4$^+$ T lymphocytes (**A, C and E**) or leukemic T cell line Jurkat (**B, D and F**) were treated with either PMA or ATP. A 30 minute treatment with 100 nM PMA was used as a positive control for leukemic T cell line Jurkat. **A and B:** cells were treated with increasing concentrations of PMA for 30 minutes (n=3). **C and D:** Cells were treated for 5 minutes or 1 hour with increasing concentrations of ATP (0.01 – 5 mM) (n=3). **A-C** For concentration response curves the maximum observed down-regulation of cell surface CD62L following agonist treatment is set as 100% and other concentrations are normalise to this. **E. and F.** Cells were treated with 3 mM ATP for the times indicated (n=3). Surface CD62L expression was measured by flow cytometry as described. One Way ANOVA was used to compare treatment groups *** p<0.001

4.1.13. P2X7R inhibitors block ATP induced, but not anti-CD3/CD28 induced down-regulation of cell surface CD62L

In chapter 3 the expression of P2X7R was confirmed in naïve $CD4^+$ T lymphocytes this, coupled with almost millimolar EC_{50} values, suggest an involvement of P2X7R in ATP induced loss of CD62L surface expression. This needed to be confirmed pharmacologically as T lymphocytes express ATP sensitive P2Y2 receptors which can also cause ADAM activation and substrate cleavage (422). Two P2X7R antagonists were used in this study: the competitive A438079 and non-competitive antagonist AZ11645373 (Figure 1.17). A438079 was previously used to confirm P2X7R was responsible for currents evoked by ATP in naïve $CD4^+$ T lymphocytes (Figure 3.5 E and F). A438079 caused a concentration dependent inhibition of CD62L loss induced by 1 hour 3 mM ATP treatment with an IC_{50} value of 2.25 µM (n=3) (Figure 4.9 A). AZ11645373 also caused a concentration dependent inhibition of CD62L loss with an IC_{50} value of 1.35 µM (n=3) (Figure 4.9 A). However, A438079 had no effect on loss of cell surface CD62L expression induced by anti-CD3/CD28 treatment of naïve $CD4^+$ T lymphocytes (Figure 4.9 B).

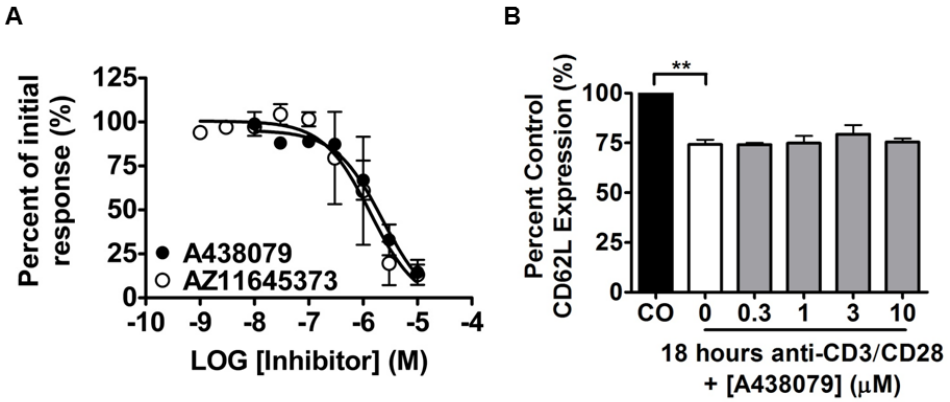

Figure 4.9: Loss of cell surface CD62L expression in response to ATP, but not anti-CD3/C28 antibody coated beads requires the P2X7R. Freshly isolated naive CD4 T lymphocytes were pre-treated with vehicle (DMSO) or the P2X7R antagonists A438079 or AZ11645373 at the indicated concentrations for 30 minutes. **A.** 3 mM ATP was then applied for 1 hour and CD62L surface expression was measure using flow cytometry as described. The initial loss of surface CD62L expression with vehicle pre-treatment was normalised to a 100% response. Inhibition was then defined as the percentage of this initial response remaining following inhibitor treatment. **B.** Alternatively cells were treated with anti-CD3/CD28 antibody coated beads for 18 hours and CD62L expression measured as described (n=3). Student's t-test was used to compare MFI of CO to bead treated cells **p<0.01. Effect of A438079 was measured by One Way ANOVA followed by Tukey's post-test.

4.1.14. Variation between loss of cell surface CD62L responses in human donors

Human P2X7R can be alternatively spliced and exhibits SNPs; this can lead to lead to differences in the ability of P2X7R to respond to ATP. Two donors were compared, one which significantly down regulated cell surface expression of CD62L in response to 1 hour 3 mM ATP treatment (Figure 4.10 Donor A), and a second which showed no significant loss (Figure 4.10 Donor B). The difference between these donors was significant in respect to ATP induced loss of surface CD62L down-regulation; however both donors showed significant anti-CD3/CD28 induced loss.

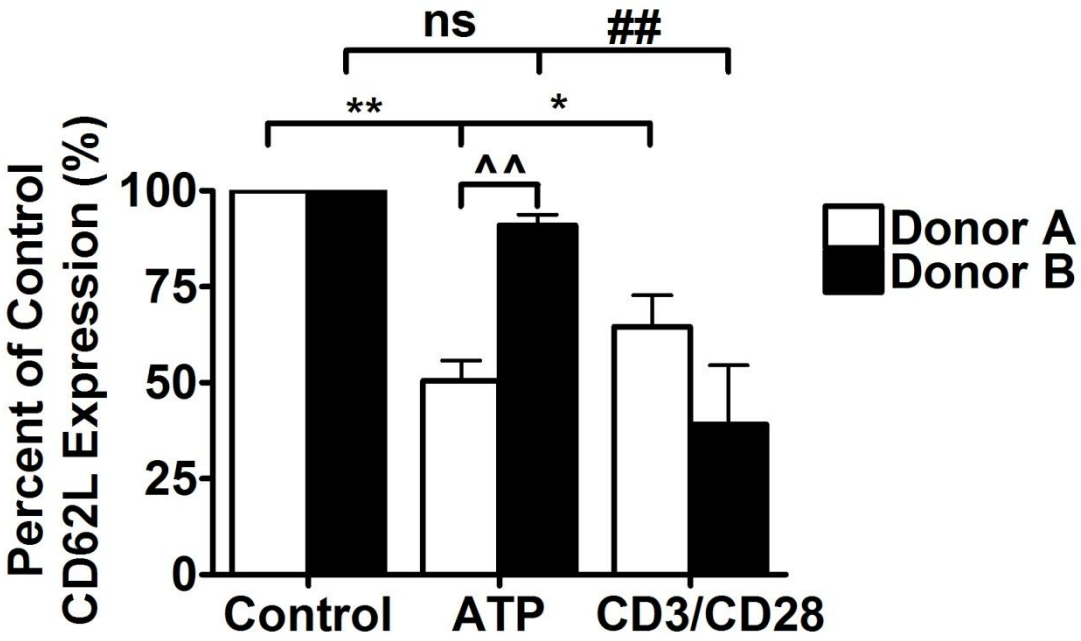

Figure 4.10: Variation of ATP and anti-CD3/CD28 antibody coated bead responses in two donors. Freshly isolated naïve $CD4^+$ T lymphocytes were treated with vehicle (DMSO), 3 mM ATP for 1 hour or anti-CD3/CD28 antibody coated beads for 18 hours (n=3). Surface CD62L expression was measured by flow cytometry as described. One Way ANOVA was used to compare treatment groups in individual donors followed by Tukey's post-test * $p<0.05$, **/## $p<0.01$. Two Way ANOVA was used to compare donors ^^ $p<0.01$.

4.1.15. Involvement of MMPs in ATP induced loss of cell surface CD62L from naïve CD4$^+$ T lymphocytes

The loss of CD62L from the surface of a number of different cell types in response to mitogenic and apoptotic signals is dependent on ADAM17 activity. ATP causes rapid release of MMP9 from PBMCs (312) and BzATP induced CD62L loss from mouse CD4$^+$ T lymphocytes is MMP dependent (423). Therefore, it was investigated whether CD62L loss in response to ATP from human naïve CD4$^+$ T lymphocytes is dependent on the actions of MMPs. Gelatin Zymography was first used to observe if MMPs were induced following ATP treatment of cells.

Bands of digested gel were observed at approximately 72 and 90 kDa in the supernatant of both resting and PMA treated leukemic Jurkat T lymphocytes (n=3) (Figure 4.11 A). These bands potentially correspond to active MMP2 and 9 respectively. PMA treatment did not increase the levels of either MMP above control. Whilst low levels of MMP9 was detected in supernatant samples of untreated naïve CD4$^+$ T lymphocytes, no increase in MMP9 activity was observed when these cells were treated with 1 mM ATP for up to 1 hour (n=2) or 5 mM ATP for 30 minutes (n=1) (Figure 4.11 B). Treatment of mouse splenocytes with 50 µM GM6001 has been shown to inhibit ATP induced CD27 down-regulation (424); GM6001 is a broad spectrum MMP inhibitor. Human naïve CD4$^+$ T lymphocytes were pre-treated with either DMSO, as a vehicle, or increasing concentrations of GM6001 for 30 minutes. Pre-treatment with 100 µM GM6001 significantly inhibited CD62L loss in response to 1 hour 3mM ATP treatment (Figure 4.11 C).

4.1.16. Measurement of soluble CD62L in the supernatant of cells

The cleavage of CD62L by ADAM proteases causes the release of a soluble fragment of CD62L (sCD62L), which is released into the extracellular environment where it is biologically active. The method chosen here for measuring CD62L down-regulation was to measure the loss of cell surface CD62L expression. However, it should be possible to also measure the release of sCD62L into the supernatant of treated cells. This has previously been shown for human PBMCs

treated with BzATP and was fully inhibited by oATP and partially by KN62, two P2X7R antagonists (245). Here, whole cell lysates and supernatants collected from vehicle, PMA and ATP treated naïve $CD4^+$ T lymphocytes were measured for CD62L expression by immunoblotting. Lymphocyte CD62L has an expected molecular weight of 74 kDa (108). However, the anti-CD62L antibody used here recognises a number of bands in the whole cell lysate (WCL) (Figure 4.11 D). Two of the predominant bands are just below the 72 kDa marker and could therefore represent CD62L from either the membrane or the cytosol. PMA causes significant loss of cell surface CD62L expression from human naïve $CD4^+$ T lymphocytes, it has previously been reported that in response to PMA treatment human lymphocytes shed a 62 kDa fragment of CD62L into the supernatant (108). PMA was therefore used as a positive control for measuring sCD62L in supernatant. Immunoblotting of supernatants for sCD62L revealed a smear of protein between 72 and 55 kDa which may contain sCD62L or other protein(s) recognised by the anti-CD62L antibody (Figure 4.11 D). Two other bands are visible in the supernatant, one of approximately 50 kDa just below the smear in all samples and a second at approximately 43 kDa, which is only visible in the ATP treated sample.

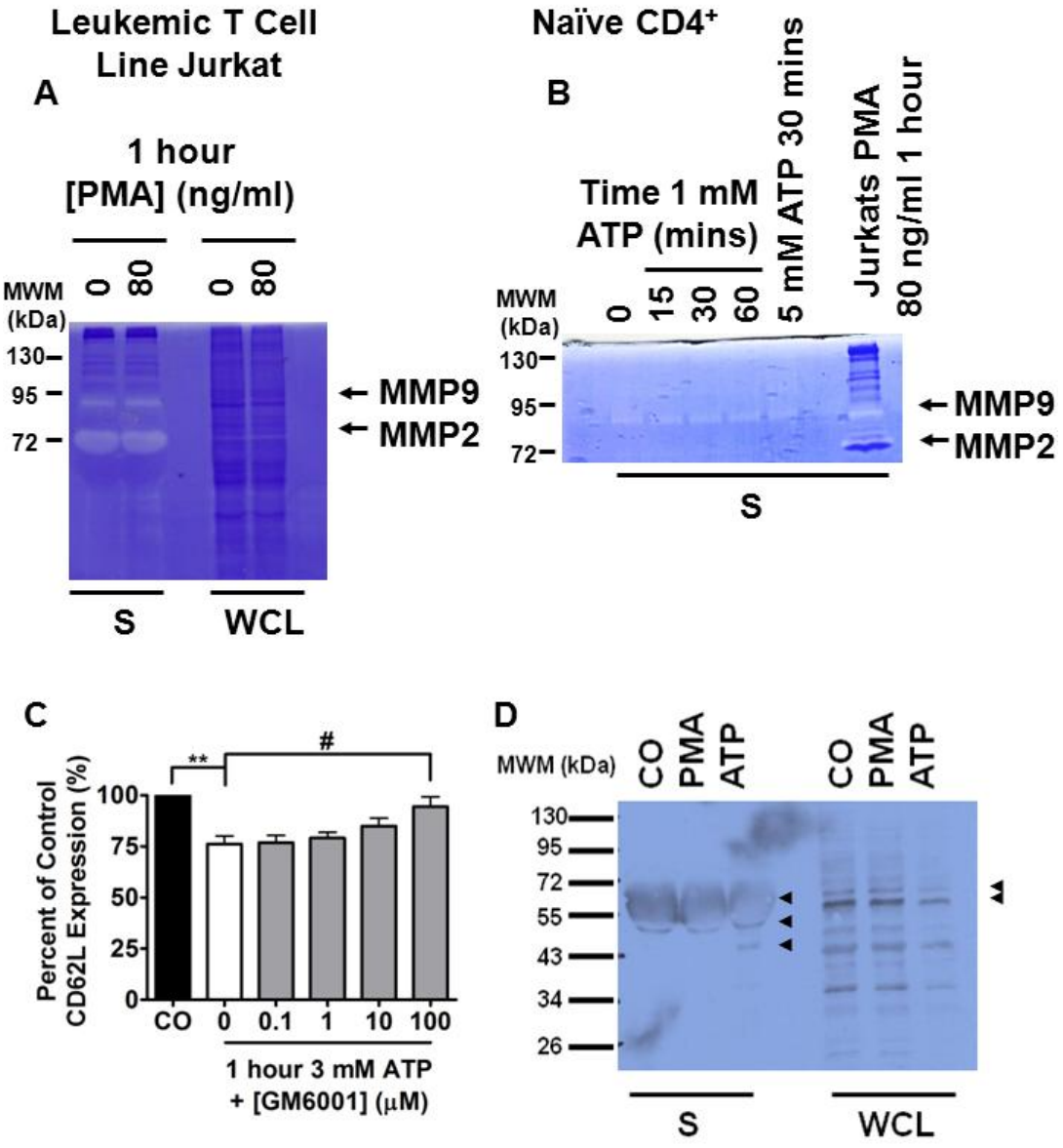

Figure 4.11: Supernatant from leukemic T cell line Jurkat and human naïve CD4$^+$ T lymphocytes contain MMPs; MMPs are responsible for ATP induced loss of cell surface CD62L expression. A. Jurkat T cells were removed from culture, washed and treated with vehicle or 80 ng/ml PMA for 1 hour. Supernatants (S) and whole cell lysates (WCL) were collected as described and separated by SDS-PAGE using Gelatin gels. Gels were developed as described and stained with Coomassie blue to reveal protein (n=3). **B.** Freshly isolated naïve CD4$^+$ T lymphocytes were treated with vehicle, 1 mM ATP for 15-60 minutes or 5 mM ATP for 30 minutes (n=2). Gelatin zymography was performed as for **A. C.** Cells were pre-treated for 30 minutes with vehicle (DMSO) or indicated concentrations of GM6001 before 1 hour 3 mM ATP treatment (n=3). Initial response analysed by Student's t-test **p<0.01 and GM6001 treated groups were compared to DMSO control by One Way ANOVA. **D.** Naïve CD4$^+$ T lymphocytes were treated with vehicle (DMSO), 100 nM PMA for 30 minutes or 3 mM ATP for 1 hour. Cells were lysed and CD62L expression in WCL and S were measured by immunoblotting with anti-CD62L antibody (n=1).

4.1.17. Hydrolysis of ATP is not responsible for down-regulation of cell surface CD62L expression.

ATP can be rapidly hydrolysed to AMP by cell surface CD39 (168, 169), this can be further hydrolysed to adenosine by CD73 (170) (Figure 1.16). CD39 is expressed on cells of the immune system, and in combination with CD73 is important for the function of Treg cells (171, 172), expression of CD39 along with P2X7R is up-regulated in chronic pancreatitis and pancreatic cancer (171). Flow cytometry was employed to measure the expression of CD39 on freshly isolated human naïve $CD4^+$ T lymphocytes. Only 3.83 ± 1.64 % (n=3 ± SEM) of naïve $CD4^+$ T lymphocytes were positive for CD39 whereas analysis of the whole PBMC revealed 25.03 ± 10.65 % (n=3 ± SEM) $CD39^+$ cells (Figure 4.12 A and B).

Adenosine can cause pro-inflammatory or anti-inflammatory responses from immune cells, this depends on the P1 adenosine receptor family members expressed and on the concentration of adenosine (179, 181). Adenosine generated by CD73 expressed on HEV negatively regulates L-selectin dependent migration of lymphocytes into draining lymph nodes (DLNs) (425). Increasing concentrations of adenosine from 2.5 µM to 2.5 mM for 1 hour did not have a significant effect on cell surface CD62L expression (Figure 4.12 C). In the same experiments 3 mM ATP was applied for 1 hour, as expected this treatment did cause a significant loss of cell surface CD62L (Figure 4.12 C). Addition of exogenous apyrase grade VI (which preferentially hydrolyses ATP to ADP) at 4 Units/ml had no effect on basal CD62L levels, but caused a significant inhibition of 3 mM ATP induced loss of cell surface CD62L expression (Figure 4.12 D).

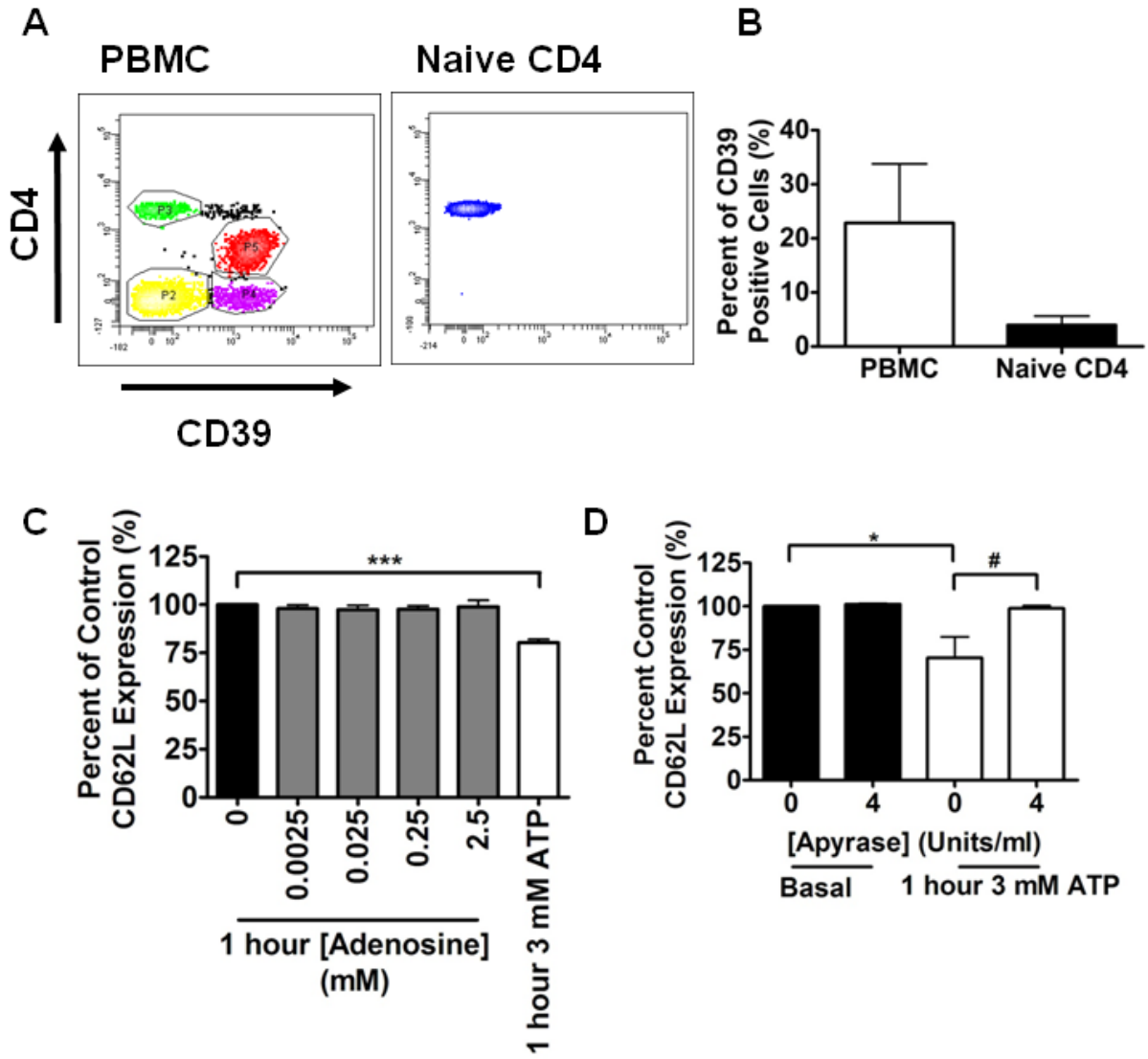

Figure 4.12: Naive CD4 T lymphocytes express low levels of CD39, adenosine does not cause loss of cell surface CD62L and apyrase prevents ATP induced loss A. PBMC and naïve $CD4^+$ T lymphocytes were freshly isolated, washed and labelled with antibody against CD39 and CD4. **B.** Percentages of cells expressing CD39 (n=3). **C.** Naive CD4 T lymphocytes were treated with increasing concentrations of adenosine or 3 mM ATP for 1 hour before CD62L expression measurement as described (n=3). **D.** Naive CD4 T lymphocytes were pre-treated with vehicle or 4 Units/ml Apyrase (Grade VI) for 30 minutes before treatment with 3 mM ATP for 1 hour (n=3). One Way ANOVA followed by Tukey's post-test used to determine significance */#$p<0.05$, ***$p<0.001$.

4.2. Investigation of the mechanisms of ATP induced CD62L down-regulation

4.2.1. Rationale and Aim

P2X7R has been shown to lead to the phosphorylation of a number of signalling proteins in a variety of cell types, including the MAPKs Erk1/2 and p38, PKC, PKD, JNK, Src and Akt (205, 238, 255, 330, 334–336, 426–428) (Figure 1.20). Several of these pathways are also implicated in ADAM17 mediated processing of substrates including CD62L, it was therefore desirable to explore the potential involvement of these pathways in ATP induced CD62L down-regulation.

4.2.2. ATP induced CD62L down-regulation is calcium independent

Increase in intracellular calcium levels through ionophore mediated influx or depletion of intracellular stores can lead to processing of CD62L (122). However, previous studies looking at P2X7R mediated CD62L down-regulation demonstrated that extracellular calcium was not required (207). This calcium independent mechanism was also observed in this thesis using human naïve $CD4^+$ T lymphocytes. No significant difference was observed in the ability of ATP to cause loss of CD62L surface expression when the agonist was applied in buffer with, or without $CaCl_2$ (Figure 4.13 A).

To confirm that calcium mobilisation by other mechanisms could lead to CD62L cell surface loss in human naïve $CD4^+$ T lymphocytes, cells were treated with either Ionomycin (a calcium ionophore) or Thapsigargin (a SERCA pump blocker) for 1 hour before measuring CD62L surface expression. Ionomycin was unable to induce a significant down-regulation of cell surface CD62L expression, this observation is in contrast to a study by Le Gall et al (122), but consistent with Jamieson et al (207) (Figure 4.13 B). Thapsigargin caused a significant concentration dependent loss of cell surface CD62L (Figure 4.13 C).

ATP treatment may not only lead to an increase in intracellular calcium through cation influx, but it could also couple to intracellular store release. To test this, a PLC inhibitor U73112 and its inactive analogue U73433 were intended for use. However, whilst U73433 had no effect on basal surface expression of CD62L the

active PLC inhibitor U73112 alone caused a visible decrease in CD62L expression (Figure 4.13 D). This prevented the use of this compound to investigate the coupling of P2X7R to PLC activation in CD62L down-regulation as a possible mechanism (Figure 4.13 E).

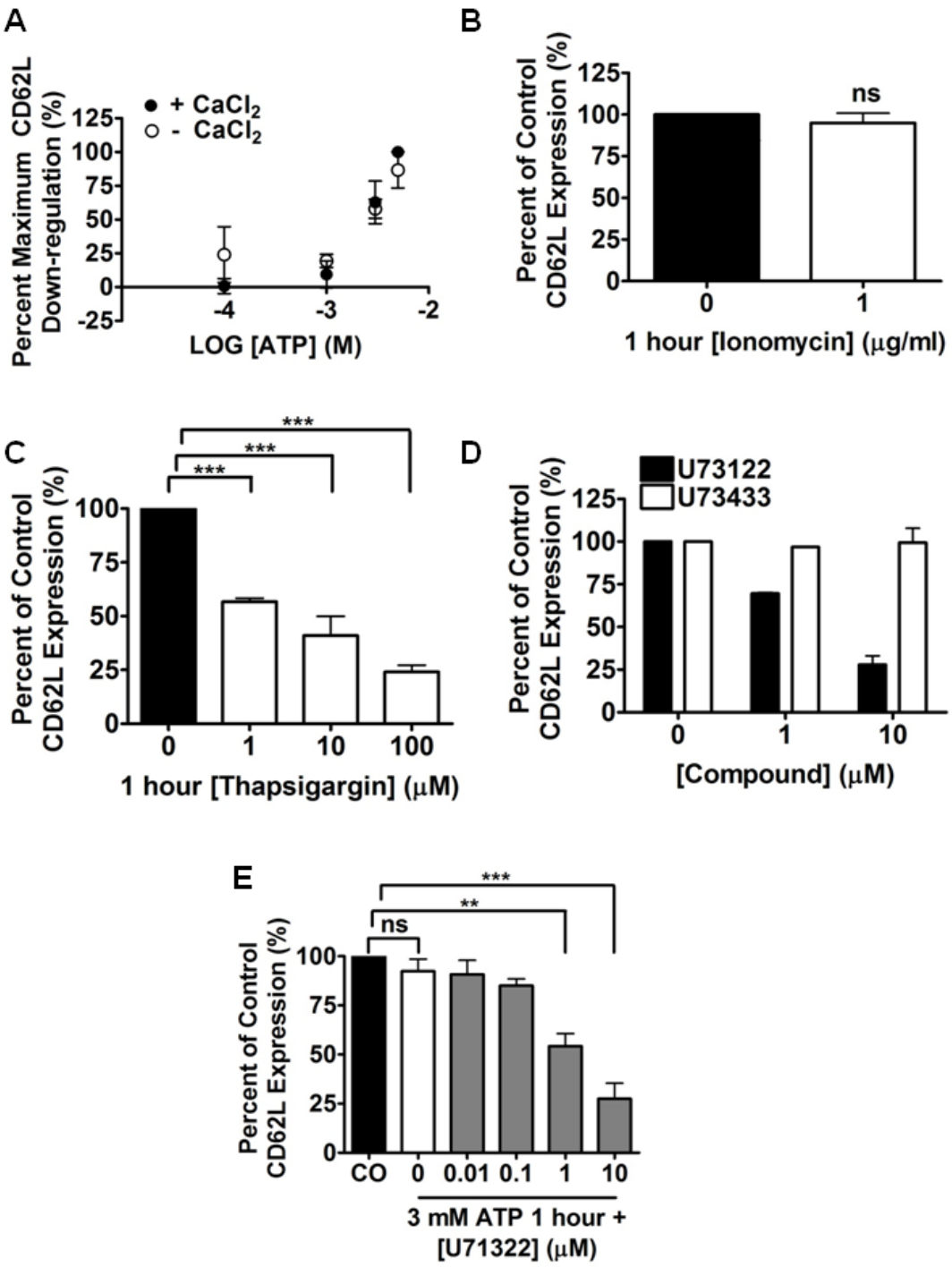

Figure 4.13: ATP induced CD62L down-regulation is not dependent on extracellular calcium, but modulation of intracellular calcium can affect surface expression of CD62L. A. Freshly isolated naïve $CD4^+$ T lymphocytes were treated with vehicle, or 3 mM ATP for 1 hour in buffer containing or free of $CaCl_2$. CD62L expression was measured by flow cytometry as described. **B.** Cells were treated with Ionomycin for 1 hour (n=3). **C.** Cells were treated with increasing concentrations of Thapsigargin (n=3). **D.** Cells were treated with vehicle (DMSO) or the PLC inhibitor U73122 or its inactive analogue U73433 for 90 minutes (n=2). **E.** Cells were pre-treated with vehicle or U73122 for 30 minutes before 1 hour 3 mM ATP treatment (n=3). One Way ANOVA followed by Tukey's post-test used to determine significance ***p<0.001

4.2.3. Phosphorylation of signalling proteins in response to ATP treatment

4.2.3.1. PI3K/Akt Pathway

Akt is an important down-stream protein in the PI3K/mTOR pathway and can also be activated independently by IKBKE (429). Full activation occurs following phosphorylation of two residues: Ser473 and Thr308 (Figure 1.6). Measurement of phosphorylation of these residues on Akt by immunoblotting is commonly used to show activation of the PI3K pathway. The class IB p110γ can be activated by ligands for the chemokine GPCRs CXCR3 and CXCR4 as well as others. Indeed both chemokines CXCL11 (CXCR3) and CXCL12 (CXCR4) caused an increase in Akt Ser473 phosphorylation (n=2 ± STDEV) (Figure 4.14 A and B). In astrocytes Akt is phosphorylated on Ser473 and Thr308 within 2 minutes of 100 μM BzATP treatment (334). Akt phosphorylation was significantly inhibited by the pan-isoform PI3K inhibitors LY294002, Wortmannin, the Src inhibitor PP2 and by extracellular calcium chelation. Akt is also phosphorylated in response to ATP treatment in mouse embryonic stem cells (255); however in mouse thymocytes 2 hour 1 mM treatment did not increase Akt phosphorylation (255). In mouse $CD4^+$ and $CD8^+$ T lymphocytes Akt down-regulates CD62L expression by phosphorylating FOXO1 and turning off CD62L gene transcription (114). Therefore, the hypothesis formed was that ATP may activate the PI3K pathway and cause CD62L down-regulation by Akt activation.

After 15 minutes treatment with 1 mM ATP a non-significant 1.77 ± 0.55 (n=3 ± SEM $p>0.05$) fold increase in Akt phosphorylation was observed (4.15 A and C). To investigate whether P2X7R was involved the antagonist A438079 was applied to cells at a concentration of 1 μM 30 minutes before ATP treatment. Pre-treatment with A438079 alone appears to increase Akt phosphorylation 1.68 ± 0.47 fold. However, after 15 minutes ATP treatment Akt phosphorylation is only 1.09 ± 0.43 fold above control when A438079 is pre-applied compared to 1.77 ± 0.55 for vehicle pre-treatment; this inhibition is however not significant (n=3 ± SEM $p>0.05$).

Activation of the PI3K/mTOR pathway can also lead to activation of S6K and subsequent phosphorylation of S6 ribosomal subunit; a step required for increased protein synthesis (53, 417). Therefore, phosphorylation of S6 can be

used as a further read out of activation of the PI3K/mTOR pathway. S6 was phosphorylated following CXCL11 and CXCL12 treatment (Figure 4.15 A and B). S6 was more robustly phosphorylated upon 1 mM ATP treatment than Akt with a peak of 13.01 ± 8.08 fold (n=3 ± SEM p>0.05) increase in S6 phosphorylation after 5 minutes (Figure 4.15 A and C). Pre-treatment with A438079 appears to have a small, but insignificant effect on S6phosphorylation in response to ATP (Figure 4.15 C).

4.2.3.2. MAPK Pathways

Erk1/2 MAPK is one of the most extensively studied signalling proteins down-stream of P2X7R activation by ATP or BzATP. ATP induced Erk1/2 phosphorylation has been shown to have a role in thymocyte death which was interestingly independent of extracellular calcium (255). A 5 minute 1 mM ATP treatment was sufficient to induce Erk1/2 phosphorylation in mouse splenocytes (255). Erk1/2 are also phosphorylated via P2X7R in astrocytes (335–337). In the study by Sinclair et al which highlighted a role for PI3K in TCR induced CD62L loss, Erk1/2 involvement was also described by using the MEK1 inhibitor PD98059 (114). Another MAPK, p38 was phosphorylated in response to ATP in murine thymocytes (255). Threonine phosphorylation of ADAM17 by Erk1/2 and p38 MAPK aids its trafficking to the cell surface, where it acts to down-regulate its substrates including CD62L (129–132).

Erk1/2 phosphorylation following chemokine stimulation has been described elsewhere (430) and CXCL11 and CXCL12 treatment was used as a positive control for Erk1/2 phosphorylation (Figure 4.16 A and B). Indeed, 5 minute 10 nM CXCL11 or CXCL12 treatment caused 7.90 ± 3.57 and 8.32 ± 3.58 fold increases in Erk1/2 respectively (n=3 ± SEM p>0.05). After 15 minute treatment with 1 mM ATP a noticeable but insignificant 4.40 ± 2.21 fold increase in Erk1/2 phosphorylation was observed; this was reduced to a 2.38 ± 1.35 fold increase when cells were pre-treated with 1 μM A438079 for 30 minutes (n=3 ± SEM p>0.05) (Figure 4.16 A and C).

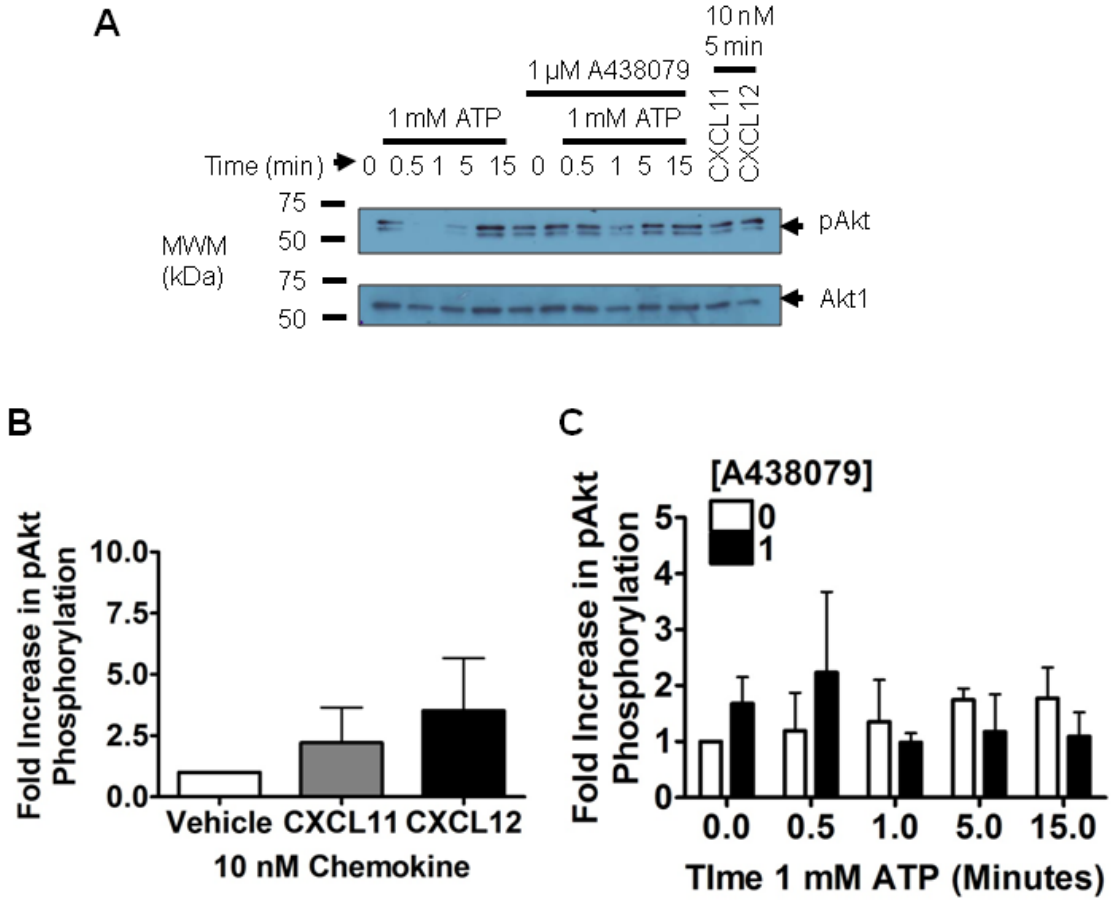

Figure 4.14: Measurement of Akt Phosphorylation down-stream of P2X7R. SEB cells were expanded from PBMC as described in materials and methods, IL2 was removed and cells re-suspended in fresh complete RMPI-1640 on day 8 post isolation and used for experiment on day 9. Cells were washed three times, re-suspended in serum free RMPI-1640 at a concentration of 2 x 10^6 per ml, pre-treated with vehicle (media) or 1 µM A438079 for 30 minutes. Cells were then treated with vehicle, 1 mM ATP or 10 nM CXCL11/12 for the indicated time periods. All cells were lysed as described, loaded onto poly-acrylamide gels and proteins separated under reducing conditions using SDS-PAGE. Proteins were transferred to nitro-cellulose membrane, blocked and immuno-blotted for Ser473 phosphorylation of Akt using antibody from Santa Cruz. Membranes were stripped of antibody, blocked and re-probed for Akt1 using anti-Akt1 antibody (Santa Cruz). Blots were analysed using Image J as described, first pAkt was normalised to Akt1 for equal protein loading and then all treatments were normalised as a fold change of pAkt above vehicle alone treated cells.). **A.** Representative western blot showing pAkt (upper panel) and Akt (lower panel). MWM = molecular weight markers **B.** Effect of 5 minutes 10 nM chemokines CXCL11 and CXCL12 on Akt phosphorylation (n=2). **C.** Effect of 1 mM ATP on pAkt levels in vehicle or 1 µM A438079 pre-treated cells (n=3) Two Way ANOVA followed by Tukey's post-test was performed to measure significance.

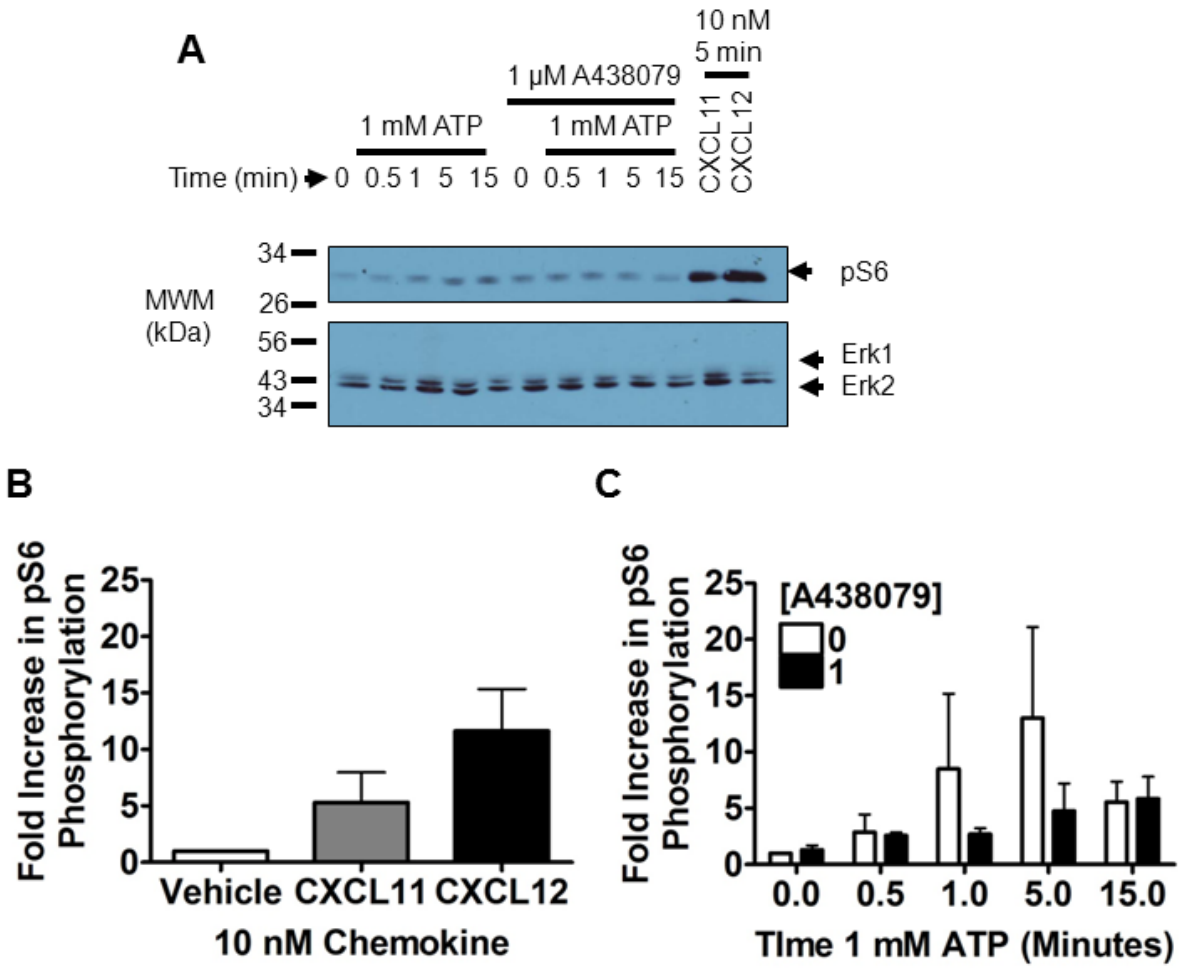

Figure 4.15: Measurement of S6 ribosomal subunit Phosphorylation down-stream of P2X7R. SEB cells were expanded from PBMC as described in materials and methods, IL2 was removed and cells re-suspended in fresh complete RMPI-1640 on day 8 post isolation and used for experiment on day 9. Cells were washed three times, re-suspended in serum free RMPI-1640 at a concentration of 2 x 10^6 per ml, pre-treated with vehicle (media) or 1 μM A438079 for 30 minutes. Cells were then treated with vehicle, 1 mM ATP or 10 nM CXCL11/12 for the indicated time periods. All cells were lysed as described, loaded onto poly-acrylamide gels and proteins separated under reducing conditions using SDS-PAGE. Proteins were transferred to nitro-cellulose membrane, blocked and immuno-blotted for phosphorylation of S6 using antibody from Cell Signalling Technologies. Membranes were stripped of antibody, blocked and re-probed for S6 using anti-Erk1 antibody (Santa Cruz). Blots were analysed using Image J as described, first pS6 was normalised to Erk1 for equal protein loading and then all treatments were normalised as a fold change of pS6 above vehicle alone treated cells. **A.** Representative western blot showing pS6 (upper panel) and Erk (lower panel). MWM = molecular weight markers. **B.** Effect of 5 minutes 10 nM chemokines CXCL11 and CXCL12 on S6 phosphorylation (n=2). **C.** Effect of 1 mM ATP on pS6 levels in vehicle or 1 μM A438079 pre-treated cells (n=3). Two Way ANOVA followed by Tukey's post-test was performed to measure significance.

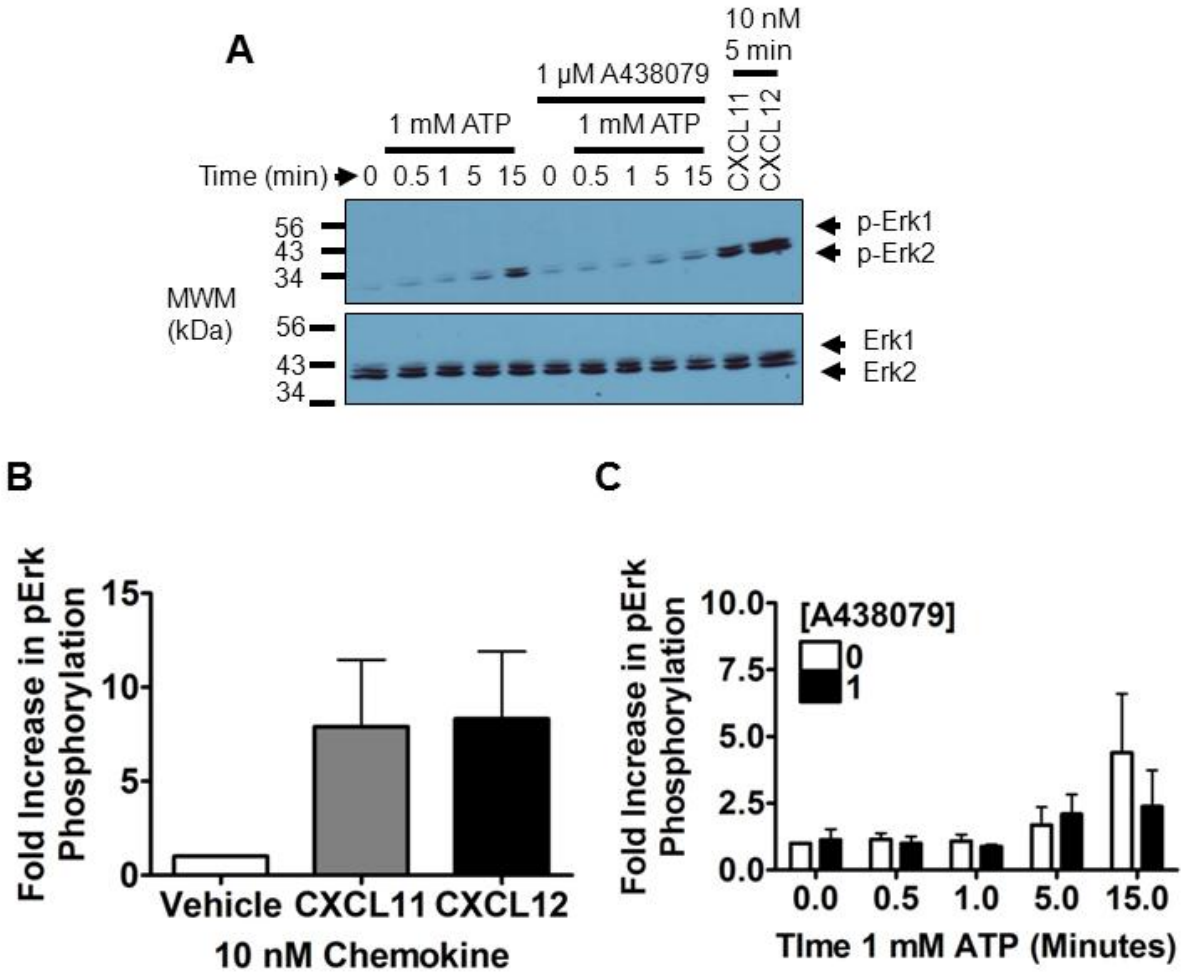

Figure 4.16: Measurement of Erk Phosphorylation down-stream of P2X7R. SEB cells were expanded from PBMC as described in materials and methods, IL2 was removed and cells re-suspended in fresh complete RMPI-1640 on day 8 post isolation and used for experiment on day 9. Cells were washed three times, re-suspended in serum free RMPI-1640 at a concentration of 2 x 10^6 per ml, pre-treated with vehicle (media) or 1 µM A438079 for 30 minutes. Cells were then treated with vehicle, 1 mM ATP or 10 nM CXCL11/12 for the indicated time periods. All cells were lysed as described, loaded onto poly-acrylamide gels and proteins separated under reducing conditions using SDS-PAGE. Proteins were transferred to nitro-cellulose membrane, blocked and immuno-blotted for phosphorylation of Erk1/2 using antibody from Cell Signalling Technologies. Membranes were stripped of antibody, blocked and re-probed for Erk1/2 using anti-Erk1 antibody (Santa Cruz). Blots were analysed using Image J as described, first pErk1/2 was normalised to Erk1 for equal protein loading and then all treatments were normalised as a fold change of pErk1/2 above vehicle alone treated cells. **A.** Representative western blot showing pErk1/2 (upper panel) and Erk (lower panel). MWM = molecular weight markers. **B.** Effect of 5 minutes 10 nM chemokines CXCL11 and CXCL12 on Erk1/2 phosphorylation (n=2). **C.** Effect of 1 mM ATP on pErk1/2 levels in vehicle or 1 µM A438079 pre-treated cells (n=3). Two Way ANOVA followed by Tukey's post-test was performed to measure significance.

4.2.4. The PI3K/mTOR, Erk1/2 and p38 MAPK signalling pathways are not required for ATP induced down-regulation of cell surface CD62L

Having observed that the PI3K/mTOR and Erk1/2 may be activated by ATP treatment, inhibitors of PI3K, Erk1/2 and p38 (another MAPK) were used to see if these pathways were involved in ATP induced loss of cell surface CD62L expression. To prevent Akt activation via PI3K cells were pre-treated for 30 minutes with the pan-isoform specific inhibitor ZSTK474 (or DMSO as a vehicle control). Cells were then treated for 1 hour with 3 mM ATP and cell surface CD62L expression measured. ZSTK474 (0.01 – 10 μM) failed to significantly inhibit ATP induced down-regulation of cell surface CD62L (Figure 4.17 A). Pre-treatment with the MEK1 inhibitor PD98059 at 0.01 – 10 μM, also had no effect on ATP induced loss of cell surface CD62L expression (Figure 4.18 B). Although the coupling of P2X7R activation to the p38 MAPK pathway was not investigated here, the p38 inhibitor SB203580 had no effect on 3 mM ATP induced down-regulation of cell surface CD62L expression (Figure 4.18 C).

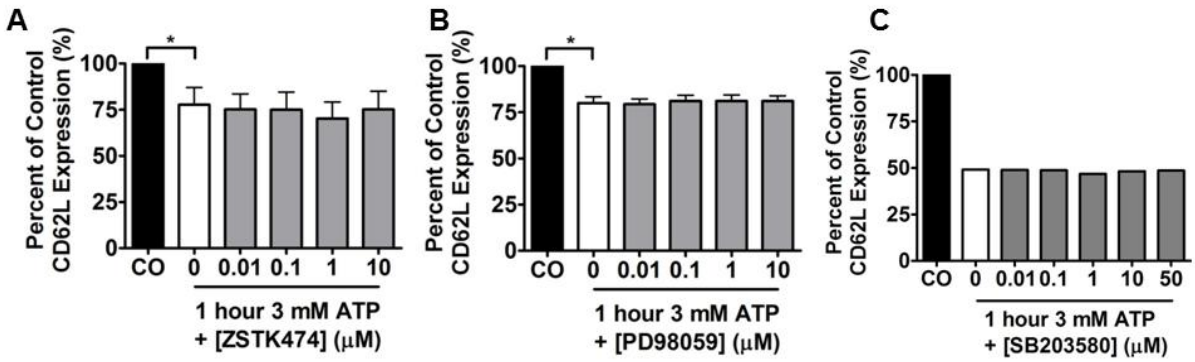

Figure 4.17: A number of kinases are not required for ATP induced CD62L down-regulation. Freshly isolated naive CD4 T lymphocytes were pre-treated with vehicle (DMSO) or small molecule inhibitors at the given concentrations: **A.** ZSTK474 (n=3) **B.** PD98059 (n=3) or **C.** SB203580 (n=2) for 30 minutes, Cells were then treated with 3 mM ATP for 1 hour. CD62L expression was analysed by flow cytometry as described. Student's t-test was used to compare MFI of CO to ATP treated cells *p<0.05. Effect of inhibitors was measured by One Way ANOVA followed by Tukey's post-test.

4.2.5. PKC is required for loss of cell surface CD62L expression in response to PMA, but not anti-CD3/CD28 antibody coated beads or ATP

Previously, PMA was shown to cause significant loss of CD62L expression from the surface of human naïve $CD4^+$ T lymphocytes and the leukemic T cell line Jurkat (Figure 4.7 and Figure 4.8 A and B). PMA is known to activate PKC and this signalling protein has been implicated in PMA induced CD62L processing; indeed PKC can directly phosphorylate ADAM17. Treatment of naïve $CD4^+$ T lymphocytes with 100 nM PMA for 30 minutes caused a significant down-regulation of CD62L from the cell surface. The PKC antagonist Gö6976 inhibits the classical PKC isoforms and 1 µM and 10 µM Gö6976 significantly inhibited PMA induced down-regulation of cell surface CD62L expression (Figure 4.18 A). However, anti-CD3/CD28 induced CD62L down-regulation was independent of classical PKC signalling (Figure 4.18 B).

Treatment of osteoclasts with ATP leads to the translocation of the classical PKC isoforms PKCα and PKCβI to the cell surface (340). It was therefore desirable to investigate whether PKC is responsible for loss of cell surface CD62L expression in response to ATP. Using naïve $CD4^+$ T lymphocytes isolated at the same time from donors showing PMA/PKC mediated CD62L loss, the involvement of PKC in ATP induced loss of cell surface CD62L expression was investigated. Pre-treatment with Gö6976 had no effect on ATP induced CD62L down-regulation, suggesting classical PKC isoforms are not involved (Figure 4.18 C). BzATP can also cause the activation of PKCδ; Rottlerin is a non-specific PKC antagonist which inhibits the novel PKC isoform, PKCδ (336). Pre-treatment of cells with Rottlerin did not significantly inhibit ATP induced loss of cell surface CD62L expression, but unexpectedly pre-treatment with 10 µM Rottlerin enhanced ATP induced CD62L loss (Figure 4.18 D).

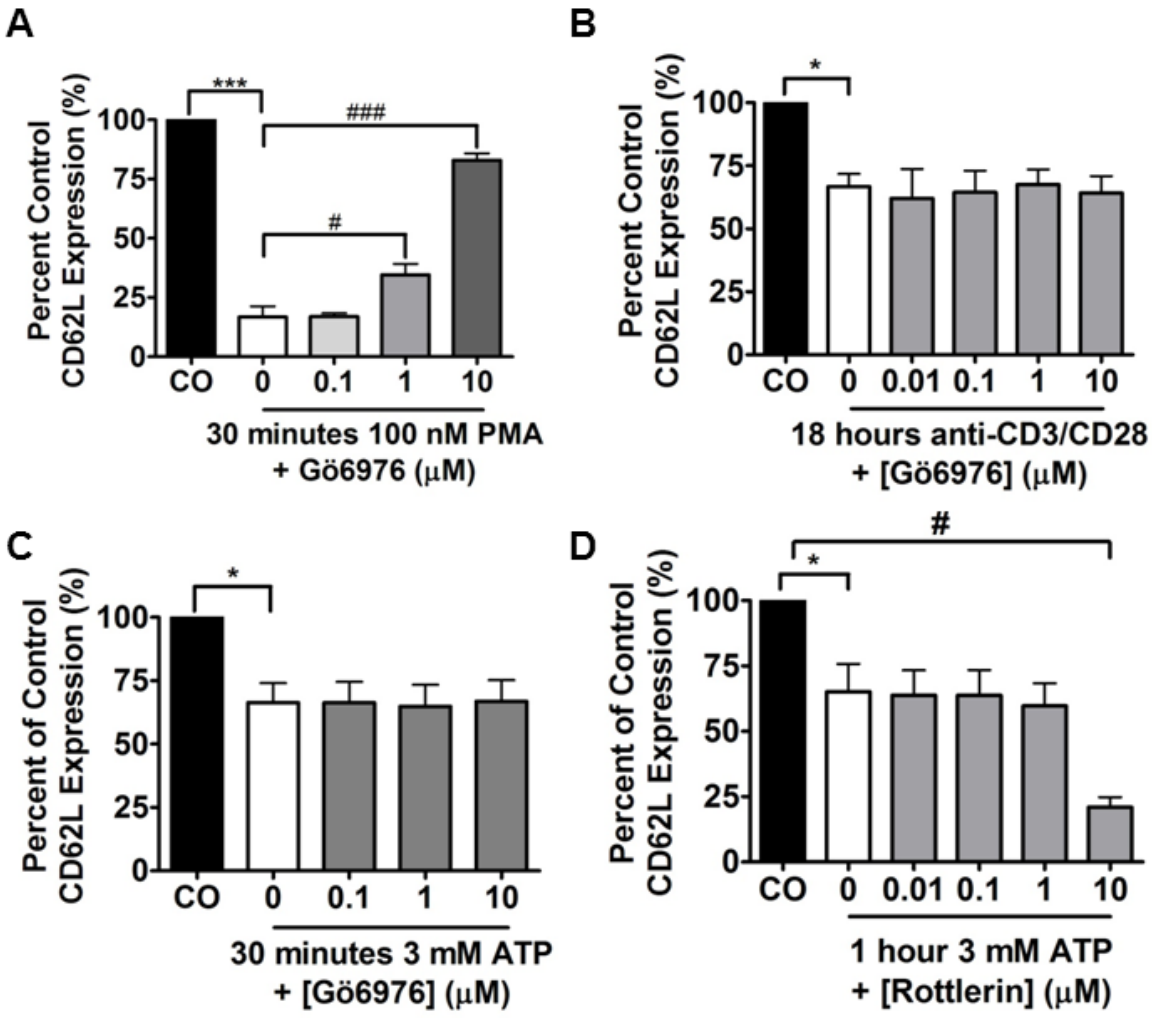

Figure 4.18: PKC is responsible for PMA, but not anti-CD3/CD28 antibody coated bead or ATP induced loss of cell surface CD62L. Freshly isolated naïve $CD4^+$ T lymphocytes were pre-treated with vehicle (DMSO), Gö6976 (**A-C**) or Rottlerin (**D**) for 30 minutes (n=3). Cells were then treated with: **A** 100 nM PMA for 30 minutes, **B** anti-CD3/CD28 antibody coated beads for 18 hours, **C** 3 mM ATP for 30 minutes or **D** 1 hour. CD62L expression was analysed by flow cytometry as described, the effect of PMA/ anti-CD3/CD28 antibody coated bead/ATP treatment on MFI was analysed by Student's t-test *p<0.05 and ***p<0.001. CD62L MFI was then normalised as a percent of control (100%) expression, DMSO treated groups were compared to inhibitors by One Way ANOVA followed by Tukey's post-test #p<0.05 and ###p<0.001.

4.2.6. Results Section 4.1 Summary

- Activation of naïve $CD4^+$ T lymphocytes causes CD62L down-regulation
- This down-regulation is significant after 18 hours of anti-CD3/CD28 antibody coated micro-bead treatment
- PI3K/mTOR and Erk1/2 MAPK signalling are not required for anti-CD3/CD28 bead mediated CD62L down-regulation
- ATP induced down-regulation of cell surface CD62L from naïve $CD4^+$ T lymphocytes but not the leukemic T cell line Jurkat.
- ATP induced CD62L down-regulation was rapid, peaking at 15 minutes
- ATP induced CD62L down-regulation occurs with an EC_{50} value of 888.6 μM for 1 hour treatment
- The P2X7R antagonists A438079 and AZ11645373 inhibited 1 hour 3 mM ATP induced CD62L down-regulation with IC_{50} values of 2.25 and 1.35 μM respectively.
- CD62L surface down-regulation induced by ATP was dependent on the actions of MMPs
- Naive $CD4^+$ T lymphocytes express low levels of CD39. The hydrolysis of ATP prevented CD62L down-regulation, whilst adenosine had no effect.

4.2.7. Results Section 4.2 Summary

- CD62L loss from naive $CD4^+$ T lymphocytes was independent of extracellular calcium. However, modulation of intracellular calcium stores causes CD62L loss
- Treatment with ATP causes a noticeable but insignificant increase in the phosphorylation of Erk1/2 and S6 ribosomal subunit.
- A less marked effect was observed for Akt phosphorylation.
- It is unclear whether this phosphorylation is dependent on P2X7R
- Inhibitors of PI3K and MEK have no effect on ATP induced CD62L down-regulation
- PKC is required for PMA, but not anti-CD3/CD28 antibody coated bead or ATP induced down-regulation of cell surface CD62L

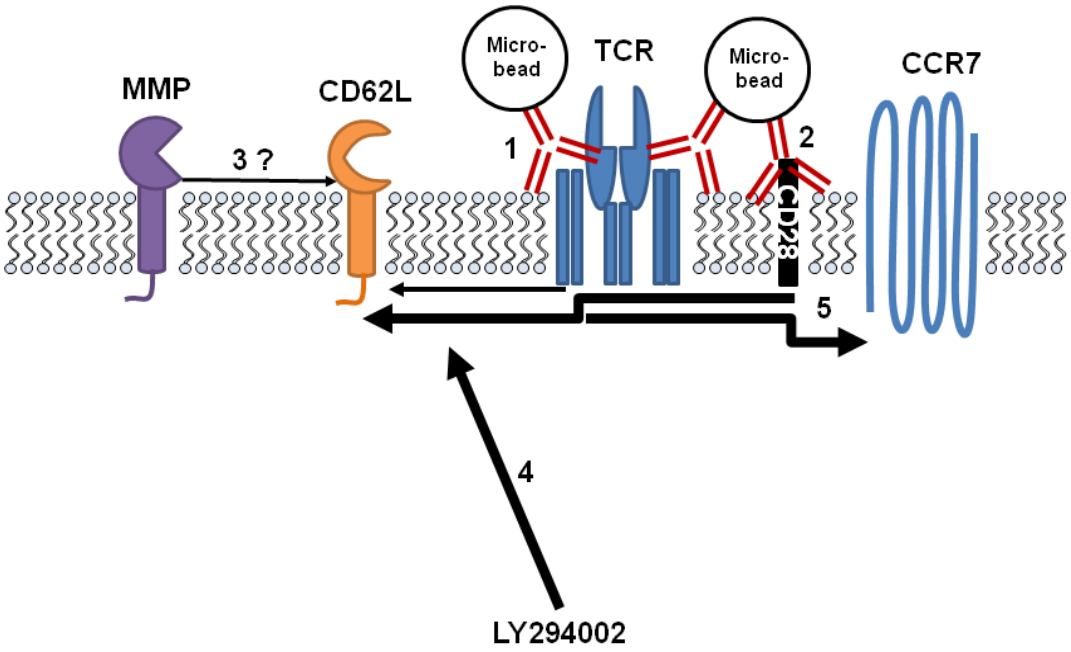

Figure 4.19: Anti-CD3/CD28 antibody coated bead induced down-regulation of surface CD62L and CCR7 1. Anti-CD3 antibody coated beads cause down-regulation of CD62L; this is enhanced by also stimulating CD28 with anti-CD3/CD28 antibody coated beads (**2**). **3.** This process did not appear to involve the action of MMPs. **4.** Pre-incubation with the Pan-PI3K inhibitor LY294002 enhanced anti-CD3 and anti-CD3/CD28 antibody coated bead induced loss of CD62L expression. **5.** Anti-CD3/CD28 antibody coated beads also cause loss of cell surface CCR7 expression.

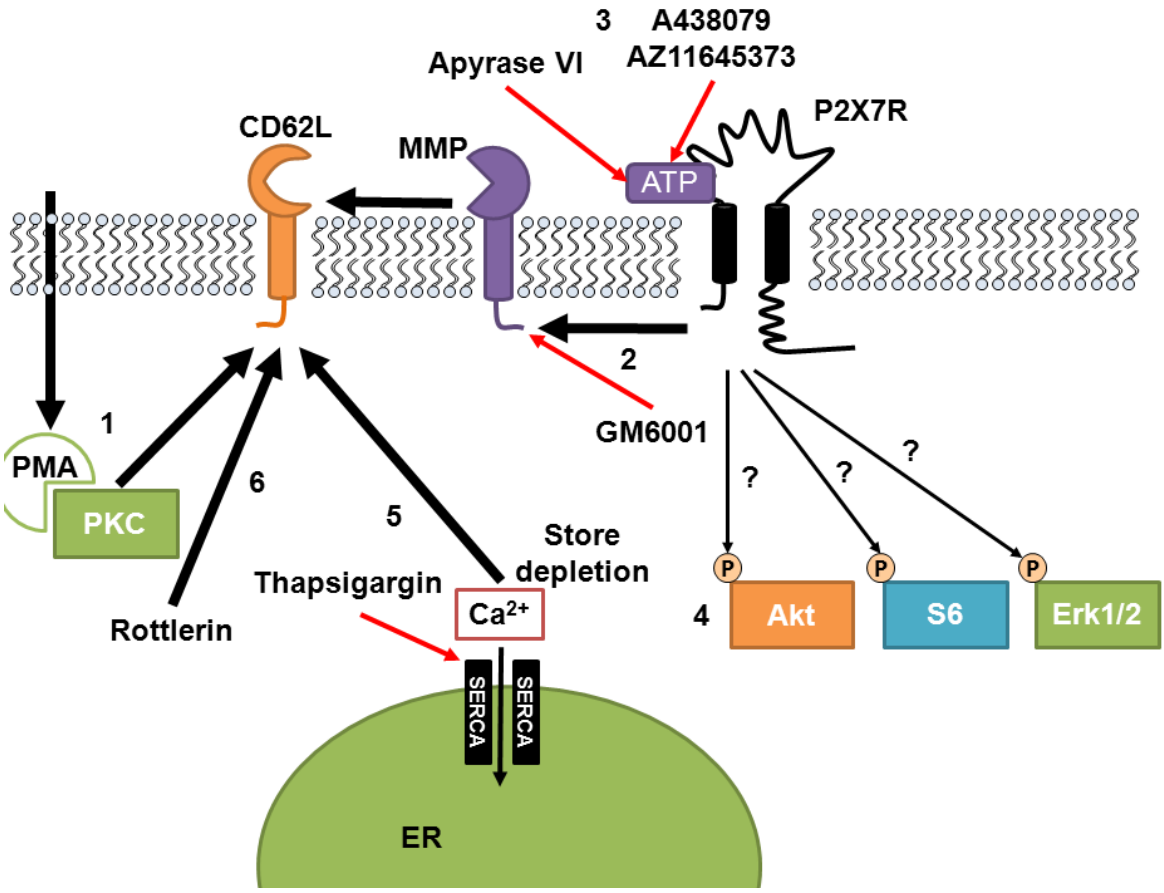

Figure 4.20: PMA, Ca^{2+} store depletion and ATP, through P2X7R, cause down-regulation of cell surface CD62L expression. 1. PMA causes significant down-regulation of surface CD62L expression through PKC activation. **2.** The broad spectrum MMP inhibitor GM6001 reveals that MMPs are responsible for ATP induced loss of cell surface CD62L expression. **3.** ATP acts through P2X7R, as the competitive and non-competitive P2X7R antagonists A438079 and AZ11645373 respectively inhibit loss of CD62L surface expression. ATP induced loss is also inhibited by grade VI apyrase. **4.** The signalling proteins Akt, S6 ribosomal subunit and Erk1/2 are phosphorylated in response to ATP, however this effect is minimal and these signalling pathways are not responsible for ATP induced CD62L loss. **5.** External calcium is not required for ATP induced loss of CD62L surface expression; however Ca2+ store depletion does induce significant CD62L loss. **6.** The non-specific PKC inhibitor Rottlerin enhances ATP induced loss of CD62L surface expression.

4.3. Results Chapter 4 Discussion

4.3.1. CD3/CD28 mediated down-regulation of cell surface CD62L

This study revealed that anti-CD3/CD28 antibody coated bead induced down-regulation of CD62L from the surface of naïve $CD4^+$ T lymphocytes was independent of PI3K/mTOR, Erk1/2 and PKC signalling. This is in direct contrast to a study by Sinclair et al which explored the mechanisms for loss of cell surface CD62L in murine T lymphocytes (114).

There are several possible reasons for differences between published data and data presented in this thesis. Firstly, this thesis employed anti-CD3/CD28 antibody coated beads; this was because in human $CD4^+$ T lymphocytes soluble anti-CD3 antibody alone caused very little CD62L down-regulation compared to mouse $CD4^+$ T lymphocytes. CD28 is an established co-stimulatory receptor for T lymphocytes during activation and may contribute to CD62L down-regulation. In one study, the leukemic T cell line Jurkat was treated with soluble anti-CD3 or anti-CD28 antibodies and CD62L expression compared. Ligation of CD3 was sufficient to cause 73% down-regulation of cell surface CD62L, whereas ligation of CD28 caused 35% loss of CD62L surface expression (431). The treatment of isolated lymph node cells with anti-CD28 antibody for 10 hours also caused a marked reduction in the cell surface expression of CD62L, alongside an up-regulation of LFA-1 (432). *In vivo*, inhibition of CD28 by CTLA4Ig caused a decrease in the number of $CD62L^{low}$ effector memory T lymphocytes found in the spleen and mesenteric lymph nodes of mice treated with influenza hemagglutinin (HA) or ovalbumin (OVA) peptides (433). However, it is unclear from this study if this is due to reduced shedding of cell surface CD62L and the authors suggest it is likely due to ineffective conversion of central to effector memory T lymphocytes. Therefore, it may be that co-stimulation allows coupling to novel mechanisms of CD62L down-regulation. However, in this thesis the relative contribution of anti-CD3 and anti-CD28 antibodies to down-regulation was not explored.

Secondly, although mouse models provide a useful tool for investigating immunity and inflammation, there are several important differences between the mouse and human immune system (434). For instance, the level of CD28 expression by $CD4^+$

and $CD8^+$ T lymphocytes varies between humans and mice. The mouse anti-CD3 antibody (2C11) and human anti-CD3 antibody (UCHT-1) both bind to epitopes in the CD3ε receptor (435, 436). However, data presented in this thesis suggests the signal transduction following CD3 ligation that leads to CD62L down-regulation may differ between species. Finally, it is possible that the micro-beads used may also provide a mechanistic signal imitating cell-cell contact induced CD62L down-regulation (437).

It was surprising that long term inhibition of PI3K or MEK/Erk1/2 did not affect CD62L expression in *ex vivo* expanded $CD4^+$ T lymphocytes. However, confounding factors are present in this long term culture model: the bead to cell ratio is increased from 1:1 (in 18 hour study) to 3:1; IL-2 is also added to maintain cell growth which has been shown, in $CD8^+$ T lymphocytes, to contribute to CD62L loss (110). After 7 days *ex vivo* culture, CD62L expression may actually be increased above initial naïve $CD4^+$ expression levels. This increase could be due, in part, to enrichment of central memory T lymphocytes which re-express high levels of CD62L to home back to SLOs for memory based antigen surveillance (89). Indeed, when T lymphocytes were expanded *ex vivo* from PBMC using SEB they display a biphasic CD62L expression profile, with a population of cells showing very high levels of expression. A study also using anti-CD3/CD28 antibody coated beads and IL-2 to activate human umbilical cord blood, observed 92% $CD3^+/CD62L^+$ cells after 14 days (438).

4.3.2. ATP induced loss of CD62L surface expression

Although the leukemic T cell line Jurkat and human naïve $CD4^+$ T lymphocytes express functional P2X7Rs, there are differences in their ability to down-regulate cell surface CD62L in response to ATP. Several signalling pathways are perturbed in the leukemic T cell line Jurkat including PI3K signalling, however this cell type is complex and it would be difficult to elucidate the reason for the lack of ATP induced CD62L surface loss (377). The basal levels of CD62L expression were lower for the leukemic T cell line Jurkat compared to human naïve $CD4^+$ T lymphocytes, this may be, in part, due to the absence of PTEN expression; restoration of PTEN expression increases CD62L expression on Jurkats (133).

What is clear however, is that down-regulation of cell surface CD62L on naïve $CD4^+$ T lymphocytes in response to ATP does not require PKC and the leukemic T cell line Jurkat down-regulates surface CD62L in response to PMA. The concentration dependence of PMA for CD62L down-regulation is similar to that observed in a mouse B cell line expressing CD62L (130). These observations suggest that a pathway other than PKC is responsible for the differences between the action of ATP on the leukemic T cell line Jurkat and naïve $CD4^+$ T lymphocytes.

Previous studies involving CD62L down-regulation from T lymphocytes have focussed on mouse $CD4^+$ T lymphocytes and subpopulations of human PBMC cells including naïve $CD4^+$ T lymphocytes; here CD62L down-regulation in response to ATP is confirmed in isolated human naïve $CD4^+$ T lymphocytes (245, 284, 395). The kinetics of CD62L down-regulation in naïve $CD4^+$ T lymphocytes showed rapid down-regulation, however this was not as rapid as for B lymphocytes from patients with BCLL. These cells down-regulate almost 95% of CD62L within 5 minutes, however BCLL cells have enhanced P2X7R expression (208, 254). ATP was more potent in BCLL cells with an EC_{50} of 31.3 ± μM (7 minute treatment) (208) compared to 877 μM (5 minute treatment) for naïve $CD4^+$ T lymphocytes for data presented in this thesis.

Previous studies have used first generation P2X7R inhibitors such as oATP and KN62 to show that P2X7R is involved in ATP induced down-regulation of cell surface CD62L (208, 245). This study utilised the second generation P2X7R antagonists A438079 and AZ116453743 to confirm P2X7R activation is indeed responsible for CD62L down-regulation in response to ATP. However, other purinergic receptors could also be involved in this process. This study did not investigate the expression of P2Y receptors on naïve $CD4^+$ T lymphocytes; however electrophysiology indicated a small outward current in response to 0.1 mM ATP which could be mediated by P2Y receptors. Indeed, P2Y2 receptors have been shown to affect ADAM17 substrate processing and this receptor subtype is expressed in T lymphocytes (422, 439, 440). A reduction in the concentration of exogenously applied ATP could lead to reduced P2X receptor activation and enhanced P2Y receptor activation. The lack of CD39 expression on

naïve $CD4^+$ T lymphocytes suggests that exogenous ATP degradation would not occur rapidly with these cells *in vitro*; however *in vivo* bystander cells could express high levels of CD39 and CD73. As shown in Figure 4.10, within PMBC there are populations of cells which are $CD4^+CD39^+$ which are likely to be Treg cells (172). Exogenous application of apyrase significantly inhibited loss of cell surface CD62L expression, therefore *in vivo* Treg cells may be able to inhibit ATP induced CD62L down-regulation from the surface of other cells.

4.3.3. Signalling mechanisms involved in ATP induced loss of cell surface CD62L

Having established that P2X7R activation couples to CD62L down-regulation from naïve $CD4^+$ T lymphocytes, it was possible to address the third aim of this project and assess the involvement of PI3K signalling in this process.

Firstly calcium mobilisation was investigated as a mechanism; this is because previous studies have shown that calcium can promote down-regulation of CD62L from the cell surface. The calcium ionophore Ionomycin (2.5 µM) has been shown to cause loss of cell surface CD62L processing from mouse T and B lymphocytes through ADAM10 and 17 (122). However, 10 µm Ionomycin was only able to cause a 14% loss of cell surface CD62L in lymphocytes from human patients with B-CLL (207). This thesis demonstrated that treatment with 1.3 µM Ionomycin was insufficient to cause CD62L down-regulation; however, higher concentrations were not explored. Un-expectedly treatment of naïve CD4+ T lymphocytes with U73122 caused loss of cell surface CD62L expression; this appears to be a specific effect because the inactive analogue U73433 had no effect on CD62L levels. This could be explained by the observation that U73122 can release Ca^{2+} from intracellular store in permeabilised mouse pancreatic acinar cells (441). Indeed, the use of Thapsigargin in this thesis caused significant down-regulation of CD62L from the cell surface of naïve $CD4^+$ T lymphocytes. The fact that ATP induced CD62L down-regulation was not significantly affected by removal of extracellular Ca^{2+} is in agreement with Jamieson et al (207).

A number of previous studies have investigated the activation of signalling proteins down-stream of P2X7R; here activation of the PI3K/mTOR and Erk1/2 pathways was investigated (205, 238, 255, 330, 334–336, 426–428). For immunoblotting, T lymphocytes activated by SEB were used because they are easier to isolate in large numbers and contain more protein than naïve $CD4^+$ T lymphocytes. Treatment with 1 mM ATP led only to small increases in the phosphorylation of components of these signalling pathways, whereas other experiments have shown this concentration to be sufficient for significant responses. In addition, A438079 only partially reduced ATP induced phosphorylation of Erk1/2. Electrophysiological experiments confirmed that 10 μM A438079 significantly inhibited ATP induced currents in naïve $CD4^+$ T lymphocytes. These experiments did, however provide a hint that the PI3K/mTOR and Erk1/2 pathways may be activated in T lymphocytes by ATP.

This study demonstrates that although ATP induced loss of cell surface CD62L expression requires the action of MMPs; remarkably it is independent of the PI3K, Erk1/2, p38 MAPK and PKC signalling pathways. Although initially unexpected, this finding correlates with data for ATP induced CD27 loss from mouse splenocytes (313). Another study also showed that ATP induced TGFα release from AP-TGFα transfected CHO cells through P2Y receptors was Erk1/2 and PKC independent (422). Recent data have revealed that Akt can be activated independently of PI3K, therefore P2X7R may activate Akt to induce CD62L in a manner independent of PI3K (429). Additionally, the lack of PI3K/mTOR and Erk1/2 involvement in down-regulation of surface CD62L expression in response to CD3/CD28 ligation of T lymphocytes was also not reconciled with mouse studies here (114).

Several other mechanisms could be responsible for CD62L processing in response to ATP. Neutrophils down-regulate CD62L from their cell surface in response to osmotic stress, the mechanism for this involves shrinkage of cells and the action of p38 MAPK and MMPs (442). Although cell shrinkage has previously been reported in response to ATP, data from this thesis suggests that this is not the case for human naïve $CD4^+$ T lymphocytes (206, 278). Additionally, the p38 MPAK inhibitor SB203580 had no effect on ATP induced down-regulation of cell

surface CD62L expression. During apoptosis, the mitochondria changes the lipid composition of its membrane and *de novo* synthesis of the lipid ceramide is promoted by BzATP and ATP through P2X7R in mouse thymocytes (279). This increased ceramide synthesis is required for activation of the apoptotic caspases 3 and 7 in macrophages (443). Streptolysin O is a pore forming toxic from bacteria which causes an increase in ceramide production in human granulocytes (444). This ceramide increase following Streptolysin O treatment was responsible for loss of cell surface CD62L expression from these cells. This effect was recapitulated by exogenous application of ceramide. However, ceramide production in response to ATP was not measured in this thesis and as other markers of apoptosis were not induced, it is unlikely that ceramide is responsible for CD62L down-regulation in human naïve $CD4^+$ T lymphocytes.

5. Chapter 5: Modulation of P2X7R function by uncoupling mitochondrial electron transport

5.1. Reactive Oxygen Species (ROS) Generation in Human Naive $CD4^+$ T Lymphocytes

5.1.1. Rational

The previous chapter established that CD62L down-regulation from the surface of human naïve $CD4^+$ T lymphocytes is dependent upon the activation of P2X7R and the action of MMPs. Experiments using small molecule inhibitors of signalling proteins of the PI3K and MAPK pathways showed that unexpectedly these did not transduce P2X7R activation to CD62L processing. An interesting observation was made when two of these compounds (LY294002 and Rottlerin) were used at concentrations above the published IC_{50} values for inhibition of their intended targets (PI3K and PKC respectively). At these higher concentrations, LY294002 and Rottlerin enhanced anti-CD3 antibody coated bead and ATP induced CD62L cell surface down-regulation respectively. One off target effect of these compounds is the enhanced production of reactive oxygen species (ROS). LY294002 is a potent anti-cancer agent through its inhibition of PI3K and DNA-PK, however, recent data suggests that it may also increase production of H_2O_2 (59). Rottlerin, when used at relatively high concentrations (e.g. 10 μM) can increase the consumption of O_2 in cells, and this effect is thought to be through increased ROS generation by modulation of the mitochondrial electron transport chain.

Additionally, P2X7R activation can cause the increased production of ROS in cells; this can drive a number of biochemical processes including the processing of IL-1β by macrophages. ROS can act as second messengers through their ability to oxidise cysteine residues in target proteins (445, 446). Indeed, ROS can cause increased processing of ADAM17 substrates through a mechanism involving either direct reduction of cysteine residues in ADAM17 or down-regulation of ADAM17 stabilising protein disulfide isomerases (PDIs) (421, 447). MMP1 and MMP9 can also be activated by ROS (448).

The observations that:

- ATP, through P2X7R, can increase intracellular ROS production
- Off target ROS enhancing effects of LY294002 and Rottlerin may enhance CD62L down-regulation
- ADAM17 and MMPs can be activated by ROS to cleave their substrates

Led to formation of the hypothesis that:

1. ATP activates P2X7R
2. P2X7R couples to increased ROS generation
3. ROS activates MMPs such as ADAM17
4. This causes CD62L processing

5.1.2. Aim

Firstly, using intracellular ROS sensing dyes and pharmacological tools, the role of ATP in ROS generation in naïve $CD4^+$ T lymphocytes was explored. This was followed by a strategy to determine if ROS mediates P2X7R dependent CD62L loss, as well as other processes.

5.1.3. ROS generation in the acute monocytic leukaemia cell line THP-1

Previous work established that in macrophages activation of NADPH oxidase by P2X7R was required for ATP induced IL-1β processing (246), however little is known about the role of P2X7R in ROS generation in T lymphocytes (449). A 2',7'-dichlorodihydrofluorescein diacetate (H2DCFDA "DCF") based fluorescence assay was used to measure ROS generation in freshly isolated naïve $CD4^+$ T lymphocytes, SEB activated T lymphocytes and the leukemic cell lines Jurkat and THP-1. The acute monocytic leukaemia cell line THP-1 was previously used to establish an assay for ethidium bromide uptake (Figure 3.6), therefore this cell type was also assessed for its ability to generate ROS in response to ATP. Unexpectedly, undifferentiated THP-1 monocytes (Figure 5.1 A and B) and macrophage-like IFNγ and LPS differentiated cells (Figure 5.1 C and D) did not show significant ROS formation in response to ATP.

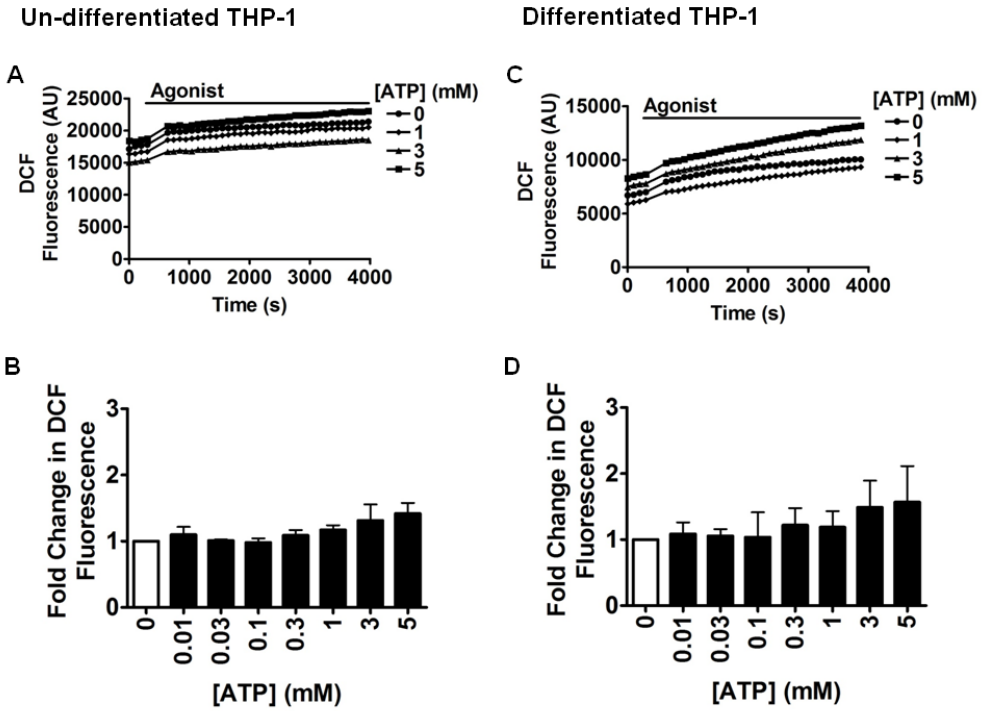

Figure 5.1: ATP does not induce significant ROS generation in the acute monocytic leukaemia cell line THP-1. Un-differentiated THP-1 cells were removed from culture **A** and **B** (n=3 ± SEM) or differentiated overnight with IFNγ and LPS **C** and **D** (n=2 ± range). Cells were loaded with DCF as described, treated with agonist and fluorescence recorded. Example kinetics of ATP induced ROS generation are given in **A** and **C.** Changes in DCF fluorescence were recorded over 1 hour of agonist stimulation and the fold changes above vehicle treatment are displayed in **B** and **D**. One Way ANOVA followed by Tukey's post-test used to determine significance.

5.1.4. ROS generation in SEB activated T lymphocytes and the leukemic T cell line Jurkat

ROS has been investigated as a mediator of cellular signalling following activation of T lymphocytes. Therefore, human T lymphocytes activated *ex vivo* with SEB and the leukemic T cell line Jurkat were assessed for ROS generation in response to ATP. SEB activated T lymphocytes show a significant increase in their ROS generation after 1 hour 5 mM ATP treatment (Figure 5.2 A and B), this was independent of extracellular $CaCl_2$ and $MgCl_2$ (Figure 5.2 C). The leukemic T cell line Jurkat also showed increased ROS generation in response to ATP, with 3 and 5 mM ATP evoking significant increases in ROS (Figure 5.2 D and E). Similarly to SEB activated T cells there was no significant difference in the effect of ATP applied in the absence or presence of extracellular $CaCl_2$ and $MgCl_2$ (Figure 5.2 F).

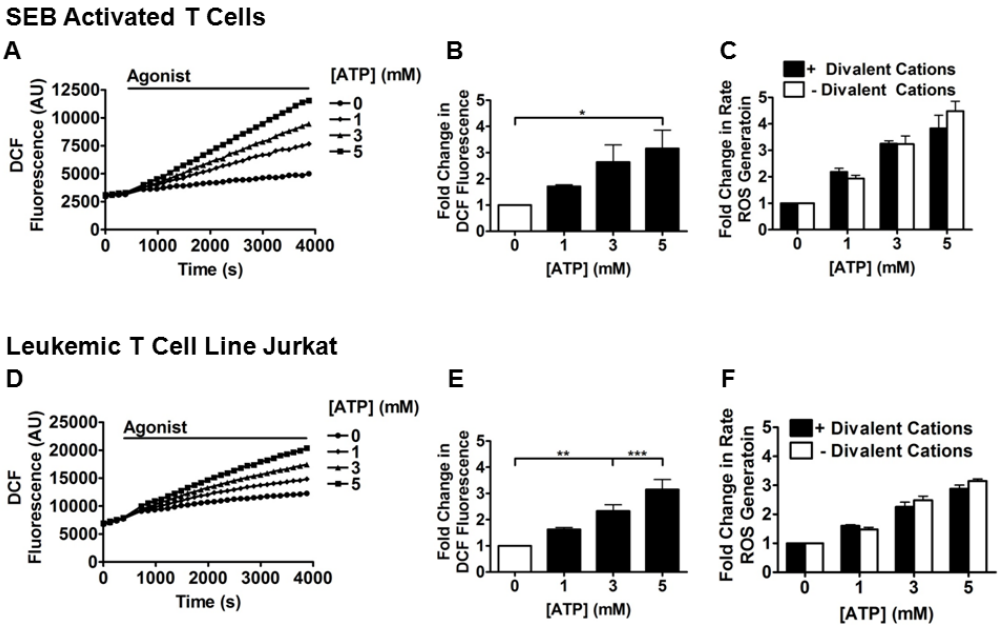

Figure 5.2: ATP induces ROS generation in SEB activated T lymphocytes and the leukemic T cell line Jurkat. T lymphocytes activated with SEB *ex vivo* (Removed from culture 9 days post activation) and the leukemic T cell line Jurkat were removed from culture. Cells were loaded with DCF as described, treated with agonist and fluorescence recorded. **A and D.** Example kinetics of ATP induced ROS generation. **B and E.** After 1 hour a final reading was recorded and expressed as a fold change over vehicle control (n=3). **C and D.** After loading with DCF cells were placed in buffer containing or free of $CaCl_2$ and $MgCl_2$ and treated with increasing concentrations of ATP (n=3). Histograms represent fold change in DCF generation over 1 hour normalised to vehicle control. One Way ANOVA followed by Tukey's post-test used to determine significance *p<0.05, **p<0.01 and ***p<0.001

5.1.5. ROS generation in naïve CD4$^+$ T lymphocytes

ROS generated in response to PMA is involved in activation of ADAM17 and subsequent processing of TNF p75 receptor from a human monocytic cell line (125). In chapter 4 PMA induced down-regulation of surface CD62L expression through PKC activation was demonstrated, here 100 nM PMA is also shown to induce a small but insignificant increase in DCF fluorescence in naïve CD4$^+$ T lymphocytes (Figure 5.3 A).

Activation of T lymphocytes leads to an increase in ROS production. Anti-CD3 antibody induces an increase in DCF fluorescence in murine T lymphocytes; as well as an increase in DHE fluorescence (a dye used to measure superoxide (O_2^-) production) (450). Here, treatment of freshly isolated human naïve CD4$^+$ T lymphocytes with 10 µg/ml anti-CD3 antibody UCHT1 for 1 hour caused a small non-significant increase in DCF fluorescence (Figure 5.3 B). Data from other groups (but not supported by data from chapter 3 here) suggest that P2X7R is required for T lymphocyte activation (259, 261, 268). It was hypothesised that P2X7R could still have a role in ROS generation following T lymphocyte activation; however pre-treatment with 10 µM A438079 did not inhibit ROS generation in response to UHCT1 treatment (Figure 5.3 B).

Exogenous ATP could still activate P2X7R and lead to ROS generation independent of T lymphocyte activation, therefore this was investigated next. Treatment of freshly isolated naïve CD4$^+$ T lymphocytes with ATP resulted in a concentration dependent increase in DCF fluorescence. Following 1 hour 5 mM ATP treatment, naïve CD4$^+$ cells show a significant increase in the rate of ROS generation compared to vehicle treatment (Figure 5.3 C and D).

5.1.6. Mechanisms of ROS generation

As ATP induced CD62L down-regulation is P2X7R dependent, P2X7R was assessed for its involvement in ATP induced ROS formation using A438079. Surprisingly A438079 did not inhibit 5 mM ATP induced increase in DCF fluorescence (Figure 5.3 E). The cellular components responsible for ROS generation in response to ATP were next investigated, as ATP can modulate NADPH oxidase (246, 451). DPI is an inhibitor of flavocytochrome containing enzymes, which include: flavocytochrome P450, nitric oxide synthase, NADPH

oxidase and complex I of the mitochondrial electron transport chain (Table 5.1). The increase in DCF fluorescence in response to 5 mM ATP was not inhibited by 1 hour pre-treatment with 100 μM DPI (Figure 5.3 F). Treatment with the complex I inhibitor rotenone had no effect on ATP induced increase in DCF fluorescence, suggesting that ATP does not increase ROS through mitochondrial complex I (Figure 5.3 G).

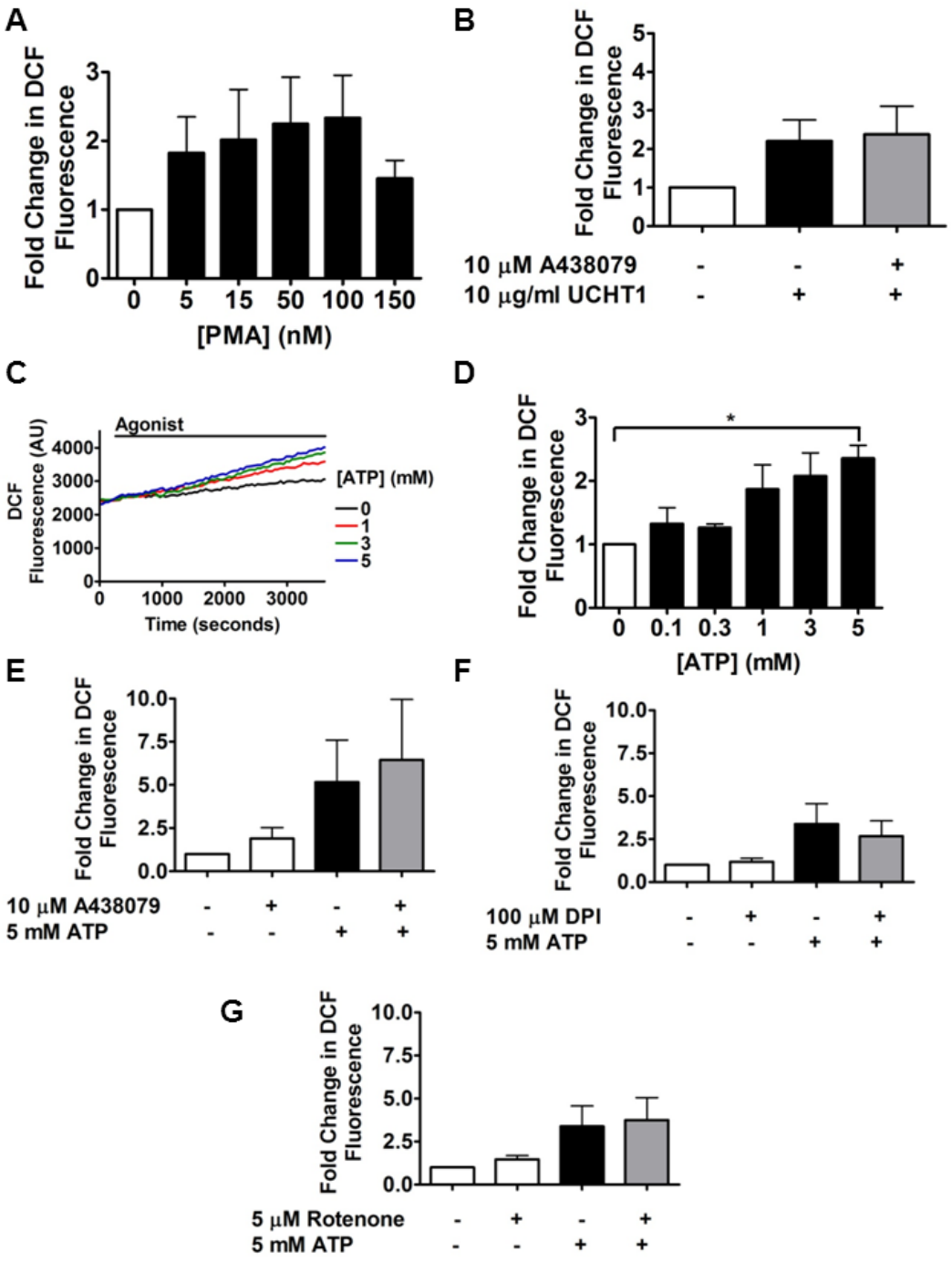

Figure 5.3: Mitogen and ATP induced ROS generation in naïve CD4$^+$ T lymphocytes. ROS in response to ATP is independent of P2X7R and unaffected by Rotenone or DPI. A. Freshly isolated naïve CD4$^+$ T lymphocytes were loaded with DCF as described, treated with agonist and fluorescence recorded. After 1 hour a final reading was recorded and expressed as a fold change over vehicle control. **A.** Effect of PMA on ROS (n=4). **B.** Cells were pre-treated with vehicle or A438079 for 30 minutes then effect of UCHT1 (anti-CD3 antibody) on ROS measured (n=5). **C.** Example kinetic of ATP induced ROS generation. **D.** Effect of ATP on ROS (n=5). Cells were pre-treated with **E.** A438079 or **F.** Rotenone for 30 minutes or **G.** DPI for 1 hour before ATP treatment (n=3). One Way ANOVA followed by Tukey's post-test used to determine significance *p<0.05

5.1.7. Exogenous application of hydrogen peroxide (H_2O_2) causes down-regulation of cell surface CD62L expression

Use of DCF detects generation of ROS which include H_2O_2. Exogenous H_2O_2 has previously been shown to cause loss of cell surface CD62L expression (421). Results here confirm that exogenous application of 100 µM H_2O_2 rapidly causes significant loss of cell surface CD62L expression (Figure 5.4 A). Peak CD62L loss was observed after 15 minutes H_2O_2 treatment. ROS generated in response to ATP treatment could potentially cause loss of CD62L surface expression, therefore inhibitors of ROS generating proteins were used to explore this possibility (Table 5.1).

Compound	Target	Source	IC_{50} Values
Apocynin	NADPH Oxidase (NOX2)	Sigma	NOX2 = 10 µM
DPI	Flavin containing enzymes. (flavocytochrome P450, nitric oxide synthase, NADPH Oxidase and Complex I)	Sigma	NOX2 = 0.9 µM Respiration = 13 µM
Rotenone	Complex I of mitochondrial electron transport chain	Sigma	3.4 ± 0.4 nM[a] (452) 1.4 µM[b] (159)
Antimycin A	Complex III of mitochondrial electron transport chain	Sigma	13.3 ± 0.7 nM[a] (452) 0.24 µM[b] (159)

Table 5.1 Table of inhibitors of ROS generating proteins

Inhibitors and uncouplers of ROS generating proteins used in this study are given in this table along with a range of their IC_{50} values. [a]Blockage of NADH oxidation by cardiac SR and [b]Inhibition of oxygen consumption in middle aged rats.

5.1.8. DPI enhances ATP induced down-regulation of cell surface CD62L expression independently of NADPH oxidase

DPI inhibits flavin containing enzymes including NADPH oxidase and complex I of the mitochondrial electron transport chain. Unexpectedly, DPI significantly enhanced ATP induced CD62L loss (Figure 5.4 B); however inhibition of NAPDH oxidase (NOX2) with apocynin did not replicate the enhancing effect on CD62L down-regulation (Figure 5.4 C). This observation suggested that complex I of the mitochondrial electron transport chain might be responsible for this enhancement. Inhibition of electron transport through complexes in the respiratory chain can lead to the leaking of electrons and generation of ROS including O_2^-. As mentioned previously, Rottlerin pre-treatment also enhances ATP induced CD62L loss and studies suggest Rottlerin may enhance ROS generation by mitochondria at 10 µM (418, 453). The mitochondrial electron transport chain was therefore investigated as a possible mechanism for enhanced ATP induced down-regulation of cell surface CD62L expression.

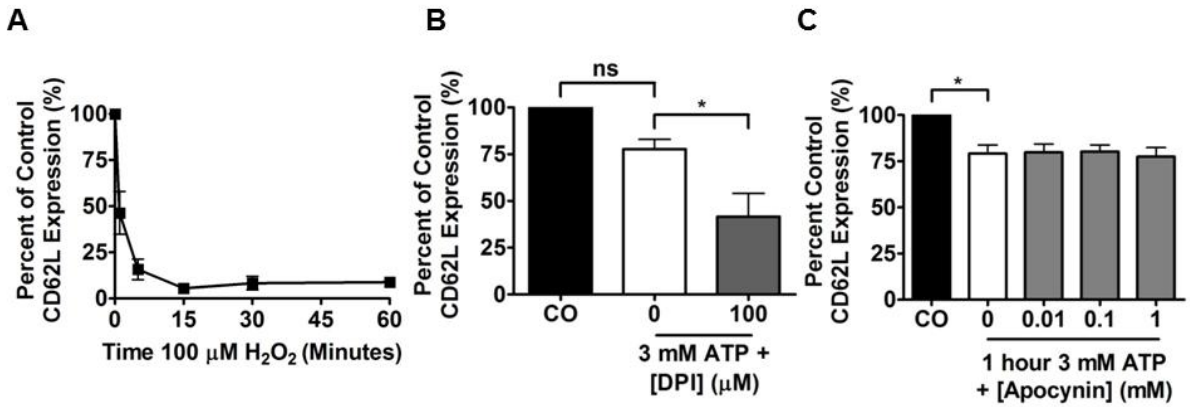

Figure 5.4: Exogenous H_2O_2 causes CD62L loss from naïve $CD4^+$ T lymphocytes. DPI but not apocynin enhances ATP induced CD62L loss. A. Freshly isolated naïve $CD4^+$ T lymphocytes were treated with 100 µM H_2O_2 for increasing periods of time (n=3). Cells were pre-treated with vehicle (DMSO), or **B.** 100 µM DPI for 1 hour or **C.** increasing concentrations of apocynin for 30 minutes, then treated with vehicle or 3 mM ATP for 1 hour (n=3). CD62L expression was measured using flow cytometry as described. One Way ANOVA followed by Tukey's post-test was used to determine significance *p<0.05

5.1.9. Uncoupling of mitochondrial electron transport at complex I or III causes enhanced ATP dependent down-regulation of cell surface CD62L expression via P2X7R

Rotenone and antimycin A, small molecule inhibitors of complex I and complex III of the mitochondrial electron transport chain respectively, were used to investigate the role of mitochondrial ROS in ATP induced CD62L down-regulation through P2X7R. Before ATP treatment, cells were pre-treated with a range of concentrations of rotenone or antimycin A close to published IC_{50} values for these compounds (Table 5.1). Both rotenone and antimycin A had no effect on basal levels of cell surface CD62L expression (Figure 5.5 A and B), but significantly enhanced CD62L down-regulation in response to ATP treatment (Figure 5.5 C and D). An additional 50.27 ± 2.25 % (n=8 ± SEM) loss of CD62L expression was observed with 5 μM rotenone pre-treatment when compared with DMSO. For pre-treatment with 1 μM antimycin A, an additional 41.57 ± 4.08 % (n=3 ± SEM) loss of CD62L expression was observed compared with DMSO. As the effect of rotenone and antimycin A on CD62L expression was only observed when cells were subsequently treated with 3 mM ATP, P2X7R was most likely involved in this process. Cells were pre-treated with 5 μM rotenone (Figure 5.5 E) or 1 μM antimycin A (Figure 5.5 F) in the presence or absence of 10 μM A438079 before 3 mM ATP was applied for 1 hour. Pre-treatment with A438079 significantly inhibited not only the CD62L loss induced by ATP alone, but also when cells were pre-treated with rotenone or antimycin A. The enhancement effect of rotenone and antimycin A therefore involves P2X7R and evidence exists for the regulation of ion channels including P2X2 by ROS (454, 455). The effect of these compounds on the concentration of ATP required to elicit CD62L down-regulation through P2X7R was next investigated. ATP was applied in increasing concentrations to naïve $CD4^+$ T lymphocytes pre-treated with vehicle (DMSO), 5 μM rotenone A or 1 μM antimycin A (Figure 5.6 A). For down-regulation of cell surface CD62L expression in response to ATP, the EC_{50} value was decreased from 1.58 mM (DMSO) to 0.43 mM when cells were pre-treated with either rotenone or antimycin A (Figure 5.6 B). However, pre-treatment of cells with increasing concentrations of antimycin A (Figure 5.7 A) or rotenone (Figure 5.7 B) did not significantly enhance anti-CD3/CD28 antibody induced CD62L down-regulation.

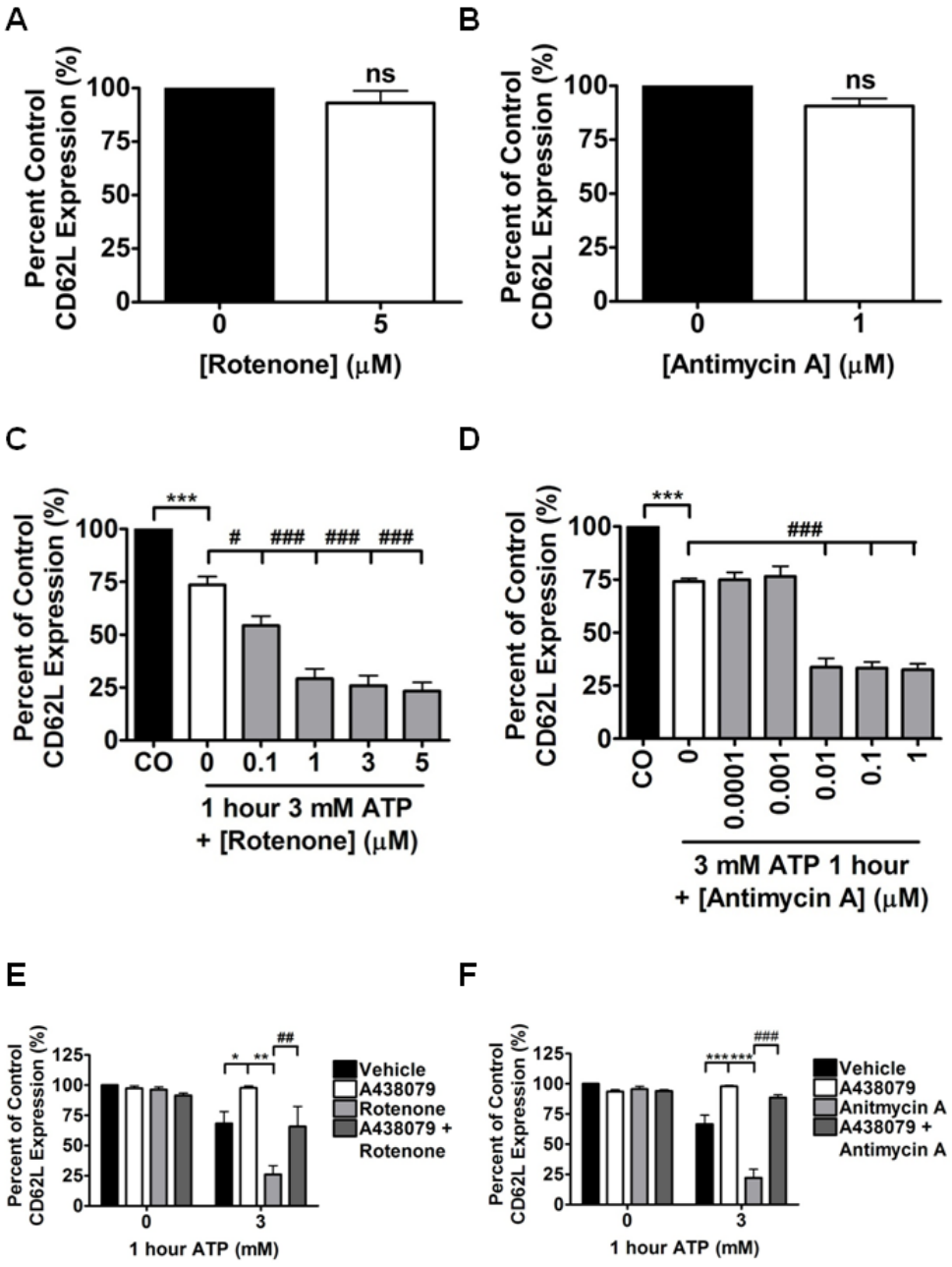

Figure 5.5: Antimycin A and rotenone enhance ATP induced CD62L down-regulation in a P2X7R dependent manner. Freshly isolated naïve $CD4^+$ T lymphocytes were pre-treated with vehicle (DMSO), or increasing concentrations of **A and C:** Rotenone (n=8) or **B and D:** Antimycin A (n=3) for 30 minutes. Cells were then treated with vehicle **(A and B)** or 3 mM ATP for 1 hour **(C and D)**. **E.** Cells were pre-treated with DMSO, 10 μM A438079, 5 μM rotenone or both A438079 and rotenone for 30 minutes before treatment with 3 mM ATP for 1 hour (n=3). **F.** Cells were pre-treated with DMSO, 10 μM A438079, 1 μM antimycin A or both A438079 and antimycin A for 30 minutes before treatment with 3 mM ATP for 1 hour (n=3). One Way ANOVA followed by Tukey's post-test or Two Way ANOVA followed by post-test were used to determine significance */#p<0.05, **/##p<0.01 and ***/###p<0.001

A

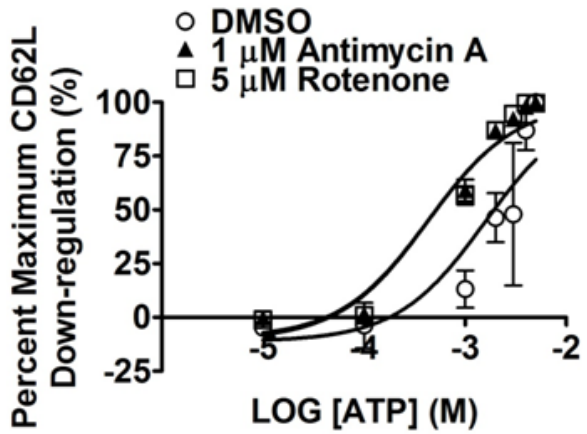

B

Compound	ATP EC_{50} (mM)
DMSO	1.58
1 μM Antimycin A	0.43
5 μM Rotenone	0.43

Figure 5.6: Antimycin A and rotenone increase potency for ATP induced CD62L down-regulation. A. Freshly isolated naive $CD4^+$ T lymphocytes were pre-treated with vehicle (DMSO), 5 μM rotenone or 1 μM antimycin A (n=3). Cells were then treated with increasing concentrations of ATP from 0.01-5 mM for 1 hour and CD62L expression measured as described. **B.** GraphPad Prism 4 was used to concentration response curves, pEC50 values for ATP for each of the pre-treatments are given in the corresponding table.

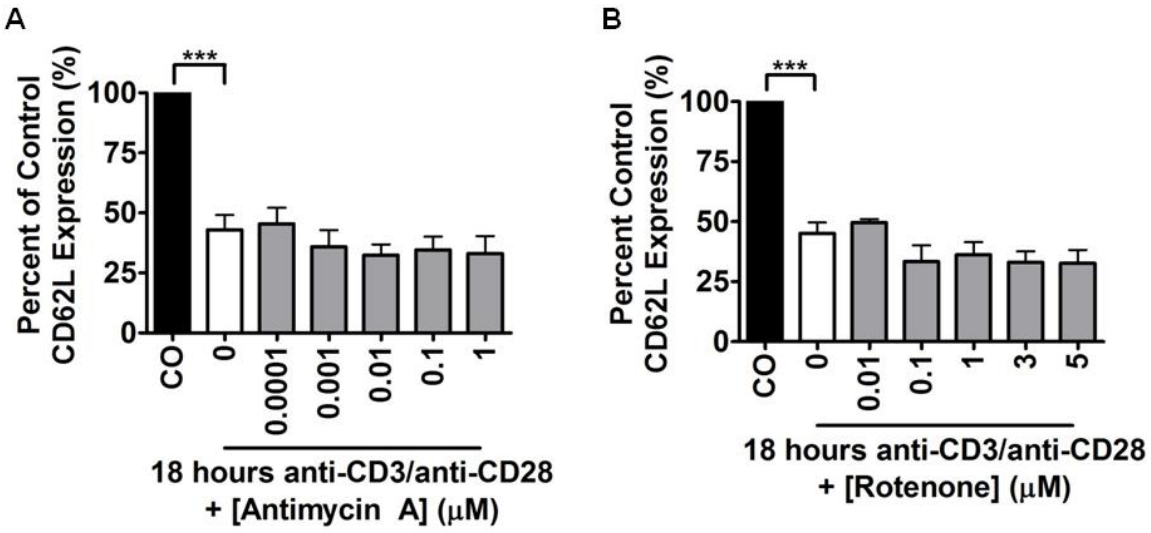

Figure 5.7: Antimycin A and rotenone do not affect CD62L down-regulation in response to 18 hour anti-CD3/CD28 antibody treatment. Freshly isolated naive $CD4^+$ T lymphocytes were pre-treated with DMSO, or increasing concentrations of **A.** Antimycin A or **B.** Rotenone for 30 minutes. Cells were then treated with anti-CD3/CD28 antibody coated beads for 18 hours and CD62L expression levels measured and analysed as described (n=3). One Way ANOVA followed by Tukey's post-test used to determine significance ***p<0.001

5.1.10. Rotenone and antimycin A enhance basal mitochondrial O_2^-

Previous work has demonstrated that uncoupling of the mitochondrial electron transport chain at complex I and III by rotenone or antimycin A respectively can increase the basal levels of O_2^- (158–160). In isolated mouse liver mitochondria antimycin A induced O_2^- generation (measured using MitoSOX Red) with an EC_{50} value of 11.4 ± 1.8 μM (159). Here it was confirmed that rotenone and antimycin A significantly increase basal levels of mitochondrial O_2^- in naïve $CD4^+$ T lymphocytes (Figure 5.8 A-C). This process was dependent on the concentration of each compound used. When cells were pre-treated with rotenone or antimycin A at the same concentrations, then treated with 3 mM ATP for 1 hour there was no significant enhancement of mitochondrial O_2^- above basal levels.

As previously mentioned, small amounts of ROS are generated after treatment of naïve $CD4^+$ T lymphocytes with anti-CD3 antibody (UCHT1) or PMA. O_2^- generation in activated T lymphocytes has also been reported (450); therefore MitoSOX Red was used to investigate if mitochondrial O_2^- increased after UCHT1 or PMA treatment. No significant increase in MitoSOX Red fluorescence was observed after UCHT1 or PMA treatment, suggesting O_2^- is not produced in the mitochondria following ligation of CD3 with anti-CD3 antibody (Figure 5.8 D).

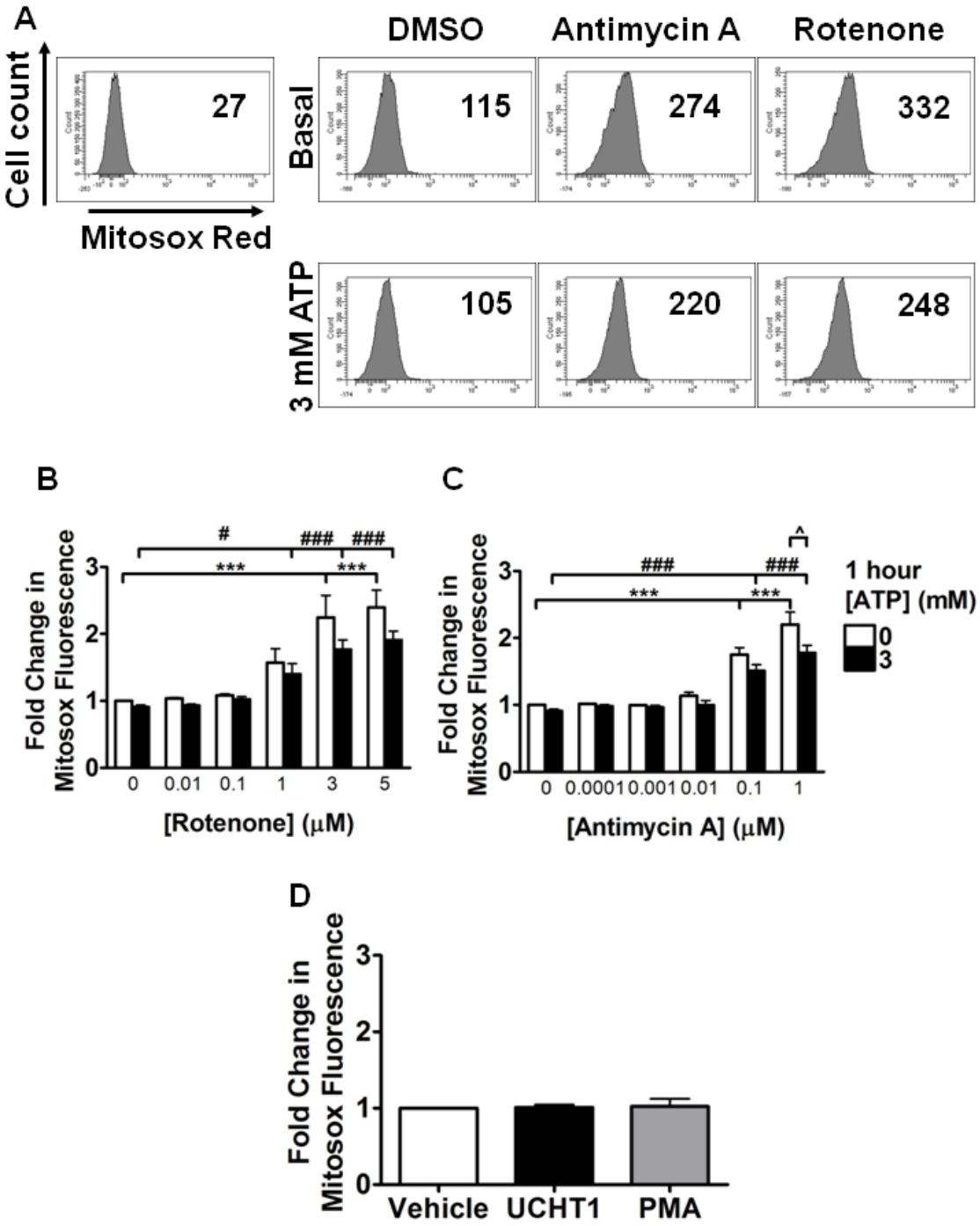

Figure 5.8: Antimycin A and rotenone significantly increase mitochondrial O_2^- levels independent of ATP. Freshly isolated naïve $CD4^+$ T lymphocytes were loaded with MitoSOX Red as described, pre-treated with vehicle (DMSO), rotenone or antimycin A for 30 minutes then vehicle or 3 mM ATP for 1 hour. MitoSOX Red Fluorescence was measured using Flow cytometry. **A.** Example flow cytometry histograms. **B.** Cells were treated with DMSO or rotenone and then vehicle or 3 mM ATP for 1 hour (n=3). **C.** Cells were treated with DMSO or antimycin A and then vehicle or 3 mM ATP for 1 hour (n=3). **D.** Effect of UCHT1 and PMA on mitochondrial O_2^- levels (n=3). One Way or Two Way ANOVA followed by Tukey's post-test used to determine significance #/^p<0.05, ***/###p<0.001

5.1.11. Effect of SOD mimetic Mn-cpx 3 on ROS generation and CD62L down-regulation

In cells O_2^- can be converted into H_2O_2 by the enzyme superoxide dismutase (SOD). SOD is just one component of a complex antioxidant system within cells that reduces damage to cellular components by ROS, or terminates ROS mediated signalling. H_2O_2 can be rapidly converted to H_2O by catalase and its reactivity with intracellular proteins such as ADAM17 is lost. The ability of H_2O_2 to induce CD62L down-regulation has been reported before and was confirmed for naïve $CD4^+$ T lymphocytes in this study (421) (Figure 5.4 A). Therefore, it is possible that mitochondrial O_2^- produced by rotenone and antimycin A is converted to H_2O_2 by SOD, and this is the ROS required for enhanced CD62L down-regulation by ATP. To investigate this, a cell permeable mimetic of SOD, Mn-cpx 3, was employed. The rational was that if O_2^- was required for enhanced CD62L loss, Mn-cpx 3 would *inhibit* CD62L down-regulation, whereas if H_2O_2 was required then Mn-cpx 3 would *enhance* CD62L down-regulation.

Mn-cpx 3 was first tested for its ability to enhance H_2O_2 production in naïve $CD4^+$ T lymphocytes. Indeed, while 30 minute pre-incubation with 30 µM Mn-cpx 3 had no effect on the basal rate of DCF fluorescence increase over 1 hour, it markedly enhanced DCF fluorescence when 3 mM ATP was applied (Figure 5.9 A and B). When cells were pre-treated with both Mn-cpx 3 and rotenone or antimycin A there did not appear to be an increase in DCF fluorescence compared to Mn-cpx 3 plus DMSO. This indicated that mitochondrial O_2^- generated by rotenone and antimycin A does not lead to enhanced cellular ROS detected by DCF. Mn-cpx 3 had no effect on basal CD62L expression levels, it did not enhance CD62L down-regulation induced by ATP alone, and unexpectedly had no effect on the enhancing effect of antimycin A (Figure 5.9 C).

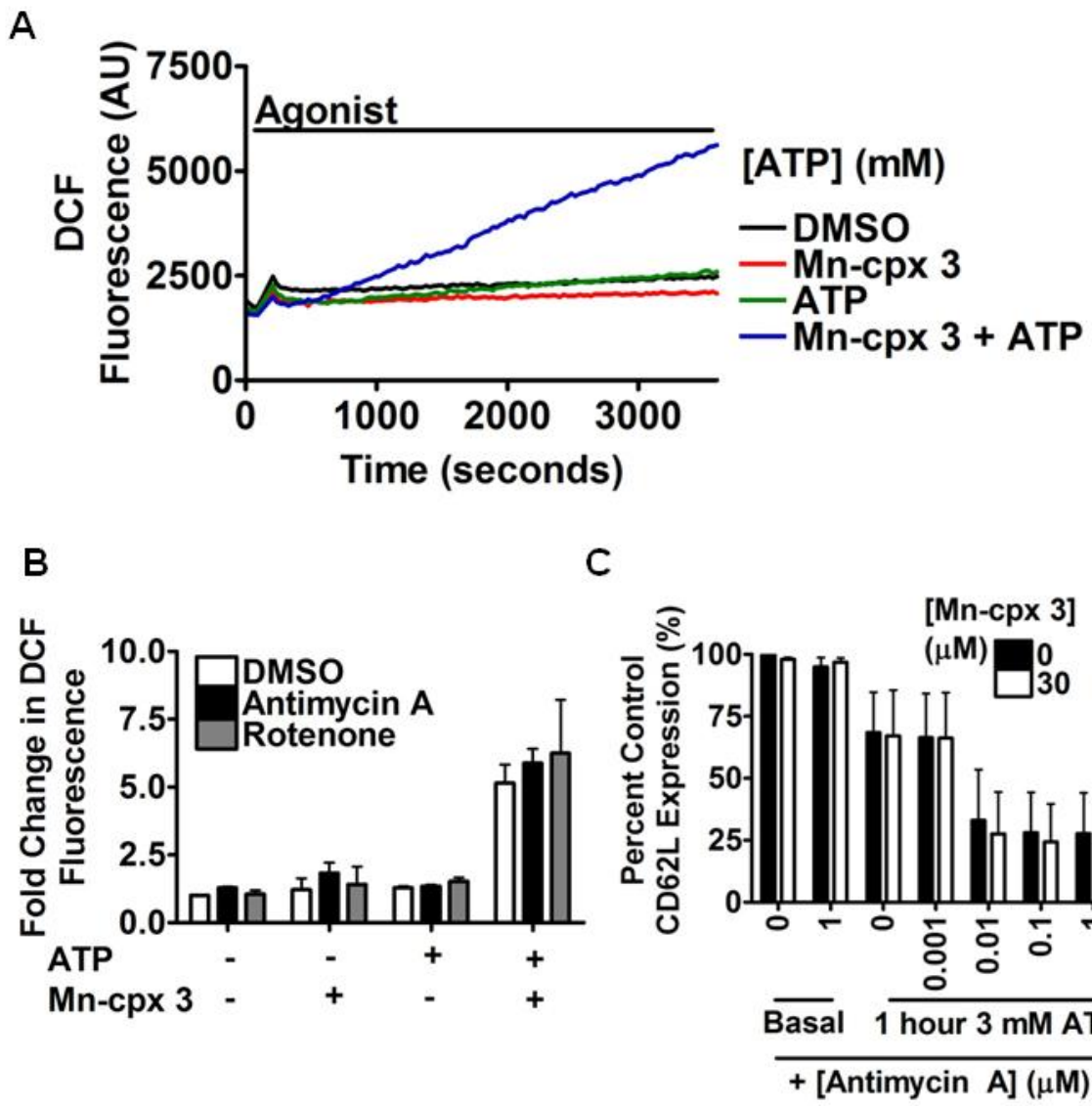

Figure 5.9: A SOD mimetic Mn-cpx 3 increases ATP induced DCF fluorescence, but has no effect on ATP or ATP + antimycin A induced CD62L down-regulation. Freshly isolated naïve $CD4^+$ T lymphocytes were loaded with DCF and pre-treated with vehicle (DMSO) or 30 μM Mn-cpx 3 for 30 minutes. DCF fluorescence was measured as described and vehicle or 3 mM ATP applied for 1 hour. **A.** Example kinetic of DCF fluorescence over 1 hour. **B.** Cells were pre-treated with DMSO or 30 μM Mn-cpx +/- DMSO, 5 μM rotenone or 1 μM antimycin A for 30 minutes then vehicle or 3 mM ATP applied for 1 hour (n=2 ± STDEV). **C.** Cells were pre-treated with DMSO or 30 μM Mn-cpx +/- increasing concentrations of antimycin A for 30 minutes, followed by 3 mM ATP for 1 hour and CD62L expression was measured using flow cytometry as described (n=3). Two Way ANOVA followed by post-test were used to determine significance.

5.1.12. Comparison of effects of antimycin A and rotenone between naive CD4$^+$ and SEB activated T lymphocytes

Naive CD4$^+$ T lymphocytes and effector Th cells demonstrate differential sensitivity to ROS such as H_2O_2 (456), therefore it was hypothesised that the ability of antimycin A and rotenone to enhance loss of cell surface CD62L expression through P2X7R may differ between these cell types.

Naïve CD4$^+$ T lymphocytes were isolated, and T lymphocytes from the same donor activated *ex vivo* from PBMCs using SEB. Cells were used on the day of isolation (naïve CD4$^+$) or 7 days post activation (SEB T cells) and experiment paired for each donor. SEB activated T cells show higher basal MitoSOX red fluorescence than naïve CD4$^+$ T lymphocytes (Figure 5.10 A). As shown in Figure 5.8, 1 µM antimycin A and 5 µM rotenone significantly enhance mitochondrial O_2^- generation. SEB activated T lymphocytes are significantly less sensitive to enhanced mitochondrial O_2^- generation in response to antimycin A, when compared to naïve CD4$^+$ T lymphocytes (Figure 5.10 B). However, this effect was not observed for rotenone pre-treatment.

When naïve CD4$^+$ T lymphocytes are activated they down-regulate CD62L, however central memory T lymphocytes re-express high levels of CD62L, this allows migration into the lymphatic system. Therefore, SEB activated T lymphocytes have biphasic CD62L expression but still respond to ATP by down-regulating CD62L expression in a P2X7R dependent manner, with an EC_{50} value of 804.2 µM (Figure 5.10 C and D).

When naïve CD4+ T lymphocytes are compared to SEB activated T lymphocytes from the same donors, there is a small difference between the effect of antimycin A and rotenone on ATP induced CD62L down-regulation, but this was statistically insignificant (Figure 5.10 E and F).

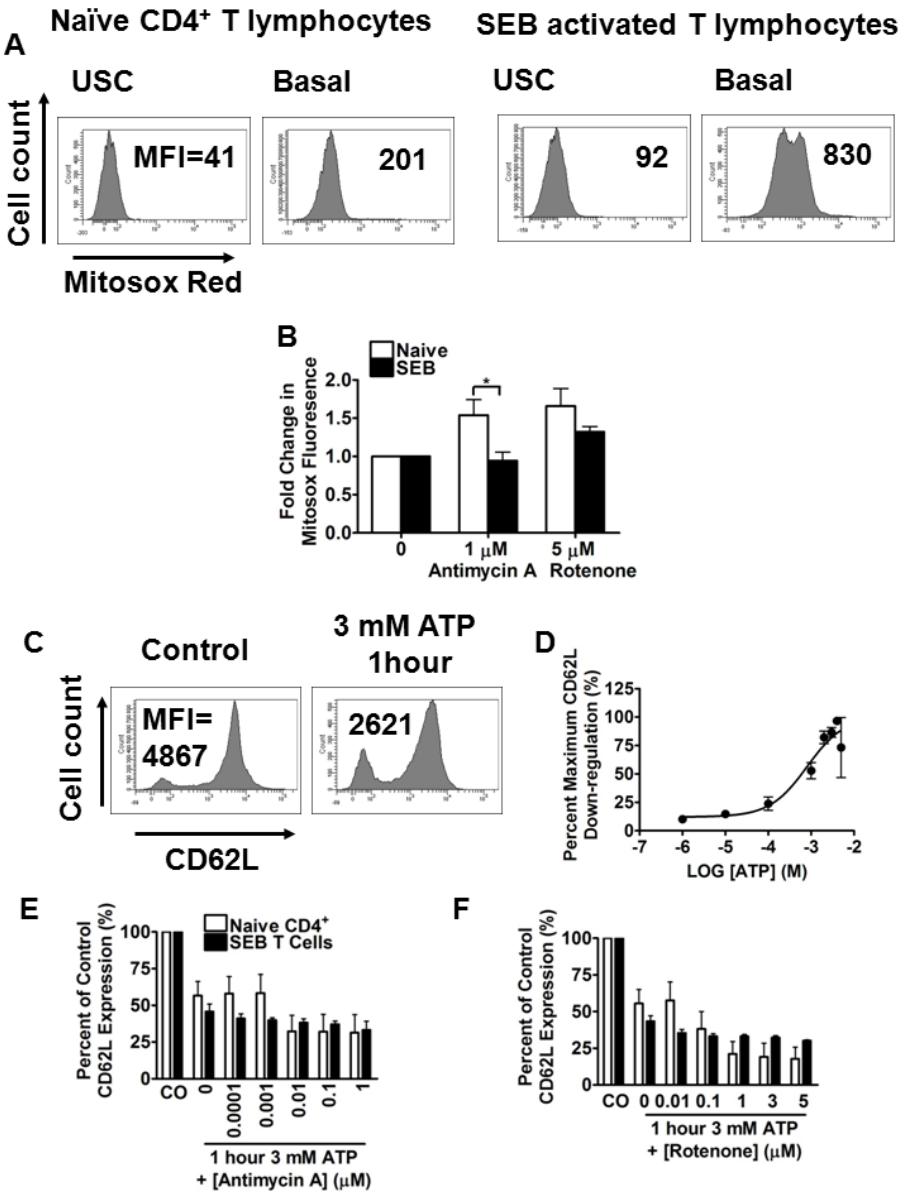

Figure 5.10: Comparison of effects of antimycin A and rotenone on mitochondrial superoxide generation and CD62L expression between naïve CD4$^+$ and SEB activated T lymphocytes. Freshly isolated naïve CD4$^+$ T or SEB T lymphocytes (Day 9 post activation) were loaded with MitoSOX Red as described. MitoSOX Red Fluorescence was measured using Flow cytometry. **A.** Histograms representing basal MitoSOX Red Fluorescence **B.** Cells were treated with vehicle (DMSO), rotenone or antimycin A for 90 minutes (n=3). **C and D**. T lymphocytes were activated *ex vivo* by SEB and removed from culture 9 days post activation. Cells were treated with increasing concentrations of ATP and cell surface CD62L expression measured as described (n=3). **E.** Cells were pre-treated with increasing concentrations of rotenone for 30 minutes before 1 hour 3 mM ATP treatment. CD62L expression was measured by flow cytometry as described (n=3). **F.** Cells were pre-treated with increasing concentrations of antimycin A for 30 minutes before 1 hour 3 mM ATP treatment (n=3). CD62L expression was measured by flow cytometry as described. Two Way ANOVA followed by post-test was used to determine significance between groups *p<0.05

5.1.13. Effect of rotenone and antimycin A on naïve $CD4^+$ T lymphocyte proliferation

Having demonstrated enhancement of ATP induced CD62L down-regulation by rotenone and antimycin A, other T lymphocyte processes were investigated for sensitivity to these compounds. If, like with CD62L expression, these compounds alone have no effect they may still enhance ATP responses through P2X7R. Although in chapter 3 inhibition of P2X7R by A438079 was shown to have no effect on proliferation, it was hypothesised that rotenone and antimycin A could potentially increase sensitivity of P2X7R to ATP and reveal a role for the receptor in proliferation. In a CFSE assay of proliferation, both rotenone and antimycin A significantly inhibited proliferation of naïve $CD4^+$ T lymphocytes after 7 days *ex vivo* culture (Figure 5.12 A-C). As this effect occurred in the absence of ATP, the role of mitochondrial uncoupling and P2X7R in proliferation was not explored further.

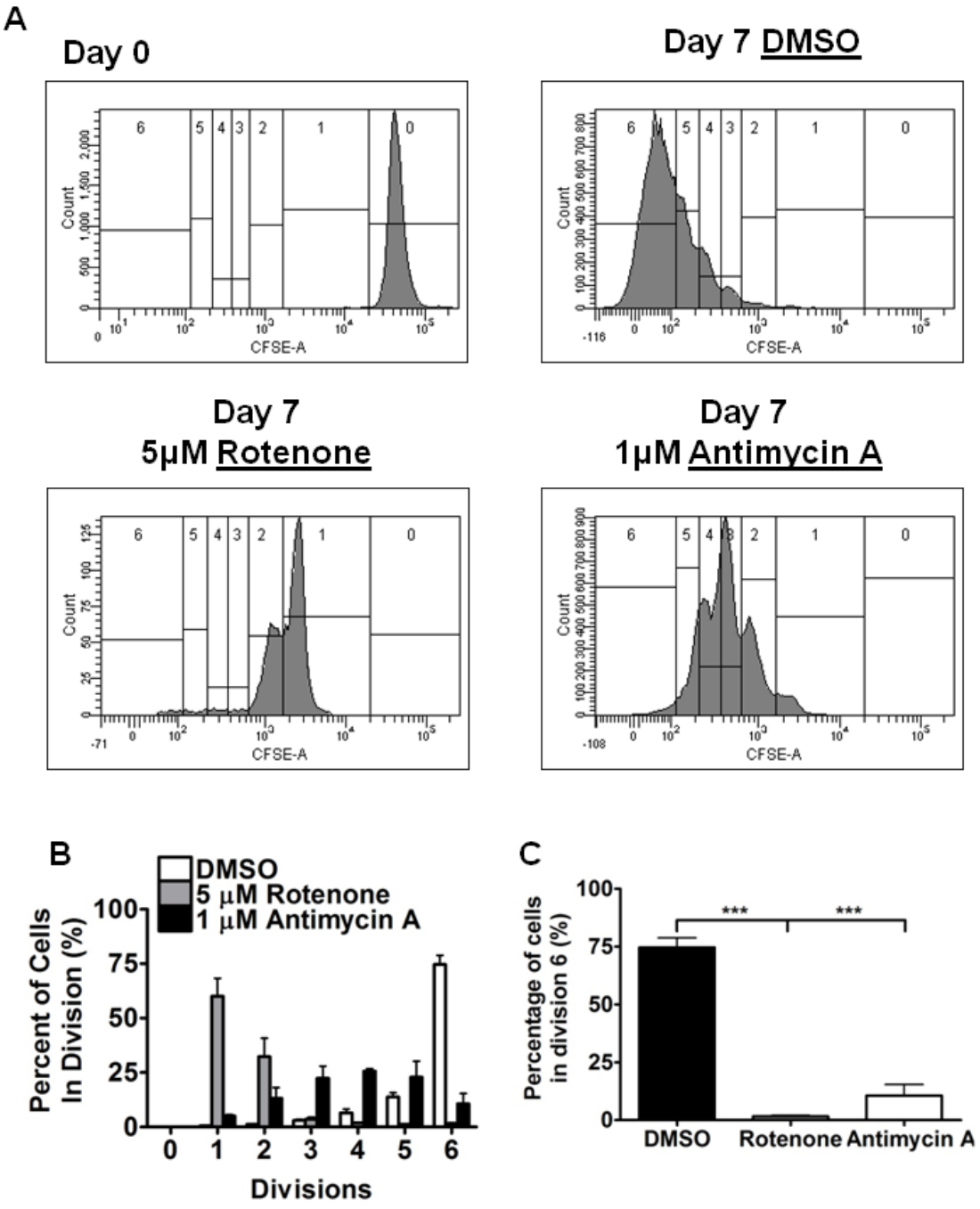

Figure 5.11: Antimycin A and rotenone significantly inhibit proliferation of human T lymphocytes. Freshly isolated naïve $CD4^+$ T lymphocytes were labelled with CFSE as described. Cells were analysed on the same day (Day 0) or pre-treated with vehicle (DMSO), 5 µM rotenone or 1 µM antimycin A for 30 minutes followed by addition of anti-CD3/ CD28 antibody coated beads to cells at a ratio of 3:1. IL2 was added at a final concentration of 36 Units/ml and cells cultured for 7 days before analysis for CFSE fluorescence. **A.** Representative flow cytometry histograms displaying population divisions 0-6. **B.** Comparison of the effect of rotenone and antimycin A on percentage of cells in each division (n=3). **C.** Statistical analysis of percentage of cells in final division 6 (minimum CFSE fluorescence) (n=3). Two Way ANOVA followed by post-test used to determine significance ***p<0.001

5.1.14. Effect of rotenone and antimycin A on naïve $CD4^+$ T lymphocyte migration

Purinergic receptors, particularly P1 adenosine and P2Y receptors have been studied for their role in cell migration, however little work on the role of P2X7R has been undertaken to date. Here the P2X7R antagonist A438079 suggested a small but insignificant inhibitory effect on migration of naïve $CD4^+$ T lymphocytes towards the chemokine CXCL12 (Figure 5.12 A). Using the Neuroprobe Boyden Chamber-like assay, migration of T lymphocytes activated by SEB appears to be unaffected by A438079 pre-treatment (Figure 5.12 B). However, a more detailed analysis of migration during live cell imaging using IBIDI µslides suggests that 1 µM A438079 may enhance basal motility while decreasing directed migration of SEB activated T lymphocytes (Figure 5.12 C). Indeed, basal velocity, accumulated and euclidean distance were all increased following 1 µM A438079 treatment; whereas, these parameters were all reduced compared to vehicle treated control cells when a CXCL-11 gradient was present. Migration of naïve $CD4^+$ T lymphocytes towards CXCL12 or basally (without chemokine) was therefore investigated with rotenone and antimycin A. As with proliferation both compounds caused a marked decrease in migration in the absence of ATP (Figure 5.13). Therefore, the combined effect of ATP and rotenone or antimycin A was not investigated in naïve $CD4^+$ T lymphocyte migration.

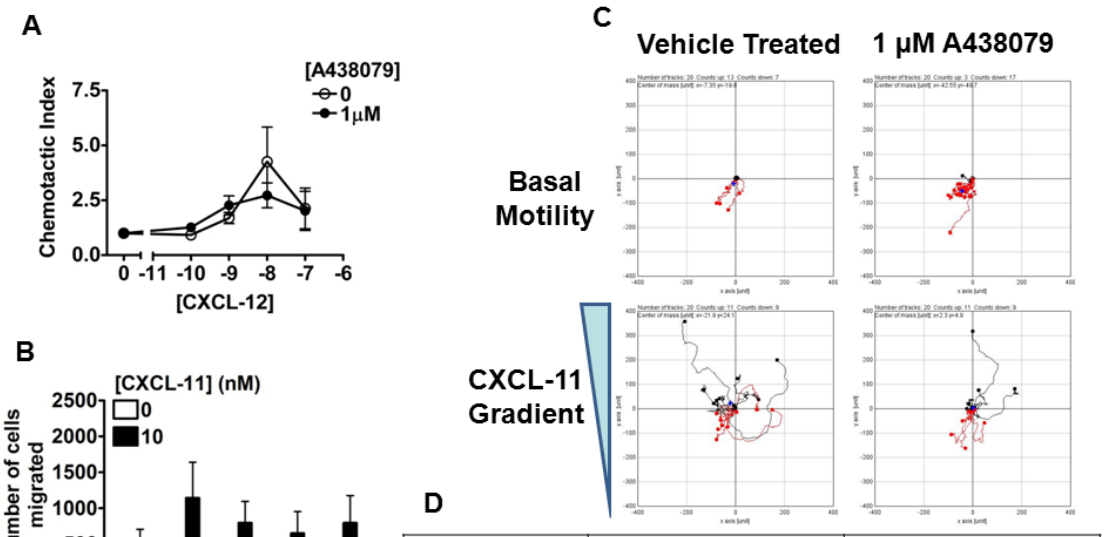

	Basal Motility		CXCL-11	
	Control	A438079	Control	A438079
Velocity (µm/sec)	0.15	0.25	0.35	0.26
A. Distance (µm)	134,52	219.4	308.48	229.3
E. Distance (µm)	27.62	70.58	108.29	58.1

Figure 5.12: Effect of P2X7R inhibition on naive CD4$^+$ and SEB activated human T lymphocyte migration. A. Naïve CD4$^+$ T lymphocytes were freshly isolated and pre-treated with vehicle or 1 µM A438079 for 30 minutes. The *in vitro* basal migration of cells and migration towards the chemokine CXCL-12 was then assessed by a Neuroprobe assay (n=3). **B and C.** T lymphocytes activated *ex vivo* by SEB were removed from culture after 9 days, and pre-treated with vehicle or 0.01 – 10 µM A438079 (**B**) or 1 µM A438079 (**C**) for 30 minutes. The *in vitro* basal migration of cells and migration towards the chemokine CXCL-11 was then assessed by a Neuroprobe assay (n=3). **C and D.** IBIDI µslides were briefly used to assess *in vitro* basal migration or migration towards CXCL-11 (n=1).

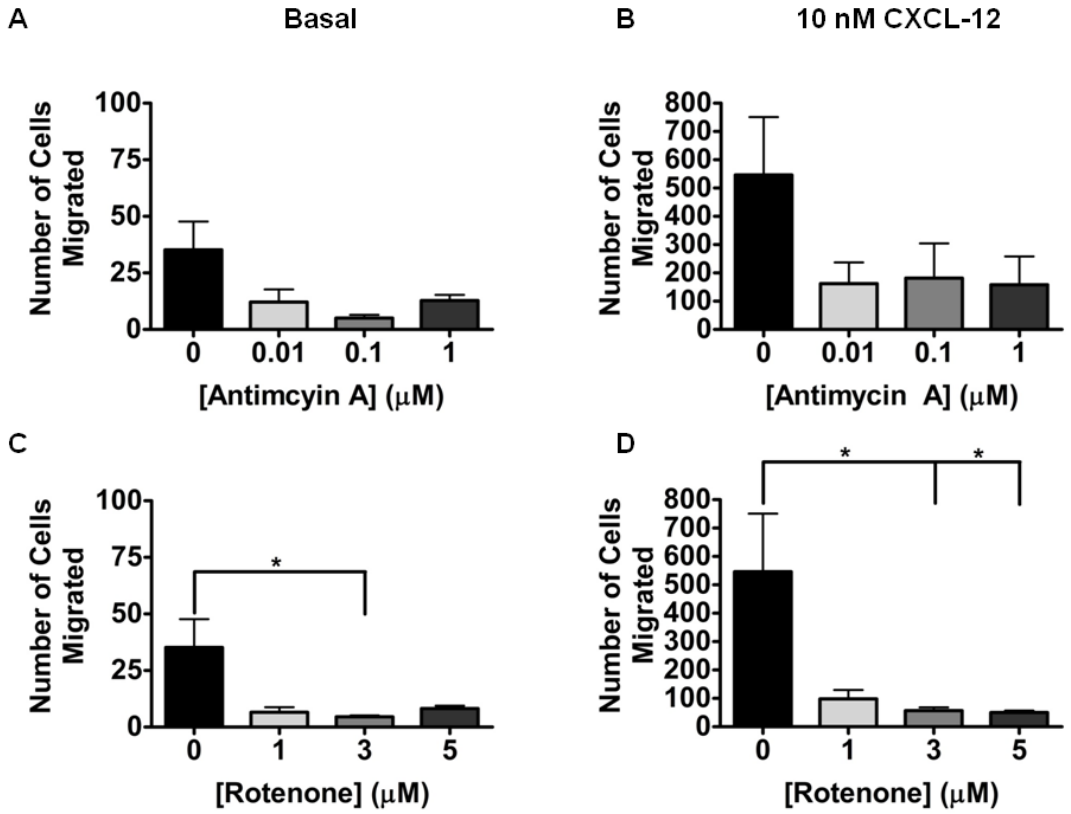

Figure 5.13: Antimycin A and rotenone reduce migration of naive CD4$^+$ human T lymphocytes. Freshly isolated naïve CD4$^+$ T lymphocytes were pre-treated with DMSO or increasing concentrations of rotenone or antimycin A. Cells were then assessed for their ability to migrate independent of chemokine (Basal) or towards the chemokine CXCL-12 using the previously described Neuroprobe migration assay. **A.** Effect of antimycin A on basal migration (n=3) **B.** Effect of antimycin A on CXCL-12 directed migration (n=3). **C.** Effect of rotenone on basal migration (n=3). **D.** Effect of rotenone on CXCL-12 directed migration (n=3). One Way ANOVA followed by Tukey's post-test used to determine significance *p<0.05

5.1.15. Effect of rotenone and antimycin A on naïve CD4$^+$ T lymphocyte apoptosis

Next the effect of rotenone and antimycin A on apoptosis was investigated; neither compound alone had significant effect on PS translocation or PI uptake. Treatment with 3 mM ATP for 1 hour had no effect on annexin V binding, however when cells were pre-treated with rotenone or antimycin A significant annexin V binding was revealed (Figure 5.14 A). Staining for PI was very weak, however the percentage of cells staining positive for PS translocation and for PI uptake following ATP treatment was significantly enhanced by pre-treatment with rotenone and antimycin A (Figure 5.14 B). Despite ATP alone having no effect, PS translocation observed with rotenone and antimycin A in combination with ATP was blocked by A438079 (Figure 5.14 A).

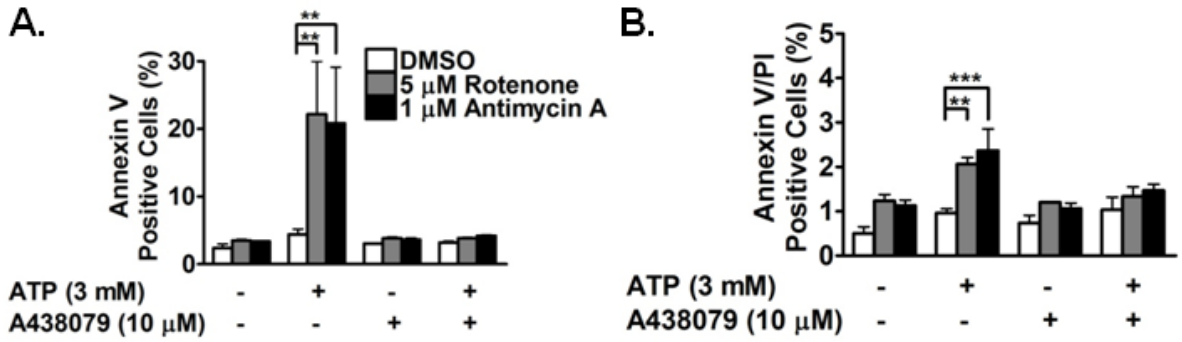

Figure 5.14: Antimycin A and rotenone enhance PS exposure and PI uptake in naïve CD4$^+$ T lymphocytes. Naïve CD4$^+$ T lymphocytes were freshly isolated from peripheral human blood and re-suspended in complete RMPI-1640. Cells were pre-treated with vehicle (DMSO), 5 µM rotenone or 1 µM antimycin A and/or 10 µM A438079 for 30 minutes then treated with 3 mM ATP for 1 hour. Cells were stained with annexin V and PI as described in materials and methods. **A.** The percentage of cells positive for annexin V is given for each treatment condition (n=3). **B.** The percentage of cell positive for both annexin V and PI is given for each treatment condition (n=3). Two way ANOVA followed by post hoc test was used to determine significance between groups **p<0.01, ***p<0.001.

5.1.16. Results Section 5 Summary

- T lymphocyte activation by anti-CD3 antibody or PMA cause small insignificant increases in ROS generation in naïve $CD4^+$ T lymphocytes
- ATP causes significant increases in ROS in naïve $CD4^+$, SEB activated T lymphocytes and the leukemic T cell line Jurkat independent of extracellular $CaCl_2$ or $MgCl_2$
- The P2X7R inhibitor A438079 did not inhibit ROS generation
- The source of ROS was not determined
- ROS machinery inhibitors do not affect basal CD62L levels
- DPI, rotenone and antimycin A, but not apocynin, significantly enhance ATP induced CD62L down-regulation suggesting mitochondrial ROS involvement
- This increase was P2X7R dependent, and rotenone and antimycin A enhance ATP sensitivity
- Rotenone and antimycin A treatment enhance mitochondrial O_2^- levels independent of ATP
- It is unclear whether conversion of O_2^- to H_2O_2 is required
- Exposure of PS is also be enhanced by rotenone and antimycin A, through ATP and P2X7R

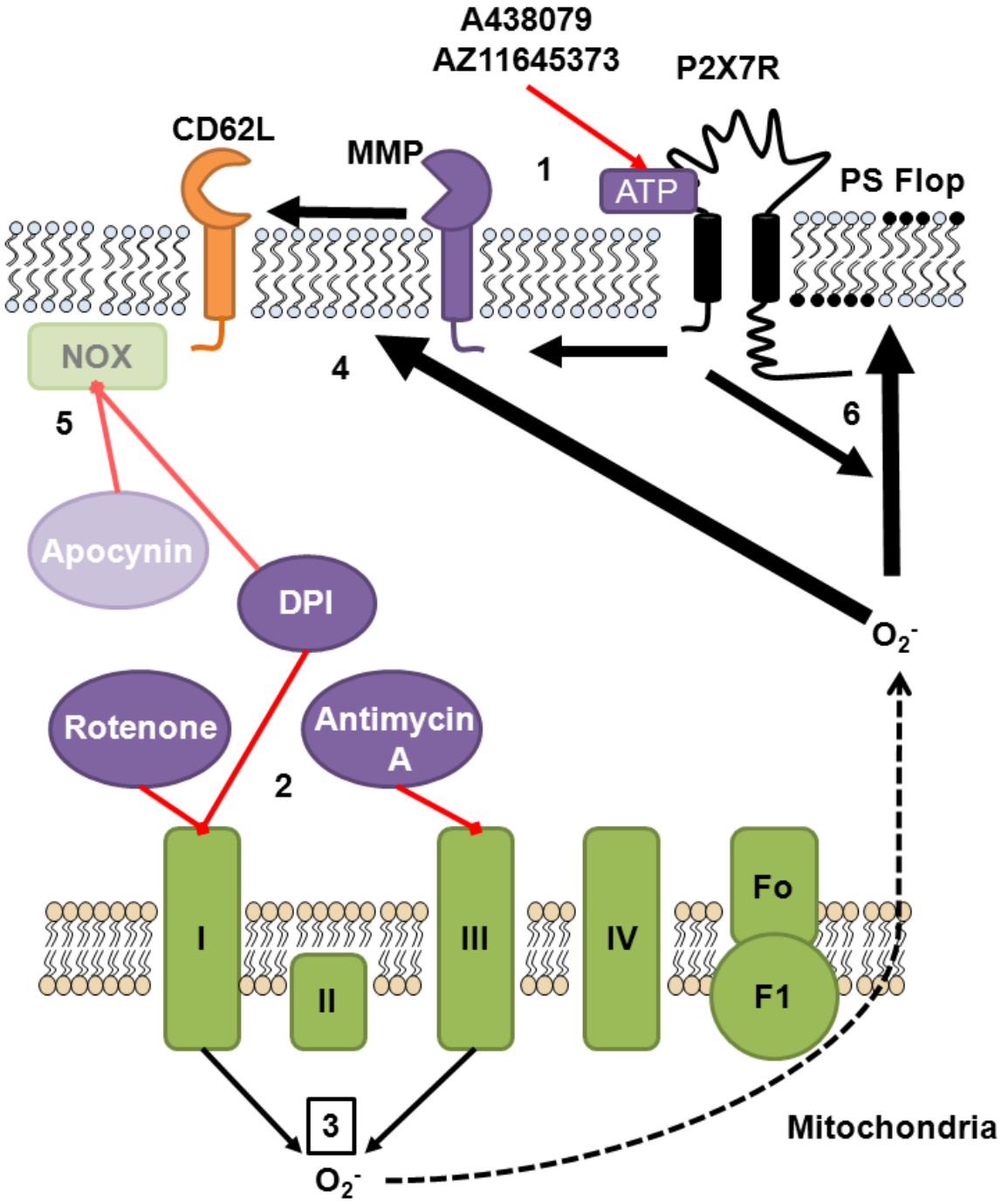

Figure 5.15: Effect of uncouplers of complex I and III of the mitochondrial electron transport on ATP induced loss of cell surface CD62L expression. 1. ATP induces loss of cell surface CD62L expression through P2X7R. **2.** Rotenone and Antimycin A are uncouplers of complex I and complex III of the mitochondrial electron transport chain respectively. **3.** Rotenone and Antimycin A significantly increase mitochondrial superoxide levels. **4.** Pre-treatment with these compounds or DPI, an inhibitor of flavin containing enzymes such as complex I, but not Apocynin (**5**), an NADPH oxidase inhibitor, significantly enhance ATP induced CD62L down-regulation. **6.** Pre-treatment with Rotenone or Antimycin A reveals P2X7R dependent externalisation of Phosphatidyl serine.

5.2. Results Chapter 5 Discussion

5.2.1. Modulation of mitochondrial ROS enhances P2X7R function

Several lines of evidence led to the formation of a hypothesis that ROS were involved in the mechanism responsible for CD62L down-regulation through P2X7R. Firstly, LY294002 enhanced CD62L down-regulation in response to anti-CD3/CD28 antibody coated beads. This observation may be explained by the ability of this PI3K inhibitor to cause increased H_2O_2 production (59). H_2O_2 is a known activator of ADAM17 and leads to enhanced ADAM17 substrate cleavage (421), CD62L loss in response to H_2O_2 was confirmed by data presented in this thesis. Secondly, the PKC inhibitor Rottlerin enhanced down-regulation of cell surface CD62L induced by ATP. Rottlerin has been shown to increase O_2 consumption by mitochondria in a PKC independent manner, suggesting it is a mitochondrial uncoupling agent (418).

ROS generation is an important part of T lymphocyte activation and differentiation (294, 457, 458), however in this study significant cytosolic or mitochondrial ROS could not be detected in response to anti-CD3 antibody or PMA (450, 459). ATP induced significant generation of cytosolic ROS; however the source of this ROS was not confirmed here. Unexpectedly, A438079 did not inhibit ATP induced ROS generation; as ATP induced CD62L was inhibited by A438079, ROS was therefore unlikely to be the mechanism connecting ATP to down-regulation of cell surface CD62L.

Nevertheless, the involvement of ROS in ATP induced down-regulation of cell surface CD62L was explored using inhibitors of ROS generating proteins. Unexpectedly, DPI caused an enhancement of ATP induced loss of cell surface CD62L expression independently of NADPH oxidase. Inhibitors of the mitochondrial electron transport chain complex I and III, rotenone and antimycin A also enhanced ATP induced CD62L processing. This observation is in contrast to the effect of these compounds on P2Y2 mediated TGF-α shedding (422). A decrease in the ATP EC_{50} indicates that these compounds enhance the potency for ATP in the process of CD62L down-regulation; although the threshold concentration of 1mM remained unaltered. The fact that the threshold did not

change suggests that P2X receptors other than P2X7 were not involved in this effect.

Increased mitochondrial O_2^- generation was recently observed in the acute monocytic leukaemia cell line THP-1 following treatment with rotenone and antimycin A (160). This study by Zhou et al. also employed MitoSOX Red to measure O_2^- levels; however, higher concentrations of rotenone and antimycin A were used than those presented in this thesis (10 and 73 µM respectively (160), compared to 5 and 1 µM here). Rotenone and antimycin A also promoted IL-1β processing in THP-1 cells through activation of caspase 1 by the NLRP3 inflammasome (160).

In this thesis, it was also investigated if mitochondrial uncoupling by rotenone and antimycin A would influence the ability of ATP, through P2X7R, to bring about cellular changes other than CD62L processing. However, it was observed that rotenone significantly inhibited basal and CXCL-12 directed migration of naïve $CD4^+$ T lymphocytes. The polarisation of mitochondria to the uropod of cells is critical for migration; therefore, Rotenone and antimycin A would indeed be expected to inhibit T lymphocyte migration (460). Both rotenone and antimycin A significantly inhibited proliferation of naïve $CD4^+$ T lymphocytes activated with anti-CD3/CD28 antibody coated beads and IL-2. This is in agreement with the inhibition of $CD8^+$ T lymphocyte proliferation by rotenone (461). In this study by Yi et al. 0.01 – 5 µM rotenone cause significant inhibition of proliferation in response to plate bound anti-CD3 and anti-CD28 antibodies (461).

Un-expectedly, rotenone and antimycin A did not significantly enhance apoptosis of naïve $CD4^+$ T lymphocytes, despite causing production of significant amounts of O_2^- over the same time period. Rotenone has been shown to cause apoptosis of a breast cancer cell line through enhanced ROS generation and activation of the stress kinases JNK and p38 MAPK (164). In another study, treatment of the leukemic T cell line Jurkat with antimycin A alone was insufficient to induce apoptosis (462), however, combination of antimycin A with the adenine nucleotide translocator (ANT) inhibitor bongkrekic acid (BA) did cause significant apoptosis of cells. It is important to note that the concentration used in the study by Wang et al. was lower than in this thesis, 0.02 compared to 1 µM.

5.2.2. O_2^- as a modulator of P2XRs

Uncoupling of mitochondrial electron transport can lead to the increased leakage of mitochondrial ROS such as O_2^-, indeed increased mitochondrial O_2^- generation for Rotenone and antimycin A treated naïve $CD4^+$ T lymphocytes was observed. Increased mitochondrial O_2^- generation may therefore represent a novel mechanism of P2X7R modulation. The conversion of O_2^- to H_2O_2 by SOD does not appear to be responsible, as Mn-cpx 3 had no effect on CD62L down-regulation.

P2X receptors can be modulated by a number of cellular mechanisms including direct post translational modifications such as phosphorylation, or by interaction with second messengers such as lipids including PIP_2 (463–465). ROS can promote lipid raft formation in T lymphocytes (449) and a number of P2XRs including P2X7R have been reported to associate in lipid rafts (383, 466–469). Association of P2X7R with lipid rafts is mediated by palmitoylation: the covalent attachment of palmitate (a 16-carbon fatty acid) to cysteine residues (383). However, it is unlikely that rotenone and antimycin A treatment enhances palmitoylation of P2X7 as data suggest that palmitoylation is in fact inhibited by ROS (470, 471).

ROS have been implicated in direct modulation of ion channels including P2X2R (454, 455). Interestingly both of these studies demonstrated that inhibition of Complex I or III by rotenone and antimycin A/Myxothiazol could enhance P2X2R activation, which agrees with data presented in this thesis for the first time in P2X7R. One study suggests that the Cys430 residue is responsible for this and the effect can be mimicked by exogenous application of H_2O_2. P2X2R has the second largest C-terminal region of P2XRs; P2X7R has the largest P2X C-terminus and this contains a number of cysteine residues which could act to potentiate receptor activation in a similar manner (173).

Here, SEB activated T lymphocytes did not produce significant mitochondrial O_2^- in response to rotenone and antimycin A treatment. It has been reported that channels expressed by activated T lymphocytes are less sensitive to modulation by ROS (456). Taken together these observations could explain why ATP mediated CD62L down-regulation from the surface of SEB activated T lymphocytes is not enhanced by rotenone or antimycin A.

6. Discussion

6.1. Overview

This thesis began by confirming expression of P2X7R in human T lymphocytes and leukemic cell lines using immunoblotting and voltage clamp electrophysiology. This was followed by a detailed analysis of its function in human naïve $CD4^+$ T lymphocytes. This project aimed to explore whether PI3K signalling was responsible for integrating P2X7R activation with T lymphocyte function.

ATP was shown to couple to uptake of the dye ethidium bromide, although this process was insensitive to inhibition by the P2X7R antagonist A438079. However, pore formation did not result in subsequent death of these cells by apoptosis or necrosis. P2X7R was shown to be dispensable for the proliferation of these cells following activation by anti-CD3/CD28 antibody coated beads. This two-signal system of T lymphocyte activation was used initially to set up an assay to explore regulation of cell surface expression of CD62L by ATP. Unlike in mouse $CD4^+$ T lymphocytes, CD62L down-regulation from the surface of human $CD4^+$ T lymphocytes was insensitive to inhibitors of the PI3K/mTOR and Erk1/2 signalling pathways.

Interestingly, while naïve $CD4^+$ T lymphocytes down-regulated cell surface CD62L in response to PMA and ATP, the leukemic T cell line Jurkat was un-responsive to ATP. The pharmacology of ATP induced surface CD62L down-regulation was explored in naïve $CD4^+$ T lymphocytes and was shown to require P2X7R. Again, inhibitors of PI3K/mTOR and Erk1/2 pathways could not prevent this down-regulation, PKC and p38 MAPK inhibition were also ineffectual. While investigating ROS as a component of ATP induced CD62L down-regulation, a novel mechanism whereby uncoupling of complex I or III of the mitochondrial electron transport chain caused enhanced CD62L down-regulation through P2X7R was discovered. This uncoupling also revealed P2X7R dependent PS translocation, which was absent in cells where mitochondrial function was not altered.

Although specific results have already been discussed in previous sections, a more detailed discussion of the implications of these findings will now follow. This will focus on the role of P2X7R and mitochondrial ROS in disease, present a model for a novel protective P2X7R mechanism and conclude by highlighting questions raised by the data and discussion in this thesis.

6.2. P2X7R and mitochondrial ROS in disease

Increased reactive oxygen and nitrogen species, including O_2^-, generation and mutated mtDNA or damaged mitochondrial electron chain components are implicated in the pathology of a number autoimmune of diseases including SLE, RA, MS and ALS.

In RA hypoxic synovial tissue undergoes mtDNA damage, which is reversible by the antioxidant SOD. Although SOD levels are significantly higher in PBMCs of RA patients, the overall trapping antioxidant capacity (TRAP) was lower in these cells (472). The lymphocytes of RA patients also produce increased ROS and this could potentially affect P2X7R activity (473); indeed P2X7R is implicated in RA (411, 474). SLE is associated with mitochondrial hyperpolarisation, enhanced ROS generation (475, 476) and increased soluble CD62L (477), in addition mtDNA is associated with SLE (478). As in RA, the activity of antioxidant enzymes including SOD are significantly lower in patients with SLE (479).

Mutation of SOD1 can cause amyotrophic lateral sclerosis (ALS), a paralysing disease involving degeneration of the motor neurones (480). In mice this disease can be modelled by introducing a G93A mutation into mSOD1 and the pathology of the disease involves the mitochondrial permeability transition pore (mPTP). The majority of the pathology of this disease is driven by damage to motor neurones, however T lymphocytes play an important role in endogenous neuro-protection and numbers of $CD4^+$ T lymphocytes from the blood of patients with ALS are increased (481, 482). Increased numbers of NKT cells are found in the spinal cord, spleen and liver in G93AmSOD1 mice compared to WT mice (483). Interestingly the levels of all T cells in the spleen compared to WT were significantly increased in G93AmSOD1 compared to WT mice. This suggests that there are T lymphocyte circulation defects in G93AmSOD1 mice. Re-introduction of wild type SOD1 may be a route of therapeutic intervention in ALS (484).

Mutations in SOD would be expected to cause increased O_2^- levels and data from this thesis suggest that this would potentially make naïve $CD4^+$ T lymphocytes more susceptible to ATP. Indeed, P2X7R has been implicated in ALS and extracellular ATP in released by lesions in ALS (351, 485). P2X7R in ALS may lead to enhanced CD62L down-regulation, causing the retention of cells in the

spleen as seen in the CD62L$^{-/-}$ mouse (483). However, fewer T lymphocytes are observed in the spleen of older mice, this may be due to enhanced ability of CD4^{+} cells to undergo apoptosis (486). Apoptosis of these cells would prevent them protecting against ALS and potentially exacerbate the condition. The observation from this thesis that modulation of the mitochondrial electron transport reveals P2X7R dependent PS exposure, could potentially explain enhanced apoptosis of these naïve CD4^{+} T lymphocytes.

EAE is a mouse model of MS and P2X7R expression was increased after EAE induction in brain homogonies (350). Indeed, a study showed that mice lacking P2X7R developed an increased incidence and greater severity of EAE when immunised with MOG$_{35-55}$ peptide (348). This second study by Chen et al. observed that following induction of EAE in P2X7R$^{-/-}$ mice there was a marked reduction in the ability of lymphocytes to undergo apoptosis. Indeed, increased number of CD3^{+} cells were observed in the CNS of P2X7R$^{-/-}$ mice. In EAE, antigen induced cell death (AICD) is important for recovery from the acute phase of the disease. P2X7R induced cell death may also be important for protecting from EAE and the loss of this protective mechanism in the P2X7R$^{-/-}$ mouse may account for the increased disease incidence and/or severity.

However a second study reported that P2X7R deficiency was in fact associated with decreased disease incidence and clinical score in mice lacking P2X7R in a MOG$_{35-55}$ peptide model of MS (349). The discrepancies in these studies could be explained by the fact that this second study by Sharp et al. (349) used P2X7-/- mice provided by GSK, whereas, Chen et al. used P2X7R$^{-/-}$ mice provided by Pfizer (348). As mentioned in section 1.10, GSK P2X7R$^{-/-}$ mice contain a functional splice variant with an alternative TMD1 that escapes inactivation and in fact leads to hyper responsive T lymphocytes (365, 366). While Pfizer mice do express splice variants with the truncated exon 13 as well as a novel hybrid isoform, these were shown to be non-functional (367). If cell death through P2X7R is indeed and important protective mechanism for the resolution of EAE, then hyper-responsive T lymphocytes from GSK P2X7$^{-/-}$ mice would be expected to undergo enhanced apoptosis and could explain the reduced indicdence and clinical score observed by Sharp et al (349).

Taken together, these studies suggest that P2X7R induced cell death involving the externalisation of PS (measured by annexin V binding by Chen et al. (348)) may act as a protective mechanism against EAE. Recently, increased survival of naïve $CD4^+$ T lymphocytes has been demonstrated in EAE/MS, this could potentially occur through an absence of P2X7R induced apoptosis of cells due to expression of SNPs or non-functional P2X7R splice variants (487, 488).

6.3. ATP and PS as “find me” and “eat me” signals

ATP was chosen as the agonist for P2X7R activation in this study because it is the endogenous P2X7R ligand and no selective P2X7R agonists exist; while BzATP is more potent than ATP at P2X7R it also activates other P2XRs. It is important when analysing the results of experiments involving ATP as an agonist, to consider the source and stability of ATP in the environment around the cell. Possible sources of ATP include: autocrine/pancrine release and release from cells undergoing necrosis. Autocrine release occurs through Pannexin-1 hemichannels, is involved in activation of P2X7R during T lymphocyte activation and can also activate P2YRs (261, 268). While necrosis would result in the un-restrained release of cellular contents including ATP into the extracellular environment, cells undergoing apoptosis release ATP through Pannexin-1 hemichannels (280, 489, 490). Purines can act as chemoattractant for phagocytes, therefore ATP release from apoptotic cells may enhance their own phagocytic clearance (318, 320, 325, 326, 491). Other soluble pro- and anti-inflammatory factors can also influence the phagocytosis of apoptotic cells, such as LPS, TNF-α and IFN-γ (492, 493).

Once phagocytes encounter apoptotic cells they require specific signals to recognise, engage and eventually opsonise these cells. These “Eat me” signals are an established concept and involve a wide variety of molecules expressed on the surface of cells undergoing apoptosis, including PS. PS is normally confined to the inner leaflet of the plasma membrane, however apoptotic cells rapidly externalise PS altering membrane A-symmetry (394, 494, 495). Indeed, PS expressed by lymphocytes undergoing apoptosis is required for their phagocytosis

by macrophages (496). Phagocytes express receptors for PS, for example the receptor TIM4 is expressed by macrophages and administration of antibodies against this receptor block phagocytosis *in vivo* (497).

Previous studies have shown that treatment of a number of cell types including: mouse thymocytes and mature T lymphocytes with ATP, causes externalisation of PS to the cell surface. However, data in this thesis suggest that ATP alone is not sufficient to cause significant PS exposure in human naïve $CD4^+$ T lymphocytes. Interestingly, it was revealed that cells could be primed using rotenone or antimycin A pre-treatment to significantly externalise PS through P2X7R. This may present a novel P2X7R dependent mechanism for the increased phagocytosis of cells with damaged mitochondria. Although this study used pharmacological uncoupling of mitochondrial electron transport, damaged mitochondria also display enhanced ROS generation and can promote inflammation (Section 6.2). Removal of cells with damaged mitochondria would be desirable to prevent un-restrained inflammation. Individuals with reduced P2X7R function, through SNPs or expression of inactive and inactivating splice variants could potentially lack a novel mechanism of T lymphocyte clearance (Figure 6.1). This highlights the need for further research into the modulation of P2X7R by ROS and how this, coupled with the emergent role of P2X7R splice variants in human immune cells, may contribute to inflammation and disease.

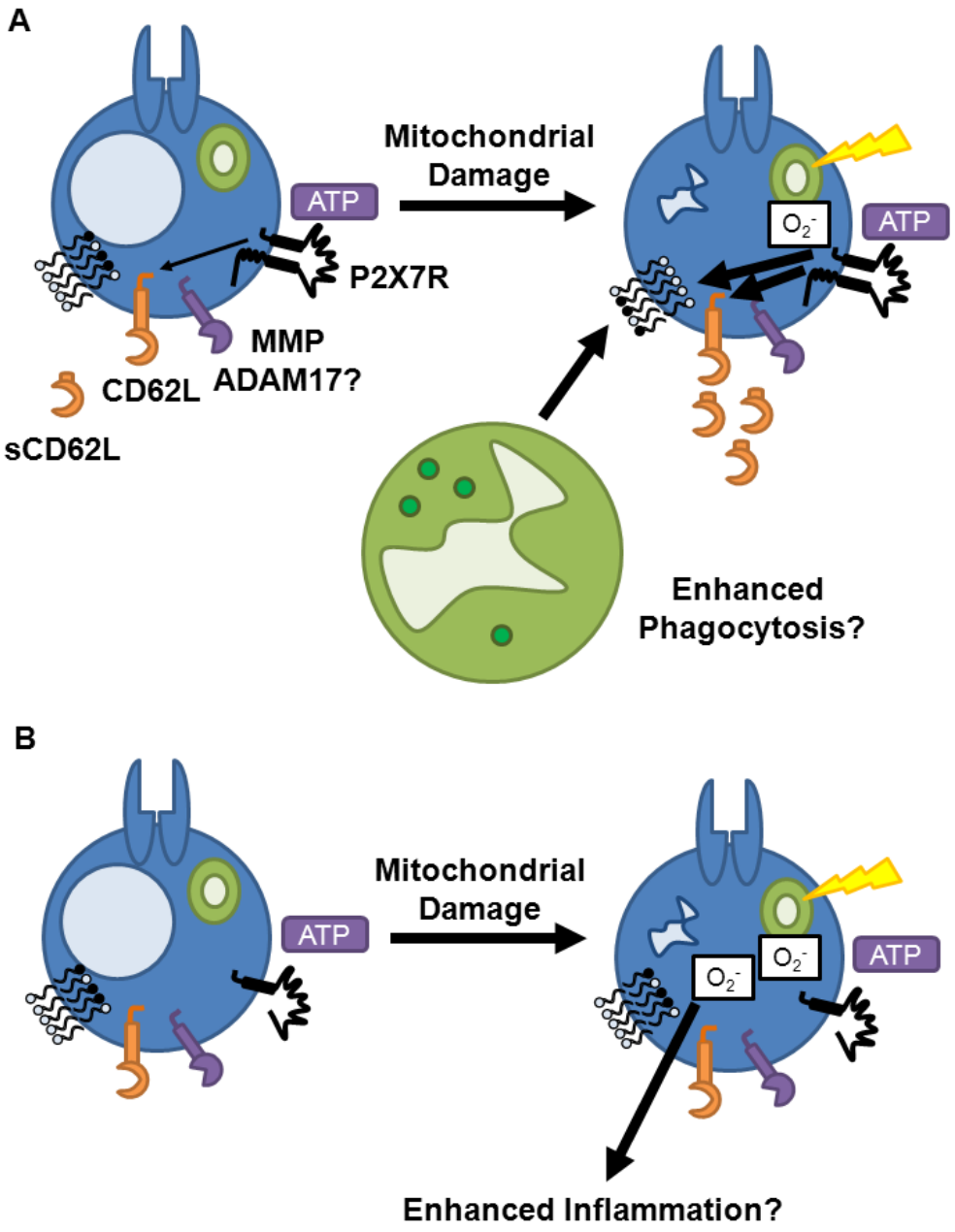

Figure 6.1: Model of the potential role of enhanced P2X7R function in naïve CD4$^+$ T lymphocytes. A. ATP induces CD62L down-regulation from the surface of naïve CD4$^+$ T lymphocytes in an MMP dependent manner. Upon damage to mitochondria, this CD62L down-regulation may be enhanced and PS exposure through P2X7R revealed (shown here by uncoupling of mitochondrial electron transport). sCD62L in the supernatant may have potential biological function, including blocking TEM of cells. Exposed PS may act as a "find me" signal for phagocytes to opsonise naïve CD4$^+$ T lymphocytes with damaged mitochondria. **B.** If expression of functional P2X7R is altered, for example by the expression of a non-functional P2X7R slice variant, then CD62L processing in response to ATP would be expected to be inhibited. When mitochondrial damage occurs PS exposure through P2X7R would not occur, cells would escape phagocytosis and potentially enhance inflammation.

6.4. Summary and Future direction

This thesis confirms P2X7R expression by leukemic cell lines, SEB activated T lymphocytes and human naïve $CD4^+$ T lymphocytes. It also makes novel findings which expand our understanding about the role of P2X7R in T lymphocyte function. PI3K signalling, as well as the PKC, Erk1/2 and p38 MAPK pathways were not involved in ATP induced CD62L down-regulation. Additionally, a species difference between the signalling pathways involved in CD3 and CD3/CD28 induced down-regulation of cell surface CD62L expression was revealed. Finally, uncoupling of mitochondrial electron transport positively regulates P2X7R induced CD62L down-regulation and reveals ATP induced PS exposure through P2X7R. Whilst the implication of this has been discussed in detail above, several questions are raised:

- What is responsible for the differences between down-regulation of cell surface CD62L in mouse and human naïve $CD4^+$ T lymphocytes?
- What mechanism links P2X7R activation to MMP induced CD62L down-regulation in the absence of mitochondrial perturbation?
- In diseases which have a mitochondrial component, is enhanced P2X7R activity responsible for disease pathophysiology?
- Are there other P2X7R dependent processes in naïve $CD4^+$ T lymphocytes which are enhanced by uncoupling of mitochondrial electron transport?
- Does the increased PS exposure on naïve $CD4^+$ T lymphocytes result in enhanced phagocytosis?
- Which P2X7R splice variants are expressed by naïve $CD4^+$ T lymphocytes?
- Does the expression of non-functional P2X7R splice variants inhibit ATP induced PS exposure, and subsequent phagocytosis?

7. References

1. Serhan, C. N. 2007. Resolution phase of inflammation: novel endogenous anti-inflammatory and proresolving lipid mediators and pathways. *Annu Rev Immunol* 25: 101-37.

2. Lanzavecchia, A., and F. Sallusto. 2005. Understanding the generation and function of memory T cell subsets. *Curr Opin Immunol* 17: 326-32.

3. Dougan, M., and G. Dranoff. 2009. Immune therapy for cancer. *Annu Rev Immunol* 27: 83-117.

4. Vesely, M. D., M. H. Kershaw, R. D. Schreiber, and M. J. Smyth. 2011. Natural innate and adaptive immunity to cancer. *Annu Rev Immunol* 29: 235-71.

5. Berger, E. A., P. M. Murphy, and J. M. Farber. 1999. Chemokine receptors as HIV-1 coreceptors: roles in viral entry, tropism, and disease. *Annu Rev Immunol* 17: 657-700.

6. Janeway, C. A., and R. Medzhitov. 2002. Innate immune recognition. *Annu Rev Immunol* 20: 197-216.

7. Minai-Fleminger, Y., and F. Levi-Schaffer. 2009. Mast cells and eosinophils: the two key effector cells in allergic inflammation. *Inflamm Res* 58: 631-8.

8. Knol, E. F., and M. Olszewski. 2011. Basophils and mast cells: Underdog in immune regulation? *Immunol Lett* 138: 28-31.

9. Chuquimia, O. D., D. H. Petursdottir, M. J. Rahman, K. Hartl, M. Singh, and C. Fernández. 2012. The Role of Alveolar Epithelial Cells in Initiating and Shaping Pulmonary Immune Responses: Communication between Innate and Adaptive Immune Systems. *PloS one* 7: e32125.

10. Sallusto, F., C. R. Mackay, and A. Lanzavecchia. 2000. The role of chemokine receptors in primary, effector, and memory immune responses. *Annu Rev Immunol* 18: 593-620.

11. Segal, A. W. 2005. How neutrophils kill microbes. *Annu Rev Immunol* 23: 197-223.

12. Soehnlein, O., and L. Lindbom. 2010. Phagocyte partnership during the onset and resolution of inflammation. *Nat Rev Immunol* 10: 427-39.

13. Guermonprez, P., J. Valladeau, L. Zitvogel, C. Théry, and S. Amigorena. 2002. Antigen presentation and T cell stimulation by dendritic cells. *Annu Rev Immunol* 20: 621-67.

14. Ward, S. G., and F. M. Marelli-Berg. 2009. Mechanisms of chemokine and antigen-dependent T-lymphocyte navigation. *Biochem J* 418: 13-27.

15. Cyster, J. G. 2005. Chemokines, sphingosine-1-phosphate, and cell migration in secondary lymphoid organs. *Annu Rev Immunol* 23: 127-59.

16. Boursalian, T. E., and K. Bottomly. 1999. Stability of naive and memory phenotypes on resting CD4 T cells in vivo. *J Immunol* 162: 9-16.

17. von Andrian, U. H., and T. R. Mempel. 2003. Homing and cellular traffic in lymph nodes. *Nat Rev Immunol* 3: 867-78.

18. Campbell, J. J., J. Pan, and E. C. Butcher. 1999. Cutting edge: developmental switches in chemokine responses during T cell maturation. *J Immunol* 163: 2353-7.

19. Tan, J. T., E. Dudl, E. LeRoy, R. Murray, J. Sprent, K. I. Weinberg, and C. D. Surh. 2001. IL-7 is critical for homeostatic proliferation and survival of naive T cells. *Proc Natl Acad Sci U S A* 98: 8732-7.

20. Guimond, M., R. G. Veenstra, D. J. Grindler, H. Zhang, Y. Cui, R. D. Murphy, S. Y. Kim, R. Na, L. Hennighausen, S. Kurtulus, B. Erman, P. Matzinger, M. S. Merchant, and C. L. Mackall. 2009. Interleukin 7 signaling in dendritic cells regulates the homeostatic proliferation and niche size of CD4+ T cells. *Nat Immunol* 10: 149-57.

21. Li, J., G. Huston, and S. L. Swain. 2003. IL-7 promotes the transition of CD4 effectors to persistent memory cells. *J Exp Med* 198: 1807-15.

22. Calzascia, T., M. Pellegrini, A. Lin, K. M. Garza, A. R. Elford, A. Shahinian, P. S. Ohashi, and T. W. Mak. 2008. CD4 T cells, lymphopenia, and IL-7 in a multistep pathway to autoimmunity. *Proc Natl Acad Sci U S A* 105: 2999-3004.

23. Alber, G., D. K. Hammer, and B. Fleischer. 1990. Relationship between enterotoxic- and T lymphocyte-stimulating activity of staphylococcal enterotoxin B. *J Immunol* 144: 4501-6.

24. Ward, S. G. 1996. CD28: a signalling perspective. *Biochem J* 318 (Pt 2: 361-77.

25. Ying, H., L. Yang, G. Qiao, Z. Li, F. Yin, D. Xie, J. Zhang, E. Alerts, and L. Zhang. 2010. Cutting edge: CTLA-4--B7 interaction suppresses Th17 cell differentiation. *J Immunol* 185: 1375-8.

26. Scalapino, K. J., and D. I. Daikh. 2008. CTLA-4: a key regulatory point in the control of autoimmune disease. *Immunol Rev* 223: 143-55.

27. Movva, S., and C. Verschraegen. 2009. The monoclonal antibody to cytotoxic T lymphocyte antigen 4, ipilimumab (MDX-010), a novel treatment strategy in cancer management. *Expert Opin Biol Ther* 9: 231-41.

28. Fife, B. T., and J. A. Bluestone. 2008. Control of peripheral T-cell tolerance and autoimmunity via the CTLA-4 and PD-1 pathways. *Immunol Rev* 224: 166-82.

29. Quann, E. J., E. Merino, T. Furuta, and M. Huse. 2009. Localized diacylglycerol drives the polarization of the microtubule-organizing center in T cells. *Nat Immunol* 10: 627-35.

30. Quann, E. J., X. Liu, G. Altan-Bonnet, and M. Huse. 2011. A cascade of protein kinase C isozymes promotes cytoskeletal polarization in T cells. *Nat Immunol* 12: 647-54.

31. Roose, J. P., M. Mollenauer, V. A. Gupta, J. Stone, and A. Weiss. 2005. A diacylglycerol-protein kinase C-RasGRP1 pathway directs Ras activation upon antigen receptor stimulation of T cells. *Mol Cell Biol* 25: 4426-41.

32. Genot, E., and D. A. Cantrell. 2000. Ras regulation and function in lymphocytes. *Curr Opin Immunol* 12: 289-94.

33. Trucy, M., C. Barbat, A. Fischer, and F. Mazerolles. 2006. CD4 ligation induces activation of protein kinase C zeta and phosphoinositide-dependent-protein kinase-1, two kinases required for down-regulation of LFA-1-mediated adhesion. *Cell Immunol* 244: 33-42.

34. Deane, J. A., and D. A. Fruman. 2004. Phosphoinositide 3-kinase: diverse roles in immune cell activation. *Annu Rev Immunol* 22: 563-98.

35. Alcázar, I., M. Marqués, A. Kumar, E. Hirsch, M. Wymann, A. C. Carrera, and D. F. Barber. 2007. Phosphoinositide 3-kinase gamma participates in T cell receptor-induced T cell activation. *J Exp Med* 204: 2977-87.

36. Guillermet-Guibert, J., K. Bjorklof, A. Salpekar, C. Gonella, F. Ramadani, A. Bilancio, S. Meek, A. J. H. Smith, K. Okkenhaug, and B. Vanhaesebroeck. 2008. The p110beta isoform of phosphoinositide 3-kinase signals downstream of G protein-coupled receptors and is functionally redundant with p110gamma. *Proc Natl Acad Sci U S A* 105: 8292-7.

37. Ward, S. G., and D. A. Cantrell. 2001. Phosphoinositide 3-kinases in T lymphocyte activation. *Curr Opin Immunol* 13: 332-8.

38. Parry, R. V., J. L. Riley, and S. G. Ward. 2007. Signalling to suit function: tailoring phosphoinositide 3-kinase during T-cell activation. *Trends Immunol* 28: 161-8.

39. Vanhaesebroeck, B., M. J. Welham, K. Kotani, R. Stein, P. H. Warne, M. J. Zvelebil, K. Higashi, S. Volinia, J. Downward, and M. D. Waterfield. 1997. P110delta, a novel phosphoinositide 3-kinase in leukocytes. *Proc Natl Acad Sci U S A* 94: 4330-5.

40. Okkenhaug, K., A. Bilancio, G. Farjot, H. Priddle, S. Sancho, E. Peskett, W. Pearce, S. E. Meek, A. Salpekar, M. D. Waterfield, A. J. H. Smith, and B. Vanhaesebroeck. 2002. Impaired B and T cell antigen receptor signaling in p110delta PI 3-kinase mutant mice. *Science* 297: 1031-4.

41. Harriague, J., and G. Bismuth. 2002. Imaging antigen-induced PI3K activation in T cells. *Nat Immunol* 3: 1090-6.

42. Fruman, D. A., and G. Bismuth. 2009. Fine tuning the immune response with PI3K. *Immunol Rev* 228: 253-72.

43. Hers, I., E. E. Vincent, and J. M. Tavaré. 2011. Akt signalling in health and disease. *Cell Signal* 23: 1515-27.

44. Liu, H., D. C. Radisky, C. M. Nelson, H. Zhang, J. E. Fata, R. A. Roth, and M. J. Bissell. 2006. Mechanism of Akt1 inhibition of breast cancer cell invasion reveals a protumorigenic role for TSC2. *Proc Natl Acad Sci U S A* 103: 4134-9.

45. Irie, H. Y., R. V. Pearline, D. Grueneberg, M. Hsia, P. Ravichandran, N. Kothari, S. Natesan, and J. S. Brugge. 2005. Distinct roles of Akt1 and Akt2 in regulating cell migration and epithelial-mesenchymal transition. *J Cell Biol* 171: 1023-34.

46. Gao, D., H. Inuzuka, A. Tseng, R. Y. Chin, A. Toker, and W. Wei. 2009. Phosphorylation by Akt1 promotes cytoplasmic localization of Skp2 and impairs APCCdh1-mediated Skp2 destruction. *Nat Cell Biol* 11: 397-408.

47. Gao, D., H. Inuzuka, A. Tseng, and W. Wei. 2009. Akt finds its new path to regulate cell cycle through modulating Skp2 activity and its destruction by APC/Cdh1. *Cell Div* 4: 11.

48. Moore, S. F., R. W. Hunter, and I. Hers. 2011. mTORC2 Protein-mediated Protein Kinase B (Akt) Serine 473 Phosphorylation Is Not Required for Akt1 Activity in Human Platelets. *J Cell Biochem* 286: 24553-60.

49. Guo, J.-P., D. Coppola, and J. Q. Cheng. 2011. IKBKE activates Akt independent of phosphatidylinositol 3-kinase/PDK1/mTORC2 and PH domain to sustain malignant transformation. *J Cell Biochem* 286: 37389-37398.

50. Gao, T., F. Furnari, and A. C. Newton. 2005. PHLPP: a phosphatase that directly dephosphorylates Akt, promotes apoptosis, and suppresses tumor growth. *Mol Cell* 18: 13-24.

51. Harris, S. J., R. V. Parry, J. Westwick, and S. G. Ward. 2008. Phosphoinositide lipid phosphatases: natural regulators of phosphoinositide 3-kinase signaling in T lymphocytes. *J Cell Biochem* 283: 2465-9.

52. Blunt, M. D., and S. G. Ward. 2012. Targeting PI3K isoforms and SHIP in the immune system: new therapeutics for inflammation and leukemia. *Curr Opin Pharmacol* .

53. Weichhart, T., and M. D. Säemann. 2009. The multiple facets of mTOR in immunity. *Trends Immunol* 30: 218-26.

54. Kok, K., B. Geering, and B. Vanhaesebroeck. 2009. Regulation of phosphoinositide 3-kinase expression in health and disease. *Trends Biochem Sci* 34: 115-27.

55. Harris, S. J., J. G. Foster, and S. G. Ward. 2009. PI3K isoforms as drug targets in inflammatory diseases: lessons from pharmacological and genetic strategies. *Curr Opin Investig Drugs* 10: 1151-62.

56. Vlahos, C., W. Matter, K. Hui, and R. Brown. 1994. A specific inhibitor of phosphatidylinositol 3-kinase, 2-(4- morpholinyl)-8-phenyl-4H-1-benzopyran-4-one (LY294002). *J Biol Chem* 269: 5241-5248.

57. Arcaro, A., and M. P. Wymann. 1993. Wortmannin is a potent phosphatidylinositol 3-kinase inhibitor: the role of phosphatidylinositol 3,4,5-trisphosphate in neutrophil responses. *Biochem J* 296 (Pt 2: 297-301.

58. Gharbi, S. I., M. J. Zvelebil, S. J. Shuttleworth, T. Hancox, N. Saghir, J. F. Timms, and M. D. Waterfield. 2007. Exploring the specificity of the PI3K family inhibitor LY294002. *Biochem J* 404: 15-21.

59. Poh, T. W., and S. Pervaiz. 2005. LY294002 and LY303511 sensitize tumor cells to drug-induced apoptosis via intracellular hydrogen peroxide production independent of the phosphoinositide 3-kinase-Akt pathway. *Cancer Res* 65: 6264-74.

60. Berndt, A., S. Miller, O. Williams, D. D. Le, B. T. Houseman, J. I. Pacold, F. Gorrec, W. C. Hon, Y. Liu, C. Rommel, P. Gaillard, T. Rückle, M. K. Schwarz, K. M. Shokat, J. P. Shaw, and R. L. Williams. 2010. The p110delta structure: mechanisms for selectivity and potency of new PI(3)K inhibitors. *Nat Chem Biol* 6: 244.

61. Feldman, M. E., B. Apsel, A. Uotila, R. Loewith, Z. A. Knight, D. Ruggero, and K. M. Shokat. 2009. Active-site inhibitors of mTOR target rapamycin-resistant outputs of mTORC1 and mTORC2. *PLoS Biol* 7: e38.

62. Liu, Q., S. Kirubakaran, W. Hur, M. Niepel, K. Westover, C. C. Thoreen, J. Wang, J. Ni, M. P. Patricelli, K. Vogel, S. Riddle, D. L. Waller, R. Traynor, T. Sanda, Z. Zhao, S. A. Kang, J. Zhao, A. T. Look, P. K. Sorger, D. M. Sabatini, and N. S. Gray. 2012. Kinome-wide selectivity profiling of ATP-competitive mTOR (mammalian target of rapamycin) inhibitors and characterization of their binding kinetics. *J Cell Biochem* 1-32.

63. Hirai, H., H. Sootome, Y. Nakatsuru, K. Miyama, S. Taguchi, K. Tsujioka, Y. Ueno, H. Hatch, P. K. Majumder, B. S. Pan, and H. Kotani. 2010. MK-2206, an allosteric Akt inhibitor, enhances antitumor efficacy by standard chemotherapeutic agents or molecular targeted drugs in vitro and in vivo. *Mol Cancer Ther* 9: 1956-67.

64. Tan, S., Y. Ng, and D. E. James. 2011. Next-generation Akt inhibitors provide greater specificity: effects on glucose metabolism in adipocytes. *Biochem J* 435: 539-44.

65. Levy, D. S., J. A. Kahana, and R. Kumar. 2009. AKT inhibitor, GSK690693, induces growth inhibition and apoptosis in acute lymphoblastic leukemia cell lines. *Blood* 113: 1723-9.

66. Powis, G., R. Bonjouklian, M. M. Berggren, a Gallegos, R. Abraham, C. Ashendel, L. Zalkow, W. F. Matter, J. Dodge, and G. Grindey. 1994. Wortmannin, a potent and selective inhibitor of phosphatidylinositol-3-kinase. *Cancer Res* 54: 2419-23.

67. Yaguchi, S., Y. Fukui, I. Koshimizu, H. Yoshimi, T. Matsuno, H. Gouda, S. Hirono, K. Yamazaki, and T. Yamori. 2006. Antitumor activity of ZSTK474, a new phosphatidylinositol 3-kinase inhibitor. *Journal of the National Cancer Institute* 98: 545-56.

68. Folkes, A. J., K. Ahmadi, W. K. Alderton, S. Alix, S. J. Baker, G. Box, I. S. Chuckowree, P. A. Clarke, P. Depledge, S. A. Eccles, et al. 2008. The identification of 2-(1H-indazol-4-yl)-6-(4-methanesulfonyl-piperazin-1-ylmethyl)-4-morpholin-4-yl-thieno[3,2-d]pyrimidine (GDC-0941) as a potent, selective, orally bioavailable inhibitor of class I PI3 kinase for the treatment of cancer . *J Med Chem* 51: 5522-32.

69. Knight, Z. A., B. Gonzalez, M. E. Feldman, E. R. Zunder, D. D. Goldenberg, O. Williams, R. Loewith, D. Stokoe, A. Balla, B. Toth, et al. 2006. A pharmacological map of the PI3-K family defines a role for p110alpha in insulin signaling. *Cell* 125: 733-47.

70. Jackson, S. P., S. M. Schoenwaelder, I. Goncalves, W. S. Nesbitt, C. L. Yap, C. E. Wright, V. Kenche, K. E. Anderson, S. M. Dopheide, Y. Yuan, et al. 2005. PI 3-kinase p110beta: a new target for antithrombotic therapy. *Nat Med* 11: 507-14.

71. Sadhu, C., B. Masinovsky, K. Dick, C. G. Sowell, and D. E. Staunton. 2003. Essential role of phosphoinositide 3-kinase delta in neutrophil directional movement. *J Immunol* 170: 2647-54.

72. Ikeda, H., T. Hideshima, M. Fulciniti, G. Perrone, N. Miura, H. Yasui, Y. Okawa, T. Kiziltepe, L. Santo, S. Vallet, et al. 2010. PI3K/p110{delta} is a novel therapeutic target in multiple myeloma. *Blood* 116: 1460-8.

73. Camps, M., T. Rückle, H. Ji, V. Ardissone, F. Rintelen, J. Shaw, C. Ferrandi, C. Chabert, C. Gillieron, B. Françon, et al. 2005. Blockade of PI3Kgamma suppresses joint inflammation and damage in mouse models of rheumatoid arthritis. *Nat Med* 11: 936-43.

74. Doukas, J., W. Wrasidlo, G. Noronha, E. Dneprovskaia, R. Fine, S. Weis, J. Hood, A. Demaria, R. Soll, and D. Cheresh. 2006. Phosphoinositide 3-kinase

gamma/delta inhibition limits infarct size after myocardial ischemia/reperfusion injury. *Proc Natl Acad Sci U S A* 103: 19866-71.

75. Maira, S. M., F. Stauffer, J. Brueggen, P. Furet, C. Schnell, C. Fritsch, S. Brachmann, P. Chène, A. De Pover, K. Schoemaker, et al. 2008. Identification and characterization of NVP-BEZ235, a new orally available dual phosphatidylinositol 3-kinase/mammalian target of rapamycin inhibitor with potent in vivo antitumor activity. *Mol Cancer Ther* 7: 1851-63.

76. Garlich, J. R., P. De, N. Dey, J. D. Su, X. Peng, A. Miller, R. Murali, Y. Lu, G. B. Mills, V. Kundra, et al. 2008. A vascular targeted pan phosphoinositide 3-kinase inhibitor prodrug, SF1126, with antitumor and antiangiogenic activity. *Cancer Res* 68: 206-15.

77. Chresta, C. M., B. R. Davies, I. Hickson, T. Harding, S. Cosulich, S. E. Critchlow, J. P. Vincent, R. Ellston, D. Jones, P. Sini, et al. 2010. AZD8055 is a potent, selective, and orally bioavailable ATP-competitive mammalian target of rapamycin kinase inhibitor with in vitro and in vivo antitumor activity. *Cancer Res* 70: 288-98.

78. Mosmann, T. R., H. Cherwinski, M. W. Bond, M. A. Giedlin, and R. L. Coffman. 1986. Two types of murine helper T cell clone. I. Definition according to profiles of lymphokine activities and secreted proteins. *J Immunol* 136: 2348-57.

79. Coffman, R. L. 2006. Origins of the T(H)1-T(H)2 model: a personal perspective. *Nat Immunol* 7: 539-41.

80. Duhen, T., R. Geiger, D. Jarrossay, A. Lanzavecchia, and F. Sallusto. 2009. Production of interleukin 22 but not interleukin 17 by a subset of human skin-homing memory T cells. *Nat Immunol* 10: 857-63.

81. Trifari, S., C. D. Kaplan, E. H. Tran, N. K. Crellin, and H. Spits. 2009. Identification of a human helper T cell population that has abundant production of interleukin 22 and is distinct from T(H)-17, T(H)1 and T(H)2 cells. *Nat Immunol* 10: 864-71.

82. Eyerich, S., K. Eyerich, A. Cavani, and C. Schmidt-Weber. 2010. IL-17 and IL-22: siblings, not twins. *Trends Immunol* 31: 354-61.

83. Soroosh, P., A. Taylor, and T. A. Doherty. 2009. Th9 and allergic disease. *Immunology* 127: 450-8.

84. Zhu, J., and W. E. Paul. 2010. Heterogeneity and plasticity of T helper cells. *Cell research* 20: 4-12.

85. Bluestone, J. A., C. R. Mackay, J. J. O'Shea, and B. Stockinger. 2009. The functional plasticity of T cell subsets. *Nat Rev Immunol* 9: 811-6.

86. Annunziato, F., and S. Romagnani. 2009. Heterogeneity of human effector CD4+ T cells. *Arthritis Res Ther* 11: 257.

87. Butcher, E. C., and L. J. Picker. 1996. Lymphocyte homing and homeostasis. *Science* 272: 60-6.

88. Segura, E., J. Valladeau-Guilemond, M.-H. Donnadieu, X. Sastre-Garau, V. Soumelis, and S. Amigorena. 2012. Characterization of resident and migratory dendritic cells in human lymph nodes. *J Exp Med* 209: 653-661.

89. Weninger, W., M. A. Crowley, N. Manjunath, and U. H. von Andrian. 2001. Migratory properties of naive, effector, and memory CD8(+) T cells. *J Exp Med* 194: 953-66.

90. Puri, K. D., E. B. Finger, G. Gaudernack, and T. A. Springer. 1995. Sialomucin CD34 is the major L-selectin ligand in human tonsil high endothelial venules. *J Cell Biol* 131: 261-70.

91. Berg, E. L., A. T. Mullowney, D. P. Andrew, J. E. Goldberg, and E. C. Butcher. 1998. Complexity and differential expression of carbohydrate epitopes associated with L-selectin recognition of high endothelial venules. *Am J Pathol* 152: 469-77.

92. Yoshida, R., M. Nagira, M. Kitaura, N. Imagawa, T. Imai, and O. Yoshie. 1998. Secondary lymphoid-tissue chemokine is a functional ligand for the CC chemokine receptor CCR7. *J Cell Biochem* 273: 7118-22.

93. Iijima, M., and P. Devreotes. 2002. Tumor suppressor PTEN mediates sensing of chemoattractant gradients. *Cell* 109: 599-610.

94. Funamoto, S., R. Meili, S. Lee, L. Parry, and R. A. Firtel. 2002. Spatial and temporal regulation of 3-phosphoinositides by PI 3-kinase and PTEN mediates chemotaxis. *Cell* 109: 611-23.

95. Smith, L. D., E. S. Hickman, R. V. Parry, J. Westwick, and S. G. Ward. 2007. PI3Kgamma is the dominant isoform involved in migratory responses of human T lymphocytes: effects of ex vivo maintenance and limitations of non-viral delivery of siRNA. *Cell Signal* 19: 2528-39.

96. Giagulli, C., E. Scarpini, L. Ottoboni, S. Narumiya, E. C. Butcher, G. Constantin, and C. Laudanna. 2004. RhoA and zeta PKC control distinct modalities of LFA-1 activation by chemokines: critical role of LFA-1 affinity triggering in lymphocyte in vivo homing. *Immunity* 20: 25-35.

97. Engelhardt, B., and H. Wolburg. 2004. Mini-review: Transendothelial migration of leukocytes: through the front door or around the side of the house? *Eur J Immunol* 34: 2955-63.

98. Wagner, N., J. Löhler, T. F. Tedder, K. Rajewsky, W. Müller, and D. A. Steeber. 1998. L-selectin and beta7 integrin synergistically mediate lymphocyte migration to mesenteric lymph nodes. *Eur J Immunol* 28: 3832-9.

99. Tedder, T. F., D. A. Steeber, and P. Pizcueta. 1995. L-selectin-deficient mice have impaired leukocyte recruitment into inflammatory sites. *J Exp Med* 181: 2259-64.

100. Arbonés, M. L., D. C. Ord, K. Ley, H. Ratech, C. Maynard-Curry, G. Otten, D. J. Capon, and T. F. Tedder. 1994. Lymphocyte homing and leukocyte rolling and migration are impaired in L-selectin-deficient mice. *Immunity* 1: 247-60.

101. Steeber, D. A., N. E. Green, S. Sato, and T. F. Tedder. 1996. Humoral immune responses in L-selectin-deficient mice. *J Immunol* 157: 4899-907.

102. Tang, M. L., L. P. Hale, D. A. Steeber, and T. F. Tedder. 1997. L-selectin is involved in lymphocyte migration to sites of inflammation in the skin: delayed rejection of allografts in L-selectin-deficient mice. *J Immunol* 158: 5191-9.

103. Gallatin, W. M., I. L. Weissman, and E. C. Butcher. 1983. A cell-surface molecule involved in organ-specific homing of lymphocytes. *Nature* 304: 30-4.

104. Tedder, T. F., C. M. Isaacs, T. J. Ernst, G. D. Demetri, D. A. Adler, and C. M. Disteche. 1989. Isolation and chromosomal localization of cDNAs encoding a novel human lymphocyte cell surface molecule, LAM-1. Homology with the mouse lymphocyte homing receptor and other human adhesion proteins. *J Exp Med* 170: 123-33.

105. Siegelman, M., M. van de Rijn, and I. Weissman. 1989. Mouse lymph node homing receptor cDNA clone encodes a glycoprotein revealing tandem interaction domains. *Science* 243: 1165-1172.

106. Watanabe, T., Y. Song, Y. Hirayama, T. Tamatani, K. Kuida, and M. Miyasaka. 1992. Sequence and expression of a rat cDNA for LECAM-1. *Biochim Biophys Acta* 1131: 321-4.

107. Berg, M., and S. P. James. 1990. Human neutrophils release the Leu-8 lymph node homing receptor during cell activation. *Blood* 76: 2381-8.

108. Schleiffenbaum, B., O. Spertini, and T. F. Tedder. 1992. Soluble L-selectin is present in human plasma at high levels and retains functional activity. *J Cell Biol* 119: 229-38.

109. Picker, L. J., J. R. Treer, B. Ferguson-Darnell, P. A. Collins, D. Buck, and L. W. Terstappen. 1993. Control of lymphocyte recirculation in man. I. Differential regulation of the peripheral lymph node homing receptor L-selectin on T cells during the virgin to memory cell transition. *J Immunol* 150: 1105-21.

110. Finlay, D. K., L. V. Sinclair, C. Feijoo, C. M. Waugh, T. J. Hagenbeek, H. Spits, and D. A. Cantrell. 2009. Phosphoinositide-dependent kinase 1 controls migration and malignant transformation but not cell growth and proliferation in PTEN-null lymphocytes. *J Exp Med* 206: 2441-54.

111. Dong, Z. M., L. Jackson, and J. W. Murphy. 1999. Mechanisms for induction of L-selectin loss from T lymphocytes by a cryptococcal polysaccharide, glucuronoxylomannan. *Infect Immun* 67: 220-9.

112. Monteseirín, J., E. Llamas, H. Sánchez-Monteseirín, I. Bonilla, M. J. Camacho, J. Conde, and F. Sobrino. 2001. IgE-mediated downregulation of L-selectin (CD62L) on lymphocytes from asthmatic patients. *Allergy* 56: 164-8.

113. Vega, A., R. El Bekay, P. Chacón, I. Ventura, and J. Monteseirín. 2010. Angiotensin II induces CD62L shedding in human neutrophils. *Atherosclerosis* 209: 344-51.

114. Sinclair, L. V., D. Finlay, C. Feijoo, G. H. Cornish, A. Gray, A. Ager, K. Okkenhaug, T. J. Hagenbeek, H. Spits, and D. A. Cantrell. 2008. Phosphatidylinositol-3-OH kinase and nutrient-sensing mTOR pathways control T lymphocyte trafficking. *Nat Immunol* 9: 513-21.

115. Finlay, D., and D. Cantrell. 2010. Phosphoinositide 3-kinase and the mammalian target of rapamycin pathways control T cell migration. *Ann N Y Acad Sci* 1183: 149-57.

116. Savage, N. D. L., S. H. Harris, A. G. Rossi, B. De Silva, S. E. M. Howie, G. T. Layton, and J. R. Lamb. 2002. Inhibition of TCR-mediated shedding of L-selectin (CD62L) on human and mouse CD4+ T cells by metalloproteinase inhibition: analysis of the regulation of Th1/Th2 function. *Eur J Immunol* 32: 2905-14.

117. Preece, G., G. Murphy, and A. Ager. 1996. Metalloproteinase-mediated regulation of L-selectin levels on leucocytes. *J Cell Biochem* 271: 11634-40.

118. Black, R. A., C. T. Rauch, C. J. Kozlosky, J. J. Peschon, J. L. Slack, M. F. Wolfson, B. J. Castner, K. L. Stocking, P. Reddy, S. Srinivasan, et al. 1997. A metalloproteinase disintegrin that releases tumour-necrosis factor-alpha from cells. *Nature* 385: 729-33.

119. Moss, M. L., S. L. Jin, M. E. Milla, D. M. Bickett, W. Burkhart, H. L. Carter, W. J. Chen, W. C. Clay, J. R. Didsbury, D. Hassler, et al. 1997. Cloning of a disintegrin metalloproteinase that processes precursor tumour-necrosis factor-alpha. *Nature* 385: 733-6.

120. Peschon, J. J. 1998. An Essential Role for Ectodomain Shedding in Mammalian Development. *Science* 282: 1281-1284.

121. Condon, T. P., S. Flournoy, G. J. Sawyer, B. F. Baker, T. K. Kishimoto, and C. F. Bennett. 2001. ADAM17 but not ADAM10 mediates tumor necrosis factor-alpha and L-selectin shedding from leukocyte membranes. *Antisense Nucleic Acid Drug Dev* 11: 107-16.

122. Le Gall, S. M., P. Bobé, K. Reiss, K. Horiuchi, X.-D. Niu, D. Lundell, D. R. Gibb, D. Conrad, P. Saftig, and C. P. Blobel. 2009. ADAMs 10 and 17 represent differentially regulated components of a general shedding machinery for

membrane proteins such as transforming growth factor alpha, L-selectin, and tumor necrosis factor alpha. *Mol Biol Cell* 20: 1785-94.

123. Garbers, C., N. Jänner, A. Chalaris, M. L. Moss, D. M. Floss, D. Meyer, F. Koch-Nolte, S. Rose-John, and J. Scheller. 2011. Species specificity of ADAM10 and ADAM17 proteins in interleukin-6 (IL-6) trans-signaling and novel role of ADAM10 in inducible IL-6 receptor shedding. *J Cell Biochem* 286: 14804-11.

124. Wang, Y., A. C. Zhang, Z. Ni, A. Herrera, and B. Walcheck. 2010. ADAM17 activity and other mechanisms of soluble L-selectin production during death receptor-induced leukocyte apoptosis. *J Immunol* 184: 4447-54.

125. Zhang, Z., P. Oliver, J. R. Lancaster, P. O. Schwarzenberger, M. S. Joshi, J. Cork, and J. K. Kolls. 2001. Reactive oxygen species mediate tumor necrosis factor alpha-converting, enzyme-dependent ectodomain shedding induced by phorbol myristate acetate. *FASEB J* 15: 303-5.

126. Horiuchi, K., S. Le Gall, M. Schulte, T. Yamaguchi, K. Reiss, G. Murphy, Y. Toyama, D. Hartmann, P. Saftig, and C. P. Blobel. 2007. Substrate selectivity of epidermal growth factor-receptor ligand sheddases and their regulation by phorbol esters and calcium influx. *Mol Biol Cell* 18: 176-88.

127. Nagano, O., D. Murakami, D. Hartmann, B. De Strooper, P. Saftig, T. Iwatsubo, M. Nakajima, M. Shinohara, and H. Saya. 2004. Cell-matrix interaction via CD44 is independently regulated by different metalloproteinases activated in response to extracellular Ca(2+) influx and PKC activation. *J Cell Biol* 165: 893-902.

128. Alexander, S. R., T. K. Kishimoto, and B. Walcheck. 2000. Effects of selective protein kinase C inhibitors on the proteolytic down-regulation of L-selectin from chemoattractant-activated neutrophils. *J Leukoc Biol* 67: 415-22.

129. Lemjabbar-Alaoui, H., S. S. Sidhu, A. Mengistab, M. Gallup, and C. Basbaum. 2011. TACE/ADAM-17 phosphorylation by PKC-epsilon mediates premalignant changes in tobacco smoke-exposed lung cells. *PloS one* 6: e17489.

130. Killock, D. J., and A. Ivetić. 2010. The cytoplasmic domains of TNFalpha-converting enzyme (TACE/ADAM17) and L-selectin are regulated differently by p38 MAPK and PKC to promote ectodomain shedding. *Biochem J* 428: 293-304.

131. Díaz-Rodríguez, E., J. C. Montero, A. Esparís-Ogando, L. Yuste, and A. Pandiella. 2002. Extracellular signal-regulated kinase phosphorylates tumor necrosis factor alpha-converting enzyme at threonine 735: a potential role in regulated shedding. *Mol Biol Cell* 13: 2031-44.

132. Soond, S. M., B. Everson, D. W. H. Riches, and G. Murphy. 2005. ERK-mediated phosphorylation of Thr735 in TNFalpha-converting enzyme and its potential role in TACE protein trafficking. *J Cell Sci* 118: 2371-80.

133. Fabre, S., F. Carrette, J. Chen, V. Lang, M. Semichon, C. Denoyelle, V. Lazar, N. Cagnard, A. Dubart-Kupperschmitt, M. Mangeney, et al. 2008. FOXO1 regulates L-Selectin and a network of human T cell homing molecules downstream of phosphatidylinositol 3-kinase. *J Immunol* 181: 2980-9.

134. Kerdiles, Y. M., D. R. Beisner, R. Tinoco, A. S. Dejean, D. H. Castrillon, R. A. DePinho, and S. M. Hedrick. 2009. Foxo1 links homing and survival of naive T cells by regulating L-selectin, CCR7 and interleukin 7 receptor. *Nat Immunol* 10: 176-84.

135. Feng, X., H. Wang, H. Takata, T. J. Day, J. Willen, and H. Hu. 2011. Transcription factor Foxp1 exerts essential cell-intrinsic regulation of the quiescence of naive T cells. *Nat Immunol* 12: 544-50.

136. Rena, G., S. Guo, S. C. Cichy, T. G. Unterman, and P. Cohen. 1999. Phosphorylation of the transcription factor forkhead family member FKHR by protein kinase B. *J Cell Biochem* 274: 17179-83.

137. Lange, C. M., T. Y. V. Tran, H. Farnik, S. Jungblut, T. Born, T. O. Wagner, and T. O. Hirche. 2010. Increased frequency of regulatory T cells and selection of highly potent CD62L+ cells during treatment of human lung transplant recipients with rapamycin. *Transpl Int* 23: 266-76.

138. Zetterberg, E., and J. Richter. 1993. Correlation between serum level of soluble L-selectin and leukocyte count in chronic myeloid and lymphocytic leukemia and during bone marrow transplantation. *Eur J Haematol* 51: 113-9.

139. Extermann, M., M. Bacchi, N. Monai, M. Fopp, M. Fey, A. Tichelli, M. Schapira, and O. Spertini. 1998. Relationship between cleaved L-selectin levels and the outcome of acute myeloid leukemia. *Blood* 92: 3115-22.

140. Hanson, E. M., V. K. Clements, P. Sinha, D. Ilkovitch, and S. Ostrand-Rosenberg. 2009. Myeloid-derived suppressor cells down-regulate L-selectin expression on CD4+ and CD8+ T cells. *J Immunol* 183: 937-44.

141. Wölfl, M., K. Merker, H. Morbach, S. W. Van Gool, M. Eyrich, P. D. Greenberg, and P. G. Schlegel. 2011. Primed tumor-reactive multifunctional CD62L+ human CD8+ T cells for immunotherapy. *Cancer Immunol Immunother* 60: 173-86.

142. Yang, S., F. Liu, Q. J. Wang, S. A. Rosenberg, and R. A. Morgan. 2011. The Shedding of CD62L (L-Selectin) Regulates the Acquisition of Lytic Activity in Human Tumor Reactive T Lymphocytes. *PloS one* 6: e22560.

143. Frauwirth, K. A., and C. B. Thompson. 2004. Regulation of T lymphocyte metabolism. *J Immunol* 172: 4661-5.

144. Lewis, R. S. 2001. Calcium signaling mechanisms in T lymphocytes. *Annu Rev Immunol* 19: 497-521.

145. Smith-Garvin, J. E., G. A. Koretzky, and M. S. Jordan. 2009. T cell activation. *Annu Rev Immunol* 27: 591-619.

146. Savignac, M., B. Mellström, and J. R. Naranjo. 2007. Calcium-dependent transcription of cytokine genes in T lymphocytes. *Pflugers Arch* 454: 523-33.

147. Oh-hora, M., and A. Rao. 2008. Calcium signaling in lymphocytes. *Curr Opin Immunol* 20: 250-8.

148. Cahalan, M. D., and K. G. Chandy. 2009. The functional network of ion channels in T lymphocytes. *Immunol Rev* 231: 59-87.

149. Frischauf, I., R. Schindl, I. Derler, J. Bergsmann, M. Fahrner, and C. Romanin. 2008. The STIM/Orai coupling machinery. *Channels (Austin)* 2: 261-8.

150. Roberts-Thomson, S. J., A. A. Peters, D. M. Grice, and G. R. Monteith. 2010. ORAI-mediated calcium entry: mechanism and roles, diseases and pharmacology. *Pharmacol Ther* 127: 121-30.

151. Balla, T., P. Várnai, and L. Hunyady. 2009. STIM and Orai: the long-awaited constituents of store-operated calcium entry. *Trends Pharmacol Sci* 30: 118-28.

152. Hogan, P. G., R. S. Lewis, and A. Rao. 2010. Molecular basis of calcium signaling in lymphocytes: STIM and ORAI. *Annu Rev Immunol* 28: 491-533.

153. Park, C. Y., P. J. Hoover, F. M. Mullins, P. Bachhawat, E. D. Covington, S. Raunser, T. Walz, K. C. Garcia, R. E. Dolmetsch, and R. S. Lewis. 2009. STIM1 clusters and activates CRAC channels via direct binding of a cytosolic domain to Orai1. *Cell* 136: 876-90.

154. Korzeniowski, M. K., I. M. Manjarrés, P. Varnai, and T. Balla. 2010. Activation of STIM1-Orai1 involves an intramolecular switching mechanism. *Sci Signal* 3: ra82.

155. Dimroth, P., G. Kaim, and U. Matthey. 2000. Crucial role of the membrane potential for ATP synthesis by F(1)F(o) ATP synthases. *J Exp Biol* 203: 51-9.

156. Embley, T. M., and W. Martin. 2006. Eukaryotic evolution, changes and challenges. *Nature* 440: 623-30.

157. Greaves, L. C., A. K. Reeve, R. W. Taylor, and D. M. Turnbull. 2012. Mitochondrial DNA and disease. *J Pathol* 226: 274-86.

158. Turrens, J. F. 1997. Superoxide production by the mitochondrial respiratory chain. *Biosci Rep* 17: 3-8.

159. Turrens, J. F., and A. Boveris. 1980. Generation of superoxide anion by the NADH dehydrogenase of bovine heart mitochondria. *Biochem J* 191: 421-7.

160. Zhou, R., A. S. Yazdi, P. Menu, and J. Tschopp. 2011. A role for mitochondria in NLRP3 inflammasome activation. *Nature* 469: 221-5.

161. Galley, H. F. 2011. Oxidative stress and mitochondrial dysfunction in sepsis. *Br J Anaesth* 107: 57-64.

162. Li, N., K. Ragheb, G. Lawler, J. Sturgis, B. Rajwa, J. A. Melendez, and J. P. Robinson. 2003. Mitochondrial complex I inhibitor rotenone induces apoptosis through enhancing mitochondrial reactive oxygen species production. *J Cell Biochem* 278: 8516-25.

163. Marchetti, P., T. Hirsch, N. Zamzami, M. Castedo, D. Decaudin, S. a Susin, B. Masse, and G. Kroemer. 1996. Mitochondrial permeability transition triggers lymphocyte apoptosis. *J Immunol* 157: 4830-6.

164. Deng, Y. T., H. C. Huang, and J. K. Lin. 2010. Rotenone induces apoptosis in MCF-7 human breast cancer cell-mediated ROS through JNK and p38 signaling. *Mol Carcinog* 49: 141-51.

165. Bulua, A. C., A. Simon, R. Maddipati, M. Pelletier, H. Park, K. Y. Kim, M. N. Sack, D. L. Kastner, and R. M. Siegel. 2011. Mitochondrial reactive oxygen species promote production of proinflammatory cytokines and are elevated in TNFR1-associated periodic syndrome (TRAPS). *J Exp Med* 208: 519-33.

166. Chen, C. M. 2011. Mitochondrial dysfunction, metabolic deficits, and increased oxidative stress in Huntington's disease. *Chang Gung Med J* 34: 135-52.

167. Burnstock, G., T. Cocks, R. Crowe, and L. Kasakov. 1978. Purinergic innervation of the guinea-pig urinary bladder. *Br J Pharmacol* 63: 125-38.

168. Kaczmarek, E., K. Koziak, J. Sévigny, J. B. Siegel, J. Anrather, A. R. Beaudoin, F. H. Bach, and S. C. Robson. 1996. Identification and characterization of CD39/vascular ATP diphosphohydrolase. *J Cell Biochem* 271: 33116-22.

169. Kansas, G. S., G. S. Wood, and T. F. Tedder. 1991. Expression, distribution, and biochemistry of human CD39. Role in activation-associated homotypic adhesion of lymphocytes. *J Immunol* 146: 2235-44.

170. Deaglio, S., K. M. Dwyer, W. Gao, D. Friedman, A. Usheva, A. Erat, J. F. Chen, K. Enjyoji, J. Linden, M. Oukka, et al. 2007. Adenosine generation catalyzed by CD39 and CD73 expressed on regulatory T cells mediates immune suppression. *J Exp Med* 204: 1257-65.

171. Künzli, B. M., P. O. Berberat, T. Giese, E. Csizmadia, E. Kaczmarek, C. Baker, I. Halaceli, M. W. Büchler, H. Friess, and S. C. Robson. 2007. Upregulation of CD39/NTPDases and P2 receptors in human pancreatic disease. *Am J Physiol Gastrointest Liver Physiol* 292: G223-30.

172. Moncrieffe, H., K. Nistala, Y. Kamhieh, J. Evans, A. Eddaoudi, S. Eaton, and L. R. Wedderburn. 2010. High expression of the ectonucleotidase CD39 on T cells from the inflamed site identifies two distinct populations, one regulatory and one memory T cell population. *J Immunol* 185: 134-43.

173. North, R. A. 2002. Molecular physiology of P2X receptors. *Physiol Rev* 82: 1013-67.

174. Mirabet, M., C. Herrera, O. J. Cordero, J. Mallol, C. Lluis, and R. Franco. 1999. Expression of A2B adenosine receptors in human lymphocytes: their role in T cell activation. *J Cell Sci* 112 (Pt 4: 491-502.

175. Huang, S., S. Apasov, M. Koshiba, and M. Sitkovsky. 1997. Role of A2a extracellular adenosine receptor-mediated signaling in adenosine-mediated inhibition of T-cell activation and expansion. *Blood* 90: 1600-10.

176. Gessi, S., K. Varani, S. Merighi, E. Cattabriga, A. Avitabile, R. Gavioli, C. Fortini, E. Leung, S. Mac Lennan, and P. A. Borea. 2004. Expression of A3 adenosine receptors in human lymphocytes: up-regulation in T cell activation. *Mol Pharmacol* 65: 711-9.

177. Gessi, S., K. Varani, S. Merighi, A. Morelli, D. Ferrari, E. Leung, P. G. Baraldi, G. Spalluto, and P. A. Borea. 2001. Pharmacological and biochemical characterization of A3 adenosine receptors in Jurkat T cells. *Br J Pharmacol* 134: 116-26.

178. Ernst, P. B., J. C. Garrison, and L. F. Thompson. 2010. Much ado about adenosine: adenosine synthesis and function in regulatory T cell biology. *J Immunol* 185: 1993-8.

179. Drygiannakis, I., P. B. Ernst, D. Lowe, and I. J. Glomski. 2011. Immunological alterations mediated by adenosine during host-microbial interactions. *Immunol Res* 50: 69-77.

180. Hoskin, D. W., J. S. Mader, S. J. Furlong, D. M. Conrad, and J. Blay. 2008. Inhibition of T cell and natural killer cell function by adenosine and its contribution to immune evasion by tumor cells (Review). *Int J Oncol* 32: 527-35.

181. Ernst, P. B., J. C. Garrison, and L. F. Thompson. 2010. Much ado about adenosine: adenosine synthesis and function in regulatory T cell biology. *J Immunol* 185: 1993-8.

182. Wang, L., S. E. W. Jacobsen, A. Bengtsson, and D. Erlinge. 2004. P2 receptor mRNA expression profiles in human lymphocytes, monocytes and CD34+ stem and progenitor cells. *BMC Immunol* 5: 16.

183. Koshiba, M., S. Apasov, V. Sverdlov, P. Chen, L. Erb, J. T. Turner, G. a Weisman, and M. V. Sitkovsky. 1997. Transient up-regulation of P2Y2 nucleotide receptor mRNA expression is an immediate early gene response in activated thymocytes. *Proc Natl Acad Sci U S A* 94: 831-6.

184. Ben Addi, A., D. Cammarata, P. B. Conley, J. M. Boeynaems, and B. Robaye. 2010. Role of the P2Y12 receptor in the modulation of murine dendritic cell function by ADP. *J Immunol* 185: 5900-6.

185. North, R. A., and A. Surprenant. 2000. Pharmacology of cloned P2X receptors. *Annu Rev Pharmacol Toxicol* 40: 563-80.

186. Khakh, B. S., W. R. Proctor, T. V. Dunwiddie, C. Labarca, and H. A. Lester. 1999. Allosteric control of gating and kinetics at P2X(4) receptor channels. *J Neurosci* 19: 7289-99.

187. Bo, X., Y. Zhang, M. Nassar, G. Burnstock, and R. Schoepfer. 1995. A P2X purinoceptor cDNA conferring a novel pharmacological profile. *FEBS Lett* 375: 129-33.

188. Woehrle, T., L. Yip, A. Elkhal, Y. Sumi, Y. Chen, Y. Yao, P. A. Insel, and W. G. Junger. 2010. Pannexin-1 hemichannel-mediated ATP release together with P2X1 and P2X4 receptors regulate T-cell activation at the immune synapse. *Blood* 116: 3475-84.

189. Rassendren, F., G. N. Buell, C. Virginio, G. Collo, R. A. North, and A. Surprenant. 1997. The permeabilizing ATP receptor, P2X7. Cloning and expression of a human cDNA. *J Cell Biochem* 272: 5482-6.

190. Sluyter, R., J. A. Barden, and J. S. Wiley. 2001. Detection of P2X purinergic receptors on human B lymphocytes. *Cell Tissue Res* 304: 231-6.

191. Chused, T. M., S. Apasov, and M. Sitkovsky. 1996. Murine T lymphocytes modulate activity of an ATP-activated P2Z-type purinoceptor during differentiation. *J Immunol* 157: 1371-80.

192. Surprenant, A., F. Rassendren, E. Kawashima, R. A. North, and G. Buell. 1996. The cytolytic P2Z receptor for extracellular ATP identified as a P2X receptor (P2X7). *Science* 272: 735-8.

193. Young, M. T., P. Pelegrin, and A. Surprenant. 2007. Amino acid residues in the P2X7 receptor that mediate differential sensitivity to ATP and BzATP. *Mol Pharmacol* 71: 92-100.

194. Jiang, L. H., F. Rassendren, A. Surprenant, and R. A. North. 2000. Identification of amino acid residues contributing to the ATP-binding site of a purinergic P2X receptor. *J Cell Biochem* 275: 34190-6.

195. Worthington, R. A., M. L. Smart, B. J. Gu, D. A. Williams, S. Petrou, J. S. Wiley, and J. A. Barden. 2002. Point mutations confer loss of ATP-induced human P2X(7) receptor function. *FEBS Lett* 512: 43-6.

196. Gu, B. J., R. Sluyter, K. K. Skarratt, A. N. Shemon, L.-P. Dao-Ung, S. J. Fuller, J. A. Barden, A. L. Clarke, S. Petrou, and J. S. Wiley. 2004. An Arg307 to

Gln polymorphism within the ATP-binding site causes loss of function of the human P2X7 receptor. *J Cell Biochem* 279: 31287-95.

197. Wilkinson, W. J., L H. Jiang, A. Surprenant, and R. A. North. 2006. Role of ectodomain lysines in the subunits of the heteromeric P2X2/3 receptor. *Mol Pharmacol* 70: 1159-63.

198. Kawate, T., J. C. Michel, W. T. Birdsong, and E. Gouaux. 2009. Crystal structure of the ATP-gated P2X(4) ion channel in the closed state. *Nature* 460: 592-8.

199. Hattori, M., and E. Gouaux. 2012. Molecular mechanism of ATP binding and ion channel activation in P2X receptors. *Nature* 485:207-12

200. Chessell, I. P., A. D. Michel, and P. P. Humphrey. 1998. Effects of antagonists at the human recombinant P2X7 receptor. *Br J Pharmacol* 124: 1314-20.

201. Di Virgilio, F., V. Bronte, D. Collavo, and P. Zanovello. 1989. Responses of mouse lymphocytes to extracellular adenosine 5'-triphosphate (ATP). Lymphocytes with cytotoxic activity are resistant to the permeabilizing effects of ATP. *J Immunol* 143: 1955-60.

202. Michel, A. D., I. P. Chessell, and P. P. Humphrey. 1999. Ionic effects on human recombinant P2X7 receptor function. *Naunyn Schmiedebergs Arch Pharmacol* 359: 102-9.

203. Virginio, C., D. Church, R. A. North, and A. Surprenant. 1997. Effects of divalent cations, protons and calmidazolium at the rat P2X7 receptor. *Neuropharmacology* 36: 1285-94.

204. Moore, S. F., and A. B. Mackenzie. 2008. Species and agonist dependent zinc modulation of endogenous and recombinant ATP-gated P2X7 receptors. *Biochem Pharmacol* 76: 1740-7.

205. Bradford, M. D., and S. P. Soltoff. 2002. P2X7 receptors activate protein kinase D and p42/p44 mitogen-activated protein kinase (MAPK) downstream of protein kinase C. *Biochem J* 366: 745-55.

206. Tsukimoto, M., M. Maehata, H. Harada, A. Ikari, K. Takagi, and M. Degawa. 2006. P2X7 receptor-dependent cell death is modulated during murine T cell maturation and mediated by dual signaling pathways. *J Immunol* 177: 2842-50.

207. Jamieson, G. P., M. B. Snook, P. J. Thurlow, and J. S. Wiley. 1996. Extracellular ATP causes of loss of L-selectin from human lymphocytes via occupancy of P2Z purinocepters. *J Cell Physiol* 166: 637-42.

208. Gu, B., L. J. Bendall, and J. S. Wiley. 1998. Adenosine triphosphate-induced shedding of CD23 and L-selectin (CD62L) from lymphocytes is mediated by the same receptor but different metalloproteases. *Blood* 92: 946-51.

209. Murgia, M., S. Hanau, P. Pizzo, M. Rippa, and F. Di Virgilio. 1993. Oxidized ATP. An irreversible inhibitor of the macrophage purinergic P2Z receptor. *J Cell Biochem* 268: 8199-203.

210. Beigi, R. D., S. B. Kertesy, G. Aquilina, and G. R. Dubyak. 2003. Oxidized ATP (oATP) attenuates proinflammatory signaling via P2 receptor-independent mechanisms. *Br J Pharmacol* 140: 507-19.

211. Wiley, J. S., J. R. Chen, M. B. Snook, and G. P. Jamieson. 1994. The P2Z-purinoceptor of human lymphocytes: actions of nucleotide agonists and irreversible inhibition by oxidized ATP. *Br J Pharmacol* 112: 946-50.

212. Gargett, C. E., and J. S. Wiley. 1997. The isoquinoline derivative KN-62 a potent antagonist of the P2Z-receptor of human lymphocytes. *Br J Pharmacol* 120: 1483-90.

213. Tokumitsu, H., T. Chijiwa, M. Hagiwara, A. Mizutani, M. Terasawa, and H. Hidaka. 1990. KN-62, 1-[N,O-bis(5-isoquinolinesulfonyl)-N-methyl-L-tyrosyl]-4-phenylpiperazi ne, a specific inhibitor of Ca2+/calmodulin-dependent protein kinase II. *J Cell Biochem* 265: 4315-20.

214. Soltoff, S. P., M. K. McMillian, and B. R. Talamo. 1989. Coomassie Brilliant Blue G is a more potent antagonist of P2 purinergic responses than Reactive Blue 2 (Cibacron Blue 3GA) in rat parotid acinar cells. *Biochem Biophys Res Commun* 165: 1279-85.

215. Gunosewoyo, H., and M. Kassiou. 2010. P2X purinergic receptor ligands: recently patented compounds. *Expert Opin Ther Pat* 20: 625-46.

216. Nelson, D. W., R. J. Gregg, M. E. Kort, A. Perez-Medrano, E. A. Voight, Y. Wang, G. Grayson, M. T. Namovic, D. L. Donnelly-Roberts, W. Niforatos, et al. 2006. Structure-activity relationship studies on a series of novel, substituted 1-benzyl-5-phenyltetrazole P2X7 antagonists. *J Med Chem* 49: 3659-66.

217. McGaraughty, S., K. L. Chu, M. T. Namovic, D. L. Donnelly-Roberts, R. R. Harris, X. F. Zhang, C. C. Shieh, C. T. Wismer, C. Z. Zhu, D. M. Gauvin, et al. 2007. P2X7-related modulation of pathological nociception in rats. *Neuroscience* 146: 1817-28.

218. Honore, P., D. Donnelly-Roberts, M. T. Namovic, G. Hsieh, C. Z. Zhu, J. P. Mikusa, G. Hernandez, C. Zhong, D. M. Gauvin, P. Chandran, et al. 2006. A-740003 [N-(1-{[(cyanoimino)(5-quinolinylamino) methyl]amino}-2,2-dimethylpropyl)-2-(3,4-dimethoxyphenyl)acetamide], a novel and selective P2X7 receptor antagonist, dose-dependently reduces neuropathic pain in the rat. *J Pharmacol Exp Ther* 319: 1376-85.

219. Alcaraz, L., A. Baxter, J. Bent, K. Bowers, M. Braddock, D. Cladingboel, D. Donald, M. Fagura, M. Furber, C. Laurent, et al. 2003. Novel P2X7 receptor antagonists. *Bioorg Med Chem Lett* 13: 4043-6.

220. Baxter, A., J. Bent, K. Bowers, M. Braddock, S. Brough, M. Fagura, M. Lawson, T. McInally, M. Mortimore, M. Robertson, et al. 2003. Hit-to-Lead studies: the discovery of potent adamantane amide P2X7 receptor antagonists. *Bioorg Med Chem Lett* 13: 4047-50.

221. Stokes, L., L. H. Jiang, L. Alcaraz, J. Bent, K. Bowers, M. Fagura, M. Furber, M. Mortimore, M. Lawson, J. Theaker, et al. 2006. Characterization of a selective and potent antagonist of human P2X(7) receptors, AZ11645373. *Br J Pharmacol* 149: 880-7.

222. Keystone, E. C., M. M. Wang, M. Layton, S. Hollis, and I. B. McInnes. 2011. Clinical evaluation of the efficacy of the P2X7 purinergic receptor antagonist AZD9056 on the signs and symptoms of rheumatoid arthritis in patients with active disease despite treatment with methotrexate or sulphasalazine. *Ann Rheum Dis* .

223. Stock, T. C., B. J. Bloom, N. Wei, S. Ishaq, W. Park, X. Wang, P. Gupta, and C. A. Mebus. 2012. Efficacy and Safety of CE-224,535, an Antagonist of P2X7 Receptor, in Treatment of Patients with Rheumatoid Arthritis Inadequately Controlled by Methotrexate. *J Rheumatol* .

224. Chessell, I. P., J. Simon, A. D. Hibell, A. D. Michel, E. A. Barnard, and P. P. Humphrey. 1998. Cloning and functional characterisation of the mouse P2X7 receptor. *FEBS Lett* 439: 26-30.

225. Buell, G. N., F. Talabot, A. Gos, J. Lorenz, E. Lai, M. A. Morris, and S. E. Antonarakis. 1998. Gene structure and chromosomal localization of the human P2X7 receptor. *Receptors Channels* 5: 347-54.

226. Lê, K. T., K. Babinski, and P. Séguéla. 1998. Central P2X4 and P2X6 channel subunits coassemble into a novel heteromeric ATP receptor. *J Neurosci* 18: 7152-9.

227. Lewis, C., S. Neidhart, C. Holy, R. A. North, G. Buell, and A. Surprenant. 1995. Coexpression of P2X2 and P2X3 receptor subunits can account for ATP-gated currents in sensory neurons. *Nature* 377: 432-5.

228. Liu, M., B. F. King, P. M. Dunn, W. Rong, A. Townsend-Nicholson, and G. Burnstock. 2001. Coexpression of P2X(3) and P2X(2) receptor subunits in varying amounts generates heterogeneous populations of P2X receptors that evoke a spectrum of agonist responses comparable to that seen in sensory neurons. *J Pharmacol Exp Ther* 296: 1043-50.

229. Nicke, A., D. Kerschensteiner, and F. Soto. 2005. Biochemical and functional evidence for heteromeric assembly of P2X1 and P2X4 subunits. *J Neurochem* 92: 925-33.

230. Torres, G. E., W. R. Haines, T. M. Egan, and M. M. Voigt. 1998. Co-expression of P2X1 and P2X5 receptor subunits reveals a novel ATP-gated ion channel. *Mol Pharmacol* 54: 989-93.

231. Townsend-Nicholson, A., B. F. King, S. S. Wildman, and G. Burnstock. 1999. Molecular cloning, functional characterization and possible cooperativity between the murine P2X4 and P2X4a receptors. *Brain Res Mol Brain Res* 64: 246-54.

232. Brown, S. G., A. Townsend-Nicholson, K. A. Jacobson, G. Burnstock, and B. F. King. 2002. Heteromultimeric P2X(1/2) receptors show a novel sensitivity to extracellular pH. *J Pharmacol Exp Ther* 300: 673-80.

233. King, B. F., A. Townsend-Nicholson, S. S. Wildman, T. Thomas, K. M. Spyer, and G. Burnstock. 2000. Coexpression of rat P2X2 and P2X6 subunits in Xenopus oocytes. *J Neurosci* 20: 4871-7.

234. Boumechache, M., M. Masin, J. M. Edwardson, D. C. Górecki, and R. Murrell-Lagnado. 2009. Analysis of assembly and trafficking of native P2X4 and P2X7 receptor complexes in rodent immune cells. *J Cell Biochem* 284: 13446-54.

235. Young, M. T., J. A. Fisher, S. J. Fountain, R. C. Ford, R. A. North, and B. S. Khakh. 2008. Molecular shape, architecture, and size of P2X4 receptors determined using fluorescence resonance energy transfer and electron microscopy. *J Cell Biochem* 283: 26241-51.

236. Young, M. T. 2010. P2X receptors: dawn of the post-structure era. *Trends Biochem Sci* 35: 83-90.

237. Adriouch, S., C. Dox, V. Welge, M. Seman, F. Koch-Nolte, and F. Haag. 2002. Cutting edge: a natural P451L mutation in the cytoplasmic domain impairs the function of the mouse P2X7 receptor. *J Immunol* 169: 4108-12.

238. Becker, D., R. Woltersdorf, W. Boldt, S. Schmitz, U. Braam, G. Schmalzing, and F. Markwardt. 2008. The P2X7 carboxyl tail is a regulatory module of P2X7 receptor channel activity. *J Cell Biochem* 283: 25725-34.

239. Wilson, H. L., S. A. Wilson, A. Surprenant, and R. A. North. 2002. Epithelial membrane proteins induce membrane blebbing and interact with the P2X7 receptor C terminus. *J Biol Chem* 277: 34017-23.

240. Adinolfi, E., M. Cirillo, R. Woltersdorf, S. Falzoni, P. Chiozzi, P. Pellegatti, M. G. Callegari, D. Sandonà, F. Markwardt, G. Schmalzing, et al. 2010. Trophic activity of a naturally occurring truncated isoform of the P2X7 receptor. *FASEB J* 24: 3393-404.

241. Collo, G., S. Neidhart, E. Kawashima, M. Kosco-Vilbois, R. A. North, and G. Buell. 1997. Tissue distribution of the P2X7 receptor. *Neuropharmacology* 36: 1277-83.

242. Gu, B. J., W. Y. Zhang, L. J. Bendall, I. P. Chessell, G. N. Buell, and J. S. Wiley. 2000. Expression of P2X(7) purinoceptors on human lymphocytes and monocytes: evidence for nonfunctional P2X(7) receptors. *Am J Physiol Cell Physiol* 279: C1189-97.

243. Suh, B. C., J. S. Kim, U. Namgung, H. Ha, and K. T. Kim. 2001. P2X7 nucleotide receptor mediation of membrane pore formation and superoxide generation in human promyelocytes and neutrophils. *J Immunol* 166: 6754-63.

244. Martel-Gallegos, G., M. T. Rosales-Saavedra, J. P. Reyes, G. Casas-Pruneda, C. Toro-Castillo, P. Pérez-Cornejo, and J. Arreola. 2010. Human neutrophils do not express purinergic P2X7 receptors. *Purinergic Signal* 6: 297-306.

245. Sengstake, S., E. M. Boneberg, and H. Illges. 2006. CD21 and CD62L shedding are both inducible via P2X7Rs. *Int Immunol* 18: 1171-8.

246. Hewinson, J., S. F. Moore, C. Glover, A. G. Watts, and A. B. MacKenzie. 2008. A key role for redox signaling in rapid P2X7 receptor-induced IL-1 beta processing in human monocytes. *J Immunol* 180: 8410-20.

247. Ferrari, D., C. Pizzirani, E. Adinolfi, R. M. Lemoli, A. Curti, M. Idzko, E. Panther, and F. Di Virgilio. 2006. The P2X7 receptor: a key player in IL-1 processing and release. *J Immunol* 176: 3877-83.

248. Ferrari, D., P. Chiozzi, S. Falzoni, M. Dal Susino, L. Melchiorri, O. R. Baricordi, and F. Di Virgilio. 1997. Extracellular ATP triggers IL-1 beta release by activating the purinergic P2Z receptor of human macrophages. *J Immunol* 159: 1451-8.

249. MacKenzie, A., H. L. Wilson, E. Kiss-Toth, S. K. Dower, R. A. North, and A. Surprenant. 2001. Rapid Secretion of Interleukin-1β by Microvesicle Shedding. *Immunity* 15: 825-835.

250. Georgiou, J. G., K. K. Skarratt, S. J. Fuller, C. J. Martin, R. I. Christopherson, J. S. Wiley, and R. Sluyter. 2005. Human epidermal and monocyte-derived langerhans cells express functional P2X receptors. *J Invest Dermatol* 125: 482-90.

251. Coutinho-Silva, R., P. M. Persechini, R. D. Bisaggio, J. L. Perfettini, A. C. Neto, J. M. Kanellopoulos, I. Motta-Ly, A. Dautry-Varsat, and D. M. Ojcius. 1999. P2Z/P2X7 receptor-dependent apoptosis of dendritic cells. *Am J Physiol* 276: C1139-47.

252. Wareham, K., C. Vial, R. C. E. Wykes, P. Bradding, and E. P. Seward. 2009. Functional evidence for the expression of P2X1, P2X4 and P2X7 receptors in human lung mast cells. *Br J Pharmacol* 157: 1215-24.

253. Wiley, J. S., and G. R. Dubyak. 1989. Extracellular adenosine triphosphate increases cation permeability of chronic lymphocytic leukemic lymphocytes. *Blood* 73: 1316-23.

254. Adinolfi, E., L. Melchiorri, S. Falzoni, P. Chiozzi, A. Morelli, A. Tieghi, A. Cuneo, G. Castoldi, F. Di Virgilio, and O. R. Baricordi. 2002. P2X7 receptor expression in evolutive and indolent forms of chronic B lymphocytic leukemia. *Blood* 99: 706-8.

255. Auger, R., I. Motta, K. Benihoud, D. M. Ojcius, and J. M. Kanellopoulos. 2005. A role for mitogen-activated protein kinase(Erk1/2) activation and non-selective pore formation in P2X7 receptor-mediated thymocyte death. *J Cell Biochem* 280: 28142-51.

256. Courageot, M. P., S. Lépine, M. Hours, F. Giraud, and J. C. Sulpice. 2004. Involvement of sodium in early phosphatidylserine exposure and phospholipid scrambling induced by P2X7 purinoceptor activation in thymocytes. *J Cell Biochem* 279: 21815-23.

257. Ross, P. E., G. R. Ehring, and M. D. Cahalan. 1997. Dynamics of ATP-induced calcium signaling in single mouse thymocytes. *J Cell Biol* 138: 987-98.

258. Apasov, S. G., M. Koshiba, T. M. Chused, and M. V. Sitkovsky. 1997. Effects of extracellular ATP and adenosine on different thymocyte subsets: possible role of ATP-gated channels and G protein-coupled purinergic receptor. *J Immunol* 158: 5095-105.

259. Schenk, U., M. Frascoli, M. Proietti, R. Geffers, J. Buer, C. Ricordi, A. M. Westendorf, F. Grassi, and E. Traggiai. 2011. ATP inhibits the generation and function of regulatory T cells through the activation of purinergic P2X receptors. *Sci Signal* 4: ra12.

260. Adriouch, S., S. Hubert, S. Pechberty, F. Koch-Nolte, F. Haag, and M. Seman. 2007. NAD+ released during inflammation participates in T cell homeostasis by inducing ART2-mediated death of naive T cells in vivo. *J Immunol* 179: 186-94.

261. Yip, L., T. Woehrle, R. Corriden, M. Hirsh, Y. Chen, Y. Inoue, V. Ferrari, P. A. Insel, and W. G. Junger. 2009. Autocrine regulation of T-cell activation by ATP release and P2X7 receptors. *FASEB J* 23: 1685-93.

262. Heiss, K., N. Jänner, B. Mähnss, V. Schumacher, F. Koch-Nolte, F. Haag, and H. W. Mittrücker. 2008. High sensitivity of intestinal CD8+ T cells to nucleotides indicates P2X7 as a regulator for intestinal T cell responses. *J Immunol* 181: 3861-9.

263. Aswad, F., and G. Dennert. 2006. P2X7 receptor expression levels determine lethal effects of a purine based danger signal in T lymphocytes. *Cell Immunol* 243: 58-65.

264. Taylor, S. R. J., D. R. Alexander, J. C. Cooper, C. F. Higgins, and J. I. Elliott. 2007. Regulatory T cells are resistant to apoptosis via TCR but not P2X7. *J Immunol* 178: 3474-82.

265. Aswad, F., H. Kawamura, and G. Dennert. 2005. High sensitivity of CD4+CD25+ regulatory T cells to extracellular metabolites nicotinamide adenine dinucleotide and ATP: a role for P2X7 receptors. *J Immunol* 175: 3075-83.

266. Hubert, S., B. Rissiek, K. Klages, J. Huehn, T. Sparwasser, F. Haag, F. Koch-Nolte, O. Boyer, M. Seman, and S. Adriouch. 2010. Extracellular NAD+ shapes the Foxp3+ regulatory T cell compartment through the ART2-P2X7 pathway. *J Exp Med* 207: 2561-8.

267. Baricordi, O. R., L. Melchiorri, E. Adinolfi, S. Falzoni, P. Chiozzi, G. Buell, and F. Di Virgilio. 1999. Increased proliferation rate of lymphoid cells transfected with the P2X(7) ATP receptor. *J Cell Biochem* 274: 33206-8.

268. Schenk, U., A. M. Westendorf, E. Radaelli, A. Casati, M. Ferro, M. Fumagalli, C. Verderio, J. Buer, E. Scanziani, and F. Grassi. 2008. Purinergic control of T cell activation by ATP released through pannexin-1 hemichannels. *Sci Signal* 1: ra6.

269. Steinberg, T. H., A. S. Newman, J. A. Swanson, and S. C. Silverstein. 1987. ATP4- permeabilizes the plasma membrane of mouse macrophages to fluorescent dyes. *J Cell Biochem* 262: 8884-8.

270. Wiley, J. S., C. E. Gargett, W. Zhang, M. B. Snook, and G. P. Jamieson. 1998. Partial agonists and antagonists reveal a second permeability state of human lymphocyte P2Z/P2X7 channel. *Am J Physiol* 275: C1224-31.

271. Locovei, S., E. Scemes, F. Qiu, D. C. Spray, and G. Dahl. 2007. Pannexin1 is part of the pore forming unit of the P2X(7) receptor death complex. *FEBS Lett* 581: 483-8.

272. Iglesias, R., S. Locovei, A. Roque, A. P. Alberto, G. Dahl, D. C. Spray, and E. Scemes. 2008. P2X7 receptor-Pannexin1 complex: pharmacology and signaling. *Am J Physiol Cell Physiol* 295: C752-60.

273. Pelegrin, P., and A. Surprenant. 2007. Pannexin-1 couples to maitotoxin- and nigericin-induced interleukin-1beta release through a dye uptake-independent pathway. *J Cell Biochem* 282: 2386-94.

274. Pelegrin, P., and A. Surprenant. 2006. Pannexin-1 mediates large pore formation and interleukin-1beta release by the ATP-gated P2X7 receptor. *EMBO J* 25: 5071-82.

275. Zanovello, P., V. Bronte, A. Rosato, P. Pizzo, and F. Di Virgilio. 1990. Responses of mouse lymphocytes to extracellular ATP. II. Extracellular ATP causes cell type-dependent lysis and DNA fragmentation. *J Immunol* 145: 1545-50.

276. Ferrari, D., M. Los, M. K. Bauer, P. Vandenabeele, S. Wesselborg, and K. Schulze-Osthoff. 1999. P2Z purinoreceptor ligation induces activation of caspases with distinct roles in apoptotic and necrotic alterations of cell death. *FEBS Lett* 447: 71-5.

277. Mackenzie, A. B., M. T. Young, E. Adinolfi, and A. Surprenant. 2005. Pseudoapoptosis induced by brief activation of ATP-gated P2X7 receptors. *J Cell Biochem* 280: 33968-76.

278. Taylor, S. R. J., M. Gonzalez-Begne, S. Dewhurst, G. Chimini, C. F. Higgins, J. E. Melvin, and J. I. Elliott. 2008. Sequential shrinkage and swelling underlie P2X7-stimulated lymphocyte phosphatidylserine exposure and death. *J Immunol* 180: 300-8.

279. Lépine, S., H. Le Stunff, B. Lakatos, J. C. Sulpice, and F. Giraud. 2006. ATP-induced apoptosis of thymocytes is mediated by activation of P2 X 7 receptor and involves de novo ceramide synthesis and mitochondria. *Biochim Biophys Acta* 1761: 73-82.

280. Qu, Y., S. Misaghi, K. Newton, L. L. Gilmour, S. Louie, J. E. Cupp, G. R. Dubyak, D. Hackos, and V. M. Dixit. 2011. Pannexin-1 is required for ATP release during apoptosis but not for inflammasome activation. *J Immunol* 186: 6553-61.

281. Koch-Nolte, F., T. Duffy, M. Nissen, S. Kahl, N. Killeen, V. Ablamunits, F. Haag, and E. H. Leiter. 1999. A new monoclonal antibody detects a developmentally regulated mouse ecto-ADP-ribosyltransferase on T cells: subset distribution, inbred strain variation, and modulation upon T cell activation. *J Immunol* 163: 6014-22.

282. Bortell, R., T. Kanaitsuka, L. A. Stevens, J. Moss, J. P. Mordes, A. A. Rossini, and D. L. Greiner. 1999. The RT6 (Art2) family of ADP-ribosyltransferases in rat and mouse. *Mol Cell Biochem* 193: 61-8.

283. Kahl, S., M. Nissen, R. Girisch, T. Duffy, E. H. Leiter, F. Haag, and F. Koch-Nolte. 2000. Metalloprotease-mediated shedding of enzymatically active mouse ecto-ADP-ribosyltransferase ART2.2 upon T cell activation. *J Immunol* 165: 4463-9.

284. Scheuplein, F., N. Schwarz, S. Adriouch, C. Krebs, P. Bannas, B. Rissiek, M. Seman, F. Haag, and F. Koch-Nolte. 2009. NAD+ and ATP released from injured cells induce P2X7-dependent shedding of CD62L and externalization of phosphatidylserine by murine T cells. *J Immunol* 182: 2898-908.

285. Adriouch, S., P. Bannas, N. Schwarz, R. Fliegert, A. H. Guse, M. Seman, F. Haag, and F. Koch-Nolte. 2008. ADP-ribosylation at R125 gates the P2X7 ion channel by presenting a covalent ligand to its nucleotide binding site. *FASEB J* 22: 861-9.

286. Seman, M., S. Adriouch, F. Scheuplein, C. Krebs, D. Freese, G. Glowacki, P. Deterre, F. Haag, and F. Koch-Nolte. 2003. NAD-induced T cell death: ADP-ribosylation of cell surface proteins by ART2 activates the cytolytic P2X7 purinoceptor. *Immunity* 19: 571-82.

287. Ohlrogge, W., F. Haag, J. Löhler, M. Seman, D. R. Littman, N. Killeen, and F. Koch-Nolte. 2002. Generation and characterization of ecto-ADP-ribosyltransferase ART2.1/ART2.2-deficient mice. *Mol Cell Biol* 22: 7535-42.

288. Kawamura, H., F. Aswad, M. Minagawa, S. Govindarajan, and G. Dennert. 2006. P2X7 receptors regulate NKT cells in autoimmune hepatitis. *J Immunol* 176: 2152-60.

289. Kawamura, H., F. Aswad, M. Minagawa, K. Malone, H. Kaslow, F. Koch-Nolte, W. H. Schott, E. H. Leiter, and G. Dennert. 2005. P2X7 receptor-dependent and -independent T cell death is induced by nicotinamide adenine dinucleotide. *J Immunol* 174: 1971-9.

290. Scheuplein, F., B. Rissiek, J. P. Driver, Y. G. Chen, F. Koch-Nolte, and D. V. Serreze. 2010. A recombinant heavy chain antibody approach blocks ART2 mediated deletion of an iNKT cell population that upon activation inhibits autoimmune diabetes. *J Autoimmun* 34: 145-54.

291. Martinon, F., A. Mayor, and J. Tschopp. 2009. The inflammasomes: guardians of the body. *Annu Rev Immunol* 27: 229-65.

292. Davis, B. K., H. Wen, and J. P. Ting. 2011. The inflammasome NLRs in immunity, inflammation, and associated diseases. *Annu Rev Immunol* 29: 707-35.

293. Sluyter, R., J. G. Dalitz, and J. S. Wiley. 2004. P2X7 receptor polymorphism impairs extracellular adenosine 5'-triphosphate-induced interleukin-18 release from human monocytes. *Genes Immun* 5: 588-91.

294. Lee, K., H. Y. Won, M. A. Bae, J. H. Hong, and E. S. Hwang. 2011. Spontaneous and aging-dependent development of arthritis in NADPH oxidase 2 deficiency through altered differentiation of CD11b+ and Th/Treg cells. *Proc Natl Acad Sci U S A* 108: 9548-53.

295. Cooper, A. M. 2009. Cell-mediated immune responses in tuberculosis. *Annu Rev Immunol* 27: 393-422.

296. Hartman, M. L., and H. Kornfeld. 2011. Interactions between naïve and infected macrophages reduce Mycobacterium tuberculosis viability. *PloS one* 6: e27972.

297. Münz, C. 2009. Enhancing immunity through autophagy. *Annu Rev Immunol* 27: 423-49.

298. Lammas, D. A., C. Stober, C. J. Harvey, N. Kendrick, S. Panchalingam, and D. S. Kumararatne. 1997. ATP-induced killing of mycobacteria by human macrophages is mediated by purinergic P2Z(P2X7) receptors. *Immunity* 7: 433-44.

299. Zaborina, O., X. Li, G. Cheng, V. Kapatral, and A. M. Chakrabarty. 1999. Secretion of ATP-utilizing enzymes, nucleoside diphosphate kinase and ATPase, by Mycobacterium bovis BCG: sequestration of ATP from macrophage P2Z receptors? *Mol Microbiol* 31: 1333-43.

300. Kusner, D. J., and J. Adams. 2000. ATP-induced killing of virulent Mycobacterium tuberculosis within human macrophages requires phospholipase D. *J Immunol* 164: 379-88.

301. Sikora, A., J. Liu, C. Brosnan, G. Buell, I. Chessel, and B. R. Bloom. 1999. Cutting edge: purinergic signaling regulates radical-mediated bacterial killing mechanisms in macrophages through a P2X7-independent mechanism. *J Immunol* 163: 558-61.

302. Fairbairn, I. P., C. B. Stober, D. S. Kumararatne, and D. A. Lammas. 2001. ATP-mediated killing of intracellular mycobacteria by macrophages is a P2X(7)-dependent process inducing bacterial death by phagosome-lysosome fusion. *J Immunol* 167: 3300-7.

303. Biswas, D., O. S. Qureshi, W. Y. Lee, J. E. Croudace, M. Mura, and D. a Lammas. 2008. ATP-induced autophagy is associated with rapid killing of intracellular mycobacteria within human monocytes/macrophages. *BMC Immunol* 9: 35.

304. Petrovski, G., G. Ayna, G. Majai, J. Hodrea, S. Benko, A. Mádi, and L. Fésüs. 2011. Phagocytosis of cells dying through autophagy induces inflammasome activation and IL-1β release in human macrophages. *Autophagy* 7: 321-30.

305. Takenouchi, T., M. Nakai, Y. Iwamaru, S. Sugama, M. Tsukimoto, M. Fujita, J. Wei, A. Sekigawa, M. Sato, S. Kojima et al. 2009. The activation of P2X7 receptor impairs lysosomal functions and stimulates the release of autophagolysosomes in microglial cells. *J Immunol* 182: 2051-62.

306. Shemon, A. N., R. Sluyter, S. L. Fernando, A. L. Clarke, L. P. Dao-Ung, K. K. Skarratt, B. M. Saunders, K. S. Tan, B. J. Gu, S. J. Fuller et al. 2006. A Thr357 to Ser polymorphism in homozygous and compound heterozygous subjects causes absent or reduced P2X7 function and impairs ATP-induced mycobacterial killing by macrophages. *J Cell Biochem* 281: 2079-86.

307. Fernando, S. L., B. M. Saunders, R. Sluyter, K. K. Skarratt, J. S. Wiley, and W. J. Britton. 2005. Gene dosage determines the negative effects of polymorphic alleles of the P2X7 receptor on adenosine triphosphate-mediated killing of mycobacteria by human macrophages. *J Infect Dis* 192: 149-55.

308. Saunders, B. M., S. L. Fernando, R. Sluyter, W. J. Britton, and J. S. Wiley. 2003. A loss-of-function polymorphism in the human P2X7 receptor abolishes ATP-mediated killing of mycobacteria. *J Immunol* 171: 5442-6.

309. Wiley, J. S., and G. R. Dubyak. 1989. Extracellular adenosine triphosphate increases cation permeability of chronic lymphocytic leukemic lymphocytes. *Blood* 73: 1316-23.

310. Zetterberg, E., and J. Richter. 1993. Correlation between serum level of soluble L-selectin and leukocyte count in chronic myeloid and lymphocytic leukemia and during bone marrow transplantation. *Eur J Haematol* 51: 113-9.

311. Labasi, J. M., N. Petrushova, C. Donovan, S. McCurdy, P. Lira, M. M. Payette, W. Brissette, J. R. Wicks, L. Audoly, and C. A. Gabel. 2002. Absence of the P2X7 receptor alters leukocyte function and attenuates an inflammatory response. *J Immunol* 168: 6436-45.

312. Sluyter, R., and J. S. Wiley. 2002. Extracellular adenosine 5'-triphosphate induces a loss of CD23 from human dendritic cells via activation of P2X7 receptors. *Int Immunol* 14: 1415-21.

313. Moon, H., H. Y. Na, K. H. Chong, and T. J. Kim. 2006. P2X7 receptor-dependent ATP-induced shedding of CD27 in mouse lymphocytes. *Immunol Lett* 102: 98-105.

314. Gu, B. J., and J. S. Wiley. 2006. Rapid ATP-induced release of matrix metalloproteinase 9 is mediated by the P2X7 receptor. *Blood* 107: 4946-53.

315. Agresti, C., M. E. Meomartini, S. Amadio, E. Ambrosini, C. Volonté, F. Aloisi, and S. Visentin. 2005. ATP regulates oligodendrocyte progenitor migration, proliferation, and differentiation: involvement of metabotropic P2 receptors. *Brain Res Brain Res Rev* 48: 157-65.

316. Agresti, C., M. E. Meomartini, S. Amadio, E. Ambrosini, B. Serafini, L. Franchini, C. Volonté, F. Aloisi, and S. Visentin. 2005. Metabotropic P2 receptor activation regulates oligodendrocyte progenitor migration and development. *Glia* 50: 132-44.

317. Haynes, S. E., G. Hollopeter, G. Yang, D. Kurpius, M. E. Dailey, W. B. Gan, and D. Julius. 2006. The P2Y12 receptor regulates microglial activation by extracellular nucleotides. *Nat Neurosci* 9: 1512-9.

318. De Simone, R., C. E. Niturad, C. De Nuccio, M. A. Ajmone-Cat, S. Visentin, and L. Minghetti. 2010. TGF-β and LPS modulate ADP-induced migration of microglial cells through P2Y1 and P2Y12 receptor expression. *J Neurochem* 115: 450-9.

319. Choi, M. S., K. S. Cho, S. M. Shin, H. M. Ko, K. J. Kwon, C. Y. Shin, and K. H. Ko. 2010. ATP induced microglial cell migration through non-transcriptional activation of matrix metalloproteinase-9. *Arch Pharm Res* 33: 257-65.

320. Irino, Y., Y. Nakamura, K. Inoue, S. Kohsaka, and K. Ohsawa. 2008. Akt activation is involved in P2Y12 receptor-mediated chemotaxis of microglia. *J Neurosci Res* 86: 1511-9.

321. Ohsawa, K., Y. Irino, Y. Nakamura, C. Akazawa, and K. Inoue. 2007. Involvement of P2X 4 and P2Y 12 Receptors in ATP-Induced Microglial Chemotaxis. *Glia* 616: 604-616.

322. Klepeis, V. E., I. Weinger, E. Kaczmarek, and V. Trinkaus-Randall. 2004. P2Y receptors play a critical role in epithelial cell communication and migration. *J Cell Biochem* 93: 1115-33.

323. Glass, R., A. Loesch, P. Bodin, and G. Burnstock. 2002. P2X4 and P2X6 receptors associate with VE-cadherin in human endothelial cells. *Cell Mol Life Sci* 59: 870-81.

324. Kaufmann, A., B. Musset, S. H. Limberg, V. Renigunta, R. Sus, A. H. Dalpke, K. M. Heeg, B. Robaye, and P. J. Hanley. 2005. “Host tissue damage” signal ATP promotes non-directional migration and negatively regulates toll-like receptor signaling in human monocytes. *J Cell Biochem* 280: 32459-67.

325. Kukulski, F., F. Ben Yebdri, J. Lecka, G. Kauffenstein, S. A. Lévesque, M. Martín-Satué, and J. Sévigny. 2009. Extracellular ATP and P2 receptors are required for IL-8 to induce neutrophil migration. *Cytokine* 46: 166-70.

326. Chen, Y., R. Corriden, Y. Inoue, L. Yip, N. Hashiguchi, A. Zinkernagel, V. Nizet, P. A. Insel, and W. G. Junger. 2006. ATP release guides neutrophil chemotaxis via P2Y2 and A3 receptors. *Science* 314: 1792-5.

327. Färber, K., S. Markworth, U. Pannasch, C. Nolte, V. Prinz, G. Kronenberg, K. Gertz, M. Endres, I. Bechmann, K. Enjyoji, et al. 2008. The ectonucleotidase cd39/ENTPDase1 modulates purinergic-mediated microglial migration. *Glia* 56: 331-41.

328. Corriden, R., Y. Chen, Y. Inoue, G. Beldi, S. C. Robson, P. A. Insel, and W. G. Junger. 2008. Ecto-nucleoside triphosphate diphosphohydrolase 1 (E-NTPDase1/CD39) regulates neutrophil chemotaxis by hydrolyzing released ATP to adenosine. *J Cell Biochem* 283: 28480-6.

329. Hyman, M. C., D. Petrovic-Djergovic, S. H. Visovatti, H. Liao, S. Yanamadala, D. Bouïs, E. J. Su, D. A. Lawrence, M. J. Broekman, A. J. Marcus, et al. 2009. Self-regulation of inflammatory cell trafficking in mice by the leukocyte surface apyrase CD39. *J Clin Invest* 119: 1136-49.

330. Kim, M., L. H. Jiang, H. L. Wilson, R. A. North, and A. Surprenant. 2001. Proteomic and functional evidence for a P2X7 receptor signalling complex. *EMBO J* 20: 6347-58.

331. Dichmann, S., M. Idzko, U. Zimpfer, C. Hofmann, D. Ferrari, W. Luttmann, C. Virchow, F. Di Virgilio, and J. Norgauer. 2000. Adenosine triphosphate-induced oxygen radical production and CD11b up-regulation: Ca(++) mobilization and actin reorganization in human eosinophils. *Blood* 95: 973-8.

332. Henríquez, M., R. Herrera-Molina, A. Valdivia, A. Alvarez, M. Kong, N. Muñoz, V. Eisner, E. Jaimovich, P. Schneider, A. F. G. Quest, et al. 2011. ATP release due to Thy-1-integrin binding induces P2X7-mediated calcium entry required for focal adhesion formation. *J Cell Sci* 124: 1581-8.

333. Daniel, C., K. Wennhold, H. J. Kim, and H. von Boehmer. 2010. Enhancement of antigen-specific Treg vaccination in vivo. *Proc Natl Acad Sci U S A* 107: 16246-16251.

334. Jacques-Silva, M. C., R. Rodnight, G. Lenz, Z. Liao, Q. Kong, M. Tran, Y. Kang, F. A. Gonzalez, G. A. Weisman, and J. T. Neary. 2004. P2X7 receptors stimulate AKT phosphorylation in astrocytes. *Br J Pharmacol* 141: 1106-17.

335. Barbieri, R., S. Alloisio, S. Ferroni, and M. Nobile. 2008. Differential crosstalk between P2X7 and arachidonic acid in activation of mitogen-activated protein kinases. *Neurochem Int* 53: 255-62.

336. Gendron, F. P., J. T. Neary, P. M. Theiss, G. Y. Sun, F. A. Gonzalez, and G. A. Weisman. 2003. Mechanisms of P2X7 receptor-mediated ERK1/2 phosphorylation in human astrocytoma cells. *Am J Physiol Cell Physiol* 284: C571-81.

337. Panenka, W., H. Jijon, L. M. Herx, J. N. Armstrong, D. Feighan, T. Wei, V. W. Yong, R. M. Ransohoff, and B. A. MacVicar. 2001. P2X7-like receptor activation in astrocytes increases chemokine monocyte chemoattractant protein-1 expression via mitogen-activated protein kinase. *J Neurosci* 21: 7135-42.

338. Lev, S., H. Moreno, R. Martinez, P. Canoll, E. Peles, J. M. Musacchio, G. D. Plowman, B. Rudy, and J. Schlessinger. 1995. Protein tyrosine kinase PYK2 involved in Ca(2+)-induced regulation of ion channel and MAP kinase functions. *Nature* 376: 737-45.

339. Grol, M. W., N. Panupinthu, J. Korcok, S. M. Sims, and S. J. Dixon. 2009. Expression, signaling, and function of P2X7 receptors in bone. *Purinergic Signal* 5: 205-21.

340. Armstrong, S., A. Pereverzev, S. J. Dixon, and S. M. Sims. 2009. Activation of P2X7 receptors causes isoform-specific translocation of protein kinase C in osteoclasts. *J Cell Sci* 122: 136-44.

341. Korcok, J., L. N. Raimundo, H. Z. Ke, S. M. Sims, and S. J. Dixon. 2004. Extracellular nucleotides act through P2X7 receptors to activate NF-kappaB in osteoclasts. *J Bone Miner Res* 19: 642-51.

342. Thompson, B. A. N., M. P. Storm, J. Hewinson, S. Hogg, M. J. Welham, and A. B. MacKenzie. 2011. A novel role for P2X7 receptor signalling in the survival of Mouse embryonic stem cells. *Cell Signal* 24: 770-8.

343. Heo, J. S., and H. J. Han. 2006. ATP stimulates mouse embryonic stem cell proliferation via protein kinase C, phosphatidylinositol 3-kinase/Akt, and mitogen-activated protein kinase signaling pathways. *Stem Cells* 24: 2637-48.

344. Sim, J. A., M. T. Young, H. Y. Sung, R. A. North, and A. Surprenant. 2004. Reanalysis of P2X7 receptor expression in rodent brain. *J Neurosci* 24: 6307-14.

345. Solle, M., J. Labasi, D. G. Perregaux, E. Stam, N. Petrushova, B. H. Koller, R. J. Griffiths, and C. A. Gabel. 2001. Altered cytokine production in mice lacking P2X(7) receptors. *J Cell Biochem* 276: 125-32.

346. Le Feuvre, R. A., D. Brough, Y. Iwakura, K. Takeda, and N. J. Rothwell. 2002. Priming of macrophages with lipopolysaccharide potentiates P2X7-mediated cell death via a caspase-1-dependent mechanism, independently of cytokine production. *J Cell Biochem* 277: 3210-8.

347. Witting, A., L. Chen, E. Cudaback, A. Straiker, L. Walter, B. Rickman, T. Mo, C. Brosnan, N. Stella, and T. Möller. 2006. Experimental autoimmune encephalomyelitis disrupts endocannabinoid-mediated neuroprotection. *Proc Natl Acad Sci U S A* 103: 6362-7.

348. Chen, L., and C. F. Brosnan. 2006. Exacerbation of experimental autoimmune encephalomyelitis in P2X7R-/- mice: evidence for loss of apoptotic activity in lymphocytes. *J Immunol* 176: 3115-26.

349. Sharp, A. J., P. E. Polak, V. Simonini, S. X. Lin, J. C. Richardson, E. R. Bongarzone, and D. L. Feinstein. 2008. P2x7 deficiency suppresses development of experimental autoimmune encephalomyelitis. *J Neuroinflammation* 5: 33.

350. Grygorowicz, T., D. Sulejczak, and L. Struzynska. 2011. Expression of purinergic P2X7 receptor in rat brain during the symptomatic phase of experimental autoimmune encephalomyelitis and after recovery of neurological deficits. *Acta Neurobiol Exp (Wars)* 71: 65-73.

351. Gandelman, M., H. Peluffo, J. S. Beckman, P. Cassina, and L. Barbeito. 2010. Extracellular ATP and the P2X7 receptor in astrocyte-mediated motor neuron death: implications for amyotrophic lateral sclerosis. *J Neuroinflammation* 7: 33.

352. King, B. F. 2007. Novel P2X7 receptor antagonists ease the pain. *Br J Pharmacol* 151: 565-7.

353. Donnelly-Roberts, D. L., and M. F. Jarvis. 2007. Discovery of P2X7 receptor-selective antagonists offers new insights into P2X7 receptor function and indicates a role in chronic pain states. *Br J Pharmacol* 151: 571-9.

354. Broom, D. C., D. J. Matson, E. Bradshaw, M. E. Buck, R. Meade, S. Coombs, M. Matchett, K. K. Ford, W. Yu, J. Yuan, et al. 2008. Characterization of N-(adamantan-1-ylmethyl)-5-[(3R-amino-pyrrolidin-1-yl)methyl]-2-chloro-benzamide, a P2X7 antagonist in animal models of pain and inflammation. *J Pharmacol Exp Ther* 327: 620-33.

355. Tsuda, M., H. Tozaki-Saitoh, and K. Inoue. 2010. Pain and purinergic signaling. *Brain Res Brain Res Rev* 63: 222-32.

356. Wang, X., G. Arcuino, T. Takano, J. Lin, W. G. Peng, P. Wan, P. Li, Q. Xu, Q. S. Liu, S. A. Goldman, et al. 2004. P2X7 receptor inhibition improves recovery after spinal cord injury. *Nat Med* 10: 821-7.

357. Carroll, W. A., D. Donnelly-Roberts, and M. F. Jarvis. 2009. Selective P2X(7) receptor antagonists for chronic inflammation and pain. *Purinergic Signal* 5: 63-73.

358. Ke, H. Z., H. Qi, A. F. Weidema, Q. Zhang, N. Panupinthu, D. T. Crawford, W. A. Grasser, V. M. Paralkar, M. Li, L. P. Audoly, et al. 2003. Deletion of the P2X7 nucleotide receptor reveals its regulatory roles in bone formation and resorption. *Mol Endocrinol* 17: 1356-67.

359. Lucae, S., D. Salyakina, N. Barden, M. Harvey, B. Gagné, M. Labbé, E. B. Binder, M. Uhr, M. Paez-Pereda, I. Sillaber, et al. 2006. P2RX7, a gene coding for a purinergic ligand-gated ion channel, is associated with major depressive disorder. *Human molecular genetics* 15: 2438-45.

360. Li, C. M., S. J. Campbell, D. S. Kumararatne, R. Bellamy, C. Ruwende, K. P. W. J. McAdam, A. V. S. Hill, and D. A. Lammas. 2002. Association of a polymorphism in the P2X7 gene with tuberculosis in a Gambian population. *J Infect Dis* 186: 1458-62.

361. Dhulipala, P. D., Y. X. Wang, and M. I. Kotlikoff. 1998. The human P2X4 receptor gene is alternatively spliced. *Gene* 207: 259-66.

362. Carpenter, D., H. J. Meadows, S. Brough, G. Chapman, C. Clarke, M. Coldwell, R. Davis, D. Harrison, J. Meakin, M. McHale, et al. 1999. Site-specific splice variation of the human P2X4 receptor. *Neurosci Lett* 273: 183-6.

363. Cheewatrakoolpong, B., H. Gilchrest, J. C. Anthes, and S. Greenfeder. 2005. Identification and characterization of splice variants of the human P2X7 ATP channel. *Biochem Biophys Res Commun* 332: 17-27.

364. Mankus, C., C. Rich, M. Minns, and V. Trinkaus-Randall. 2011. Corneal epithelium expresses a variant of P2X(7) receptor in health and disease. *PloS one* 6: e28541.

365. Taylor, S. R. J., M. Gonzalez-Begne, D. K. Sojka, J. C. Richardson, S. A. Sheardown, S. M. Harrison, C. D. Pusey, F. W. K. Tam, and J. I. Elliott. 2009. Lymphocytes from P2X7-deficient mice exhibit enhanced P2X7 responses. *J Leukoc Biol* 85: 978-86.

366. Nicke, A., Y. H. Kuan, M. Masin, J. Rettinger, B. Marquez-Klaka, O. Bender, D. C. Górecki, R. D. Murrell-Lagnado, and F. Soto. 2009. A functional P2X7 splice variant with an alternative transmembrane domain 1 escapes gene inactivation in P2X7 knock-out mice. *J Cell Biochem* 284: 25813-22.

367. Masin, M., C. Young, K. Lim, S. J. Barnes, X. J. Xu, V. Marschall, W. Brutkowski, E. R. Mooney, D. C. Gorecki, and R. Murrell-Lagnado. 2012. Expression, assembly and function of novel C-terminal truncated variants of the mouse P2X7 receptor: re-evaluation of P2X7 knockouts. *Br J Pharmacol* 165: 978-93.

368. Feng, Y. H., X. Li, L. Wang, L. Zhou, and G. I. Gorodeski. 2006. A truncated P2X7 receptor variant (P2X7-j) endogenously expressed in cervical cancer cells antagonizes the full-length P2X7 receptor through hetero-oligomerization. *J Cell Biochem* 281: 17228-37.

369. Ghosh, S., A. Preet, J. E. Groopman, and R. K. Ganju. 2006. Cannabinoid receptor CB2 modulates the CXCL12/CXCR4-mediated chemotaxis of T lymphocytes. *Mol Immunol* 43: 2169-79.

370. Harris, S. J., R. V. Parry, J. G. Foster, M. D. Blunt, A. Wang, F. Marelli-Berg, J. Westwick, and S. G. Ward. 2011. Evidence that the lipid phosphatase SHIP-1 regulates T lymphocyte morphology and motility. *J Immunol* 186: 4936-45.

371. Hodgkin, A. L., A. F. Huxley, and B. Katz. 1952. Measurement of current-voltage relations in the membrane of the giant axon of Loligo. *J Physiol* 116: 424-48.

372. Neher, E., B. Sakmann, and J. H. Steinbach. 1978. The extracellular patch clamp: a method for resolving currents through individual open channels in biological membranes. *Pflugers Arch* 375: 219-28.

373. Gillis, S., and J. Watson. 1980. Biochemical and biological characterization of lymphocyte regulatory molecules. V. Identification of an interleukin 2-producing human leukemia T cell line. *J Exp Med* 152: 1709-19.

374. Smith, K. A. 1988. Interleukin-2: inception, impact, and implications. *Science* 240: 1169-76.

375. Imboden, J. B., A. Weiss, and J. D. Stobo. 1985. The antigen receptor on a human T cell line initiates activation by increasing cytoplasmic free calcium. *J Immunol* 134: 663-5.

376. Imboden, J. B., and G. Pattison. 1987. Regulation of inositol 1,4,5-trisphosphate kinase activity after stimulation of human T cell antigen receptor. *J Clin Invest* 79: 1538-41.

377. Astoul, E., C. Edmunds, D. A. Cantrell, and S. G. Ward. 2001. PI 3-K and T-cell activation: limitations of T-leukemic cell lines as signaling models. *Trends Immunol* 22: 490-6.

378. Abe, T., M. Ohno, T. Sato, M. Murakami, M. Kajiki, and R. Kodaira. 1991. “Differentiation Induction” culture of human leukemic myeloid cells stimulates high production of macrophage differentiation inducing factor. *Cytotechnology* 5: 75-93.

379. Fenton, M. J., M. W. Vermeulen, B. D. Clark, A. C. Webb, and P. E. Auron. 1988. Human pro-IL-1 beta gene expression in monocytic cells is regulated by two distinct pathways. *J Immunol* 140: 2267-73.

380. Humphreys, B. D., and G. R. Dubyak. 1998. Modulation of P2X7 nucleotide receptor expression by pro- and anti-inflammatory stimuli in THP-1 monocytes. *J Leukoc Biol* 64: 265-73.

381. Humphreys, B. D., and G. R. Dubyak. 1996. Induction of the P2z/P2X7 nucleotide receptor and associated phospholipase D activity by lipopolysaccharide and IFN-gamma in the human THP-1 monocytic cell line. *J Immunol* 157: 5627-37.

382. Newbolt, A., R. Stoop, C. Virginio, a Surprenant, R. A. North, G. Buell, and F. Rassendren. 1998. Membrane topology of an ATP-gated ion channel (P2X receptor). *J Cell Biochem* 273: 15177-82.

383. Gonnord, P., C. Delarasse, R. Auger, K. Benihoud, M. Prigent, M. H. Cuif, C. Lamaze, and J. M. Kanellopoulos. 2009. Palmitoylation of the P2X7 receptor, an ATP-gated channel, controls its expression and association with lipid rafts. *FASEB J* 23: 795-805.

384. Sun, C., J. Chu, S. Singh, and R. D. Salter. 2010. Identification and characterization of a novel variant of the human P2X(7) receptor resulting in gain of function. *Purinergic Signal* 6: 31-45.

385. J. M. Lackie. 2007. *Dictionary of Cell and Molecular Biology*,. Plumbland Consulting Ltd., Cumbria, U.K. :261.

386. Egerton, M., R. Scollay, and K. Shortman. 1990. Kinetics of mature T-cell development in the thymus. *Proc Natl Acad Sci U S A* 87: 2579-82.

387. Smith, C. A., G. T. Williams, R. Kingston, E. J. Jenkinson, and J. J. Owen. 1989. Antibodies to CD3/T-cell receptor complex induce death by apoptosis in immature T cells in thymic cultures. *Nature* 337: 181-4.

388. McConkey, D. J., P. Hartzell, J. F. Amador-Pérez, S. Orrenius, and M. Jondal. 1989. Calcium-dependent killing of immature thymocytes by stimulation via the CD3/T cell receptor complex. *J Immunol* 143: 1801-6.

389. Marsden, V. S., and A. Strasser. 2003. Control of apoptosis in the immune system: Bcl-2, BH3-only proteins and more. *Annu Rev Immunol* 21: 71-105.

390. Akbar, A. N., J. Savill, W. Gombert, M. Bofill, N. J. Borthwick, F. Whitelaw, J. Grundy, G. Janossy, and M. Salmon. 1994. The specific recognition by macrophages of CD8+,CD45RO+ T cells undergoing apoptosis: a mechanism for T cell clearance during resolution of viral infections. *J Exp Med* 180: 1943-7.

391. Bulanova, E., V. Budagian, Z. Orinska, F. Koch-Nolte, F. Haag, and S. Bulfone-Paus. 2009. ATP induces P2X7 receptor-independent cytokine and chemokine expression through P2X1 and P2X3 receptors in murine mast cells. *J Leukoc Biol* 85: 692-702.

392. Haag, F., S. Adriouch, A. Braß, C. Jung, S. Möller, F. Scheuplein, P. Bannas, M. Seman, and F. Koch-Nolte. 2007. Extracellular NAD and ATP: Partners in immune cell modulation. *Purinergic Signal* 3: 71-81.

393. Strasser, A., L. O'Connor, and V. M. Dixit. 2000. Apoptosis signaling. *Annu Rev Biochem* 69: 217-45.

394. Leventis, P. A., and S. Grinstein. 2010. The distribution and function of phosphatidylserine in cellular membranes. *Annu Rev Biophys* 39: 407-27.

395. Elliott, J. I., A. Surprenant, F. M. Marelli-Berg, J. C. Cooper, R. L. Cassady-Cain, C. Wooding, K. Linton, D. R. Alexander, and C. F. Higgins. 2005. Membrane phosphatidylserine distribution as a non-apoptotic signalling mechanism in lymphocytes. *Nat Cell Biol* 7: 808-16.

396. Courageot, M. P., S. Lépine, M. Hours, F. Giraud, and J. C. Sulpice. 2004. Involvement of sodium in early phosphatidylserine exposure and phospholipid scrambling induced by P2X7 purinoceptor activation in thymocytes. *J Cell Biochem* 279: 21815-23.

397. Jurisić, V., I. Spuzić, and G. Konjević. 1999. A comparison of the NK cell cytotoxicity with effects of TNF-alpha against K-562 cells, determined by LDH release assay. *Cancer Lett* 138: 67-72.

398. Nicke, A. 2008. Homotrimeric complexes are the dominant assembly state of native P2X7 subunits. *Biochem Biophys Res Commun* 377: 803-8.

399. Sorge, R. E., T. Trang, R. Dorfman, S. B. Smith, S. Beggs, J. Ritchie, J. S. Austin, D. V. Zaykin, H. V. Meulen, M. Costigan, et al. 2012. Genetically determined P2X7 receptor pore formation regulates variability in chronic pain sensitivity. *Nat Med* 18: 595-599.

400. Hibell, A. D., E. J. Kidd, I. P. Chessell, P. P. Humphrey, and A. D. Michel. 2000. Apparent species differences in the kinetic properties of P2X(7) receptors. *Br J Pharmacol* 130: 167-73.

401. Klapperstück, M., C. Büttner, T. Böhm, G. Schmalzing, and F. Markwardt. 2000. Characteristics of P2X7 receptors from human B lymphocytes expressed in Xenopus oocytes. *Biochim Biophys Acta* 1467: 444-56.

402. Freedman, B. D., Q. H. Liu, G. Gaulton, M. I. Kotlikoff, J. Hescheler, and B. K. Fleischmann. 1999. ATP-evoked Ca2+ transients and currents in murine thymocytes: possible role for P2X receptors in death by neglect. *Eur J Immunol* 29: 1635-46.

403. Kawate, T., J. L. Robertson, M. Li, S. D. Silberberg, and K. J. Swartz. 2011. Ion access pathway to the transmembrane pore in P2X receptor channels. *J Gen Physiol* 137: 579-90.

404. Virginio, C., A. MacKenzie, F. A. Rassendren, R. A. North, and A. Surprenant. 1999. Pore dilation of neuronal P2X receptor channels. *Nat Neurosci* 2: 315-21.

405. Nörenberg, W., H. Sobottka, C. Hempel, T. Plötz, W. Fischer, G. Schmalzing, and M. Schaefer. 2012. Positive allosteric modulation by ivermectin of human but not murine P2X7 receptors. *Br J Pharmacol* .

406. Kawano, A., M. Tsukimoto, T. Noguchi, N. Hotta, H. Harada, T. Takenouchi, H. Kitani, and S. Kojima. 2012. Involvement of P2X4 receptor in P2X7 receptor-

dependent cell death of mouse macrophages. *Biochem Biophys Res Commun* 419: 374-80.

407. Kawano, A., M. Tsukimoto, D. Mori, T. Noguchi, H. Harada, T. Takenouchi, H. Kitani, and S. Kojima. 2012. Regulation of P2X7-dependent inflammatory functions by P2X4 receptor in mouse macrophages. *Biochem Biophys Res Commun* 420: 102-7.

408. Seil, M., M. El Ouaaliti, U. Fontanils, I. G. Etxebarria, S. Pochet, G. Dal Moro, A. Marino, and J. P. Dehaye. 2010. Ivermectin-dependent release of IL-1beta in response to ATP by peritoneal macrophages from P2X(7)-KO mice. *Purinergic Signal* 6: 405-16.

409. Di Virgilio, F., P. Chiozzi, D. Ferrari, S. Falzoni, J. M. Sanz, A. Morelli, M. Torboli, G. Bolognesi, and O. R. Baricordi. 2001. Nucleotide receptors: an emerging family of regulatory molecules in blood cells. *Blood* 97: 587-600.

410. Tedder, T. F., A. C. Penta, H. B. Levine, and A. S. Freedman. 1990. Expression of the human leukocyte adhesion molecule, LAM1. Identity with the TQ1 and Leu-8 differentiation antigens. *J Immunol* 144: 532-40.

411. Portales-Cervantes, L., P. Niño-Moreno, L. Doníz-Padilla, L. Baranda-Candido, M. García-Hernández, M. Salgado-Bustamante, R. González-Amaro, and D. Portales-Pérez. 2010. Expression and function of the P2X(7) purinergic receptor in patients with systemic lupus erythematosus and rheumatoid arthritis. *Hum Immunol* 71: 818-25.

412. Schwarz, E. C., C. Kummerow, A. S. Wenning, K. Wagner, A. Sappok, K. Waggershauser, D. Griesemer, B. Strauss, M. J. Wolfs, A. Quintana, et al. 2007. Calcium dependence of T cell proliferation following focal stimulation. *Eur J Immunol* 37: 2723-33.

413. Rabie, T., A. Strehl, A. Ludwig, and B. Nieswandt. 2005. Evidence for a role of ADAM17 (TACE) in the regulation of platelet glycoprotein V. *J Cell Biochem* 280: 14462-8.

414. Kong, D., and T. Yamori. 2007. ZSTK474 is an ATP-competitive inhibitor of class I phosphatidylinositol 3 kinase isoforms. *Cancer Sci* 98: 1638-42.

415. Alessi, D. R., A. Cuenda, P. Cohen, D. T. Dudley, and A. R. Saltiel. 1995. PD 098059 is a specific inhibitor of the activation of mitogen-activated protein kinase kinase in vitro and in vivo. *J Cell Biochem* 270: 27489-94.

416. Martiny-Baron, G., M. G. Kazanietz, H. Mischak, P. M. Blumberg, G. Kochs, H. Hug, D. Marmé, and C. Schächtele. 1993. Selective inhibition of protein kinase C isozymes by the indolocarbazole Gö 6976. *J Cell Biochem* 268: 9194-7.

417. Gschwendt, M., H. J. Müller, K. Kielbassa, R. Zang, W. Kittstein, G. Rincke, and F. Marks. 1994. Rottlerin, a novel protein kinase inhibitor. *Biochem Biophys Res Commun* 199: 93-8.

418. Soltoff, S. P. 2001. Rottlerin is a mitochondrial uncoupler that decreases cellular ATP levels and indirectly blocks protein kinase Cdelta tyrosine phosphorylation. *J Cell Biochem* 276: 37986-92.

419. Hanke, J. H., J. P. Gardner, R. L. Dow, P. S. Changelian, W. H. Brissette, E. J. Weringer, B. A. Pollok, and P. A. Connelly. 1996. Discovery of a novel, potent, and Src family-selective tyrosine kinase inhibitor. Study of Lck- and FynT-dependent T cell activation. *J Cell Biochem* 271: 695-701.

420. Thoreen, C. C., S. A. Kang, J. W. Chang, Q. Liu, J. Zhang, Y. Gao, L. J. Reichling, T. Sim, D. M. Sabatini, and N. S. Gray. 2009. An ATP-competitive mammalian target of rapamycin inhibitor reveals rapamycin-resistant functions of mTORC1. *J Cell Biochem* 284: 8023-32.

421. Wang, Y., A. H. Herrera, Y. Li, K. K. Belani, and B. Walcheck. 2009. Regulation of mature ADAM17 by redox agents for L-selectin shedding. *J Immunol* 182: 2449-57.

422. Myers, T. J., L. H. Brennaman, M. Stevenson, S. Higashiyama, W. E. Russell, D. C. Lee, and S. W. Sunnarborg. 2009. Mitochondrial reactive oxygen species mediate GPCR-induced TACE/ADAM17-dependent transforming growth factor-alpha shedding. *Mol Biol Cell* 20: 5236-49.

423. Elliott, J. I., J. H. McVey, and C. F. Higgins. 2005. The P2X7 receptor is a candidate product of murine and human lupus susceptibility loci: a hypothesis and comparison of murine allelic products. *Arthritis Res Ther* 7: R468-75.

424. Schultz, G. S., S. Strelow, G. A. Stern, N. Chegini, M. B. Grant, R. E. Galardy, D. Grobelny, J. J. Rowsey, K. Stonecipher, and V. Parmley. 1992. Treatment of alkali-injured rabbit corneas with a synthetic inhibitor of matrix metalloproteinases. *Invest Ophthalmol Vis Sci* 33: 3325-31.

425. Takedachi, M., D. Qu, Y. Ebisuno, H. Oohara, M. L. Joachims, S. T. McGee, E. Maeda, R. P. McEver, T. Tanaka, M. Miyasaka, et al. 2008. CD73-generated adenosine restricts lymphocyte migration into draining lymph nodes. *J Immunol* 180: 6288-96.

426. Chu, Y. X., Y. Zhang, Y. Q. Zhang, and Z. Q. Zhao. 2010. Involvement of microglial P2X7 receptors and downstream signaling pathways in long-term potentiation of spinal nociceptive responses. *Brain Behav Immun* 24: 1176-89.

427. Gavala, M. L., Z. A. Pfeiffer, and P. J. Bertics. 2008. The nucleotide receptor P2RX7 mediates ATP-induced CREB activation in human and murine monocytic cells. *J Leukoc Biol* 84: 1159-71.

428. Humphreys, B. D., J. Rice, S. B. Kertesy, and G. R. Dubyak. 2000. Stress-activated protein kinase/JNK activation and apoptotic induction by the macrophage P2X7 nucleotide receptor. *J Cell Biochem* 275: 26792-8.

429. Guo, J. P., D. Coppola, and J. Q. Cheng. 2011. IKBKE activates Akt independent of phosphatidylinositol 3-kinase/PDK1/mTORC2 and PH domain to sustain malignant transformation. *J Cell Biochem* 286: 37389-98.

430. Janas, M. L., G. Varano, K. Gudmundsson, M. Noda, T. Nagasawa, and M. Turner. 2010. Thymic development beyond beta-selection requires phosphatidylinositol 3-kinase activation by CXCR4. *J Exp Med* 207: 247-61.

431. Dong, Z. M., L. Jackson, and J. W. Murphy. 1999. Mechanisms for induction of L-selectin loss from T lymphocytes by a cryptococcal polysaccharide, glucuronoxylomannan. *Infect Immun* 67: 220-9.

432. Müller, N., J. van den Brandt, F. Odoardi, D. Tischner, J. Herath, A. Flügel, and H. M. Reichardt. 2008. A CD28 superagonistic antibody elicits 2 functionally distinct waves of T cell activation in rats. *J Clin Invest* 118: 1405-16.

433. Ndejembi, M. P., J. R. Teijaro, D. S. Patke, A. W. Bingaman, M. R. Chandok, A. Azimzadeh, S. G. Nadler, and D. L. Farber. 2006. Control of memory CD4 T cell recall by the CD28/B7 costimulatory pathway. *J Immunol* 177: 7698-706.

434. Mestas, J., and C. C. W. Hughes. 2004. Of mice and not men: differences between mouse and human immunology. *J Immunol* 172: 2731-8.

435. Leo, O., M. Foo, D. H. Sachs, L. E. Samelson, and J. A. Bluestone. 1987. Identification of a monoclonal antibody specific for a murine T3 polypeptide. *Proc Natl Acad Sci U S A* 84: 1374-8.

436. Arnett, K. L., S. C. Harrison, and D. C. Wiley. 2004. Crystal structure of a human CD3-epsilon/delta dimer in complex with a UCHT1 single-chain antibody fragment. *Proc Natl Acad Sci U S A* 101: 16268-73.

437. Wroblewski, M., and A. Hamann. 1997. CD45-mediated signals can trigger shedding of lymphocyte L-selectin. *Int Immunol* 9: 555-62.

438. Mazur, M. A., C. C. Davis, and P. Szabolcs. 2008. Ex vivo expansion and Th1/Tc1 maturation of umbilical cord blood T cells by CD3/CD28 costimulation. *Biol Blood Marrow Transplant* 14: 1190-6.

439. Rowlands, D. J., M. N. Islam, S. R. Das, A. Huertas, S. K. Quadri, K. Horiuchi, N. Inamdar, M. T. Emin, J. Lindert, V. S. Ten, et al. 2011. Activation of TNFR1 ectodomain shedding by mitochondrial Ca2+ determines the severity of inflammation in mouse lung microvessels. *J Clin Invest* 121: 1986-99.

440. Camden, J. M., A. M. Schrader, R. E. Camden, F. A. González, L. Erb, C. I. Seye, and G. A. Weisman. 2005. P2Y2 nucleotide receptors enhance alpha-secretase-dependent amyloid precursor protein processing. *J Cell Biochem* 280: 18696-702.

441. Mogami, H., C. Lloyd Mills, and D. V. Gallacher. 1997. Phospholipase C inhibitor, U73122, releases intracellular Ca2+, potentiates Ins(1,4,5)P3-mediated

Ca2+ release and directly activates ion channels in mouse pancreatic acinar cells. *Biochem J* 324 (Pt 2: 645-51.

442. Rizoli, S. B., O. D. Rotstein, and A. Kapus. 1999. Cell volume-dependent regulation of L-selectin shedding in neutrophils. A role for p38 mitogen-activated protein kinase. *J Cell Biochem* 274: 22072-80.

443. Raymond, M. N., and H. Le Stunff. 2006. Involvement of de novo ceramide biosynthesis in macrophage death induced by activation of ATP-sensitive P2X7 receptor. *FEBS Lett* 580: 131-6.

444. Walev, I., D. Tappe, E. Gulbins, and S. Bhakdi. 2000. Streptolysin O-permeabilized granulocytes shed L-selectin concomitantly with ceramide generation via neutral sphingomyelinase. *J Leukoc Biol* 68: 865-72.

445. Finkel, T. 1998. Oxygen radicals and signaling. *Curr Opin Cell Biol* 10: 248-53.

446. Finkel, T. 2011. Signal transduction by reactive oxygen species. *J Cell Biol* 194: 7-15.

447. Willems, S. H., C. J. Tape, P. L. Stanley, N. A. Taylor, I. G. Mills, D. E. Neal, J. McCafferty, and G. Murphy. 2010. Thiol isomerases negatively regulate the cellular shedding activity of ADAM17. *Biochem J* 428: 439-50.

448. Shin, M. H., Y. J. Moon, J. E. Seo, Y. Lee, K. H. Kim, and J. H. Chung. 2008. Reactive oxygen species produced by NADPH oxidase, xanthine oxidase, and mitochondrial electron transport system mediate heat shock-induced MMP-1 and MMP-9 expression. *Free Radic Biol Med* 44: 635-45.

449. Lu, S. P., M. H. Lin Feng, H. L. Huang, Y. C. Huang, W. I. Tsou, and M. Z. Lai. 2007. Reactive oxygen species promote raft formation in T lymphocytes. *Free Radic Biol Med* 42: 936-44.

450. Devadas, S., L. Zaritskaya, S. G. Rhee, L. Oberley, and M. S. Williams. 2002. Discrete generation of superoxide and hydrogen peroxide by T cell receptor stimulation: selective regulation of mitogen-activated protein kinase activation and fas ligand expression. *J Exp Med* 195: 59-70.

451. Parvathenani, L. K., S. Tertyshnikova, C. R. Greco, S. B. Roberts, B. Robertson, and R. Posmantur. 2003. P2X7 mediates superoxide production in primary microglia and is up-regulated in a transgenic mouse model of Alzheimer's disease. *J Cell Biochem* 278: 13309-17.

452. Jones, T. T., and G. J. Brewer. 2010. Age-related deficiencies in complex I endogenous substrate availability and reserve capacity of complex IV in cortical neuron electron transport. *Biochim Biophys Acta* 1797: 167-76.

453. Soltoff, S. P. 2007. Rottlerin: an inappropriate and ineffective inhibitor of PKCdelta. *Trends Pharmacol Sci* 28: 453-8.

454. Coddou, C., J. F. Codocedo, S. Li, J. G. Lillo, C. Acuña-Castillo, P. Bull, S. S. Stojilkovic, and J. P. Huidobro-Toro. 2009. Reactive oxygen species potentiate the P2X2 receptor activity through intracellular Cys430. *J Neurosci* 29: 12284-91.

455. Mason, H. S., S. Bourke, and P. J. Kemp. 2004. Selective modulation of ligand-gated P2X purinoceptor channels by acute hypoxia is mediated by reactive oxygen species. *Mol Pharmacol* 66: 1525-35.

456. Bogeski, I., C. Kummerow, D. Al-Ansary, E. C. Schwarz, R. Koehler, D. Kozai, N. Takahashi, C. Peinelt, D. Griesemer, M. Bozem, et al. 2010. Differential redox regulation of ORAI ion channels: a mechanism to tune cellular calcium signaling. *Sci Signal* 3: ra24.

457. Jackson, S. H., S. Devadas, J. Kwon, L. A. Pinto, and M. S. Williams. 2004. T cells express a phagocyte-type NADPH oxidase that is activated after T cell receptor stimulation. *Nat Immunol* 5: 818-27.

458. Tse, H. M., T. C. Thayer, C. Steele, C. M. Cuda, L. Morel, J. D. Piganelli, and C. E. Mathews. 2010. NADPH oxidase deficiency regulates Th lineage commitment and modulates autoimmunity. *J Immunol* 185: 5247-58.

459. Williams, M. S., and J. Kwon. 2004. T cell receptor stimulation, reactive oxygen species, and cell signaling. *Free Radic Biol Med* 37: 1144-51.

460. Campello, S., R. A. Lacalle, M. Bettella, S. Mañes, L. Scorrano, and A. Viola. 2006. Orchestration of lymphocyte chemotaxis by mitochondrial dynamics. *J Exp Med* 203: 2879-86.

461. Yi, J. S., B. C. Holbrook, R. D. Michalek, N. G. Laniewski, and J. M. Grayson. 2006. Electron transport complex I is required for CD8+ T cell function. *J Immunol* 177: 852-62.

462. Wang, J. F., T. R. Jerrells, and J. J. Spitzer. 1996. Bcl-2 protects against apoptosis induced by antimycin A and bongkrekic acid without restoring cellular ATP levels. *Free Radic Biol Med* 20: 533-42.

463. Bernier, L. P., A. R. Ase, S. Chevallier, D. Blais, Q. Zhao, E. Boué-Grabot, D. Logothetis, and P. Séguéla. 2008. Phosphoinositides regulate P2X4 ATP-gated channels through direct interactions. *J Neurosci* 28: 12938-45.

464. Zhao, Q., D. E. Logothetis, and P. Séguéla. 2007. Regulation of ATP-gated P2X receptors by phosphoinositides. *Pflugers Arch* 455: 181-5.

465. D'Arco, M., R. Giniatullin, V. Leone, P. Carloni, N. Birsa, A. Nair, A. Nistri, and E. Fabbretti. 2009. The C-terminal Src inhibitory kinase (Csk)-mediated tyrosine phosphorylation is a novel molecular mechanism to limit P2X3 receptor function in mouse sensory neurons. *J Cell Biochem* 284: 21393-401.

466. Allsopp, R. C., U. Lalo, and R. J. Evans. 2010. Lipid raft association and cholesterol sensitivity of P2X1-4 receptors for ATP: chimeras and point mutants

identify intracellular amino-terminal residues involved in lipid regulation of P2X1 receptors. *J Cell Biochem* 285: 32770-7.

467. Vial, C., C. Y. E. Fung, A. H. Goodall, M. P. Mahaut-Smith, and R. J. Evans. 2006. Differential sensitivity of human platelet P2X1 and P2Y1 receptors to disruption of lipid rafts. *Biochem Biophys Res Commun* 343: 415-9.

468. Vial, C., and R. J. Evans. 2005. Disruption of lipid rafts inhibits P2X1 receptor-mediated currents and arterial vasoconstriction. *J Cell Biochem* 280: 30705-11.

469. Vacca, F., S. Amadio, G. Sancesario, G. Bernardi, and C. Volonté. 2004. P2X3 receptor localizes into lipid rafts in neuronal cells. *J Neurosci Res* 76: 653-61.

470. Clark, K. L., A. Oelke, M. E. Johnson, K. D. Eilert, P. C. Simpson, and S. C. Todd. 2004. CD81 associates with 14-3-3 in a redox-regulated palmitoylation-dependent manner. *J Cell Biochem* 279: 19401-6.

471. Parat, M. O., R. Z. Stachowicz, and P. L. Fox. 2002. Oxidative stress inhibits caveolin-1 palmitoylation and trafficking in endothelial cells. *Biochem J* 361: 681-8.

472. De Leo, M. E., A. Tranghese, M. Passantino, A. Mordente, M. M. Lizzio, T. Galeotti, and A. Zoli. 2002. Manganese superoxide dismutase, glutathione peroxidase, and total radical trapping antioxidant capacity in active rheumatoid arthritis. *J Rheumatol* 29: 2245-6.

473. Remans, P. H. J., M. van Oosterhout, T. J. M. Smeets, M. Sanders, W. M. Frederiks, K. A. Reedquist, P. P. Tak, F. C. Breedveld, and J. M. van Laar. 2005. Intracellular free radical production in synovial T lymphocytes from patients with rheumatoid arthritis. *Arthritis Rheum* 52: 2003-9.

474. Lister, M. F., J. Sharkey, D. A. Sawatzky, J. P. Hodgkiss, D. J. Davidson, A. G. Rossi, and K. Finlayson. 2007. The role of the purinergic P2X7 receptor in inflammation. *J Inflamm (Lond)* 4: 5.

475. Gergely, P., B. Niland, N. Gonchoroff, R. Pullmann, P. E. Phillips, and A. Perl. 2002. Persistent mitochondrial hyperpolarization, increased reactive oxygen intermediate production, and cytoplasmic alkalinization characterize altered IL-10 signaling in patients with systemic lupus erythematosus. *J Immunol* 169: 1092-101.

476. Gergely, P., C. Grossman, B. Niland, F. Puskas, H. Neupane, F. Allam, K. Banki, P. E. Phillips, and A. Perl. 2002. Mitochondrial hyperpolarization and ATP depletion in patients with systemic lupus erythematosus. *Arthritis Rheum* 46: 175-90.

477. Russell, A. I., D. S. Cunninghame Graham, S. Chadha, C. Roberton, T. Fernandez-Hart, B. Griffiths, D. D'Cruz, D. Nitsch, J. C. Whittaker, and T. J. Vyse. 2005. No association between E- and L-selectin genes and SLE: soluble L-

selectin levels do correlate with genotype and a subset in SLE. *Genes Immun* 6: 422-9.

478. Perl, A. 2010. Pathogenic mechanisms in systemic lupus erythematosus. *Autoimmunity* 43: 1-6.

479. Shah, D., R. Kiran, A. Wanchu, and A. Bhatnagar. 2010. Oxidative stress in systemic lupus erythematosus: relationship to Th1 cytokine and disease activity. *Immunol Lett* 129: 7-12.

480. Martin, L. J., B. Gertz, Y. Pan, A. C. Price, J. D. Molkentin, and Q. Chang. 2009. The mitochondrial permeability transition pore in motor neurons: involvement in the pathobiology of ALS mice. *Exp Neurol* 218: 333-46.

481. Chiu, I. M., A. Chen, Y. Zheng, B. Kosaras, S. A. Tsiftsoglou, T. K. Vartanian, R. H. Brown, and M. C. Carroll. 2008. T lymphocytes potentiate endogenous neuroprotective inflammation in a mouse model of ALS. *Proc Natl Acad Sci U S A* 105: 17913-8.

482. McCombe, P. A., and R. D. Henderson. 2011. The Role of immune and inflammatory mechanisms in ALS. *Curr Mol Med* 11: 246-54.

483. Finkelstein, A., G. Kunis, A. Seksenyan, A. Ronen, T. Berkutzki, D. Azoulay, M. Koronyo-Hamaoui, and M. Schwartz. 2011. Abnormal Changes in NKT Cells, the IGF-1 Axis, and Liver Pathology in an Animal Model of ALS. *PloS one* 6: e22374.

484. Takeuchi, S., N. Fujiwara, A. Ido, M. Oono, Y. Takeuchi, M. Tateno, K. Suzuki, R. Takahashi, I. Tooyama, N. Taniguchi, et al. 2010. Induction of protective immunity by vaccination with wild-type apo superoxide dismutase 1 in mutant SOD1 transgenic mice. *Exp Neurol* 69: 1044-56.

485. Yiangou, Y., P. Facer, P. Durrenberger, I. P. Chessell, A. Naylor, C. Bountra, R. R. Banati, and P. Anand. 2006. COX-2, CB2 and P2X7-immunoreactivities are increased in activated microglial cells/macrophages of multiple sclerosis and amyotrophic lateral sclerosis spinal cord. *BMC neurology* 6: 12.

486. Minamimura, K., W. Gao, and T. Maki. 2006. CD4+ regulatory T cells are spared from deletion by antilymphocyte serum, a polyclonal anti-T cell antibody. *J Immunol* 176: 4125-32.

487. Siegmund, K., T. Zeis, G. Kunz, T. Rolink, N. Schaeren-Wiemers, and J. Pieters. 2011. Coronin 1-mediated naive T cell survival is essential for the development of autoimmune encephalomyelitis. *J Immunol* 186: 3452-61.

488. Haegert, D. G., J. D. Hackenbroch, D. Duszczyszyn, L. Fitz-Gerald, E. Zastepa, H. Mason, Y. Lapierre, J. Antel, and A. Bar-Or. 2011. Reduced thymic output and peripheral naïve CD4 T-cell alterations in primary progressive multiple sclerosis (PPMS). *J Neuroimmunol* 233: 233-9.

489. Chekeni, F. B., M. R. Elliott, J. K. Sandilos, S. F. Walk, J. M. Kinchen, E. R. Lazarowski, A. J. Armstrong, S. Penuela, D. W. Laird, G. S. Salvesen, et al. 2010. Pannexin 1 channels mediate “find-me” signal release and membrane permeability during apoptosis. *Nature* 467: 863-7.

490. Elliott, M. R., F. B. Chekeni, P. C. Trampont, E. R. Lazarowski, A. Kadl, S. F. Walk, D. Park, R. I. Woodson, M. Ostankovich, P. Sharma, et al. 2009. Nucleotides released by apoptotic cells act as a find-me signal to promote phagocytic clearance. *Nature* 461: 282-6.

491. Haynes, S. E., G. Hollopeter, G. Yang, D. Kurpius, M. E. Dailey, W. B. Gan, and D. Julius. 2006. The P2Y12 receptor regulates microglial activation by extracellular nucleotides. *Nat Neurosci* 9: 1512-9.

492. Heasman, S. J., K. M. Giles, A. G. Rossi, J. E. Allen, C. Haslett, and I. Dransfield. 2004. Interferon gamma suppresses glucocorticoid augmentation of macrophage clearance of apoptotic cells. *Eur J Immunol* 34: 1752-61.

493. Michlewska, S., I. Dransfield, I. L. Megson, and A. G. Rossi. 2009. Macrophage phagocytosis of apoptotic neutrophils is critically regulated by the opposing actions of pro-inflammatory and anti-inflammatory agents: key role for TNF-alpha. *FASEB J* 23: 844-54.

494. Gordesky, S. E., and G. V. Marinetti. 1973. The asymetric arrangement of phospholipids in the human erythrocyte membrane. *Biochem Biophys Res Commun* 50: 1027-31.

495. Li, W. 2012. Eat-me signals: keys to molecular phagocyte biology and “appetite” control. *J Cell Physiol* 227: 1291-7.

496. Fadok, V. A., D. R. Voelker, P. A. Campbell, J. J. Cohen, D. L. Bratton, and P. M. Henson. 1992. Exposure of phosphatidylserine on the surface of apoptotic lymphocytes triggers specific recognition and removal by macrophages. *J Immunol* 148: 2207-16.

497. Miyanishi, M., K. Tada, M. Koike, Y. Uchiyama, T. Kitamura, and S. Nagata. 2007. Identification of Tim4 as a phosphatidylserine receptor. *Nature* 450: 435-9.

498. Takeda, S. 2009. Three-dimensional domain architecture of the ADAM family proteinases. *Semin Cell Dev Biol* 20: 146-52.

8. Appendix

8.1. Expression of cell surface markers on freshly isolated human naïve $CD4^+$ T lymphocytes

To confirm that high purity naïve $CD4^+$ T lymphocytes were isolated from whole blood as described in material and methods 2.2.4, levels of the cell surface markers CD4, CD62L and CCR7 were measured. Cells isolated from three independent donors on three separate occasions showed high levels of cell surface CD4 (98.33 ± 0.38 %) and CD62L (98.5 ± 0.4 %) (Figure 8.1). Additionally when the adhesion molecule CD62L was analysed alongside the chemokine receptor CCR7, cells isolated from five donors showed 91.88 ± 2.87 % cells positive for both proteins (Figure 8.2 A and B).

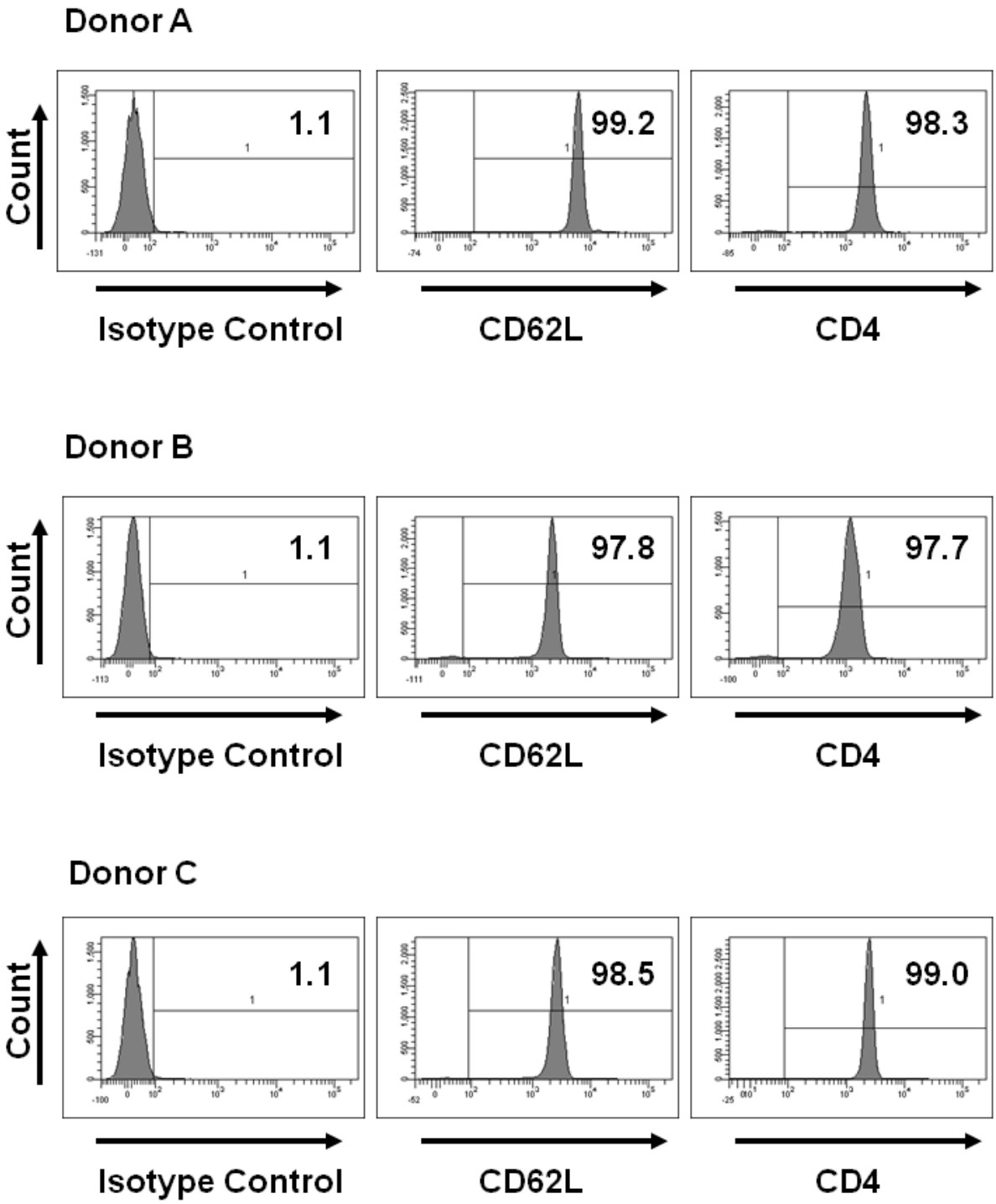

Figure 8.1: Expression of CD4 and CD62L on the surface of freshly isolated human naïve CD4$^+$ T lymphocytes. Naïve CD4+ T lymphcoytes were freshly isolated from human PBMC, as described in materials and methods. Cells were washed twice in ice cold PBS + 2% FCS and incubated for 1 hour with Isotype control (IgGκ1-FITC), CD62L-FITC or CD4-FITC Cell surface expression of molecules were measured using flow cytometry. A gate was set around 1% of the isotype control and the percentage of CD62L and CD4 positive cells are recorded along with example histograms for three independent donors.

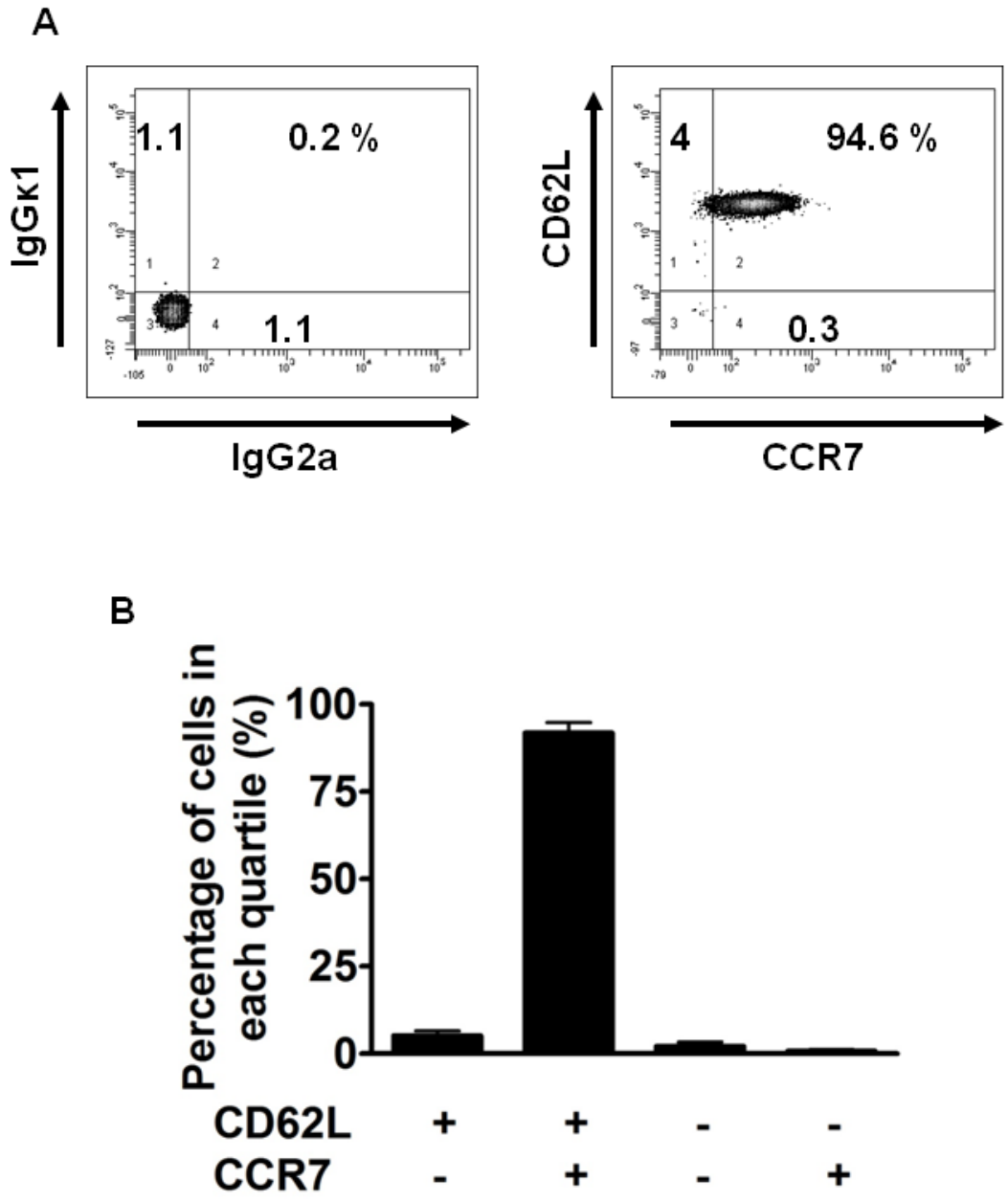

Figure 8.2: Expression of CD62L and CCR7 on the surface of freshly isolated human naïve CD4$^+$ T lymphocytes. Naïve CD4$^+$ T lymphcoytes were freshly isolated from human PBMC, as described in materials and methods. Cells were washed twice in ice cold PBS + 2% FCS and incubated for 1 hour with Isotype control (IgGκ1-FITC and IgG2a) or CD62L-FITC and CCR7-APC. Cell surface expression of molecules were measured using flow cytometry. **A.** A gate was set around 1% of the isotype control and the percentage of CD62L$^-$CCR7$^-$, CD62L$^+$CCR7$^-$, CD62L$^+$CCR7$^+$ and CD62L$^-$CCR7$^+$ positive cells are recorded. **B.** The percentage of cells (from three independent donors) in each quadratic are complied in a bar graph.

8.2. Publications

Foster JG, Blunt MD, Carter E, Ward SG. Inhibition of PI3K Signaling Spurs New Therapeutic Opportunities in Inflammatory/Autoimmune Diseases and Hematological Malignancies. *Pharmacological Reviews (In Press)*

Harris SJ, Parry RV, **Foster JG**, Blunt MD, Wang A, Marelli-Berg F, Westwick J, Ward SG. Evidence that the lipid phosphatase SHIP-1 regulates T lymphocyte morphology and motility. *J Immunol. 2011 Apr 15;186(8):4936-45*

Harris SJ, **Foster JG**, Ward SG. PI3K isoforms as drug targets in inflammatory diseases: lessons from pharmacological and genetic strategies. *Curr Opin Investig Drugs.* 2009 Nov;10(11):1151-62.

2nd UK Purine Symposium" Nottingham, UK, 17th September 2010

P2X7 receptor expression in human T lymphocytes and their role in loss of CD62L cell surface expression

Foster JG, MacKenzie AB and Ward SG

Cell Symposia: Inflammation and Disease" Lisbon, Portugal, 26th-28th September 2010

P2X7 receptor expression in human T lymphocytes and their role in loss of CD62L cell surface expression.

Foster JG, MacKenzie AB and Ward SG

Keystone Symposia Conference: PI 3-Kinase signalling pathways" Keystone, Colorado, USA, 13th-18th February 2011

Characterisation of the role of PI3K-dependent signalling in down-regulation of CD62L in human T lymphocytes

Foster JG, MacKenzie AB and Ward SG

Winter BPS Meeting" London, UK, 13-15th December 2011

Functional expression of P2X7 Receptor in T lymphocytes and its role in CD62L down-regulation

Foster JG, MacKenzie AB and Ward SG